



**HAL**  
open science

# Synthesis and studies of new optimised chelating agents for targeting chemokine receptor CXCR4

Pauline Désogère

► **To cite this version:**

Pauline Désogère. Synthesis and studies of new optimised chelating agents for targeting chemokine receptor CXCR4. Other. Université de Bourgogne, 2012. English. NNT: 2012DIJOS047. tel-00842206

**HAL Id: tel-00842206**

**<https://theses.hal.science/tel-00842206>**

Submitted on 8 Jul 2013

**HAL** is a multi-disciplinary open access archive for the deposit and dissemination of scientific research documents, whether they are published or not. The documents may come from teaching and research institutions in France or abroad, or from public or private research centers.

L'archive ouverte pluridisciplinaire **HAL**, est destinée au dépôt et à la diffusion de documents scientifiques de niveau recherche, publiés ou non, émanant des établissements d'enseignement et de recherche français ou étrangers, des laboratoires publics ou privés.



## THESIS

*Presented to obtain the title of*

# DOCTOR IN CHEMISTRY OF THE UNIVERSITY OF BURGUNDY

*By*

**Pauline DESOGERE**

*Master in Science*

---

### **Synthesis and studies of new optimized chelating agents for targeting chemokine receptor CXCR4**

---

Defended on November, 22<sup>th</sup> 2012 in front of the comity:

S. ARCHIBALD	Doctor at the University of Hull	Referee
P. PALLAVICINI	Professor at the University of Pavia	Referee
H. MAECKE	Professor at the University of Freiburg	Reviewer
J. M. BARBE	Doctor at the University of Burgundy	Reviewer
F. DENAT	Professor at the University of Burgundy	Director
C. GOZE	Doctor at the University of Burgundy	Co-Director



## **ACKNOWLEDGEMENTS**

This work was performed at the “Institut de Chimie Moléculaire de l’Université de Bourgogne” (ICMUB-P2DA, UMR 6302), Joint Research Unit between the University of Burgundy and the “Centre National de la Recherche Scientifique (C.N.R.S.) in the Laboratory of “Polyamines, Porphyrines: Développement et Applications”.

First of all, I would like to express my gratitude to Mister Steve Archibald, Doctor at the University of Hull and to Mister Piersandro Pallavicini, Professor at the University of Pavia, for accepting the task of reporter of this thesis. I am also very honored that Mister Helmut Mäcke, Professor at the University Hospital of Freiburg and Mister Jean-Michel Barbe, Doctor at the University of Burgundy have agreed to review this work.

I would like to express my sincere appreciation to my Director of thesis, Professor Franck Denat, for being supportive of various research ideas, providing academic freedom to experiment and also for help and support with future career. None of this work would have been possible without his confidence. I also deeply thank my Co-Director of thesis, Christine Goze, Doctor at the University of Burgundy, for every-day support, valuable discussions and advice on various research issues, and friendship.

I deeply thank Professor Helmut Mäcke for having initiated the AMD project and for the collaboration that was developed during my PhD. I would also like to express my gratitude to Doctor Steve Archibald for his interest in our compounds and future collaboration. I also thank Professor Rita Delgado for her participation in the cryptand project.

Thanks to Doctor Frédéric Boschetti, Director of CheMatech for his breadth of scientific experience and his key advice in macrocycle syntheses.

I place on record, my sincere gratitude to Doctor Claire Bernhard for her constant and valuable guidance and encouragements extended to me. This thesis work would not have been possible without her support and friendship.

I want to thank everyone who participated directly or indirectly to this thesis work, Sophie Poty in particular for her tremendous work in the AMD project (Good luck for the following...) and Marc Pirrotta for the large scale syntheses. I am not forgetting the trainees that I had the pleasure to supervise: Pierre Gaudriault, Delphine Thomas and Elodie Gigot.



I am deeply grateful to the entire members of the “Plateforme d’Analyses Chimiques et de Synthèse Moléculaire de l’Université de Bourgogne”. Thanks to Marie-José Penouilh and Doctor Fanny Piquet for the analyses by ESI high-resolution mass spectrometry, Marcel Soustelle for the elemental analyses, Didier Poinot for his help in experiments in the CECUB and Doctor Yoann Rousselin for the XRD and molecular modeling calculations. I also thank Doctor Christine Goze and Professor Claude Gros for the analysis by MALDI-TOF mass spectrometry.

I would like to thank all the lab members for their academic support in research and those who facilitated my every-day work: Doctor Christine Stern for her teaching experience, Doctor David Monchaud for biological questions, Doctor Michel Piquet for NMR issues, Doctor Alain Tabard, Christophe Guerville and Dominique Fraticelli for help in computing and Marc Pirrotta for technical support.

This has been particularly pleasant and comforting to work within the R13 group that I warmly thank, especially Claire Bernhard, Nicolas Sok, Mathieu Moreau, Bertand Brizet, Damien Lhenry, Sophie Poty, Marc Pirrotta, Loïc Stephan, without forgetting the CheMatech team Guillaume Paulin and Stéphane Martel.

Special thanks to all my chemist friends for their support, care and patiently listening to all my problems, complaints and jokes: Claire, Marie-Jo, Semra, Antoine, Bertrand, Marco, Guillaume P., Mathieu, Nico, Frédérique, Sarah P., Sophie, Guillaume O., Damien, Yann, Clément, Yulia, Lydie, Fred... Speaking of friendships, thank you to Caro, Tom, Mathilde, Aline, Carole, Perrine, Nico and Delphine, who can not speak chemistry language but who were always here for laughing with me, caring for me and cheering me up.

Lastly, special thanks to my family for constant support, encouragement and patience, especially my wonderful mother and my brother Antoine.

# SUMMARY

<b>ACKNOWLEDGEMENTS</b> .....	<b>3</b>
<b>SUMMARY</b> .....	<b>5</b>
<b>GLOSSARY OF ABBREVIATIONS</b> .....	<b>7</b>
<b>FOREWORD</b> .....	<b>9</b>
<b>I. INTRODUCTION</b> .....	<b>13</b>
I.1 CHEMOKINE RECEPTOR CXCR4 .....	13
I.1.1 Generalities .....	13
I.1.2 Activation of CXCR4 by SDF-1alpha .....	14
I.1.3 Involvement in several physiological and pathological processes .....	16
I.1.4 CXCR4 antagonists .....	17
I.1.5 Binding mode studies of small-molecule antagonists .....	20
I.2 CXCR4-BASED IMAGING AGENTS .....	24
I.2.1 Targeting CXCR4 radiopharmaceuticals .....	25
I.2.2 Optical imaging .....	42
I.2.3 Bimodality .....	46
I.3 RESEARCH OUTLOOK .....	48
<b>II. SYNTHESIS OF NEW CHELATING AGENTS BASED ON POLYAZACYCLOALKANES, OPTIMIZATION OF THE COORDINATION PROPERTIES FOR COPPER AND GALLIUM CHELATION.</b>	<b>53</b>
II.1 NEW METHODS OF C-FUNCTIONALIZATION OF REINFORCED TETRAAZACYCLOALKANES .....	54
II.1.1 Use of bisaminal as organic template .....	54
II.1.2 Synthesis of selectively functionalized constrained homocyclens .....	60
II.1.3 Introduction of a grafting function .....	72
II.1.4 Conclusion .....	73
II.2 NEW SYNTHETIC METHODS OF 1,4,7-TRIAZACYCLONONANE AND ITS DERIVATIVES: TOWARDS TACN-BASED BIFUNCTIONAL CHELATING AGENTS .....	74
II.2.1 Synthetic routes towards TACN derivatives .....	74
II.2.2 Obtention of new TACN derivatives by using the « aminal tool » .....	77
II.2.3 Synthesis of new BFCAs based on C-functionalized TACN .....	83
II.2.4 Conclusion .....	102
II.3 SYNTHESIS OF NEW CYCLEN-BASED CRYPTANDS .....	102
II.3.1 Cryptands based on tetraazacycloalkanes .....	102

II.3.2	<i>Synthetic pathways toward macrobicyclic systems.....</i>	106
II.3.3	<i>New cyclen-based systems bearing a diphenylether or a dibenzofuran unit.....</i>	107
II.4	CONCLUSION .....	113
<b>III.</b>	<b>NEW IMAGING AGENTS FOR TARGETING CHEMOKINE RECEPTOR CXCR4.....</b>	<b>117</b>
III.1	SYNTHESIS OF NEW AMD3100- AND AMD3465-BASED BUILDING BLOCKS .....	119
III.2	NEW IMAGING AGENTS FOR TARGETING CXCR4 .....	126
III.2.1	<i>Introduction of a fluorescent tag.....</i>	126
III.2.2	<i>Introduction of a macrocyclic chelating agent .....</i>	131
III.3	CONCLUSION.....	143
	<b>CONCLUSION .....</b>	<b>145</b>
	<b>EXPERIMENTAL SECTION.....</b>	<b>149</b>
<b>I.</b>	<b>INSTRUMENTATION .....</b>	<b>151</b>
<b>II.</b>	<b>EXPERIMENTAL PART CHAPTER II.....</b>	<b>153</b>
<b>III.</b>	<b>EXPERIMENTAL PART CHAPTER III.....</b>	<b>185</b>
<b>IV.</b>	<b>X-RAY DATA .....</b>	<b>210</b>
	<b>REFERENCES.....</b>	<b>215</b>
	<b>PUBLICATIONS AND COMMUNICATIONS .....</b>	<b>229</b>

## GLOSSARY OF ABBREVIATIONS

**Arg:** Arginine  
**Asp:** Aspartic acid  
**BFCA:** Bifunctional Chelating Agent  
**Bn:** Benzyl  
**CB:** Cross-bridged  
**COSY:** Correlation Spectroscopy  
**CPK:** Coray, Pauling, Koltun  
**CXCL12:** Chemokine ligand 12  
**CXCR4:** Chemokine receptor 4  
**DDQ:** 2,3-dichloro-5,6-dicyano-1,4-benzoquinone  
**DIPEA:** *N-N*-diisopropylethylamine  
**DMAP:** 4-dimethylaminopyridine  
**DMF:** dimethylformamide  
**DMSO:** dimethylsulfoxide  
**DOTA:** 2,2',2'',2'''-(1,4,7,10-tetraazacyclododecane-1,4,7,10-tetrayl)tetraacetic acid  
**DTPA:** diethylene triamine pentaacetic acid  
**EDCI:** 1-ethyl-3-(3-dimethylaminopropyl)carbodiimide  
**EDTA:** Ethylenediaminepentaacetic acid  
**ESI:** Electrospray Ionisation  
**Et:** Ethyl  
**Glu:** Glutamic acid  
**GPCR:** G-protein-coupled receptor  
**Gly:** Glycine  
**HBTU:** O-Benzotriazole-tetramethyl-uronium-hexafluoro-phosphate  
**His:** Histidine  
**HIV:** Human Immunodeficiency Virus  
**HMBC:** Heteroatom Multiple-Bond Correlation  
**HMQC:** Heteronuclear Multiple Quantum Coherence  
**HOBt:** 4-hydroxybenzotriazole  
**HPC:** Hematopoietic Progenitor Cell  
**HPLC:** High-Performance Liquid Chromatography  
**HSC:** Hematopoietic Stem Cell  
**IR:** Infrared  
**Lys:** Lysine  
**MRI:** Magnetic Resonance Imaging  
**MALDI-TOF:** Matrix Assisted Laser Desorption Ionisation- Time of Flight  
**Me:** Methyl

**MOMIA:** MOnomolecular Multimodality Imaging Agent  
**Ms:** Mesityl  
**NCS:** Isothiocyanate  
**NHS:** N-hydroxysuccinimide  
**NIR:** Near Infrared  
**NMR:** Nuclear Magnetic Resonance  
**NODAGA:** 1,4,7-triazacyclononane-1-glutaric acid-4,7-diacetic acid  
**NODASA:** 1,4,7-triazacyclononane-1-succinic acid-4,7-diacetic acid  
**NOESY:** Nuclear Overhauser Enhancement Spectroscopy  
**NOTA:** 2,2',2''-(1,4,7-triazacyclononane-1,4,7-triyl)triacetic acid  
**PEG:** Polyethylene glycol  
**PET:** Positron Emission Tomography  
**Sar:** Sarcophagine  
**SPECT:** Single Photon Emission Computed Tomography  
**SDF-1:** Stromal Cell-Derived factor-1  
**SB:** Side-bridged  
**SOD:** Superoxide Dismutase  
**TACN:** 1,4,7-triazacyclononane  
**TETA:** 2,2',2'',2'''-(1,4,8,11-tetraazacyclotetradecane-1,4,8,11-tetrayl)tetraacetic acid  
**TFA:** Trifluoroacetic acid  
**TLC:** Thin Layer Chromatography  
**TM:** Transmembrane  
**TRITA:** 2,2',2'',2'''-(1,4,7,10-tetraazacyclotridecane-1,4,7,10-tetrayl)tetraacetic acid  
**Ts:** Tosyl  
**Tyr:** Tyrosine  
**UV:** Ultra Violet

## **FOREWORD**

Cancer is a devastating global health issue affecting every socioeconomic class. Despite the considerable resources dedicated to cancer fighting, it remains the leading cause of death worldwide, accounting for a total of 7.9 million deaths (around 13 % of all deaths) in 2008, as reported by the World Health Organization.<sup>1</sup> This number is expected to increase dramatically over the coming years and is projected to triple by the year 2030. There have been numerous developments in cancer research over the past two decades, including discovery of novel diagnostic strategies, therapeutics and identification of key causal factors. However, the above statistics speak for themselves and serve as a reminder that we still have a long way to go to impact this devastating disease.

Most deaths from cancer stem from metastasis, and chemokine receptors are emerging as key elements in this process. Chemokine receptor 4 (CXCR4)-chemokine ligand 12 (CXCL12) interactions have been shown to play key roles in cancer cell survival, proliferation, homing, adhesion, tumor angiogenesis, and resistance to conventional and targeted therapies.<sup>2</sup> Given its extensive involvement in cancer progression, inhibition of CXCR4-CXCL12 $\alpha$  signaling was investigated as a potential therapeutic strategy using antagonists of the natural ligand.<sup>3</sup> CXCR4 targeting antagonists also provide versatile platforms for the development of imaging agents.<sup>4</sup> The underlying rationale here is that imaging of CXCR4 can be used to detect tumors and/or highly aggressive subpopulations of tumor cells.

In cancer, molecular imaging has traditionally played a critical role in detecting and staging the disease and permits the non-invasive study of cells in their natural microenvironment, without perturbing the system under investigation.<sup>1</sup> Generally speaking, molecular imaging involves specialized instrumentation, used alone or in combination with targeting imaging agents. Signal detection of the chosen label (luminescent and/or radioactive) enables the visualization of tissue characteristics and/or biochemical markers. For molecular imaging of cancer-related biomarkers, several modalities are in use including PET (Positron Emission Tomography), SPECT (Single Photon Emission Computed Tomography), MRI (magnetic resonance imaging), CT (x-ray computed tomography), optical imaging and bioluminescence.

This thesis is in line with these thematic concerns.



# **I. Introduction**





## I. INTRODUCTION

### I.1 Chemokine receptor CXCR4

#### I.1.1 Generalities

Chemoattractant cytokines, also called chemokines, are integral components of the hematopoietic cascade and the inflammatory response, regulating lymphocyte development, homing and trafficking.<sup>5,6</sup> They are 8-10 kDa proteins that are subdivided into four families defined by the number and relative spacing of cysteine residues at the *N*-terminal end of the protein. The two major families are CC and CXC in which there are two cysteine residues that are either adjacent (CC) or separated by one amino acid residue (CXC). Two other families are CX3C in which the cysteine residues are separated by three amino acid residues, and C in which one cysteine residue is lacking.

Chemokines are transmembrane (TM) proteins belonging to the superfamily of G-protein-coupled receptors (GPCRs).<sup>7</sup> In general, within the respective families, each chemokine has more than one receptor, and each receptor generally has more than one ligand. One exception is the chemokine receptor CXCR4, expressed in a wide range of tissues, including immune and central nervous systems. It has only one reported ligand CXCL12 $\alpha$  also called stromal cell-derived factor (SDF-1).<sup>3,6</sup>

CXCR4 possesses seven transmembrane domains that are linked to an inactive G protein existing as a heterotrimer (G $\alpha$ , G $\beta$ , and G $\gamma$ ) (Figure I-1).<sup>3</sup> Its structure is three-dimensional with an acidic extracellular *N*-terminal domain, an intracellular cytoplasmic tail in a three-stranded antiparallel  $\beta$ -sheet, and a *C*-terminal  $\alpha$ -helix. The *N*-terminal domain is essential for ligand binding, whereas the *C*-terminus is important in G protein activation.

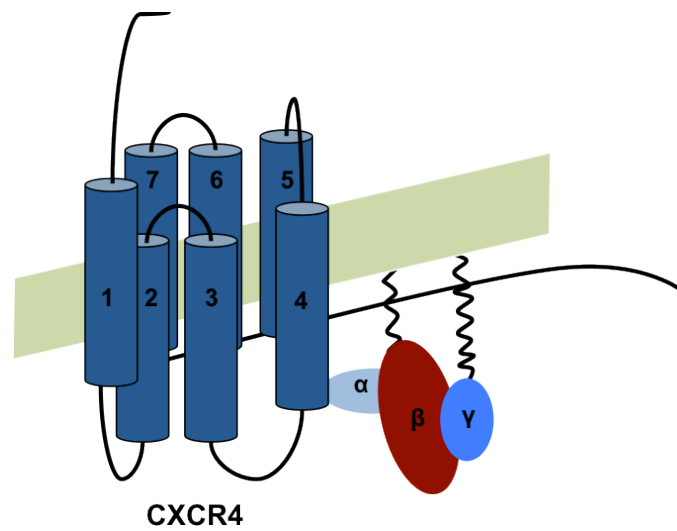


Figure I-1: Chemokine receptor CXCR4.<sup>3</sup>

Signal transduction by a GPCR occurs when an extracellular signaling molecule activates a cell surface receptor. In turn, this receptor alters intracellular molecules creating a response. The first step in this complex process is the ligation of the receptor by its high affinity ligand. This induces a conformational change that leads to the dissociation of the heterotrimer ( $G\alpha$  from the other two G-protein subunits). The dissociation exposes sites on the subunits that can interact with other molecules. The particular mechanism of SDF-1 $\alpha$ -CXCR4 interaction has been well characterized and will be described in the next part.

### ***1.1.2 Activation of CXCR4 by SDF-1alpha***

The structure of CXCL12 $\alpha$  has been determined by X-ray crystallography and NMR spectroscopy.<sup>8</sup> First eight residues of CXCL12 $\alpha$  at the *N*-terminus form an important receptor binding site (Figure I-2). The overall charge for CXCL12 $\alpha$  is +8 and the corresponding net charge of the extracellular loops of CXCR4 is -9. The positively charged residues, including Lys<sup>24</sup>, His<sup>25</sup>, Lys<sup>27</sup> and Arg<sup>41</sup>, form a cluster, which leads to the highly positive potential of CXCL12 $\alpha$ .

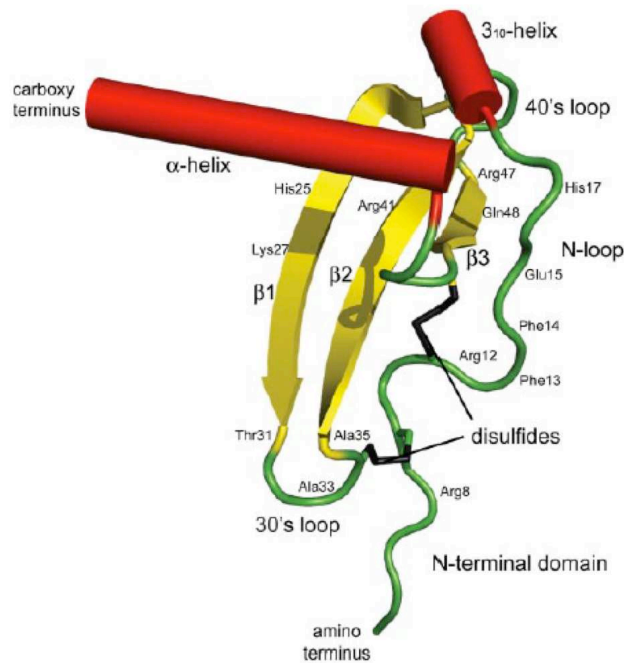


Figure I-2: CXCL12 $\alpha$  structure.<sup>8</sup> Strands are displayed as ribbons, helical regions are displayed as cylinders and loops, and random coil regions are displayed as a backbone trace. The two conserved disulphide bonds are displayed in black.

A molecular binding mechanism of CXCL12 $\alpha$  with CXCR4 has been proposed (Figure I-3).<sup>3,9-11</sup> The positively charged part of CXCL12 $\alpha$  first binds to the negatively charged extracellular loops of CXCR4 through an electrostatic interaction. Then, the positively charged *N*-terminus further binds to the corresponding negatively charged transmembrane domains. These two binding steps convert the CXCR4 to an active conformation initiating signal transfer through the membrane thus activating immune cells.

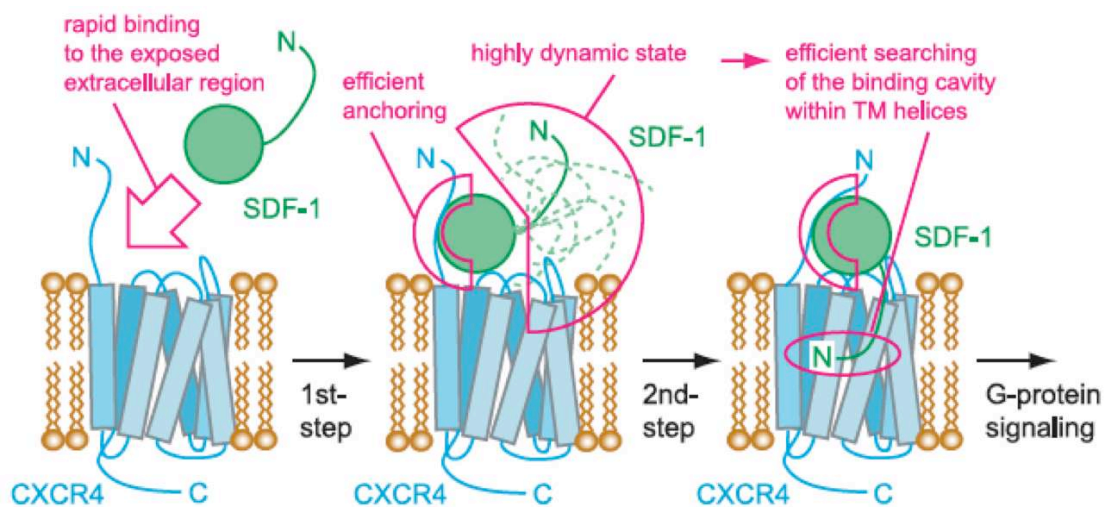


Figure I-3: Mechanism of SDF-1 $\alpha$  - CXCR4 interaction<sup>9</sup>

### 1.1.3 Involvement in several physiological and pathological processes

The activation of CXCR4 by SDF-1 $\alpha$  can lead to different downstream signaling pathways that result in a variety of physiological responses, such as chemotaxis, cell survival and proliferation, intracellular calcium flux and gene transcription (Figure I-4).<sup>12</sup> These normal physiological responses also share several downstream effectors with multiple pathological processes, including tumor cell metastases, autoimmune and inflammatory diseases.

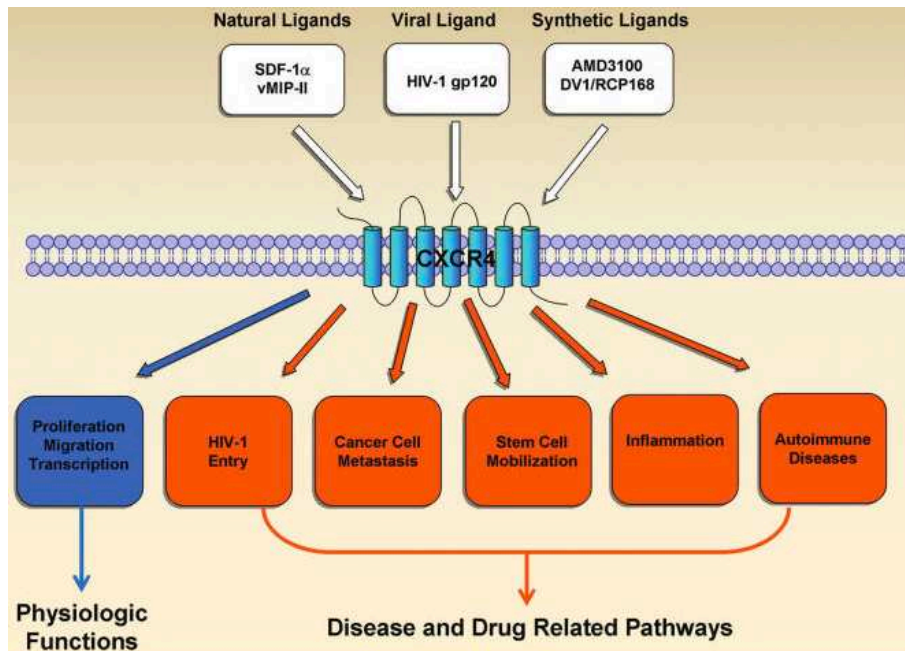


Figure I-4: Various biological functions of the chemokine receptor CXCR4.<sup>12</sup>

#### 1.1.3.1 Cancer cells metastases

Malignant cells from at least 23 different types of cancer express the chemokine receptor CXCR4 and respond to its ligand CXCL12 $\alpha$ .<sup>7,13</sup> This receptor ligand pair appears to be involved in cancer cell progression, angiogenesis, metastases, and survival. CXCR4 expression enables tumor cells to home to organs expressing abundant levels of CXCL12 $\alpha$ , such as lungs, bone, liver, brain, and bone marrow, leading to establishment of metastases. Overexpression of CXCR4 in primary tumors is directly correlated to increased risk for local recurrence, distant metastases, and poor survival rates in breast, colon, and several other cancers.

#### 1.1.3.2 Stem cells mobilization

Recent studies have indicated that the interactions between CXCR4 and CXCL12 $\alpha$  modulate hematopoietic cell mobilization and engraftment.<sup>14</sup> CXCR4 is extensively expressed in hematopoietic stem cells (HSCs) and in hematopoietic progenitor cells (HPCs), and its interaction

with CXCL12 $\alpha$  promotes the retention of CXCR4 expressing hematopoietic cells in the bone marrow microenvironment. Consequently, the blocking of CXCR4 with an antagonist results in the mobilization of hematopoietic cells.

### *1.1.3.3 Autoimmune and autoinflammatory diseases*

In a normal immune response, leukocytes gather in the site of injury or infection and defend the body from disease bearing organisms.<sup>15</sup> Chemokines play a major role in this immune response by activating the directed migration of leukocytes. However, under certain circumstances the immune response can be inappropriately activated and targeted toward normal healthy tissue leading to autoimmunity and disease. Chemokines have been shown to be associated with a number of autoinflammatory diseases including multiple sclerosis, rheumatoid arthritis, atherosclerosis, asthma, organ transplant rejection, etc.

### *1.1.3.4 HIV entry*

HIV enters T cells by the adsorption of its surface glycoproteins (gp120) to receptors on the target cell followed by fusion of the viral envelope with the cell membrane and the release of the HIV capsid into the cell.<sup>16</sup> The glycoprotein CD4 is the main receptor for HIV-1 and CXCR4 the coreceptor involved in the process.

Because of its involvement in a wide range of physiological and pathologic processes, there has been intensive biological, chemical, and pharmaceutical research to understand the modulation of chemokine-receptor functions. The ultimate goal is to translate these discoveries into novel treatment strategies for clinical applications.

## ***1.1.4 CXCR4 antagonists***

Inhibition of CXCR4-CXCL12 $\alpha$  signaling was investigated as potential therapeutic strategies using antagonists of the natural ligand. Several CXCR4-binding agents, including antibodies,<sup>17,18</sup> peptide-based antagonists and small-molecule-antagonist scaffolds such as cyclams have been developed.<sup>12,19</sup>

### I.1.4.1 Peptide derivatives

The design of new specific peptide-based CXCR4 antagonists requires the following of a general procedure. After identification of a natural antagonist and its critical residues involved in the fixation on the receptor, a library of peptides can be generated by modulation of several parameters such as structure (monomer or dimer), overall charge and size. It has been shown that CXCR4 extracellular surface is negatively charged. As a consequence, the overall charge of the antagonist is an important parameter and all high potent antagonists are positively charged.

Among the large series of natural CXCR4 ligands, SDF-1 was particularly studied.<sup>12</sup> Its *N*-terminus was determined as a critical site for CXCR4 recognition, signal transduction and antiviral activity. A wide range of peptides derived from this particular region was generated.<sup>20-22</sup> The resulting peptides exhibited similar activities compared to SDF-1 but were less potent. The same strategy was applied on another natural antagonist based on a viral chemokine (viral macrophage inflammatory protein-II so called vMIP-II).<sup>23,24</sup>

Another route towards effective anti-HIV compounds was based on derivatives of self-defense peptides of horseshoe crabs, tachyplesin and polyphemusin.<sup>25</sup> By chemical modifications of these peptides, Masuda *et al* developed a synthetic anti-HIV peptide called T22 (Figure I-5),<sup>26</sup> which is a 18-residue peptide with two disulphide bridges. A structure-activity relationship study of T22 revealed the contribution of characteristic regions to its activity and cytotoxicity. The number of Arg residues in the *N*-terminal and *C*-terminal regions of T22 is actually correlated with anti-HIV activity and the presence of disulphide rings, especially the major one, is indispensable for biological activity.

Several downsized analogues of T22 were prepared to enhance its anti-HIV activity and decrease its cytotoxicity. Among them, T140 was identified as the highest potent peptide.<sup>27-29</sup> Four residues (two arginines, one 3-(2-naphthyl)alanine, and one tyrosine) were determined as T140 critical pharmacophores<sup>30</sup> and a wide range of cyclopentapeptides was generated from these residues. The pentapeptide FC131 showed even stronger antagonist action and improved metabolic stabilities.<sup>31</sup>

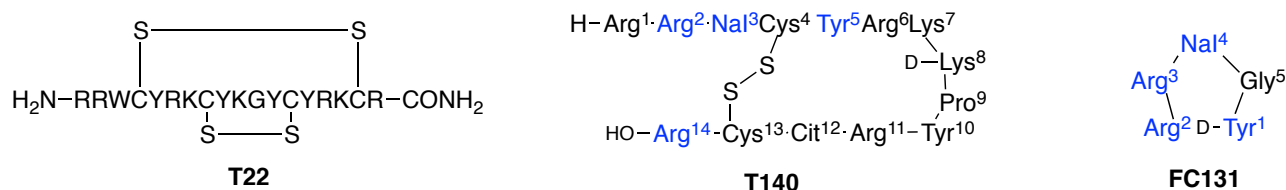


Figure I-5: Structures of T22 and its derivatives T140 and FC131. Blue residues are the indispensable residues of T140 for the potent CXCR4-antagonistic activity. Nal = L-3-(2naphthyl)alanine, Cit = L-citrulline

### I.1.4.2 Small organic molecules

In the search for new anti-HIV agents with better characteristics than the existing drugs, a novel class of compounds namely bicyclam was discovered with potent and selective anti-HIV activity.<sup>32</sup> These derivatives are highly basic and positively charged at physiological pH.

These compounds contain two macrocyclic rings, with 14 members each, linked in various ways. The prototype compound used for the development of these new agents was the monocyclam AMD1498 (1,4,8,11-tetraazacyclotetradecane) (Figure I-6).<sup>32</sup> Two compounds (AMD1657 and AMD2763) were found active against HIV-1 (Figure I-6). In AMD1657 the cyclam moieties were linked with a direct carbon-carbon bridge creating two chiral centers, in AMD2763 via an aliphatic (propylene) bridge.<sup>32</sup>

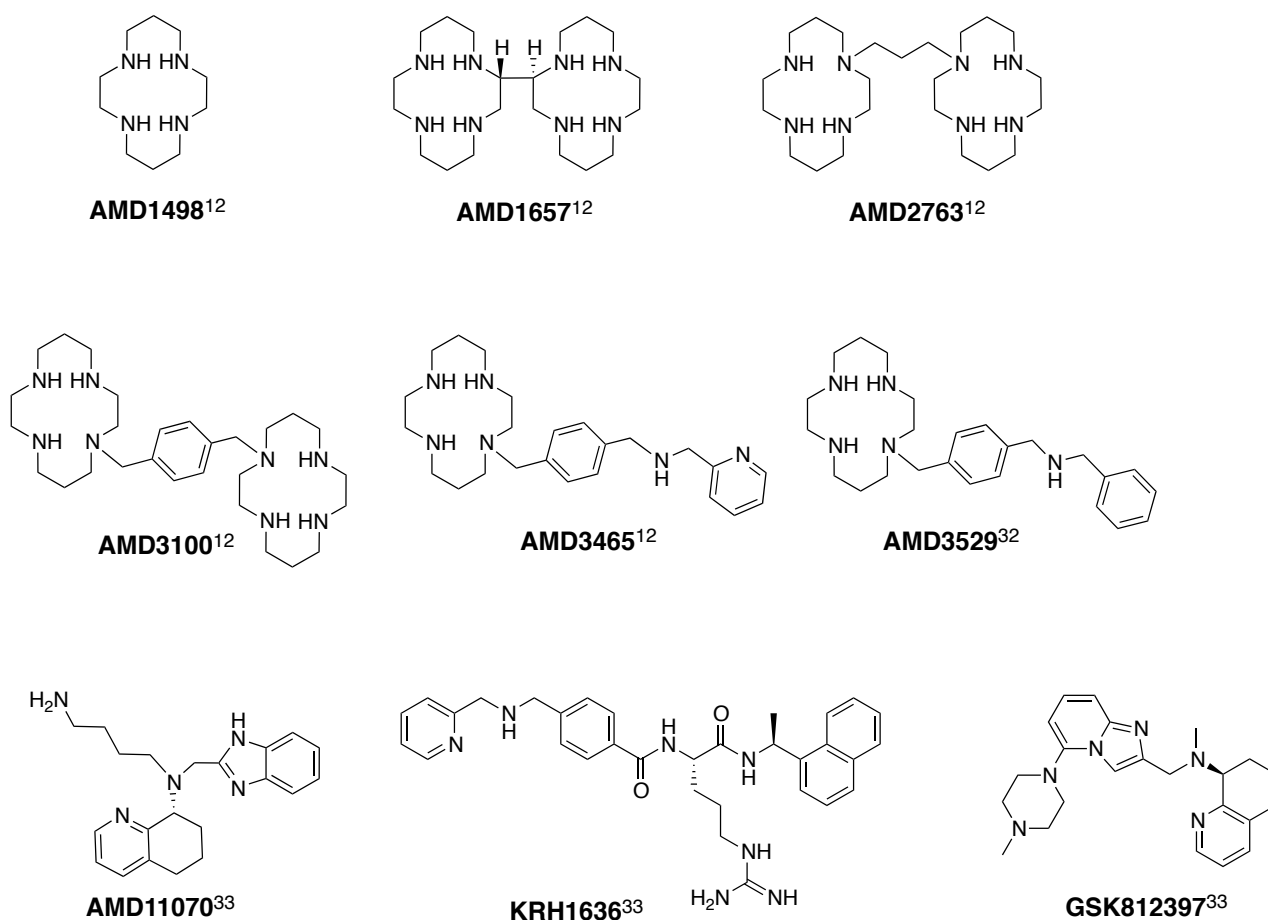


Figure I-6: Chemical structures of several small molecules CXCR4 antagonists.<sup>12,32,33</sup>

Further studies pointed out that bicyclam derivatives in which the two monocyclam rings are connected by an aromatic linker, instead of an aliphatic linker, inhibited HIV replication, in a concentration about 100-fold lower than the one required for AMD2763.<sup>32</sup>

The most potent bicyclam of these series is AMD3100, previously called JM3100 or SID791, in which the two cyclam moieties are linked by a 1,4-phenylenebis(methylene)-bridge (Figure I-6).<sup>34</sup> Clinical studies of AMD3100 in HIV-infected patients have provided proof of concept for



CXCR4 blocking in HIV therapy. However, further development was discontinued due to cardiac toxicity when injected in high doses. Clinical trials also demonstrated that AMD3100 is an efficient mobilizer of hematopoietic stem cells from the bone marrow in both healthy individuals and some individuals with cancer. AMD3100 is now marketed as Mozobil™ and used as stem colony mobilization agent in combination with granulocyte colony-stimulating factor. Configurationally restricted derivatives of AMD3100 were also developed.<sup>35,36</sup>

However, clinical applications of AMD3100 and its derivatives are limited because of their lack of oral bioavailability, which is related to their high positive charge at physiological pH. In order to improve oral absorption, analogous compounds such as monocyclam derivatives (AMD3465, AMD3529) were developed.<sup>33</sup>

AMD3465, based on a monomacrocyclic *N*-pyridinylmethylene cyclam structure, particularly retains attention. Indeed, it exhibits improved anti-HIV activity and it has been showed to be 10-fold more effective as a CXCR4 antagonist than the biscyclam AMD3100 in (<sup>125</sup>I)-CXCL12 displacement assays.<sup>37</sup>

Most recently, a novel series of heterocyclic analogues has been developed containing different moieties such as imidazole, benzimidazole, functionalized pyridine or guanidine (AMD11070, KRH1636, GSK812397) (Figure I-6).<sup>12</sup> Among them, AMD11070 is the first orally bioavailable small-molecule CXCR4 inhibitor. It is currently being studied in clinical trials as a potent antiretroviral agent.

### ***1.1.5 Binding mode studies of small-molecule antagonists***

The evolution from the macrocyclic and positively charged AMD3100 to the monocyclam AMD3465 and to the non-cyclam AMD11070 represents a progressive reduction in both molecular size and charge, but also a gain of oral bioavailability. Because they are structurally different, it is of interest to examine their mode of interaction with the receptor.

#### ***1.1.5.1 Ligand-receptor interactions***

Kawatkar *et al* demonstrated that CXCR4 antagonists based on small organic molecule have a distinct binding site, which is different from the region occupied by the *N*-terminus of SDF-1.<sup>38</sup> This suggested the coexistence of an antagonistic ligand-binding site with a SDF-1 signaling site in CXCR4. Based on site-directed mutagenesis and molecular modeling, different binding mode studies were investigated on AMD3100, AMD3465 and AMD11070 (Figure I-7).<sup>33,37,39,40</sup>

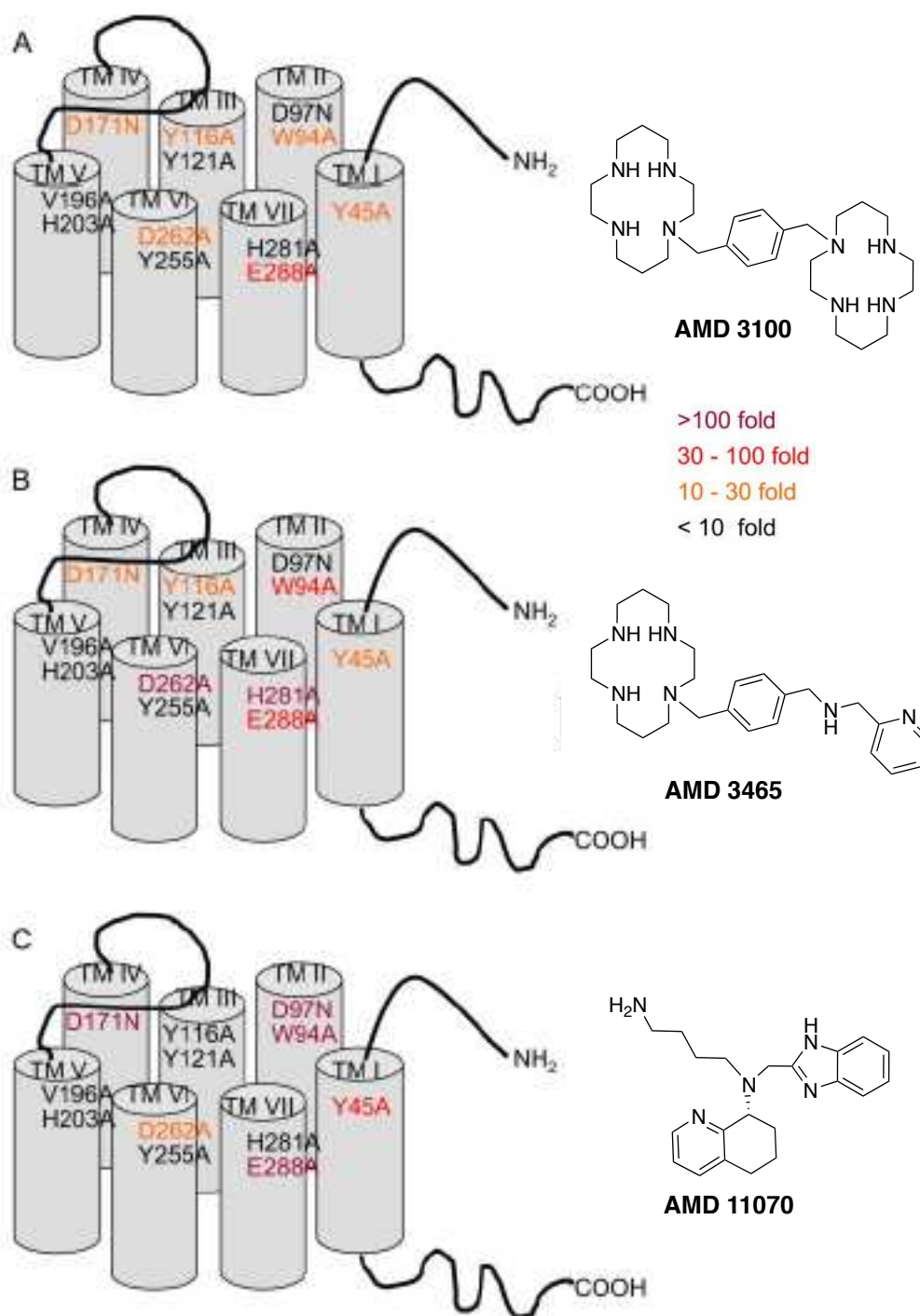


Figure I-7: Residues identified through mutagenesis to be important for the binding of AMD3100 and AMD3465 shown in a helical wheel diagram of the CXCR4 receptor. The levels of effect of each mutation on the  $K_i$  values of the compounds in  $^{125}\text{I}$ -SDF-1 competitive binding are indicated by the following font colour: purple, >100-fold increase in  $K_i$  value; red, 30- to 100-fold increase in  $K_i$  value; orange, 10- to 30-fold increase in  $K_i$  value; and black, <10-fold increase in  $K_i$  value.<sup>40</sup>

At physiological pH, AMD3100 has an overall charge of +4 due to the four protonated nitrogens (two per cyclam ring). Thus, the protonated cyclams can interact with negatively charged amino acids (such as aspartate and glutamate) in the main ligand binding pocket of the receptor. Three acidic residues Asp<sup>171</sup> (D171N), Asp<sup>262</sup> (D262A) and Glu<sup>288</sup> (E288A) are mainly involved in

the inhibitor-receptor interactions (Figure I-7A). One cyclam ring of AMD3100 interacts with Asp<sup>171</sup> in TM-IV, whereas the other ring is sandwiched between the carboxylic acid groups of Asp<sup>262</sup> and Glu<sup>288</sup> from TM-VI and -VII, respectively.<sup>39</sup>

Due to the substitution of one cyclam by a pyridine ring, AMD3465 is smaller in size and the binding pocket is more compact compared to AMD3100. However, some antagonist-receptor interactions are similar to those involved in AMD3100 binding (Figure I-7B). The overall charge of AMD3465 is +3 at physiological pH. Thus, the doubly protonated cyclam ring interacts with Asp<sup>171</sup>, the pyridine moiety with Asp<sup>262</sup> and the protonated secondary amine of the aminomethylpyridine with Glu<sup>288</sup>. Moreover, an aromatic interaction between His<sup>281</sup> (H281A) and the pyridine ring has been demonstrated.<sup>33,39</sup> This additional interaction with His<sup>281</sup> leads to the enhancement of the inhibitor binding to the receptor and therefore contributes to the higher potency of AMD3465 compared to AMD3100.

Because of its structure, AMD11070 has significantly different binding modes compared with macrocyclic molecules (Figure I-7C). At physiological pH, AMD11070 is doubly protonated and can form ionic interactions with different amino acid residues. Different binding models were proposed by Wong *et al* involving in particular hydrogen bonds between the protonated primary amine and an aspartate residue <sup>97</sup>Asp (D97N), <sup>171</sup>Asp or <sup>262</sup>Asp or between the protonated tertiary amine and <sup>288</sup>Glu. Aromatic interactions between the benzimidazole and the tyrosine residue (<sup>45</sup>Tyr or <sup>84</sup>Tyr) were also identified.<sup>40</sup> It has to be noted that <sup>97</sup>Asp is not involved in the binding with macrocyclic antagonists.

As a conclusion, these antagonists bind to overlapping but not identical amino acid residues in the transmembrane regions close to the extracellular loop of the receptor.

Concerning macrocyclic antagonists, studies also revealed that it was possible to enhance the affinity for the receptor by adding a metal cation in the cyclam ring.<sup>33,41</sup>

### *1.1.5.2 Effect of a transition metal in the cyclam cavity*

Because of the preorganization and the flexibility of their macrocyclic framework, cyclams are known to form stable complexes with transition metals. Several complexes of AMD3100 with metal cations were prepared and studied. Liang *et al* demonstrated that incorporation of Zn<sup>2+</sup>, Cu<sup>2+</sup> or Ni<sup>2+</sup> into the macrocyclic rings of AMD3100 led to the enhancement of the binding affinity to the CXCR4 receptor. To explain these results, it is of interest to understand the coordination geometry of such complexes.<sup>32</sup>

In the cyclam ring,  $Zn^{2+}$  is coordinated by the four nitrogen atoms in a planar fashion.  $Zn^{2+}$  complexes having usually a square pyramidal or an octahedral geometry, at least one coordination site is vacant in cyclam complexes allowing interactions with an axial ligand, such as a carboxylic acid. Gerlach *et al* performed the modelisation of acetate binding to cyclam and cyclam( $Zn$ ).<sup>41</sup> The optimized structures indicated that the acetate group was bound to cyclam by forming three hydrogen bonds (Figure I-8A), whereas in cyclam( $Zn$ ) it was directly coordinated to the metal ion and formed only one hydrogen bond (Figure I-8B).

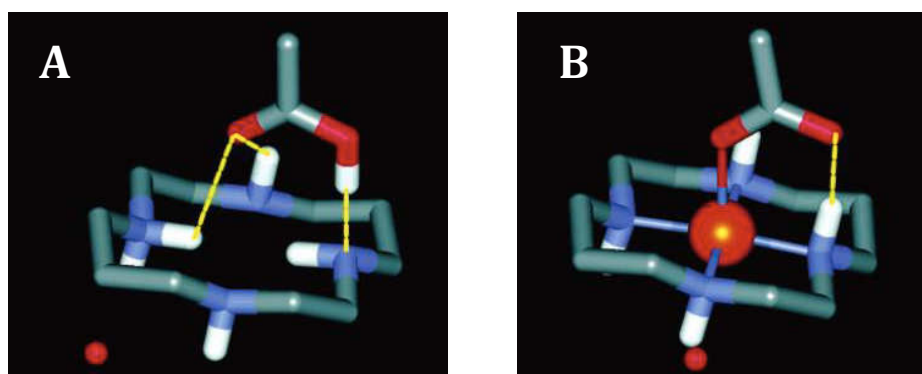


Figure I-8: Structures of cyclam complexes optimized by quantum chemistry.<sup>41</sup> Hydrogen bonds are represented in yellow dotted lines.

Gerlach *et al* showed that the affinity of AMD3100 to the CXCR4 was increased 36-fold, by incorporation of  $Zn^{2+}$  into one cyclam ring, in competition binding assays with <sup>125</sup>I-SDF-1.<sup>41</sup> Previously, we saw that Asp<sup>171</sup> and Asp<sup>262</sup> were the key residues involved in the binding of the non-metallated biscyclam compound. The enhancing effect of transition metal can be due to either an improved binding to one of the key residues or it can be caused by a metal ion interaction with another residue in the receptor. Studies indicated that upon chelation of  $Zn^{2+}$  by AMD3100, the complex does not change binding mode, but more likely its interaction with the carboxylate group of Asp<sup>262</sup> becomes stronger. (Figure I-9).<sup>41</sup> The biszinc analogue showed identical affinity to that of the corresponding mono-metallated analogue.

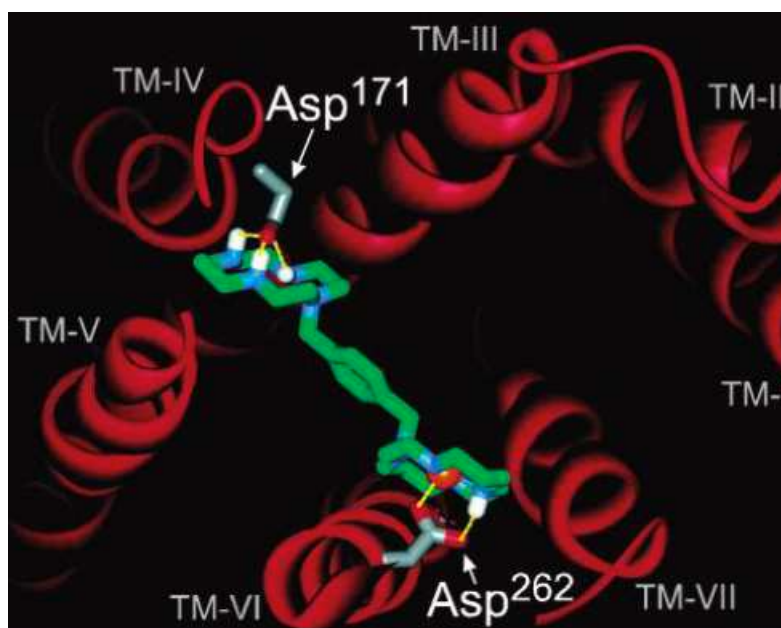


Figure I-9: Molecular model of the main ligand-binding pocket of the CXCR4 receptor with AMD3100(Zn) manually docked into favourable interactions with Asp<sup>171</sup> and Asp<sup>262</sup>.<sup>41</sup>

Cyclam complexes of Cu<sup>2+</sup> and Ni<sup>2+</sup> can adopt the same configuration than cyclam-Zn. Both AMD3100(Ni) and AMD3100(Cu) complexes showed a higher affinity than the non-metallated ligand. The affinity was respectively 7-fold and 50-fold enhanced with Cu<sup>2+</sup> and Ni<sup>2+</sup> in a cyclam ring. Ni-complex exhibited the highest potential as antagonist due to a stronger interaction with the receptor. The difference of strength of the interaction between the metal complexes and the receptor (Ni > Zn > Cu) should be related to the stability of the bond between the metal and Asp<sup>262</sup>.<sup>41</sup>

Only one example in the literature reports the effect of transition metal in the unique cyclam cavity of AMD3465.<sup>33</sup> Similarly to AMD3100, the presence of Cu<sup>2+</sup> increased the affinity to the receptor and confirmed the importance of Asp<sup>262</sup> in the electrostatic interaction between the metal and the receptor.

## I.2 CXCR4-based imaging agents

In cancer, non-invasive imaging has traditionally played a critical role in detecting and staging the disease. Advances during the past decade continue to revolutionize the role of imaging in cancer through faster and more sensitive instruments, through the development of novel imaging probes and through genetic engineering systems. For molecular imaging of cancer-related biomarkers, several modalities are in use including PET, SPECT, MRI, CT and optical imaging. Anatomical technologies such as X-ray, CT and MRI have become diagnostic staples of current clinical practice. Likewise, functional imaging modalities have found broad clinical use in oncologic disease diagnosis and staging. Functional imaging modalities include optical (bioluminescence and fluorescence), PET and SPECT.

For a diagnostic perspective, the role played by CXCR4 in invasion and metastases makes it a valuable biomarker to identify primary tumors to metastases.<sup>7,13,42</sup> For this reason a number of CXCR4 inhibitors have been developed, which have been reviewed in the previous part. Recently it was found that these CXCR4 targeting moieties also provide versatile platforms for the development of imaging agents (Figure I-10).<sup>4</sup> In the next part, we will present the different modalities used for imaging CXCR4 and the corresponding CXCR4 imaging agents, which are radioactive and/or luminescent.

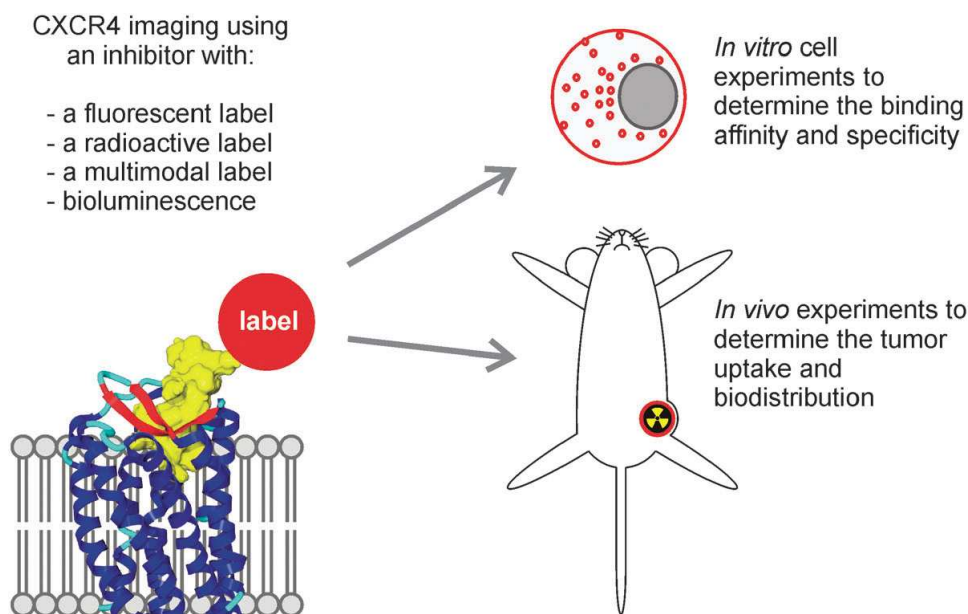


Figure I-10: Use of CXCR4 as a target for imaging (inhibitor in yellow).<sup>4</sup>

## 1.2.1 Targeting CXCR4 radiopharmaceuticals

Nuclear imaging enables the visualization and the following of molecular process and cellular function in living organisms without perturbation through the use of radiolabeled compounds. Such compounds are named radiopharmaceuticals or radiotracers and are used in such low concentrations that they have limited pharmacological effect. When specific, these tracers are based on the receptor binding of a radiolabeled vector in the diseased tissue. The target-specific moiety, such as an antibody or antibody fragment, a peptide, nanoparticles or low molecular weight ligands, is labeled with an appropriate radionuclide.

### 1.2.1.1 Generalities on PET and SPECT

Radiolabeled compounds can be visualized with either PET or SPECT. The remarkable sensitivity of such techniques and their ability to provide information complementary to the

anatomical images produced by other modalities make them ideal for imaging biomarker- and microenvironment-targeted tracers. Both modalities have become extremely important in the clinic, and while PET is generally more expensive on both clinical and pre-clinical levels, it also undoubtedly possesses a number of significant advantages over SPECT, most notably the ability to quantify images.

For a PET or SPECT exam, the radiolabeled agent is administered to the patient/subject, typically via an intravenous injection. The radioactivity is then traced through the body and its distribution determined from scans obtained with a specific camera. The gamma rays emissions of the radiotracers are detected, in the case of SPECT, by a gamma camera. In PET imaging, short-lived positron-emitting isotopes are used as radiotracers. The emission of a positron and its annihilation with an electron results in the emission of two 511 keV photons at 180° to each other; these photons are detected as a coincident event, making it possible to localize more precisely their source and reconstruct an image (Figure I-11).

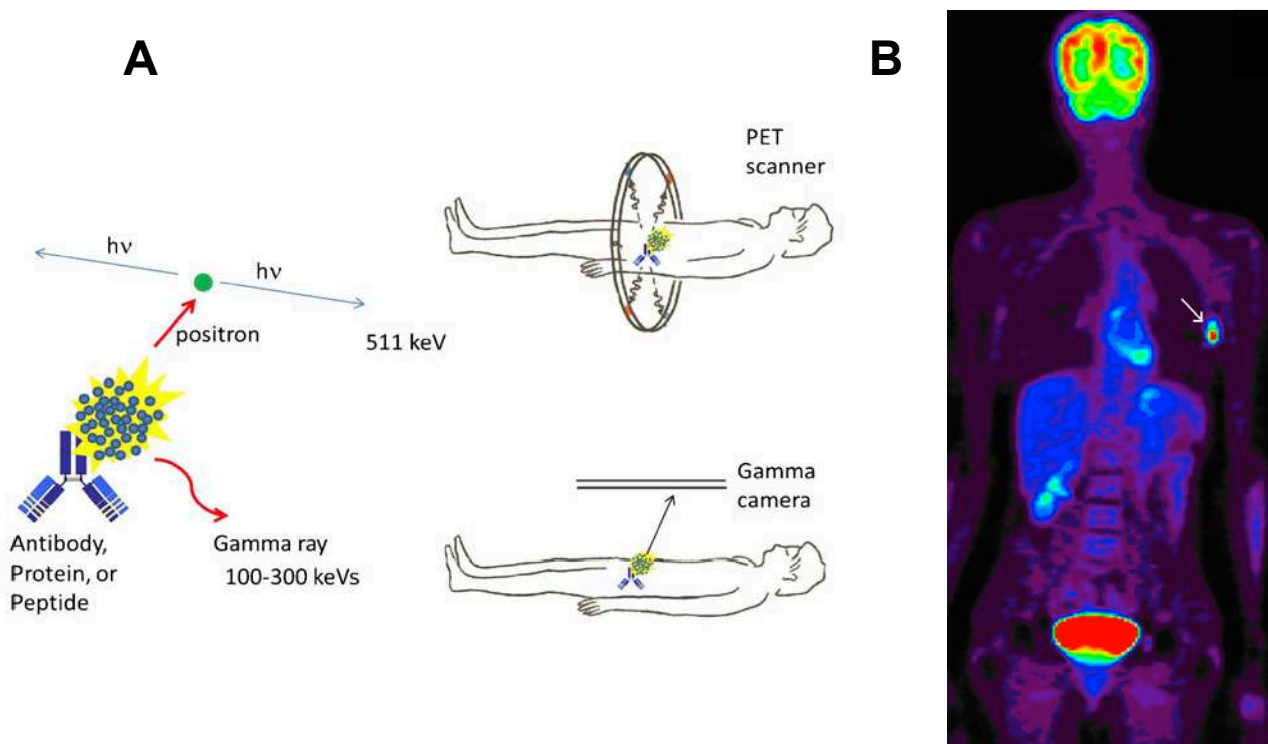


Figure I-11: **A:** Diagram illustrating the principles of PET and SPECT,<sup>43</sup> **B:** Example of a PET image.

Since the advent of PET and SPECT in both clinic and preclinic research laboratories, a number of isotopes have been used in nuclear medicine.

Table I-1 lists common radionuclides used in nuclear medicine with their half-lives, their mode of decay and the technique that employed them. The choice of radionuclide largely depends upon its nuclear properties (half-life, type of radiation, energy, and presence or lack of other particulate radiation emissions) and potential for wide clinical applications of the radiotracer.



The radioisotopes can be divided in three major groups: lightweight elements, radiohalogens and radiometals. Halogens especially  $^{18}\text{F}$  are increasingly more common in synthetic biomolecules or in many cases may be added to a molecular structure by radiochemistry process without significantly altering its biologic activity. Radiometals possess attractive radionucleidic properties for imaging. Moreover, they offer many opportunities for the design and the development of new target-specific radiotracers.

Radionuclide	Physical half-life	Mode of decay	Applications
$^{13}\text{N}$	10 min	$\beta^+$	PET
$^{11}\text{C}$	20.3 min	$\beta^+$	PET
$^{15}\text{O}$	2 min	$\beta^+$	PET
$^{18}\text{F}$	109.8 min	$\beta^+$	PET
$^{123}\text{I}$	13.2 h	$\gamma$	SPECT
$^{125}\text{I}$	59 d	$\gamma$	SPECT
$^{131}\text{I}$	8.0 d	$\gamma$	SPECT
$^{99\text{m}}\text{Tc}$	6.0 h	$\gamma$	SPECT
$^{89}\text{Zr}$	78.5 h	$\beta^+$	PET
$^{111}\text{In}$	67.9 h	$\gamma$	SPECT
$^{67}\text{Ga}$	78.2 h	$\gamma$	SPECT
$^{68}\text{Ga}$	1.1 h	$\beta^+$	PET
$^{64}\text{Cu}$	12.7 h	$\beta^+$	PET
$^{67}\text{Cu}$	61.8 h	$\gamma + \beta^-$	SPECT/therapy

Table I-1: Relevant radionuclides for medical applications.

There are numerous categories of molecular imaging agents including small molecules, peptides, high-molecular-weight antibodies, engineered protein fragments, and various nanoparticles. Each type falls within a different size range and thus possesses different pharmacokinetics, binding properties and receptor interaction modes. Within each individual class of agents, there are agents that can be directly or indirectly labeled.

### 1.2.1.2 Direct labeling

Chemical modification of proteins and small molecules with a radioactive element is a process generally used in direct labeling. Non-metallic radionuclides, possessing short radioactive half-lives ( $^{123}\text{I}$ ,  $^{18}\text{F}$ ,  $^{13}\text{N}$  and  $^{11}\text{C}$ ) are directly incorporated in the core of the targeting molecule. This method provides a mean of detection that can be extremely sensitive for assay, localization and imaging applications.



Several CXCR4 antagonists were directly radiolabeled with iodide.<sup>4</sup> For example, SDF-1 was labeled with <sup>125</sup>I and the resulting agent demonstrated poor imaging characteristics *in vivo*, limiting routine use.<sup>44</sup> It was given up for molecular imaging, however the molecule is being used in competition binding assays to evaluate the affinity of antagonists for the receptor. Monoclonal CXCR4 antibody clone 12G5, which binds the same extracellular loop as CXCL12, was also radiolabeled with <sup>125</sup>I and studied by Nimmagadda *et al.* in a glioblastoma tumor model.<sup>45</sup> Imaging data showed clear accumulation of <sup>125</sup>I-12G5 in the tumors, even though the highest level of radioactivity was seen in the spleen.

Direct imaging is an accurate method because the molecular target of interest is being studied directly. Despite the significant successes of such probes, these radiotracers possess a few critical limitations. First, their short-half-lives allow only investigations of biological processes on the order of minutes or a few hours using tracers with rapid pharmacokinetic profiles. Second, the necessity of incorporating the radioisotopes into the core structure of the tracer often requires demanding and complex syntheses.

### I.2.1.3 Indirect labeling

Indirect labeling by using a prosthetic group or an appended chelator so-called bifunctional chelating agent (BFCA) is a more generalizable method that may be applied to image many different biological processes with the same basic technique.

In the first section, we will present the use of prosthetic group for the introduction of <sup>18</sup>F on the targeting biomolecule. The second section will present a broad view of the chemical strategies explored to synthesize different families of chelators-based radiotracers.

#### I.2.1.3.1 Introduction of <sup>18</sup>F via a prosthetic group

The <sup>18</sup>F radioisotope can be indirectly incorporated into the core structure of the tracer by the use of a prosthetic group.<sup>46</sup> The use of such groups is of great interest because of ease and high yields of the chemical reactions involved and the high chemoselectivity of the radiolabeling process. The targeting molecule is normally connected to a reactive moiety at a specific position not involved in a crucial biological role. The radiolabeled prosthetic group is then linked to the reactive moiety in a chemoselective manner. We will describe the examples of CXCR4 antagonists labeled with <sup>18</sup>F via a prosthetic group.

The first example of <sup>18</sup>F-radioimaging agent based on T140 was described by Jacobson *et al* (Figure I-12).<sup>47</sup> After selective labeling on the N terminus via *N*-succinimidyl-4-<sup>18</sup>F-fluorobenzoate

conjugation, the two lysine residues were deprotected with hydrazine. The corresponding agent suffered from pronounced off target binding to red blood cells when used in tracer concentrations. CXCR4-positive tumors were distinguishable from control tumors; however, coinjection of unlabeled 4-F-T140 was necessary to see increased radioactivity in the CXCR4-positive tumors.

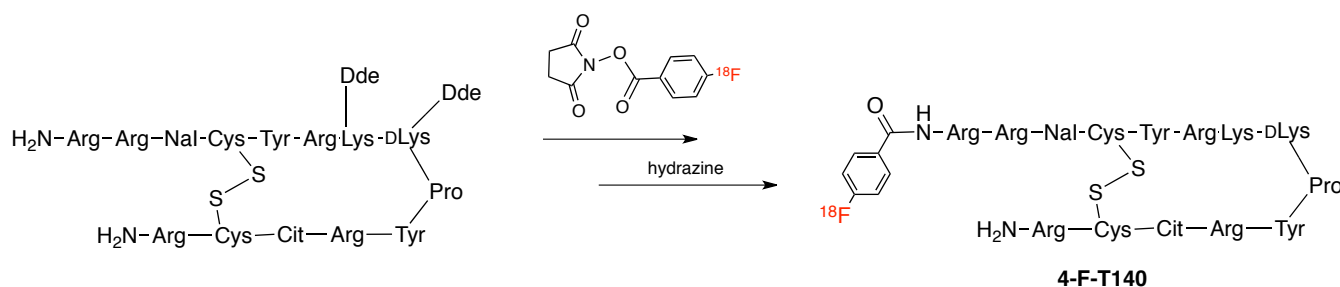


Figure I-12

FC131 was also labeled with  $^{18}\text{F}$  (Figure I-13).<sup>46</sup> The *in vivo* biodistribution of such agent showed high accumulation of radioactivity in the elimination tissues and a rapid clearance. It appears to be a suitable platform for the potential visualization of CXCR4 *in vivo*, but the little evidence of uptake in tissues that endogenously express CXCR4 suggests a low level of specific binding. Structural modifications are required to improve the performance of the tracer.

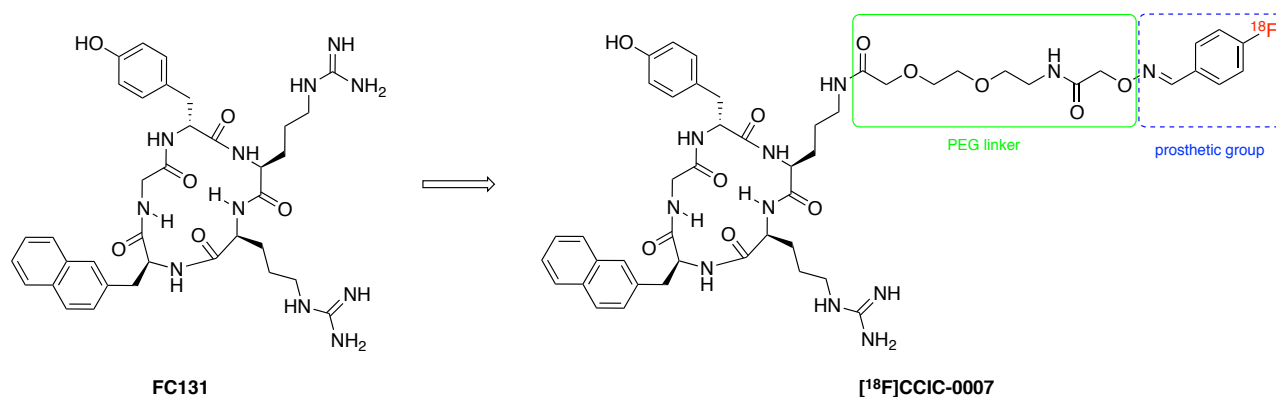


Figure I-13

### I.2.1.3.2 Introduction of a radiometal via a bifunctional chelating agent

The most reliable method of linking a metal ion to the biomolecule is to use a bifunctional chelating agent (BFCA) which is a small molecule containing two different moieties (Figure I-14).<sup>48</sup> One moiety is a ligand capable of strongly coordinating the chosen metal ion. The other moiety is a functional group able to react and form a stable covalent bond with the carrier. Additionally, an appropriate spacer that separates the chelating moiety and the bioactive fragment can also be used. The nature of such spacers is variable, and generally they are used as pharmacokinetic modifiers. For example, a polyethyleneglycol (PEG) chain will increase water solubility, whereas an aliphatic chain will increase lipophilicity.

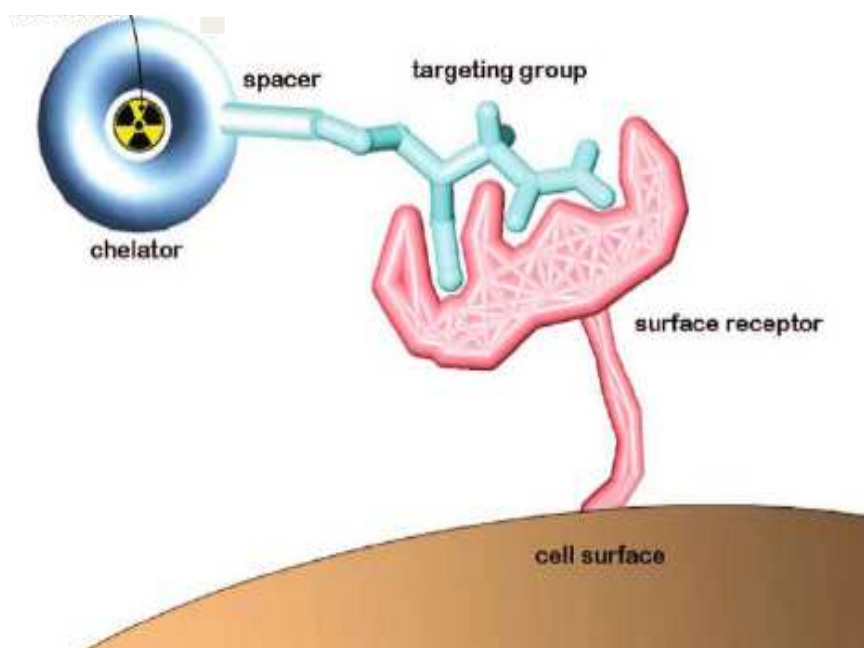


Figure I-14: Schematic representation of a chelator-based radiotracer connected to a surface receptor.<sup>48</sup>

There are several fundamental criteria that have to be taken in consideration to design a BFCA. Both formation of thermodynamically and kinetically inert metal chelate and stable covalent attachment of the chelator moiety to the biomolecule are essential parameters to create an efficient radiopharmaceutical.

#### I.2.1.3.2.1 Radiochelate choice

The choice of the right chelator is a crucial point in the stability of a final conjugate and depends on the metal ion to be complexed. Transmetallation by endogenous metal ions ( $\text{Ca}^{2+}$  or  $\text{Zn}^{2+}$  for example)<sup>49</sup> or transchelation by endogenous ligands, such as transferrin,<sup>50,51</sup> are phenomena that occur *in vivo*. Loss or dissociation of the radionuclide results in toxicity but also in poor image quality. An adapted chelator should prevent radiometal release in the organism by complying with the nature and oxidation state of the given radionuclide.<sup>52</sup>

Thus, several parameters have to be considered.<sup>53</sup> Cavity size must accommodate the ionic radius of the radiometal for an optimal encapsulation. To provide the appropriate number of donor binding groups and complete the coordination sphere of the metal, coordinating pendant arms can also be added. The stability of the metal complex is highly dependent of the coordination properties of the pendant arms and the charge of the complex relies on both nature and number of arms. The radiometals are diverse in their properties and coordination chemistry, so there is no bifunctional chelate suitable for all radionuclides.

## I.2.1.3.2.1.1 Chelators

A wide range of metal-chelating molecules based on acyclic and cyclic polyamines have been synthesized and studied (Figure I-15).<sup>48,49,54-59</sup> Acyclic ligands usually require mild conditions for complexation but they are more inclined to release the metal ion *in vivo*. Macrocyclic chelators provide metal complexes that are thermodynamically more stable and kinetically more inert than the complexes with their acyclic analogues. This increased stability has been called macrocyclic effect.

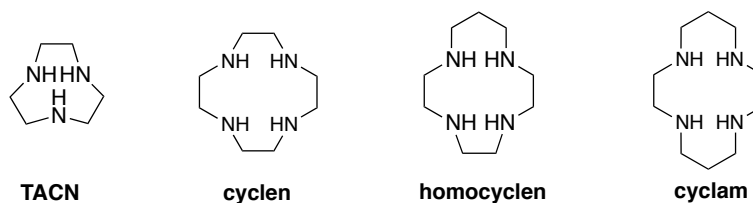


Figure I-15: Examples of polyazacycloalkanes.<sup>48</sup>

Polyamines and their derivatives bearing additional coordinating groups have been of great interest in the development of BFCAs. The use of polyaminocarboxylates such as EDTA or DTPA and macrocyclic chelators such as DOTA, NOTA, TRITA or TETA is particularly widespread in medicine (Figure I-16).<sup>55,60</sup> Acetate pendant arms provide strong binding donor groups that can complete the coordination sphere of the metal. A number of phosphonate<sup>61,62</sup> and phosphinate<sup>63-66</sup> pendant-armed polyazamacrocyclic chelators have also been synthesized. Introduction of methanephosphonic or methanephosphinic acid pendant arms has resulted in complexes having higher stability and selectivity towards cation.<sup>65,67</sup>

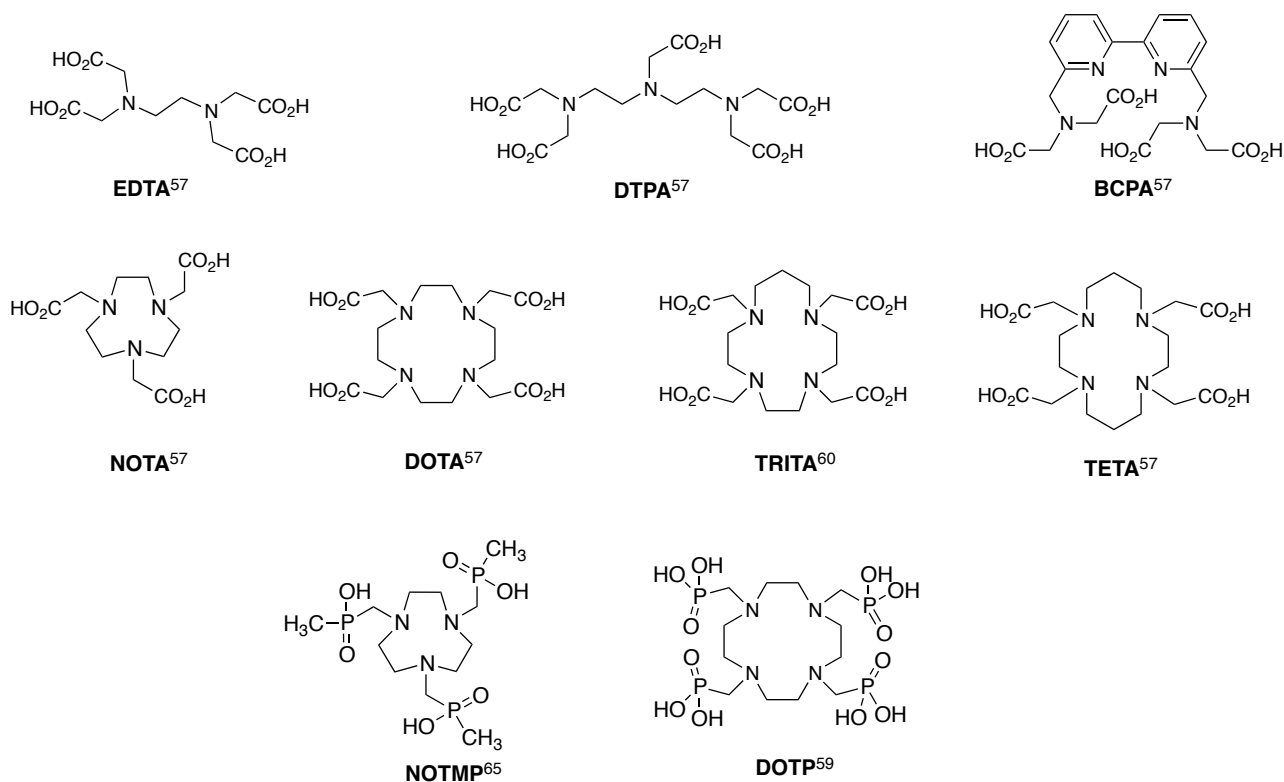


Figure I-16: Some examples of common linear and cyclic chelators.

Once selected, the chelate has to be functionalized to allow covalent attachment to the biomolecule. The introduction of the grafting function on the chelating core can be accomplished using well-established methods of selective *N*- and *C*-functionalization.

In most cases, attachment of the chelate-fragment to the biomolecule involves one of the coordinating acetate pendant arms, typically via formation of amide bonds with primary amines from lysine residues. However, the transformation of one of the carboxylic acid group into carboxamide has an influence on metal binding. This change in coordination number and donor character decreases *in vitro* and *in vivo* stability of the resulting complexes.<sup>68</sup>

Another approach consists in preparing an arm bearing both a chelating group and a grafting functionality.<sup>69-71</sup> This approach enables the coupling with the biomolecule without compromising the stability of the respective metal complexes (Figure I-17).

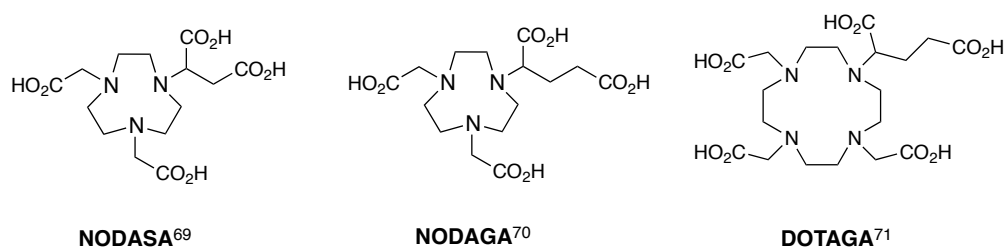


Figure I-17: Structures of azamacrocycles carrying a diacidic arm.

Alternatively, the functional group used to couple the vector can be introduced in the methylenic backbone of the chelator leaving all of the carboxylic pendant arms available for coordination to the metal.<sup>55,72,73</sup> This C-functionalization approach also avoids the multistep synthesis of a sophisticated pendant arm (Figure I-18).

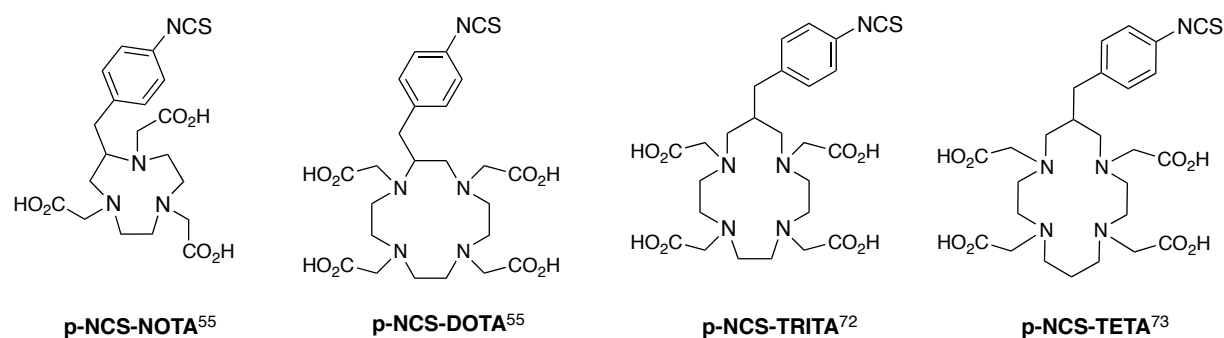


Figure I-18: C-functionalized polyazamacrocycles.

Acyclic and cyclic polyaminopolycarboxylates have been the most extensively evaluated BFCs for the labeling of peptides with trivalent and bivalent radiometals like  $\text{Ga}^{3+}$ ,  $\text{In}^{3+}$ , or  $\text{Cu}^{2+}$ . To select the adapted chelator to a metal, it is necessary to study its coordination properties, and its *in vivo* behavior. We will first concentrate on both gallium and indium. Then, we will study copper.

#### I.2.1.3.2.1.2 Gallium and indium

The group 13 elements Ga and In are post-transition metals. Their chemistry in aqueous media is exclusively limited to the oxidation state III.<sup>58</sup> In aqueous solution, the  $\text{M}^{3+}$  ions have a marked tendency to undergo hydrolysis, which is even pronounced for  $\text{Ga}^{3+}$ . At physiological pH, gallium forms essentially the gallate anion  $[\text{Ga}(\text{OH})_4]^-$ , while indium precipitates as the tris(hydroxide)  $[\text{In}(\text{OH})_3]$ .<sup>56</sup> When designing radiopharmaceuticals, it is of particular importance to obtain Ga and In complexes resistant to hydrolysis. These complexes must also have resistance towards transchelation reactions with transferrin, which is present in the plasma and involved in the receptor-mediated transport of iron into cells.<sup>50</sup> This is particularly relevant for Ga(III), that presents the highest affinity to transferrin due to the similarity of the coordination chemistry of trivalent gallium and iron.

As a classic hard acidic cation, Ga(III) is strongly bound to ligands featuring multiple anionic oxygen donor sites.<sup>48</sup> This small and highly charged cation of ionic radius 47-62 pm (coordination number CN = 4-6) is quite acidic with a pKa of 2.6 in its hydrated form. Typically chelators have been developed to sequester Ga(III) up to its maximum coordination number of 6 in a pseudo-octahedral geometry.

The significantly larger size of In(III) at 62-92 pm for CN 4-8, however, results in higher coordination numbers of 7 and even 8 in its complexes.<sup>48</sup> While still a hard acid, its higher pKa of 4.0 and faster water exchange rate also reflect its distinction from Ga(III). A slightly enhanced affinity for softer donor types compared with Ga(III) can be noted in In(III) coordination chemistry.

The labeling of peptides with  $^{67}\text{Ga}/^{68}\text{Ga}$  has been performed using mainly DOTA or NOTA derivative.<sup>48</sup> The Ga(III)-NOTA complex has an exquisite stability among gallium complexes. Moreover, the kinetic complexation of Ga(III) is faster for NOTA than for DOTA, requiring longer reaction times and higher temperature with  $^{67}\text{Ga}/^{68}\text{Ga}$  using DOTA-like chelators. The high stability constant of Ga(III)-NOTA complexes and their kinetics reflect a better fitting of the NOTA cavity size with the size of the Ga(III) ion and the involvement of all pendant arms in the coordination to the metal. To keep the possibility of a N3O3-hexadentate coordination, after linkage of the biomolecule, NOTA-like chelators containing a diacid pendant arm, such as NODASA and NODAGA have been designed and synthesized (Figure I-17). Notni *et al* recently developed a TACN-based bifunctional phosphinate ligand that allows instantaneous labeling at 60 °C and low pH (Figure I-19).<sup>63</sup>

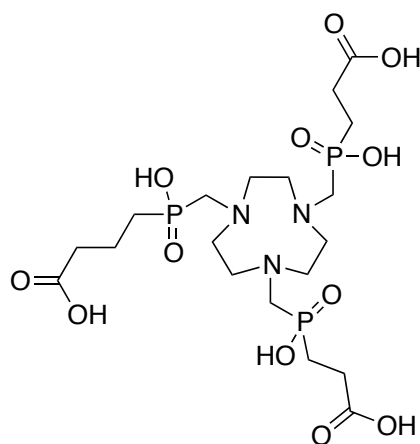


Figure I-19: Structure of a TACN-based bifunctional phosphinate ligand.<sup>63</sup>

Unlike Ga(III), the coordination requirements of In(III) are not fulfilled by NOTA-like chelators (Figure I-20).<sup>48</sup> DTPA and DOTA derivatives have been used for  $^{111}\text{In}$  labeling. DTPA is potentially octadentate and forms complexes of higher stability with In(III) compared to Ga(III). The valuable octadentate chelator DOTA has also been shown to form a robust complex with In(III). No X-ray structural data are yet available for the parent In-DOTA complex. There are, however, several reported structures of its derivatives, such as the In(III) complex of the *p*-aminoanilide analogue (DOTA-AA) (Figure I-20).



Figure I-20: Structures of Ga and In complexes with polyazacycloalcanes.<sup>74</sup>

#### I.2.1.3.2.1.3 Copper

Copper has a unique combination of diagnostic ( $^{60}\text{Cu}$ ,  $^{61}\text{Cu}$ ,  $^{62}\text{Cu}$  and  $^{64}\text{Cu}$ ) and therapeutic radionuclides ( $^{64/67}\text{Cu}$ ).<sup>75</sup> The aqueous coordination chemistry of copper is limited to its three accessible oxidation states (I-III). Cu(III), is relatively rare and difficult to attain without the use of strong  $\pi$ -donating ligands. The lowest oxidation state, Cu(I), has a diamagnetic  $d^{10}$  configuration and forms labile complexes. Cu(II) is generally less labile toward ligand exchange compared with Cu(I) and is the most widely used for radiopharmaceuticals.<sup>48</sup> It is a  $d^9$  metal of borderline softness, which favors amines, imines, and bidentate ligands like bipyridine. Coordination numbers ranging from 4 to 6 were found with geometries approximating square planar, square pyramidal, trigonal bipyramidal, and octahedral. Full envelopment of Cu(II) in its maximum six coordinate mode is favored. As a result, hexadentate chelators have become the most investigated in radiocopper chemistry. Jahn-Teller distortions in six-coordinate Cu(II) complexes are often observed as an axial elongation or a tetragonal compression. In Figure I-21 are represented some structures of Cu(II) complexes with hexadentate chelators. Among the numerous possible geometries, Cu(II) complex can be a distorted trigonal prism (Cu-NOTA), a tetragonally distorted octahedron (Cu-TE2P) or a distorted octahedron (Cu-CB-TE2A).

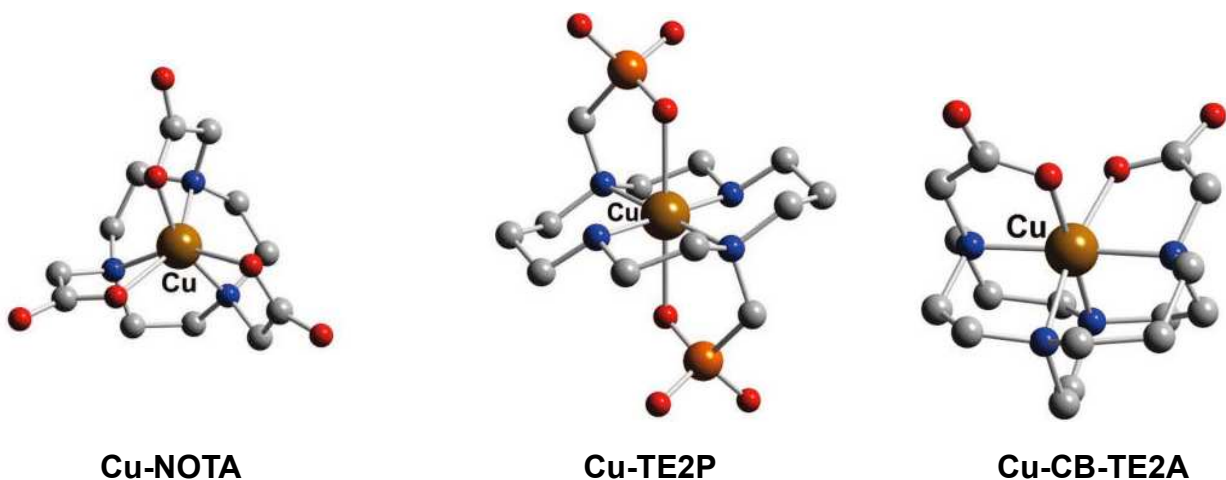


Figure I-21: Structures of Cu(II) complexes with polyazacycloalcanes.<sup>74</sup>



Copper is an essential trace element that plays a critical role in the body, and as such, under physiological conditions intracellular copper availability is restricted.<sup>48</sup> The natural accumulation of  $\text{Cu}^{2+}$  proceeds via assimilation of the naturally occurring proteins, albumin and transcuprin, in the blood. It is then carried to the liver and internalized. Copper is then sequestered for long-term storage in the form of  $\text{Cu}^+$  and  $\text{Cu}^{2+}$  ions, excreted or incorporated into metalloenzymes. Superoxide dismutase (SOD) is a homodimeric enzyme found widely distributed in the cytosol of eukaryotic cells.<sup>75</sup> This enzyme is especially abundant in the liver, kidneys and red blood cells. Each subunit of the enzyme contains one copper and one zinc atom. The SOD role in the body is to provide a defense mechanism against potential toxicity of oxygen radicals by catalyzing the disproportionation of the superoxide ion to hydrogen peroxide and oxygen. It has also been implicated in the breakdown of copper complexes *in vivo*.

To resume,  $^{64}\text{Cu}(\text{II})$  complexes must be resistant towards transchelation to proteins involved in the transport and storage of copper, and must not undergo reduction to  $\text{Cu}(\text{I})$ , as it will increase the probability of releasing the radiometal *in vivo*.

A wide range of bi-functional ligands has been investigated for  $^{64/67}\text{Cu}^{2+}$ . Typically they are based on complexing agents such as cyclic/acyclic polyaminocarboxylate and polyaminophosphonate of hexaaza-cage.<sup>48,75,76</sup>

DOTA and TETA have been largely used as bifunctional chelators for  $^{64}\text{Cu}$ -labeling of peptides, although they are not ideal chelators for  $\text{Cu}(\text{II})$ , as well documented by the *in vivo* instability of their complexes. *In vivo* experiments in rat models have shown that both  $^{64}\text{Cu}$ -DOTA and  $^{64}\text{Cu}$ -TETA undergo transchelation of  $^{64}\text{Cu}(\text{II})$  to liver and blood proteins, with this behavior being more pronounced in the case of  $^{64}\text{Cu}$ -DOTA.<sup>77</sup> NOTA has also a good affinity for divalent copper, and the corresponding  $\text{Cu}(\text{II})$ -NOTA complex presents a stability constant similar to those with DOTA and TETA.<sup>75</sup> NOTA-based bifunctional chelators allowed the  $^{64}\text{Cu}$ -labeling of different bioactive peptides with very high specific activity and under mild reaction conditions.<sup>78</sup> The resulting metallo-peptide has shown a better biodistribution profile than those labeled with  $^{64}\text{Cu}$  using DOTA or TETA derivatives as BFCs, pointing out the best properties of NOTA-derivatives to stabilize the metal *in vivo*.<sup>48</sup>

Investigations have been performed on reinforced systems, aiming to introduce novel classes of bifunctional chelators suited for *in vitro* and *in vivo* stabilization of  $\text{Cu}(\text{II})$  complexes. Such constrained azamacrocycles are represented in Figure I-22. Metabolic studies in rat models showed that  $^{64}\text{Cu}$ -CB-DO2A and  $^{64}\text{Cu}$ -CB-TE2A presented an increased *in vivo* stability compared with  $^{64}\text{Cu}$ -DOTA and  $^{64}\text{Cu}$ -TETA complexes, confirming that the introduction of the ethylenic bridge enhances the stability of these macrocyclic complexes.<sup>52,79,80</sup> This short two-carbon cross-bridge imparts additional rigidity and topological constraints. However, the kinetics of  $\text{Cu}(\text{II})$  complexation with CB-TE2A is rather slow, and the formation of  $^{64}\text{Cu}$ -CB-TE2A requires harsh

radiolabeling conditions that may induce damage to some biomolecules. The same behavior was observed for PCB-TE2A.<sup>81</sup> A new class of cross-bridged cyclam macrocycles having methanephosphonic acid pendant arms has been developed.<sup>61</sup> These compounds readily formed copper(II) complexes and the <sup>64</sup>Cu-labeled chelates demonstrated promising kinetic inertness *in vivo*. It was also found that complexation in methanol was already complete in less than 5 min at ambient temperature, which is convenient for biomolecules labeling. The synthesis of new constrained ligands was developed such as C3B-DO2A and CB-TR2A and it has been shown that the metallation can be also performed at room temperature.<sup>82</sup>

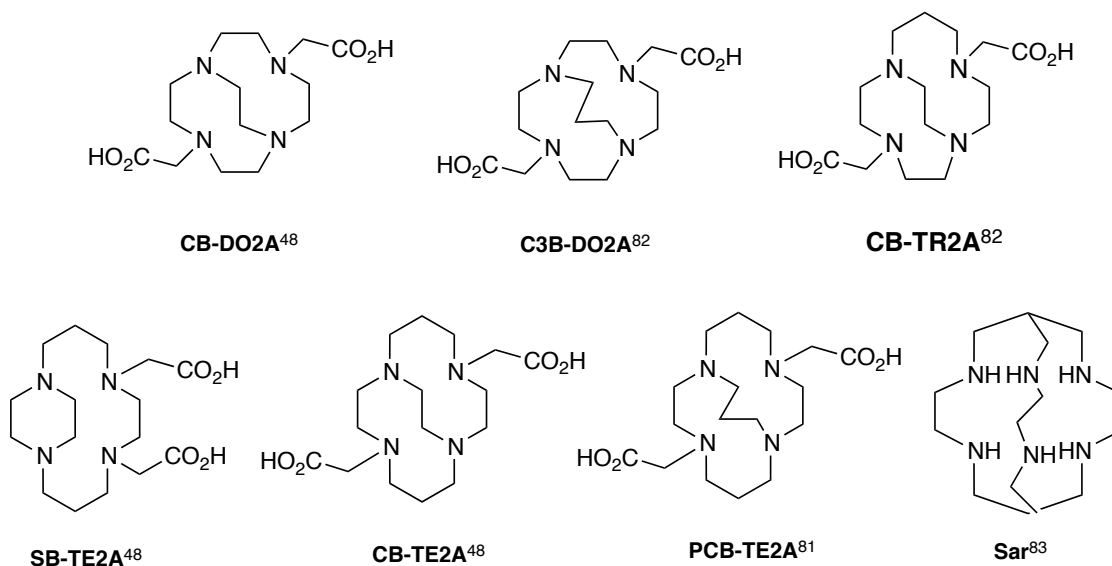


Figure I-22: Examples of constrained polyazamacrocycles.

Research for finding bifunctional chelators that efficiently bind to Cu(II) under mild reaction conditions pointed out the best properties of cryptand macrocyclic ligands of the hexaaminemacrobicyclic type, so-called “sarcophagines” (Sar).<sup>48,83,84</sup> These Sar ligands encapsulate the Cu(II) ion forming hexacoordinated and octahedral Cu(II) complexes with thermodynamic stability constant as high as the ones found with DOTA and TETA derivatives. At room temperature, the Sar ligand binds to <sup>64</sup>Cu(II) with fast complexation kinetics, at remarkably low concentrations over a pH range of 4-9. The resulting complexes show a high kinetic inertness, as shown by negligible *in vitro* transchelation.

#### I.2.1.3.2.2 Introduction of a grafting function

Once the most appropriate chelate has been selected for the desired application, a reactive group or grafting function has to be introduced on its core. Examples of reactive functionalities used to link chelates to vectors include isothiocyanates, carboxylic acids as active esters, anhydrides and maleimides.<sup>49,85,86</sup> These reactive groups can react with nucleophilic sites (amino, thiol or hydroxy groups) present on the biomolecule.

Carboxylic group is of great interest, since it can be easily activated to allow attack by an amino group, usually from a lysine residue, present in an antibody or a peptide. Among the

numerous possibilities, the preparation of anhydrides and reactive esters, derived for example from *N*-hydrosuccinimide, are highly used because they allow high selectivity and mild reaction conditions.<sup>87</sup> Isothiocyanate is another reactive group, which is widely exploited in the conjugation of carriers containing amino group, since it forms a stable thiourea bond. Concerning thiols residues on the biomolecule, they can easily and specifically react with maleimide under mild conditions.

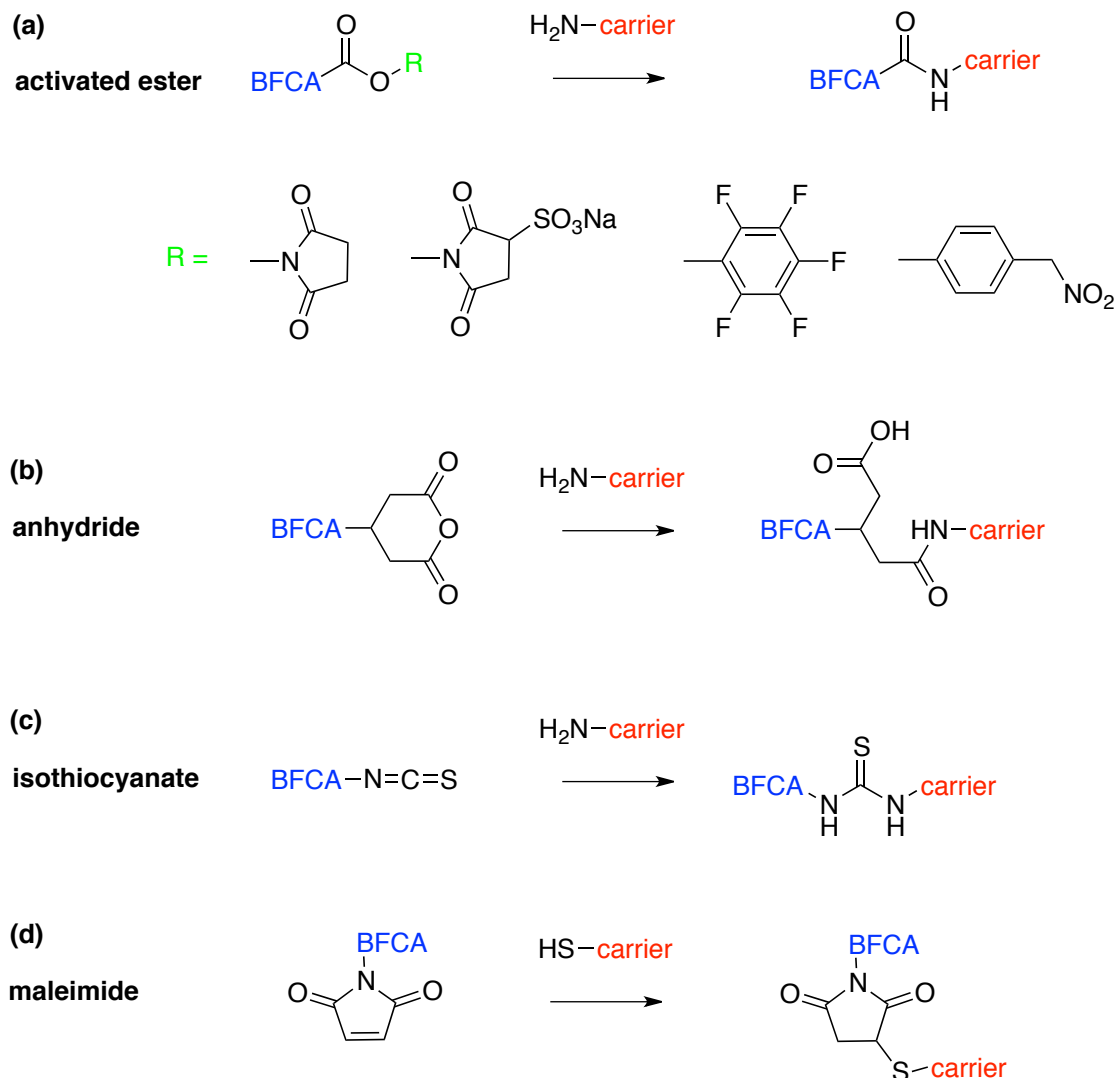


Figure I-23: Reaction scheme for BFCA-peptide conjugation.<sup>85</sup>

Click chemistry involving azides and alkynes is another bioconjugation strategy that is increasingly widespread.<sup>88-91</sup> The optimal reaction conditions for conjugation include mild aqueous conditions close to physiological pH, short reaction times and minimal purification.

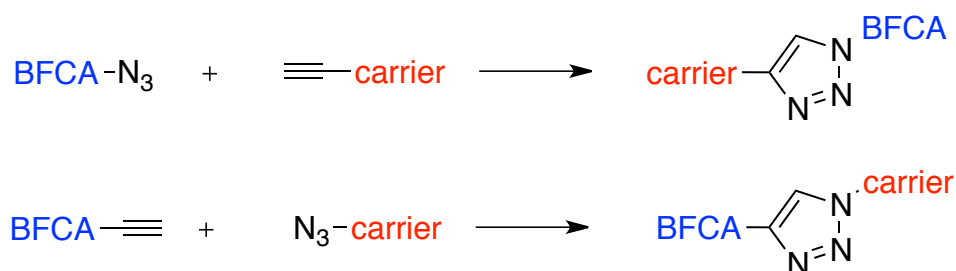


Figure I-24: Schematic representation of a « click chemistry » approach.<sup>90</sup>

### I.2.1.3.2.3 Examples of targeting CXCR4 radiopharmaceutical based on radiometal

Among all the common BFCAs available for  $^{99m}\text{Tc}$ , an acetylmercapto-derivative (so-called MAS<sub>3</sub>) was the only one being connected to a CXCR4 ligand. Thus, SDF-1 was connected to a  $^{99m}\text{Tc}$ -MAS moiety via a solid-phase prelabeling technique (Figure I-25).<sup>92,93</sup> It was evaluated as an imaging agent for myocardial infarction. Preliminary studies on rats showed a high specificity on endogenously and expressing cells. The relatively fast clearance via renal excretions also resulted in a relatively low background tissue retention. However, a high dose of  $^{99m}\text{Tc}$ -SDF-1 was required to assess the accumulation in the myocardium. In addition, its poor imaging characteristics *in vivo* limit its routine use.

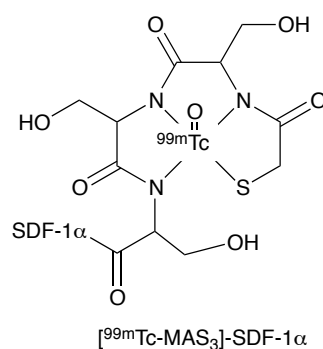


Figure I-25

Hanaoka *et al* studied a DTPA-based derivative of T140 metallated with  $^{111}\text{In}$ .<sup>94,95</sup> The complex exhibited a low affinity toward the receptor and a high accumulation of the radioactivity in the liver, kidneys and spleen. Due to its accumulation in nontarget organs,  $^{111}\text{In}$ -DTPA-Ac-TZ14011 may be unavailable as a radiopharmaceutical for screening small tumors, particularly in the kidneys and their surroundings.

The groups of Hennrich and Jacobson developed T140-based imaging agent carrying respectively one  $^{68}\text{Ga}$ -DOTA (Figure I-26A) or two  $^{64}\text{Cu}$ -DOTA (Figure I-26B) moieties on different free lysine residues.<sup>96,97</sup> Introduction of macrocycles into T140 didn't change its high binding affinity to CXCR4 or its high inhibition potency. *In vivo* studies were performed on the  $^{64}\text{Cu}$  complexes. Tumor CXCR4 expression could be imaged but with high uptakes in blood and metabolic organs due to red blood cells binding.

Jacobson *et al* developed two new derivatives of T140, DOTA-NFB and NOTA-NFB possessing an unique chelator on the *N*-terminus (Figure I-26C).<sup>98</sup> Both agents were able to bind to CXCR4 but not to red blood cells and could be injected in lower mass.

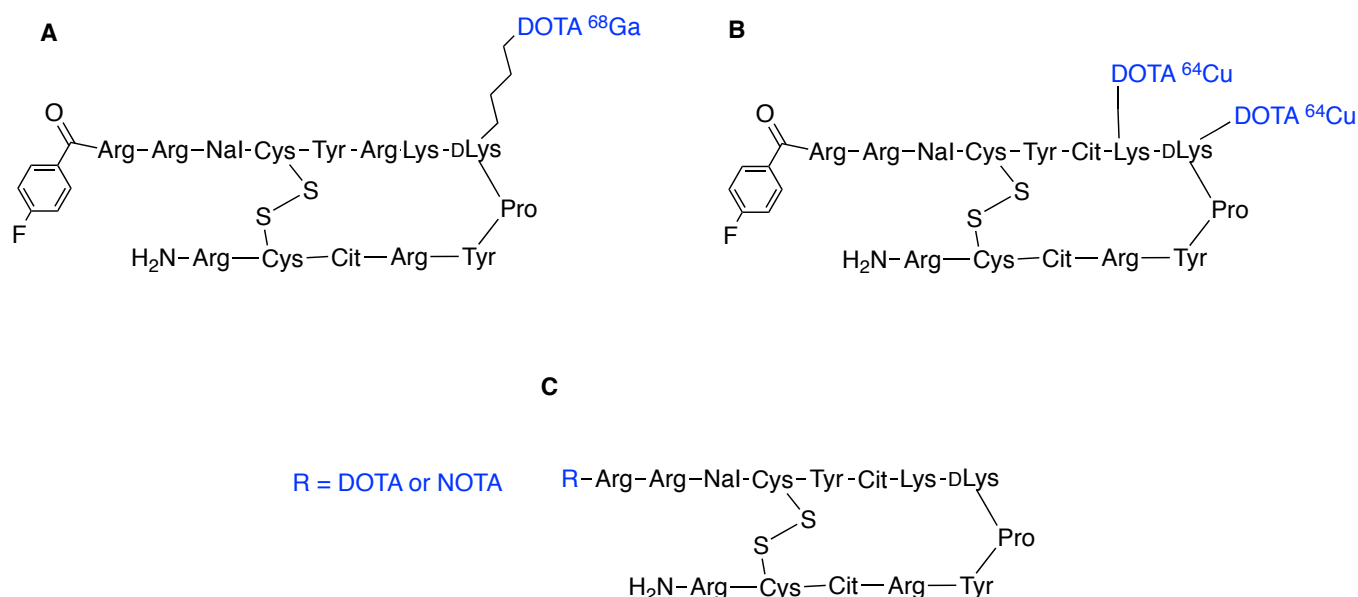


Figure I-26: Examples of T140 analogues associated with a polyazamacrocycle.

However in all previous T140-based radiotracers, high and long-lasting uptake was observed in liver and kidneys. Labeling with <sup>68</sup>Ga gave similar results.<sup>97</sup>

The addition of a bulky group such as DOTA on the small cyclic pentapeptide FC131 resulted in diminution of the binding affinity compared to FC131 (Figure I-27).<sup>99</sup> However, the molecule metallated with <sup>68</sup>Ga showed higher affinity than the non-metallated one due to a higher overall charge and a different charge distribution.

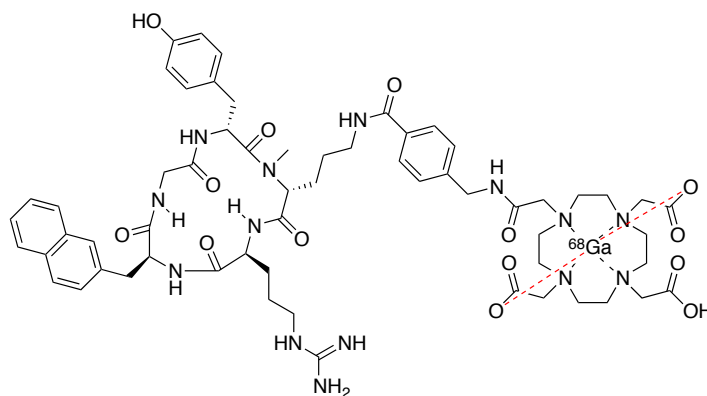


Figure I-27

To compensate the significant reduction in binding affinity due to the presence of DOTA, dimers with C<sub>2</sub> symmetry were developed (Figure I-28).<sup>100</sup> The resulting dimer displayed a lower affinity, which implied that the additional peptide hindered the binding. First *in vivo* studies demonstrated a high liver uptake making such dimers unsuitable for the detection of primary tumors or metastases, particularly in the liver and the surrounding organs.

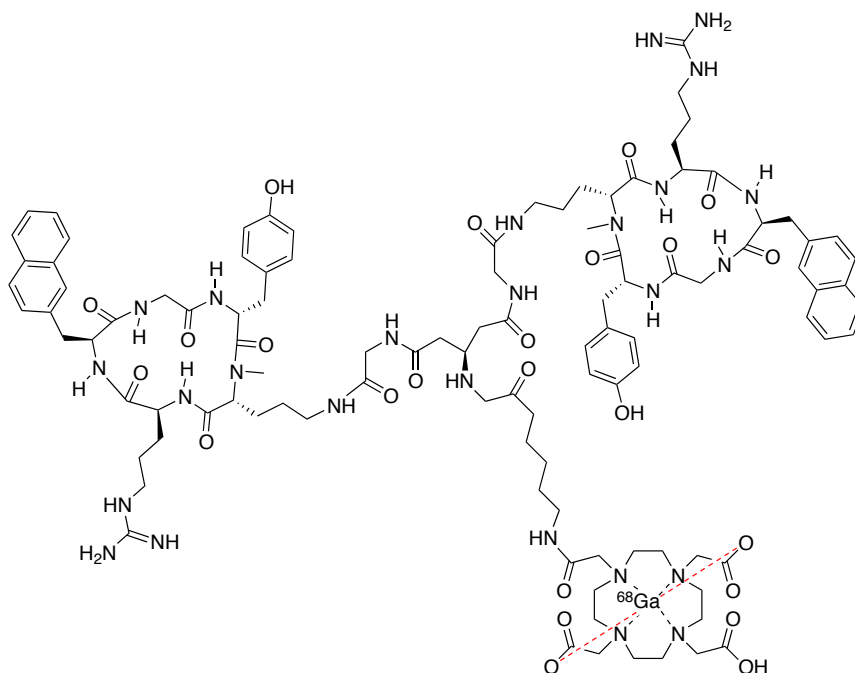


Figure I-28

In all previous examples, abnormal accumulation of radioactivity is observed in healthy tissues. As a matter of fact, the macrocycles (DOTA, NOTA) were not chosen to optimize metal coordination, but to provide maximum flexibility to the system with respect to future diverse applicability with other radiometals. Future generation of radiotracers should be based on adapted chelators that form thermodynamically and kinetically more inert complexes.

#### I.2.1.3.2.4 Particular case of AMD3100 and AMD3465

Small molecules such as AMD3100 and AMD3465 were directly radiolabeled with  $^{64}\text{Cu}$  and  $^{99\text{m}}\text{Tc}$  (Figure I-29).<sup>101-105</sup> This approach used the ability of cyclams to form stable complexes with transition metals to obtain radiotracers that possess an enhanced affinity toward the receptor due to the presence of the cation.

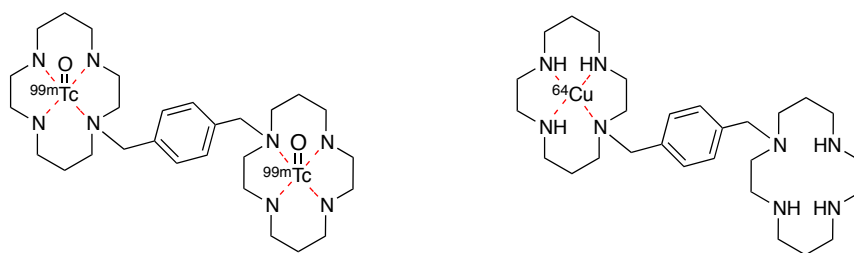


Figure I-29

The resulting tracers based on AMD3100 are suitable for PET and SPECT imaging of CXCR4-expressing tumors even though considerable uptake was observed in the liver and lymphoid organs, probably due to target-specific binding or to the presence of metastases.<sup>101-104</sup> CXCR4 is expressed in the liver and kidneys, and reduced uptake has been observed in blocking studies in these tissues, suggesting that some of the uptake seen is receptor-mediated. Another possible explanation could

be the thermodynamic instability of the copper complex resulting in a dissociation phenomenon and metal release in the organism.

$^{64}\text{Cu}$ -AMD3465 has the highest target selectivity reported for this class of agents to date.<sup>105</sup> Even though  $^{64}\text{Cu}$ -AMD3465 has improved affinity and kinetics, compared with  $^{64}\text{Cu}$ -AMD3100, considerable uptake in the liver and kidneys was also observed. Some of this accumulation could also be attributed to possible transchelation of  $^{64}\text{Cu}$  from  $^{64}\text{Cu}$ -AMD3465 to plasma proteins.

## 1.2.2 Optical imaging

The visualization of cells and tissues using light is one of the most informative and facile approaches in basic research and medical diagnostic imaging. Through the use of fluorescence microscopy, researchers have been able to observe molecular events in real time in living cells or *ex vivo* tissues samples. A number of macroscopic optical imaging techniques enable non-invasive, repetitive, whole body imaging of living small animals, using sizable field of view. Among the macroscopic optical imaging techniques, fluorescence imaging has been particularly used.

### 1.2.2.1 Fluorescence imaging

Following the administration of a fluorescent imaging agent, an excitation light of appropriate wavelength is used to illuminate the subject. This leads to excitation of the fluorophore and the subsequent emission of light that is detected via a camera and converted to an image detailing the location of emitted light (Figure I-30).

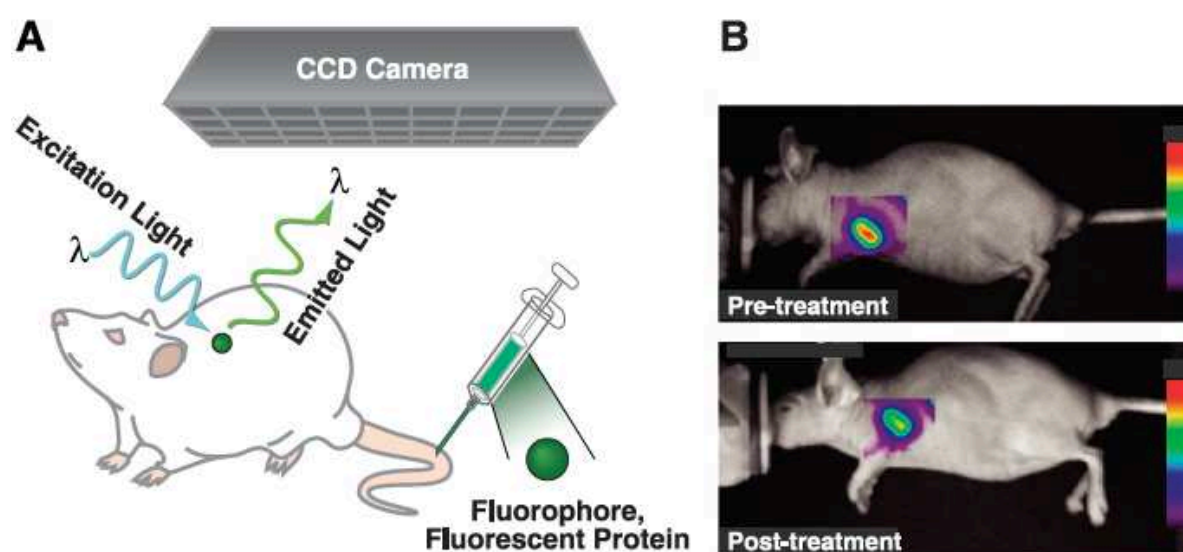


Figure I-30: Optical fluorescence molecular imaging.<sup>1</sup>

This technique has a number of limitations that need to be considered including its limited depth of penetration (<1 cm). Visualization through the skin is indeed restricted to superficial tissues such as the breast. It is however a useful tool for preclinical evaluation of imaging agents and for intraoperative applications where depth of penetration is not an issue. Furthermore, fluorescence imaging suffers from issues associated with tissues autofluorescence that decreases the sensitivity of the technique. Among the optical imaging technologies, near-infrared (NIR) fluorescence imaging within the wavelength range of 700-1000 nm has been dedicated immense attention. The low absorption and autofluorescence from organisms and tissues in the NIR spectral range minimize background interference, improve tissue depth penetration, image sensitively and noninvasively.<sup>106</sup>

Fluorescence imaging typically involves the use of targeting fluorescent-tagged molecules.<sup>107,108</sup> Small synthetic fluorophores form the bulk of the commercially available fluorescent molecules. A simple parameter for making meaningful comparisons between different fluorescent molecules is the product of the extinction coefficient and the quantum yield ( $\epsilon \times \Phi$ ). This term is directly proportional to the brightness of the dye, accounting for both the amount of light absorbed and the quantum efficiency of the fluorophore. Accurate comparisons between dye molecules must include both of these parameters. Figure I-31 lists the major classes of biologically significant organic fluorophores. The fluorescent dye can also be a protein, quantum dots or lanthanides complexes.<sup>108</sup>



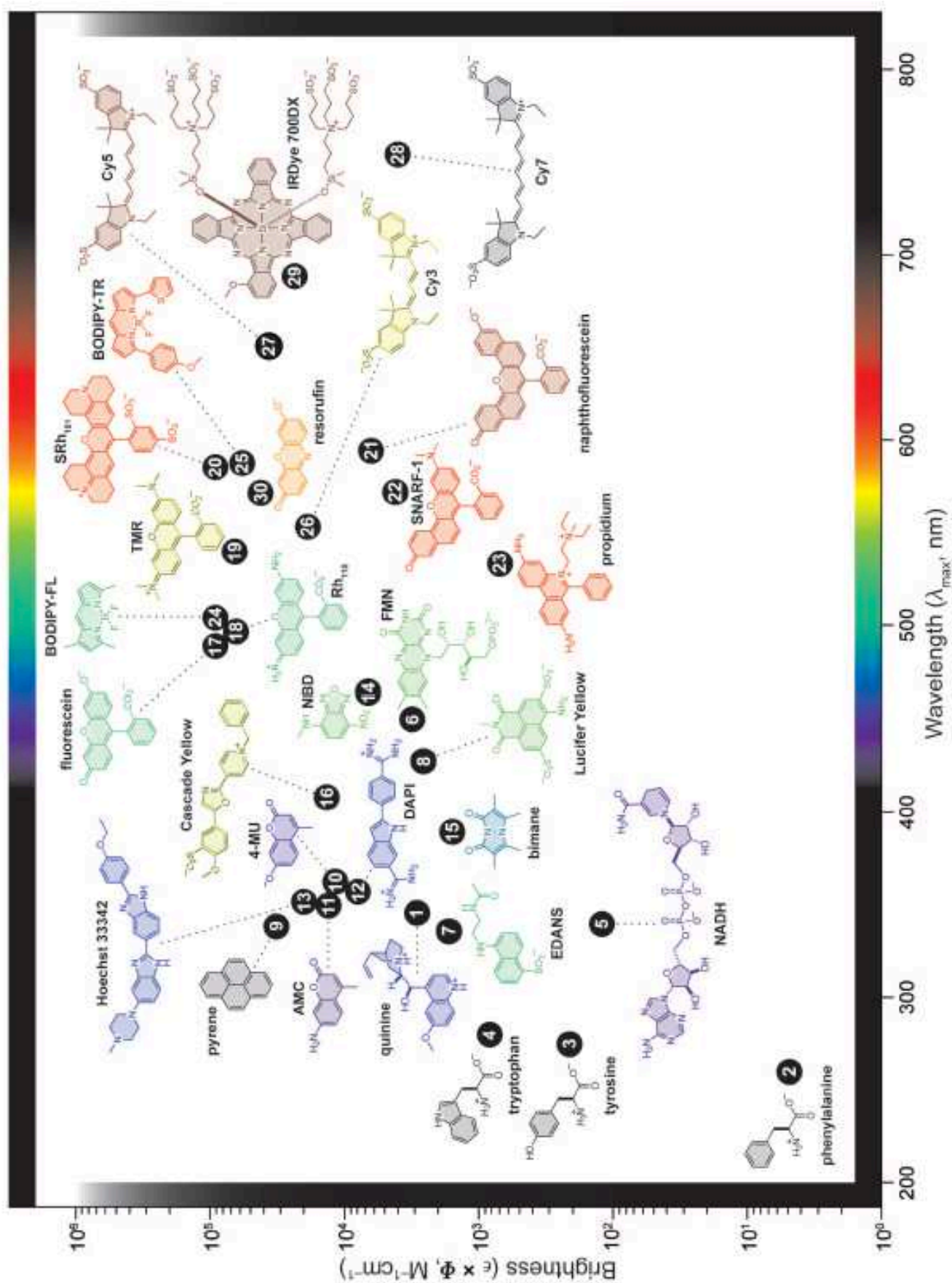


Figure I-31: Plot of fluorophore brightness vs the wavelength of maximum absorption for the major classes of organic fluorophores. The colour of the structure indicates its wavelength of maximum emission. For clarity, only the fluorophoric moiety is shown.<sup>107</sup>

### I.2.2.2 Examples of targeting CXCR4 optical agents

Several CXCR4-receptor probes have been prepared and applied for both *in vitro* and *in vivo*. Most of them are peptide-based. For example, SDF-1 was labeled with several fluorophores such as fluorescein<sup>109</sup> and cyanine<sup>110</sup>. The fluorescein-based agent was used to evaluate the mechanism of receptor activation by SDF-1. Studies of a NIR-fluorescent conjugate based on cyanine showed a high-selectivity, specificity and sensitivity *in vitro* and *in vivo* for tumor detection despite high background in the liver within the first 24 hours. Specific antagonists were also marked with a fluorescent dye: T140 was labeled with fluorescein,<sup>111,112</sup> and rhodamine.<sup>112,113</sup> Rhodamine was also introduced on FC131 and on the corresponding dimer.<sup>2</sup>

There are only two examples of small-molecule based antagonist carrying a fluorescent dye. Khan *et al* developed a rhodamine-conjugated azamacrocycle antagonist (Figure I-32).<sup>114</sup> The reinforced cyclam served as a vector for targeting CXCR4. The resulting agent didn't demonstrate any competition with anti-CXCR4 antibodies during binding competition studies. As expected, the addition of Cu in the macrocyclic cavity led to the enhancement of the binding affinity to CXCR4. Despite a significant quenching of the fluorescence, the signal was still efficient enough to be detected in biological system. However, the small molecule demonstrated a high non-specific accumulation in the cytoplasm.

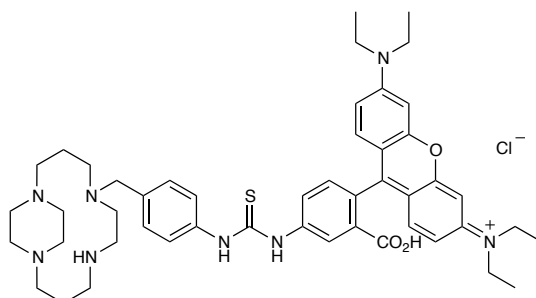


Figure I-32: Rhodamine conjugated azamacrocycle antagonist.<sup>114</sup>

Recently, a fluorescent AMD3100 analogue was synthesized by the group of Knight.<sup>115</sup> An anthracenyl moiety was introduced between two cyclams serving as a spacer and as a fluorescent tag (Figure I-33). They reported a significant reduction of the affinity to the receptor probably induced by the lipophilic character of the anthracenyl group. The binuclear Zn, Cu and Ni complexes were also investigated and the most promising results were obtained with the biszinc complexes showing a higher specificity and a reduced cytotoxicity compared to the free ligand.

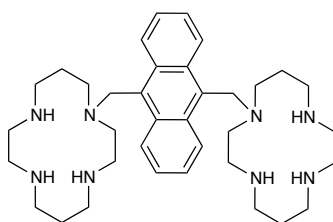


Figure I-33: Anthracenyl derivative of AMD3100.

### 1.2.3 Bimodality

The roles of imaging in disease diagnosis and treatment monitoring continue to increase because of advances in imaging technologies and concomitant improvements in detection sensitivity, spatial resolution, and quantitative information. In a perfect world, a single imaging method could furnish anatomic, physiologic, and molecular information with high sensitivity and specificity. However, none of the current imaging methods used in humans provides comprehensive medical imaging. To overcome the individual limitations of different imaging methods, taking advantage of their individual strengths, they can be combined in so-called multimodal imaging approaches.<sup>116</sup> To appreciate the potential benefits of combining optical and nuclear modalities, we have tabulated the main characteristics of each technique (Table I-2).

<b>Imaging technique</b>	<b>PET</b>	<b>SPECT</b>	<b>Fluorescence imaging</b>
Source	$\beta^+$ rays	$\gamma$ rays	Visible light or NIR
Spatial resolution	1-2 mm ( <i>in vitro</i> ) 5-7 mm ( <i>in vivo</i> )	1-2 mm ( <i>in vitro</i> ) 8-10 mm ( <i>in vivo</i> )	2-3 mm ( <i>in vivo</i> )
Depth	No limit	No limit	< 1cm
Sensitivity	pM	nM to pM	nM to pM
Amount of molecular probe used	Nanograms	Nanograms	Micrograms to milligrams

Table I-2: Characteristics of imaging modalities.<sup>1</sup>

Co-injection of two different imaging agents (one for each modality) that are distributed differently in the body imparts an increasing potential for toxicity. To link different applications, it is desirable to use one-and-the-same imaging agent, functionalized with multiple diagnostic labels. This approach requires the preparation of one multifunctional molecule so-called MOMIA (MOmonomolecular Multimodality Imaging Agent). This unique structural core ensures the same biodistribution and enables the fusion of contrast data with high spatial precision.

A potential application for such multimodal compounds is an integrated use of preoperative diagnostics and surgical planning (radioactivity-based) with intraoperative surgical image guidance (fluorescence-based) to the predefined lesion location.<sup>117,118</sup> This combination benefits from the high sensitivity of nuclear imaging and the high spatial resolution of fluorescence imaging.

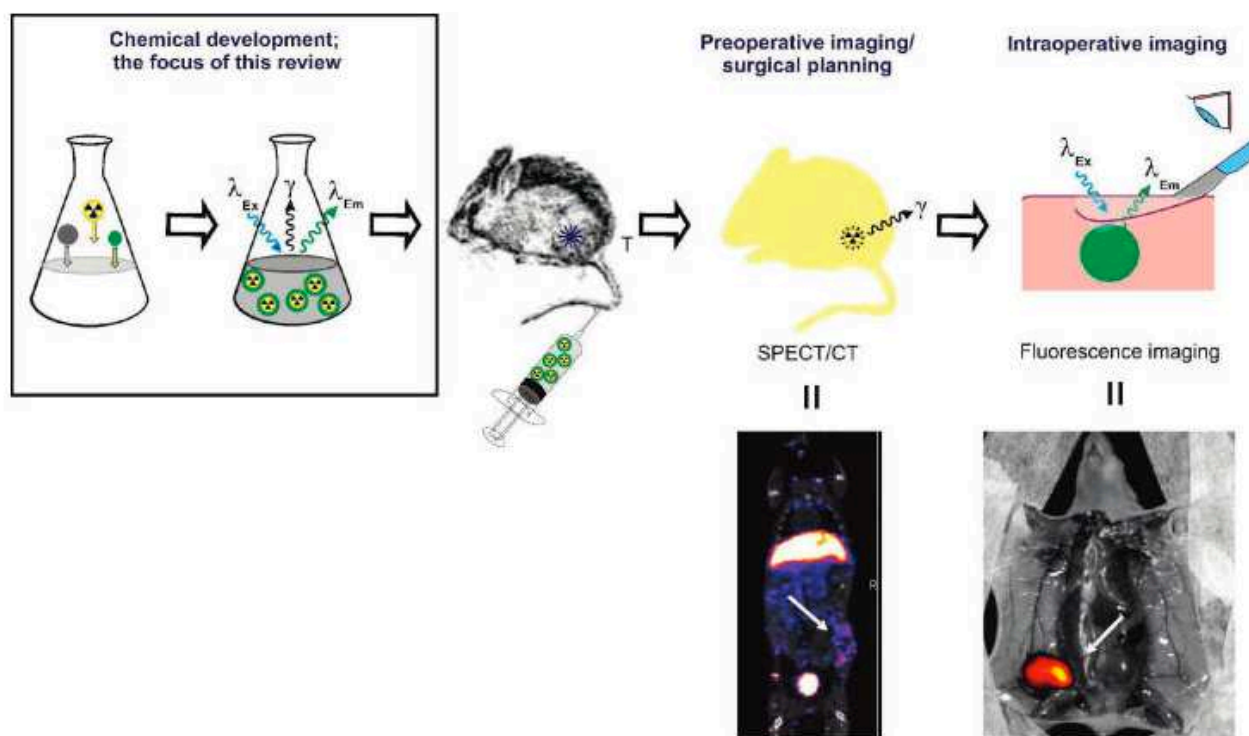


Figure I-34: Schematic overview of the development and potential use of multimodal tumor-targeting peptides.<sup>119</sup>

Kuil *et al* developed several bimodal probes for imaging CXCR4 combining a DTPA moiety for  $^{111}\text{In}$  chelation and a cyanine. The first generation of such probe was based on substituted T140 and demonstrated affinity and specific binding to CXCR4 (Figure I-35A).<sup>120</sup> However, the bimodal moiety was close to the residues involved in crucial interactions with the receptor and the conjugation of the bimodal label reduced the affinity to the receptor. In the second generation, multimeric peptide dendrimers consisting of multiple peptides and one bimodal label were prepared (Figure I-35B).<sup>121</sup> By reducing the influence of the label with additional spacers, dimeric and tetrameric systems exhibited higher affinity and higher tumor uptake than the monomer but also higher non-specific uptake.

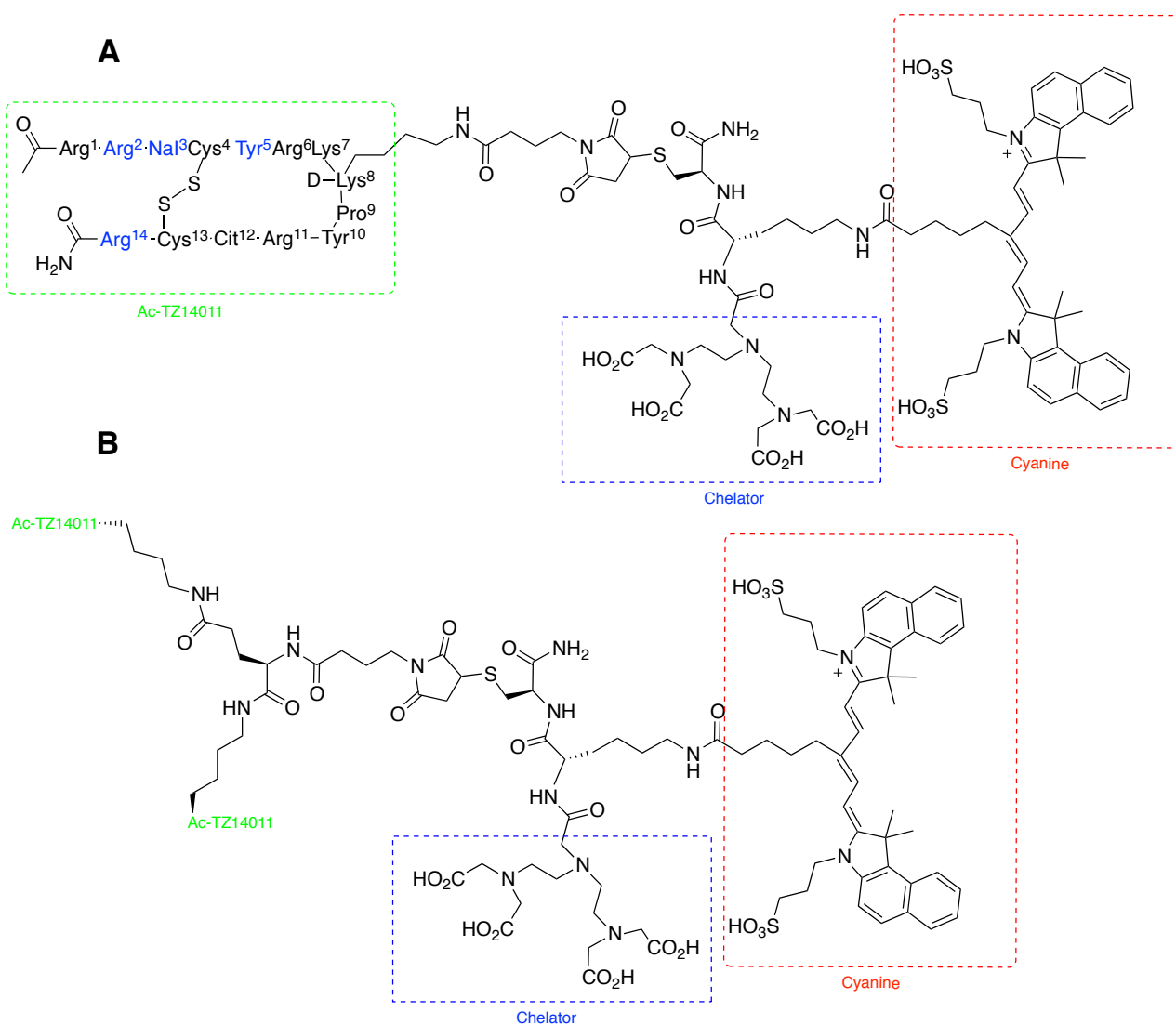


Figure I-35: Structure of bimodal probes. **A**: First generation, **B**: Dimer of the second generation.<sup>121</sup>

### I.3 Research Outlook

In this thesis work, the major focus was placed on the use of cyclic polyamines as valuable tools for the development of imaging agents. The ultimate goal of these new imaging agents is the non-invasive tumors localization and profiling of signal transduction pathways, (i) to get further insight into the molecular pathophysiology of cancer; (ii) to facilitate the design of diagnostic biomarkers; and (iii) to speed up the development of new therapeutics.

#### *First part*

The growing clinical demand for radiometals for diagnosis and therapy must be covered by the development of adapted chelators. In this effort, we were first interested in developing new macrocyclic scaffolds of high potential for copper and gallium chelation (Figure I-36). We first

focused on the development of a new powerful route towards selectively functionalized constrained homocyclens. The second part of my work was based on *C*-functionalized TACN and its derivatives. From a synthetic route previously developed in our group, we were able to facilitate and optimize the synthesis of selectively *N*- and *C*-functionalized TACN. By varying the grafting functions and the pendant coordinating arms, we prepared several really promising BFCAs for copper and gallium chelation. We also investigated the synthesis of new cryptands based on cyclen and we studied their properties towards copper complexation

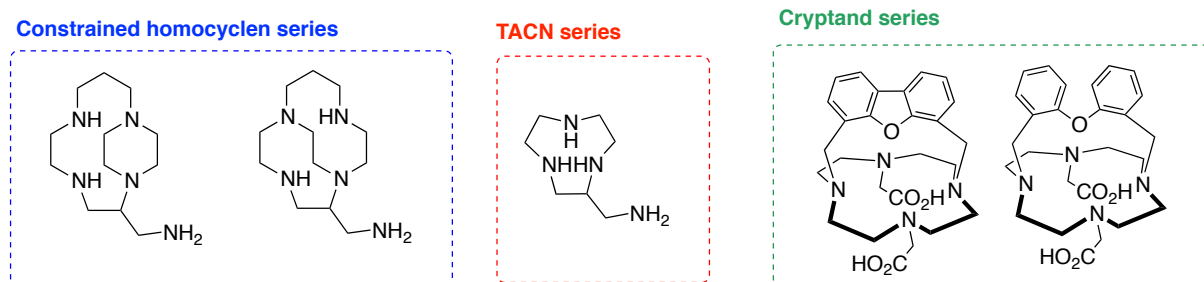


Figure I-36: New systems based on polyazamacrocycles.

### Second part

Using the gain expertise in macrocycles synthesis, we were interested in generating a new family of imaging agents based on AMD3100 and AMD3465 for targeting CXCR4 (Figure I-37). The access towards these agents first required the preparation of original building blocks in series AMD3100 and AMD3465. The conjugation of such platforms onto the appropriate probe enabled the synthesis of various systems for optical and nuclear imaging. Thus, we were able to introduce a Bodipy dye and several chelators adapted for gallium, copper and indium chelation.

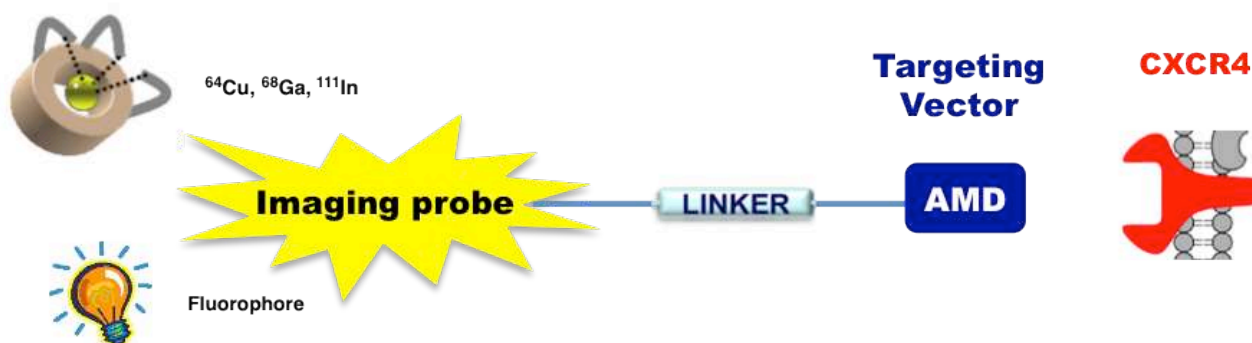


Figure I-37: Schematic representation of new imaging agents based on AMD3100 and AMD3465 for targeting CXCR4.



**II. Synthesis of new chelating agents based on polyazacycloalkanes, optimization of the coordination properties for copper and gallium chelation.**





## II. Synthesis of new chelating agents based on polyazacycloalkanes, optimization of the coordination properties for copper and gallium chelation.

Increasing use of  $^{64}\text{Cu}$  and other copper radioisotopes and  $^{68}\text{Ga}$  in nuclear medicine and in preclinical applications has produced a need for optimal bifunctional chelating agent with high stability against *in vivo* metal loss. Functionalized polyazacycloalkanes represent a class of chelating agents able to form stable complexes with a large variety of metal ions and particularly with copper. Structural factors, such as ligand rigidity, type of donor atoms and their disposition, have been shown to play significant roles in determining the binding features of polyazamacrocycles toward metal cations, and can be appropriately tuned in order to improve their selectivity. The development of new BFCAs based on macrocycles also requires the tuning of other properties such as the hydrophilic/hydrophobic character, and the addition of an appropriate linker to attach the macrocycle to the targeting vector. This can be accomplished using well-established methods of selective *N*- and *C*-functionalization. Many different synthetic methods for the selective *N*- or *C*-functionalization of polyazacycloalkanes have been reported, including high dilution techniques, use of metal cations as template, protection/deprotection sequences, functionalization on either nitrogen or carbon atoms and use of bisaminal intermediates. The *C*-functionalization approach enables the attachment of the targeting biomolecule to a carbon atom of the macrocyclic BFCA. Thus, all nitrogen atoms remain available for further introduction of pendant coordinating arms. This approach also avoids the multistep synthesis of a sophisticated pendant arm. These advantages prompted us to investigate new ways to prepare such compounds. In the first part, we will present the synthesis of new *C*-functionalized systems based on constrained homocyclen. The second part is based on *C*-functionalized TACN, *i.e.* optimization of the synthetic methodology previously developed in our group and synthesis of new promising bifunctional chelating agents.

The quest for new macrocyclic ligands continues to be an active field of research. The preparation of cryptands or other macropolycycles has attracted increasing interest owing to their suitability as frameworks for many receptor sites. Numerous studies on cage-type tetraazamacrobicycles have shown the influence of the cavity size on the selectivity for coordination of alkali, alkaline earth, and ammonium ions when such systems are used as selective receptors. Thus, they are an important class of molecules in coordination chemistry, with the coordination properties depending upon the design of the macrocyclic receptor. The preparation of new macropolycyclic polyamines is indeed a major topic. Thus we investigated the synthesis of new macrobicyclic systems based on cyclen and we studied their properties towards metal complexation.

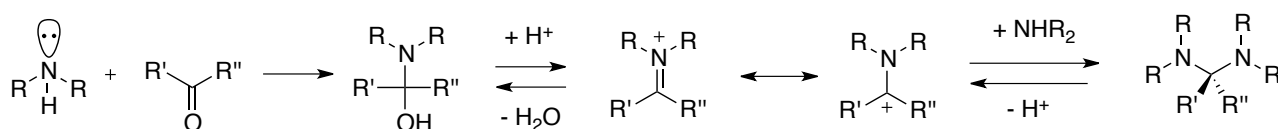
## II.1 New methods of C-functionalization of reinforced tetraazacycloalkanes

As described in chapter I, BFCAs containing topologically constrained polyazamacrocycles such as side-bridged (SB) and cross-bridged (CB) cyclams have shown remarkable properties for copper chelation. However, in most cases the radiolabeling of such ligands involves harsh conditions that are incompatible with fragile biomolecules such as antibodies.<sup>76</sup> In order to overcome this problem, the synthesis of new constrained ligands based on homocyclen was developed. Homocyclen derivatives have been much less investigated than their smaller and larger analogues, cyclen and cyclam derivatives, respectively, although it has been reported that such 13-membered ring compounds could show promising coordination properties. In particular, it has been shown that the metalation of constrained homocyclens can be performed at room temperature, which is convenient for biomolecules labeling.<sup>82</sup> Moreover the resulting Cu complexes are reasonably resistant to acid decomplexation.

Because of these promising properties, the synthesis of new BFCAs based on such constrained homocyclens is a great challenge, which can be faced using the methods of selective *N*- and *C*-functionalization developed in our group.<sup>122-124</sup> These synthetic routes involve the use of bisaminal tool. It is first necessary to understand the mechanism of formation of bisaminal intermediates, which serve as organic template for further cyclization reactions and enable selective functionalization.

### II.1.1 Use of bisaminal as organic template

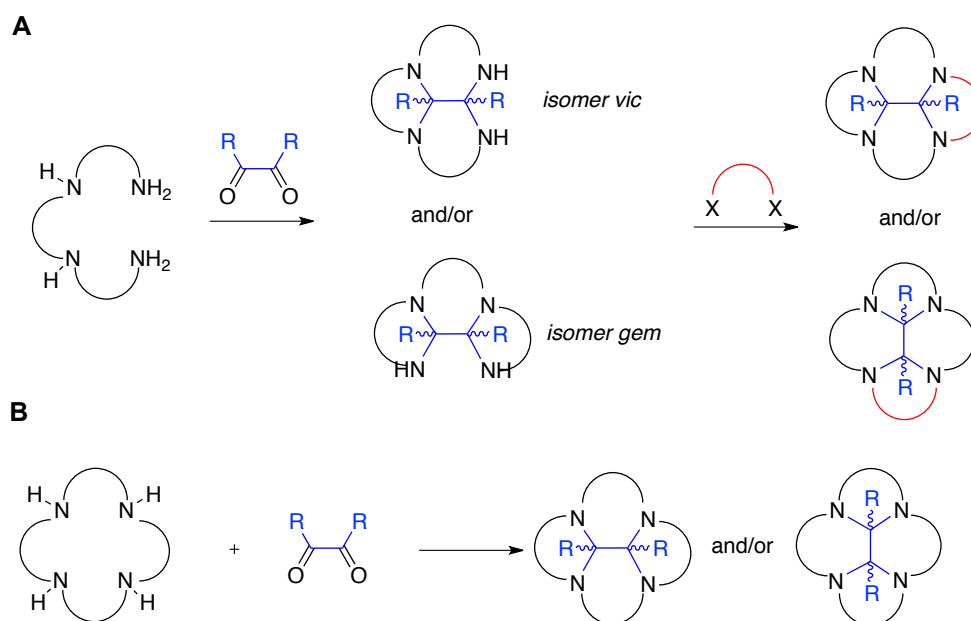
The « bisaminal route » emerged as one of the most powerful synthetic tools in the field of tetraazacycloalkanes chemistry over the past few years. Bisaminals are obtained after condensation of an aldehyde or a ketone on amines. The first step of the nucleophilic addition of amines to aldehydes or ketones leads to an imine or an iminium ion, depending on the primary or secondary nature of the amine concerned (Scheme II-1). The formation of the aminal function is the consequence of the addition of a second amine onto the  $sp^2$  carbon atom.



Scheme II-1

It is possible to synthesize cyclic bisaminals from polyamines containing ethylenic or propylenic chains. These cyclic derivatives are generally more stable than their acyclic analogues because of the formation of thermodynamically stable five- and six-membered rings. Thus, a tricyclic derivative is formed by the action of  $\alpha$ -dicarbonylated species such as glyoxal, pyruvic

aldehyde or 2,3-butanedione on a linear tetraamine (Scheme II-2A).<sup>125</sup> The resulting bisaminal bridge acts as an organic template, which induces pre-organization of the tetraamine to favor its subsequent cyclization. The  $\alpha$ -dicarbonylated species can also be introduced on tetraazacycloalkanes (Scheme II-2B) leading to the corresponding tetracyclic derivatives.



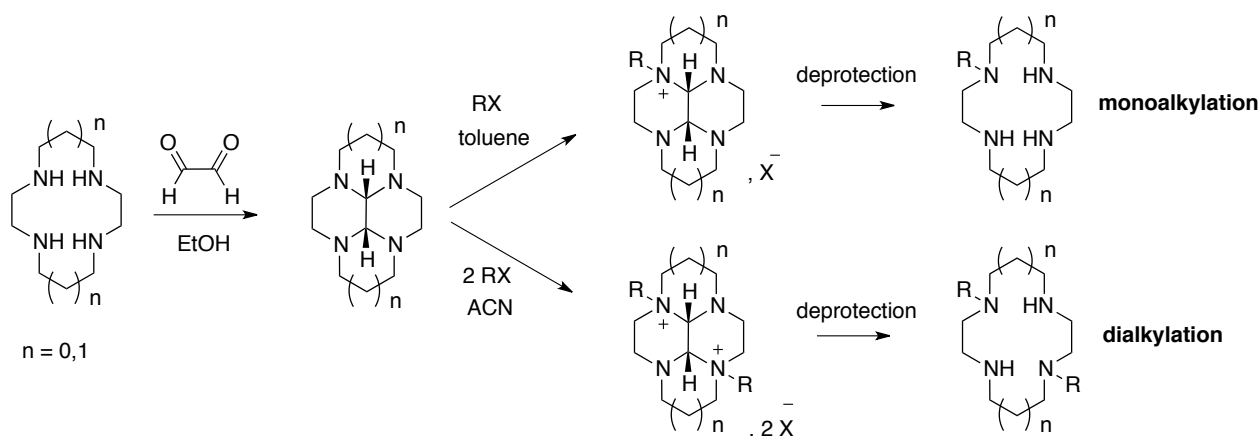
Scheme II-2

In theory, these condensation reactions should result in multiple stereoisomers according to the *vic/gem* insertion of the  $\alpha$ -dicarbonyl reagent and *cis/trans* configuration of the resulting bisaminal bridge. In fact, the reaction is highly selective and leads to only a few isomers.<sup>125</sup> Reports concerning the synthesis of these bisaminals indicate that one or several isomers can be isolated in variable proportions depending on the experimental conditions (solvent, temperature). In major cases, the formation of rings with a maximum of six members appears to constitute the driving force of the reaction. In particular, when the  $\alpha$ -dicarbonylated species is added on cyclic tetraamines, only *cis* isomers are formed.

In recent years, the bisaminal derivatives of cyclic and linear tetraamines have been extensively used and enabled the successful synthesis of tetraazamacrocycles (cyclen, cyclam and homocyclen) either with 2,3-butanedione, pyruvic aldehyde or glyoxal. The bisaminal route also enables the obtention of selectively functionalized systems. In these cases, the choice of the  $\alpha$ -dicarbonylated species is primordial to control the reactivity of the bisaminal intermediates towards selective alkylation. The “bisaminal route” allows the *N*-mono<sup>126,127</sup> and the *N,N'*-dialkylation<sup>128</sup> of several macrocycles leading to a wide range of selectively functionalized derivatives as well as their constrained analogues. This route also gave access to *C*-functionalized systems.<sup>124,129</sup> These aspects will be discussed in the next parts.

### II.1.1.1 Selective *N*-functionalization of bisaminal derivatives: towards the formation of constrained polyazamacrocycles

Several methods of selective *N*-functionalization of tetraazacycloalkanes have been developed<sup>130-136</sup> and most of them are based on alkylation of the bisaminal resulting from the condensation of glyoxal on the cyclic tetraamine.<sup>130,133-135</sup> The tetracyclic *cis*-fused bisaminal is selectively mono- or cross-di-alkylated to obtain the resulting mono- or bis-quaternary ammonium salts respectively (Scheme II-3).

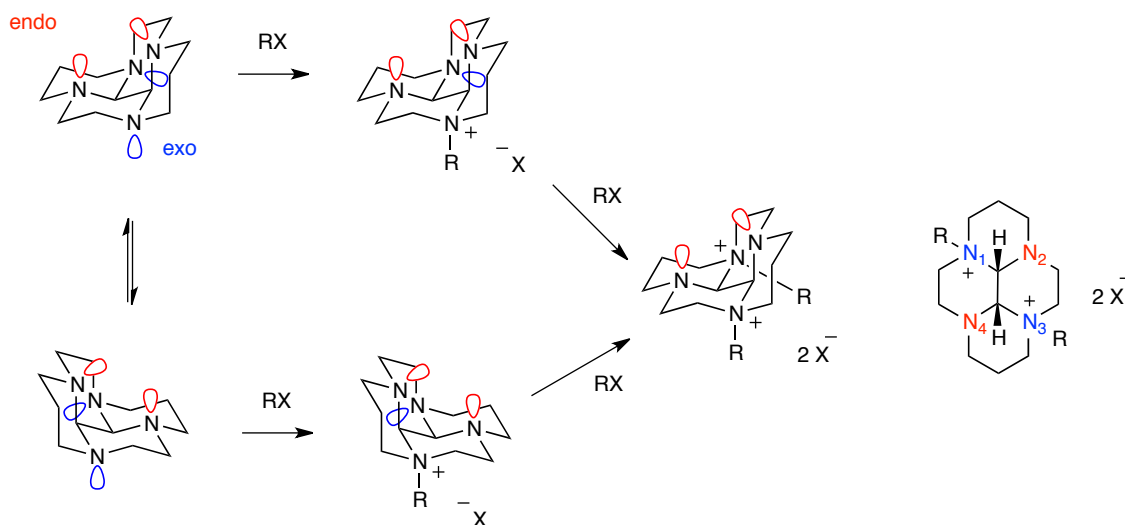


The alkylation of these bisaminals to form the corresponding ammonium is highly dependent on proper solvent selection.<sup>137</sup> When halides are employed as electrophiles, exclusive monoalkylation is observed in toluene. The success of this selectivity can be attributed to the low solubility and resulting precipitation of the ammonium salt formed in the reaction media. The formation of the dialkylated bisaminal can be achieved in a one-pot process using acetonitrile as the solvent and with proper choice of stoichiometry. Formation of alkylated macrocycles<sup>133,138</sup> (such as cyclam, cyclen and homocyclen) is then performed by hydrolysis of the ammonium salts in aqueous acid or basic solution to remove the bisaminal bridge. This route was extended to the synthesis of macropolycycles or cryptands.<sup>128,139</sup>

#### II.1.1.1.1 Mechanism of alkylation and selectivity

Weisman and co-workers have demonstrated that the bisaminal obtained from condensation of glyoxal with cyclam undergoes highly regioselective *N*-functionalization and that the substitution pattern is dictated by the macrocycle conformation.<sup>137</sup> As mentioned above, condensation of glyoxal on cyclic polyamines exclusively results in the formation of a bisaminal exhibiting a *cis* configuration. Scheme II-4 represents the two conformations of a tetracyclic bisaminal. The relatively rigid structural feature imparts a bowl-like geometry with convex and concave faces. The exo lone pairs point towards the convex face of the macrocycle, making them more nucleophilic

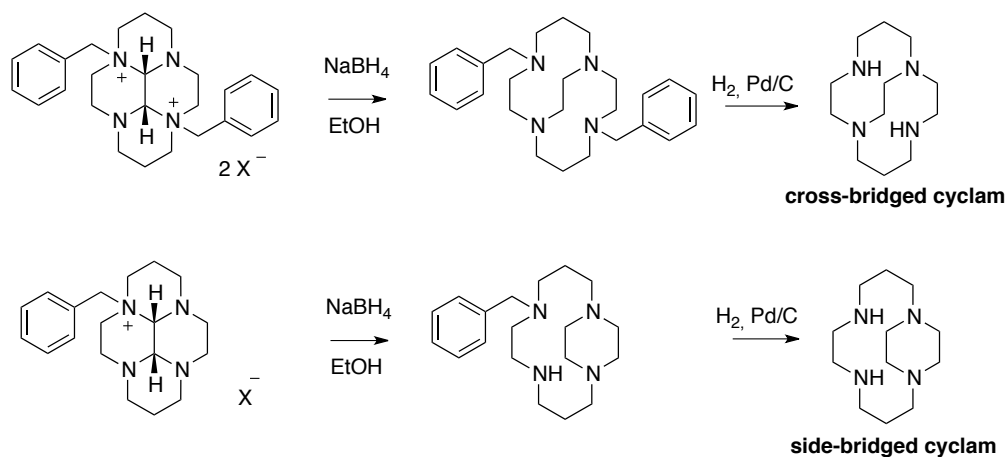
than the endo lone pairs, which point towards the interior concave face. Thus, alkylation preferentially occurs on the exo lone pair of the so-called N1 and N3 nitrogen atoms.



Scheme II-4: Alkylation of a tetracyclic bisaminal.

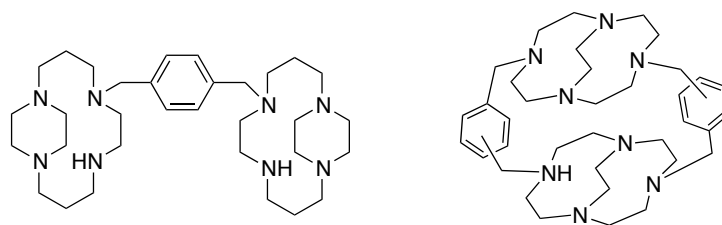
### II.1.1.1.2 Towards constrained polyazacycloalkanes

Alkylated bisaminal intermediates are valuable precursors of constrained macrocycles. The synthetic route to such system was originally developed by Weisman *et al* giving access to cross-bridged cyclams (Scheme II-5). It is based upon reductive ring cleavage with  $\text{NaBH}_4$  of the dialkylated ammonium salts resulting from glyoxal condensation followed by the hydrogenolysis of the benzyl groups.<sup>140,141</sup> This method was later derived and adopted by Kolinski to synthesize side-bridged cyclam from the monoalkylated ammonium salts.<sup>142</sup>



Scheme II-5

This route can be applied in cyclen<sup>143</sup> and homocyclen<sup>82</sup> series and also enables the synthesis of bismacrocycles and other macropolycycles (Scheme II-6).<sup>35,144</sup>



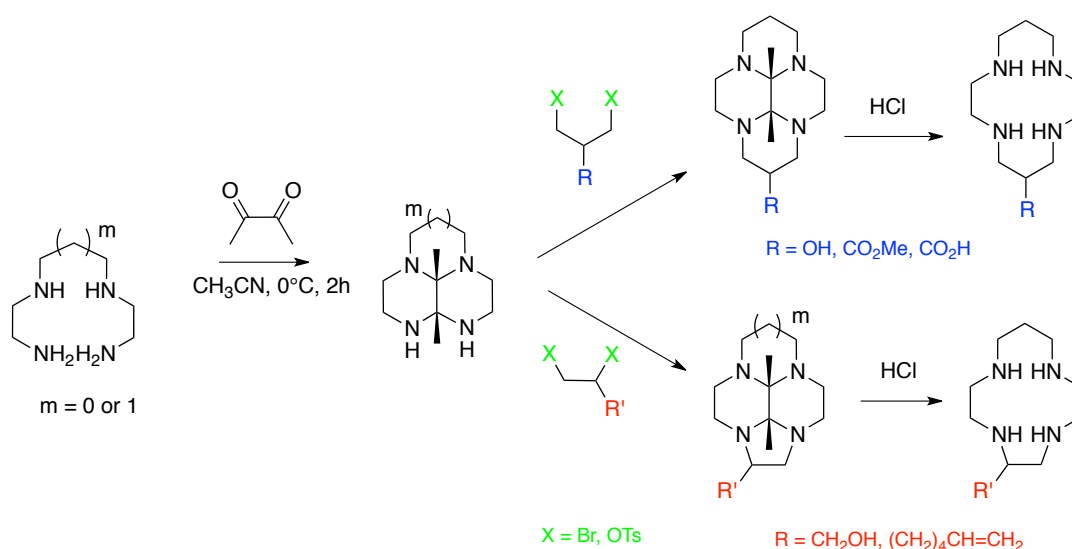
Scheme II-6: Examples of macropolycycles based on constrained tetraazacycloalkanes.<sup>35,144</sup>

The group of Yamamoto reported another synthetic way to obtain side-bridged cyclam using bisaminal tool.<sup>145</sup> This synthesis only differed in the use of DIBAL-H instead of  $\text{NaBH}_4$  as opening ring agent. However, the most commonly route to constrained macrocycles remains the one developed by Weisman and co-workers.

### II.1.1.2 C-functionalization using bisaminal methodology

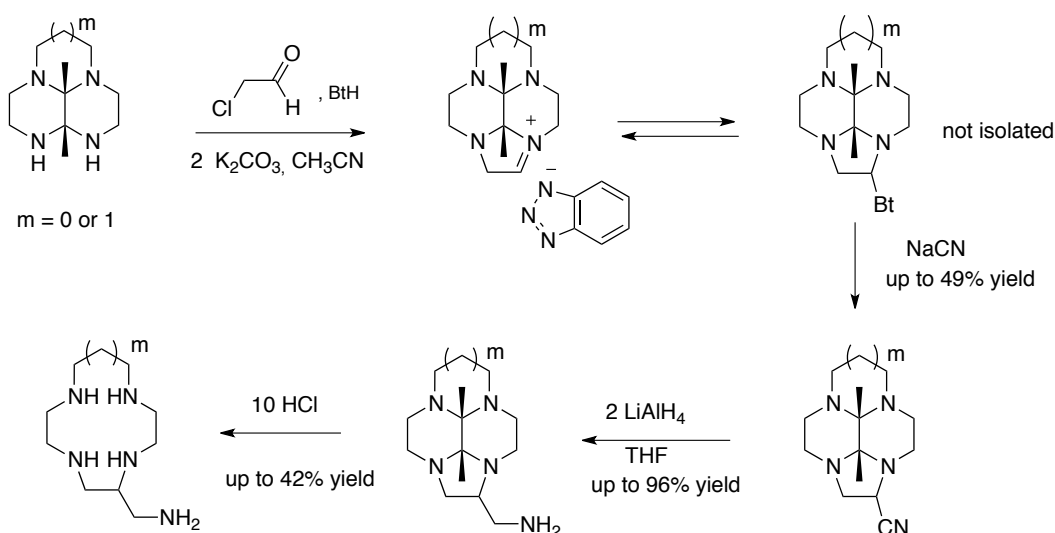
In most cases, the synthesis of C-functionalized macrocycles implies the use of C-functionalized precursors prior to cyclization. The most frequently used procedures for the synthesis of such systems are based on Richman and Atkins cyclization, involving *p*-toluenesulfonyl protecting groups.<sup>146</sup> These methods are not atom-economic and the deprotection step requires harsh conditions. The condensation of the linear tetraamine with substituted malonic esters allows the preparation of various C-functionalized cyclams.<sup>147</sup> However, reaction times are very long, yields often poor and the reduction of the diamide intermediate requires the use of borane.

The bisaminal template approach represents a powerful synthetic tool for the preparation of various C-functionalized tetraazacycloalkanes. New synthetic routes based on this approach have been developed.<sup>124,129,136</sup> Most of them use 2,3-butanedione as organic template, because the resulting fragment is easily deprotected in mild conditions.<sup>138</sup> The protected C-functionalized macrocycles were obtained following a “one-pot” procedure by reaction of a suitable biselectrophile with the tricyclic bisaminal derivative (Scheme II-7). Our group used dihalogenated or ditosylated propane or ethane derivatives, bearing a wide range of functions such as alcohol or vinyl groups (Scheme II-7).<sup>129</sup> In the same manner, Archibald *et al* synthesized a 1,3-dibromopropane bearing a nitrobenzyl moiety in three steps from the commercially available precursors.<sup>136</sup> In all cases, the bisaminal template was easily removed in acidic conditions. However, the main drawback of this approach is the preparation of the precursor bearing the desired function on a carbon atom.



Scheme II-7

A recent approach developed in our laboratory allows the introduction of a functional group onto a carbon atom of the cyclic backbone without needing to prepare a sophisticated precursor.<sup>124</sup> After rigidification of the starting linear tetraamines with 2,3-butanedione, chloroacetaldehyde was reacted with the resulting bisaminals in the presence of one equivalent of benzotriazole and potassium carbonate (Scheme II-8). The benzotriazole moiety was then displaced by a nucleophile such as sodium cyanide. Reduction with two equivalents of  $\text{LiAlH}_4$  gave the corresponding aminomethyl bisaminal derivatives in homocyclen and cyclen series, which were converted into the targeted macrocycles after removal of the bisaminal bridge by acidic hydrolysis.

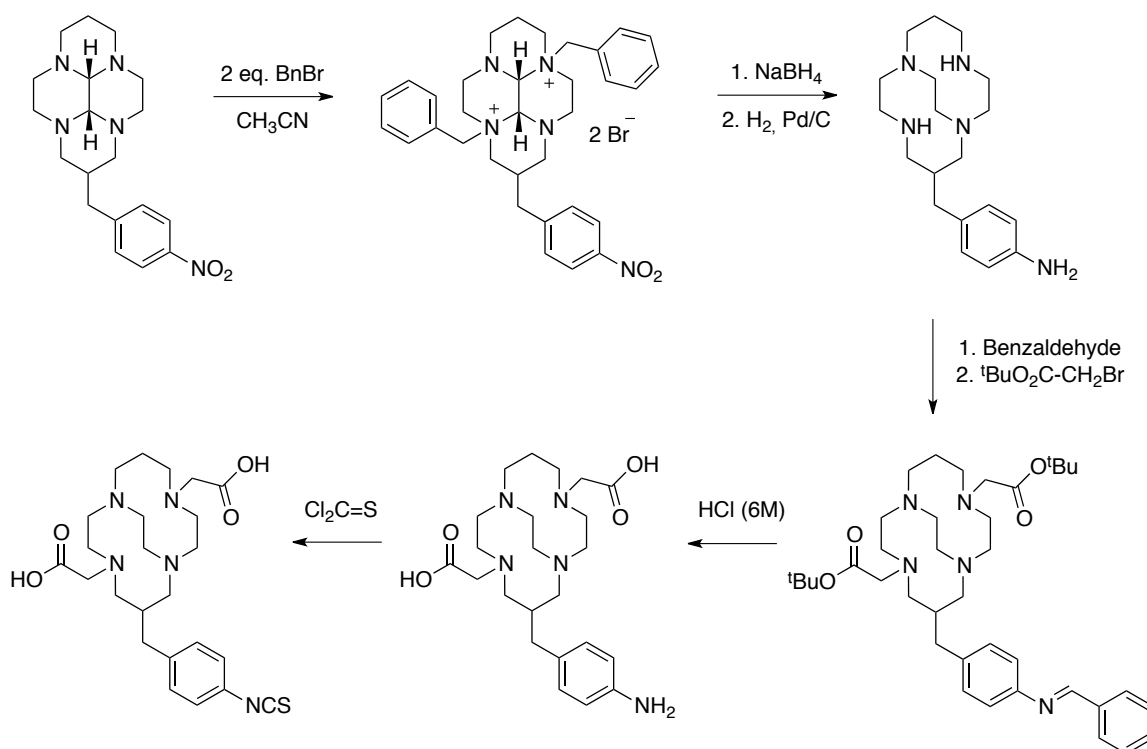


Scheme II-8



### II.1.1.3 Combining both previous approaches towards new C-functionalized cross-bridged systems

Archibald and co-workers combined both previous approaches to prepare the only example of C-functionalized constrained macrocycle reported in the literature (Scheme II-9).<sup>73</sup> A valuable bifunctional chelator was synthesized in seven steps in an overall yield of 20 % from a  $\beta$ -substituted cyclam-based bisaminal. After construction on the cross-bridged core and reduction of the nitro group, the primary amine was protected over the secondary amines using benzaldehyde. The resulting precursor is of great interest for the preparation of a wide range of di-N-substituted cross-bridged systems. In the corresponding paper, Archibald and co-workers added pendant coordinating arms, deprotected the imine in acidic conditions and introduced an isothiocyanate group for bioconjugation purposes.



Scheme II-9

### II.1.2 Synthesis of selectively functionalized constrained homocyclens

Inspired by the previous work and all synthetic methodologies developed in our group, we considered the preparation of new C-functionalized constrained homocyclens (Figure II-1).

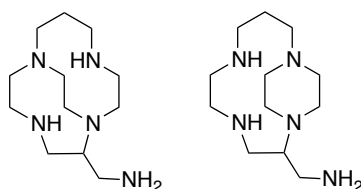
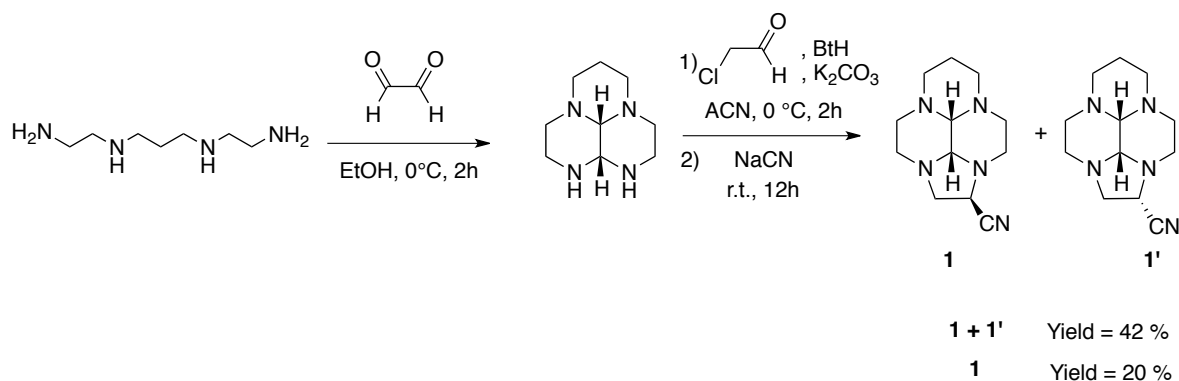


Figure II-1: New C-functionalized constrained homocyclens.

### II.1.2.1 Cyclization reaction

The bisaminal compound was synthesized by rigidification of the starting linear tetraamine with glyoxal (Scheme II-10). The condensation of chloroacetaldehyde with the resulting bis-aminal in the presence of benzotriazole and potassium carbonate in acetonitrile gave the corresponding cyclic adducts, which were not isolated. The benzotriazole was then displaced by sodium cyanide. Several stereoisomers can be expected due to the presence of many chiral centers, *i.e.* the nitrogen and carbon atoms of the aminal bridge, as well as the carbon atom bearing the nitrile group. Interestingly, we obtained a mixture of only two diastereoisomers **1** and **1'**, which could be separated by recrystallization in cyclohexane. However, only the diastereoisomer **1** was obtained pure enough to be involved in further reactions. The orientation of the nitrile group and of aminal hydrogen atoms in compound **1** was determined from the X-ray structures obtained after quaternization reaction of **1** (*vide infra*).



Scheme II-10

### II.1.2.2 Selective alkylation reactions

The addition of one equivalent of benzyl bromide on compound **1** was performed in toluene in order to precipitate the mono *N*-alkylated cationic compounds.<sup>148</sup> Potentially, the four nitrogen atoms of the aminal intermediate **1** can be alkylated by the addition of one equivalent of nucleophile (Figure II-2).

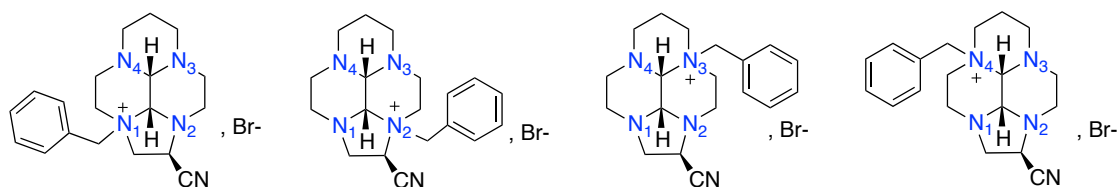
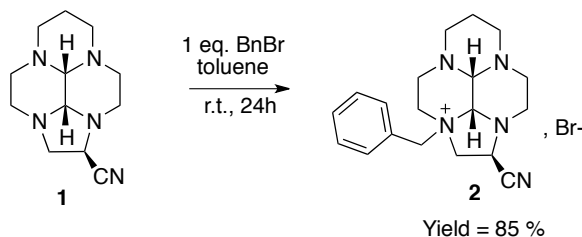


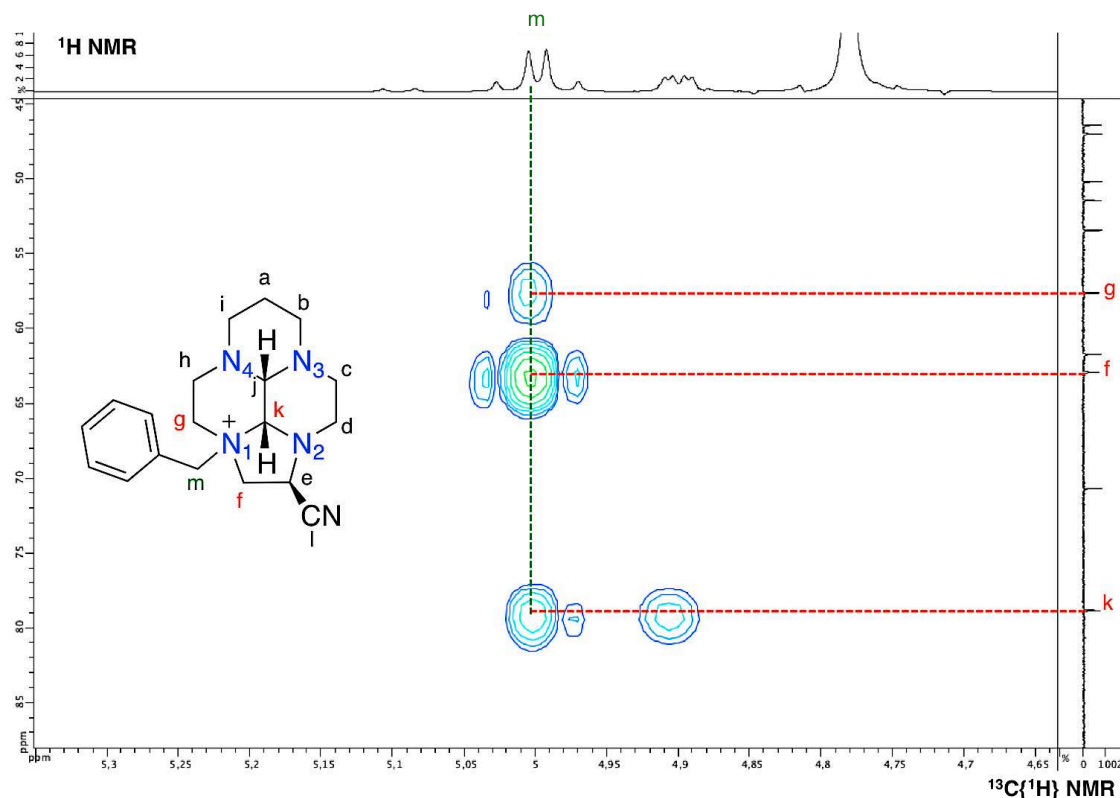
Figure II-2

Surprisingly, this addition was regioselective and led to compound **2** as the sole product, which was isolated by filtration after 24 hours in 85 % yield (Scheme II-11). The remaining 15 % corresponded to the starting material.



Scheme II-11

The structure of compound **2** was determined by COSY, HMQC, HMBC and NOESY experiments. The 2D-HMBC spectrum (Figure II-3) shows a region of cross-peaks corresponding to correlations involving  $\text{CH}_2^m$ . The correlation between the  $\text{CH}_2^m$  protons and the two carbons  $\text{C}^f$  and  $\text{C}^g$  on HMBC spectrum clearly indicates that the benzyl group was located on N1 atom and not on N3 atom.

Figure II-3: 2D-HMBC spectrum of **2** recorded at 600 MHz, 300 K in  $\text{D}_2\text{O}$ .

This result was confirmed by a NOESY analysis that is reported in Figure II-4. Through space interactions were identified with the alpha hydrogen atoms  $\text{CH}_2^g$  and  $\text{CH}_2^f$ . Taken together, these studies unambiguously demonstrated that compound **2** resulted from N1 quaternization.

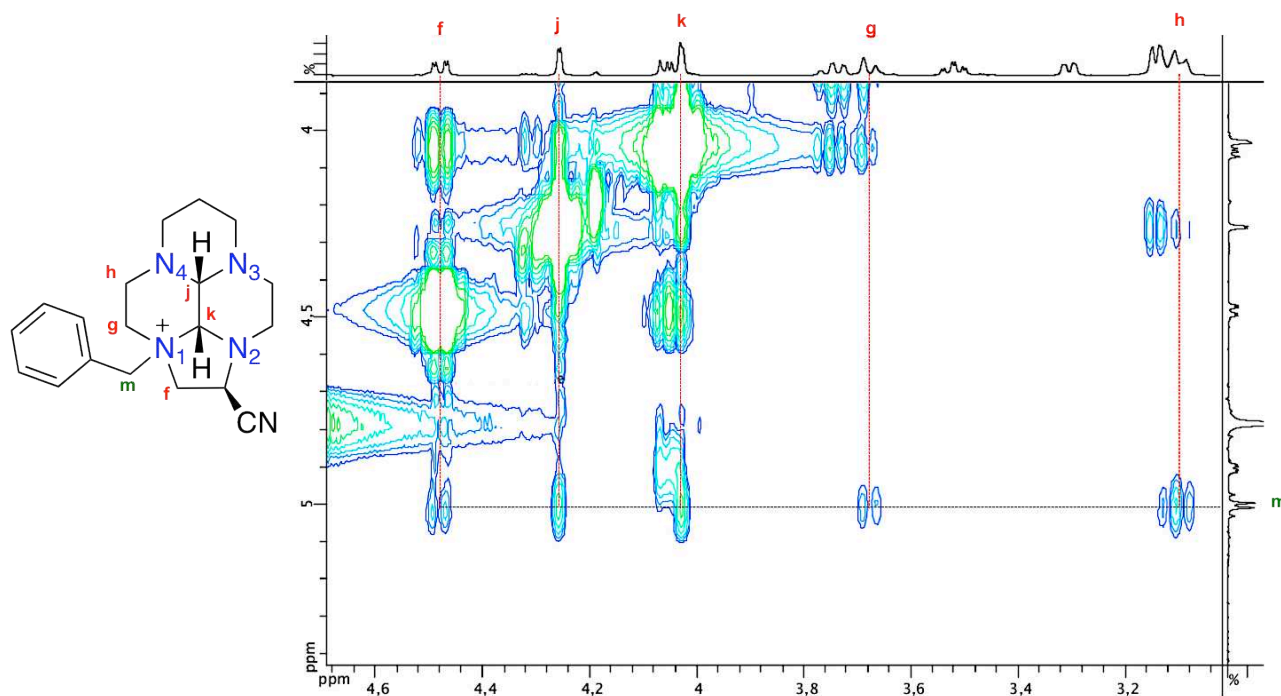


Figure II-4: NOESY  $\{^1\text{H}-^1\text{H}\}$  NMR spectrum of compound **2** (300 K, 600 MHz,  $\text{D}_2\text{O}$ ).

The NOESY spectrum also reveals strong space interactions between  $\text{CH}_2^m$  and the two aminal hydrogen atoms  $\text{CH}^j$  and  $\text{CH}^k$ , indicating that the benzyl group and the hydrogen atoms of the bis-aminal bridge are located on the same side of the molecule mean plane.

The molecule could be recrystallized in acetonitrile and its structure was elucidated by X-Ray diffraction. The crystal structure (Figure II-5) corroborates NMR data and also indicates that the nitrile group and the aminal hydrogen atoms point in the same direction.



Figure II-5: ORTEP<sup>149</sup> view of compound **2**. Thermal ellipsoids are drawn at 50 % probability. Solvent molecule is not shown for clarity.

NMR spectra of the precipitate and the crystals were compared. The spectra were strictly superimposable, proving that the quaternization reaction occurs selectively on N1. The regioselectivity of the reaction on N1 can be highlighted by comparison of the thermodynamic stability of the four potential regioisomers obtained upon alkylation of N1, N2, N3 and N4. Thus, DFT calculations were performed by varying the position and the orientation of the benzyl groups (Figure II-6). The data revealed that the most thermodynamically stable products resulted from N1 (computed form **a**) and N3 quaternization (computed form **e**).

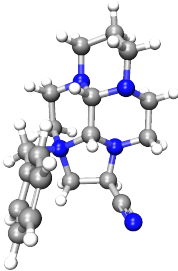
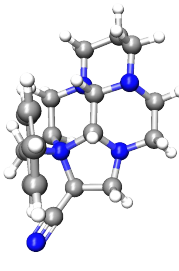
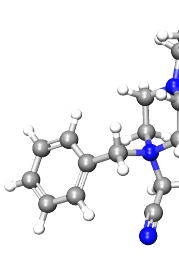
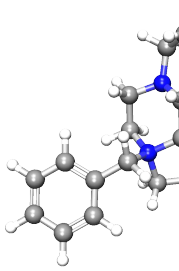
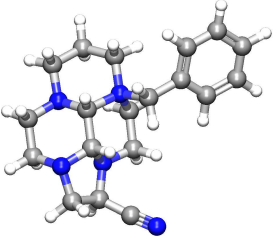
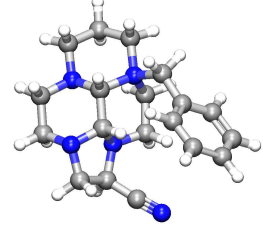
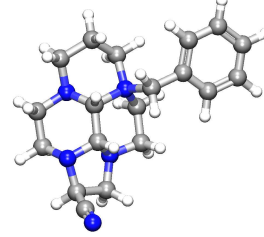
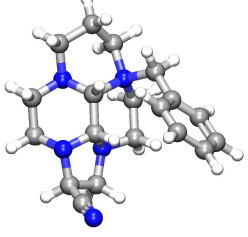
<b>a</b>	<b>b</b>	<b>c</b>	<b>d</b>
			
-1012.803090 hartrees	-1012.790170 hartrees	-1012.783836 hartrees	-1012.793636 hartrees
$\Delta G^\circ = 0 \text{ kcal.mol}^{-1}$	$\Delta G^\circ = 8.11 \text{ kcal.mol}^{-1}$	$\Delta G^\circ = 12.08 \text{ kcal.mol}^{-1}$	$\Delta G^\circ = 5.93 \text{ kcal.mol}^{-1}$
<b>e</b>	<b>f</b>	<b>g</b>	<b>h</b>
			
-1012.800964 hartrees	-1012.790918 hartrees	-1012.792373 hartrees	-1012.786831 hartrees
$\Delta G^\circ = 1.33 \text{ kcal.mol}^{-1}$	$\Delta G^\circ = 7.63 \text{ kcal.mol}^{-1}$	$\Delta G^\circ = 6.72 \text{ kcal.mol}^{-1}$	$\Delta G^\circ = 10.20 \text{ kcal.mol}^{-1}$

Figure II-6: DFT B3LYP/6-31G\*\* calculation for potential isomers formed by mono-quaternization of compound **1**.

It has to be noted that the computed form **a** is similar to the structure of compound **2** determined by X-Ray diffraction (Figure II-7).

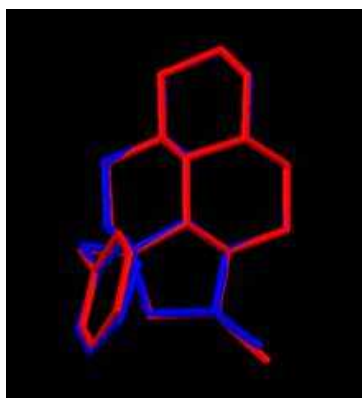


Figure II-7: Superimposition of the structure of compound **2** obtained by X-Ray (blue) and by DFT B3LYP/6-31G\*\* calculation (red).

Such orientation of the benzyl group in compound **2** is imposed by  $\pi$ - $\pi$  stacking interaction (Figure II-8).

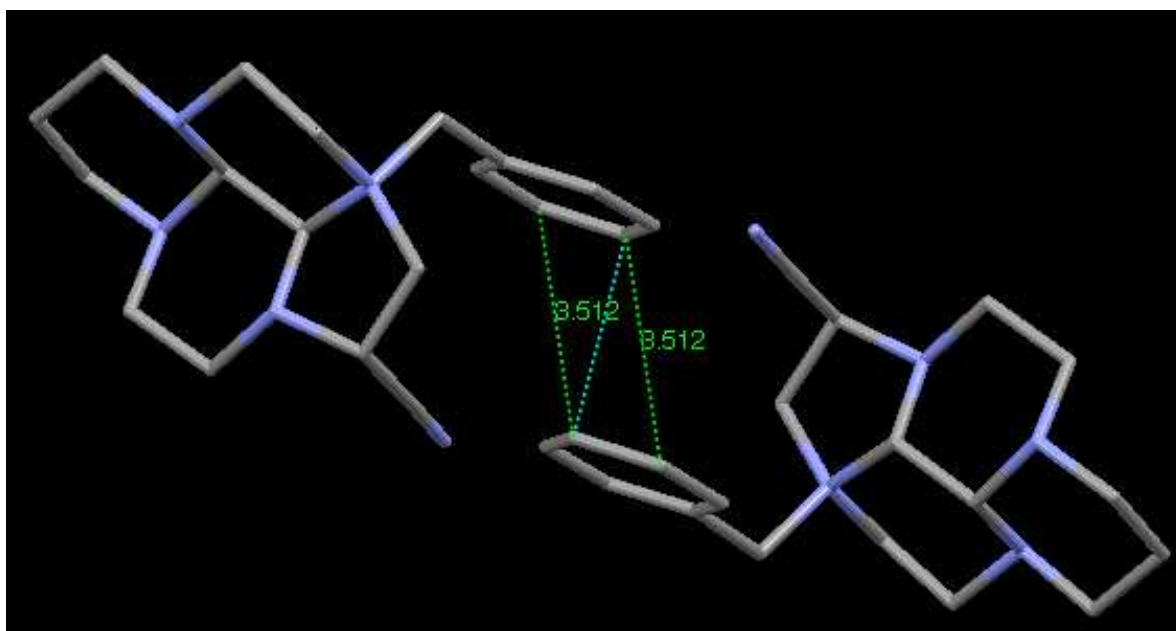


Figure II-8: Evidence of  $\pi$ - $\pi$  stacking interaction on the X-Ray structure of compound **2**. Hydrogen atoms are omitted for clarity.

At this stage, even if the thermodynamic stability studies can explain the formation of compound **2**, the difference of values between N1 and N3 is not significant ( $\Delta G^\circ = 1.33 \text{ kcal.mol}^{-1}$ ). To gain further insight into the regioselectivity, the accessibility of the lone pair on the N1 and N3 nitrogen atoms of the starting compound **1** was studied by molecular modeling calculations (Figure II-9).

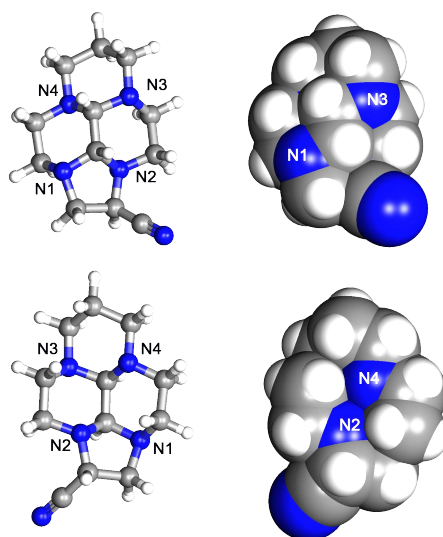
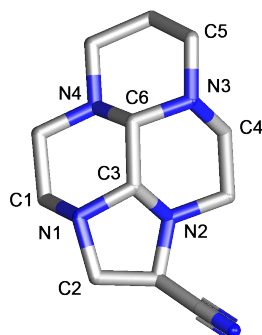


Figure II-9: Molecular view of DFT B3LYP/6-31G\*\* results for compound **1**.

The values of C-N1-C angles and of the distance between N1 and the mean plane formed by the three carbon atoms C1, C2 and C3 are reported in Figure II-10. N1 is involved in a five-membered ring and in a six-membered ring and presents a classical trigonal pyramidal geometry

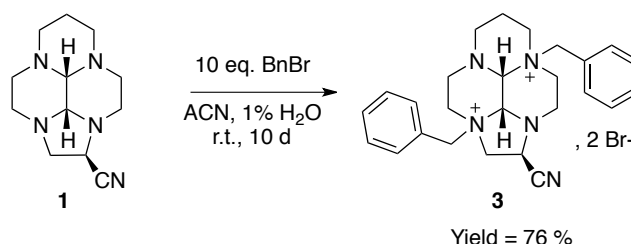
(AX3E according to VSEPR theory). The data reveal that N3, which is engaged in two six-membered rings, is closer to the (C4C5C6) plane. Taken together, these data show a higher accessibility of the lone pair on N1 than on N3.



C1-N1-C2	112.62	C4-N3-C5	113.76
C1-N1-C3	111.91	C4-N3-C6	113.87
C2-N1-C3	102.24	C5-N3-C6	109.98
(C1C2C3) to N1	0.500	(C4C5C6) to N3	0.409

Figure II-10: Angles ( $^{\circ}$ ) and distances ( $\text{\AA}$ ) measurements in compound **1**.

We then investigated the di-quaternization reaction of compound **1**. A large excess of benzyl bromide (10 equivalents) was added on compound **1** in an acetonitrile/water mixture. Compound **3** was isolated in 76 % yield after ten days at room temperature (Scheme II-12).



Scheme II-12

The crystal structure of compound **3** is shown in Figure II-11 and reveals that the quaternization occurred on N1 and N3. The trans selectivity of the di-quaternization reaction of amina derivatives has been previously reported (II.1.1.1.2).

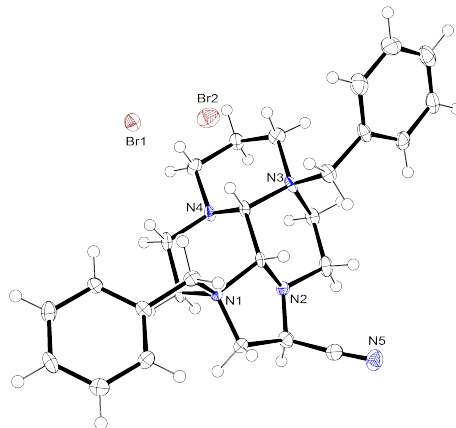
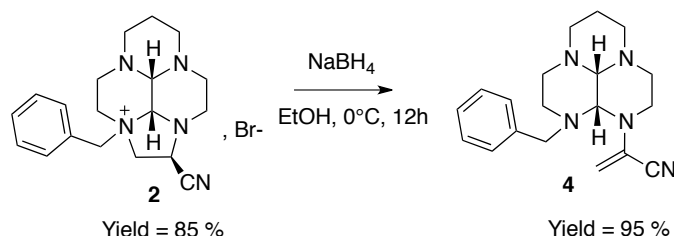


Figure II-11: ORTEP<sup>149</sup> view of compound **3**. Thermal ellipsoids are drawn at 50% probability. Water molecules are not shown for clarity.

### II.1.2.3 Reductive ring opening with sodium borohydride

Treatment of **2** with a large excess of NaBH<sub>4</sub> in ethanol didn't result in double reductive ring expansion, but led almost quantitatively to an unexpected compound containing an acrylonitrile moiety (compound **4**, Scheme II-13).



Scheme II-13

The structure of **4** was determined by spectroscopic analysis. <sup>1</sup>H NMR spectrum exhibits signals that are characteristic of the presence of terminal ethylenic protons ( $\delta = 4.57$  and 4.71 ppm).

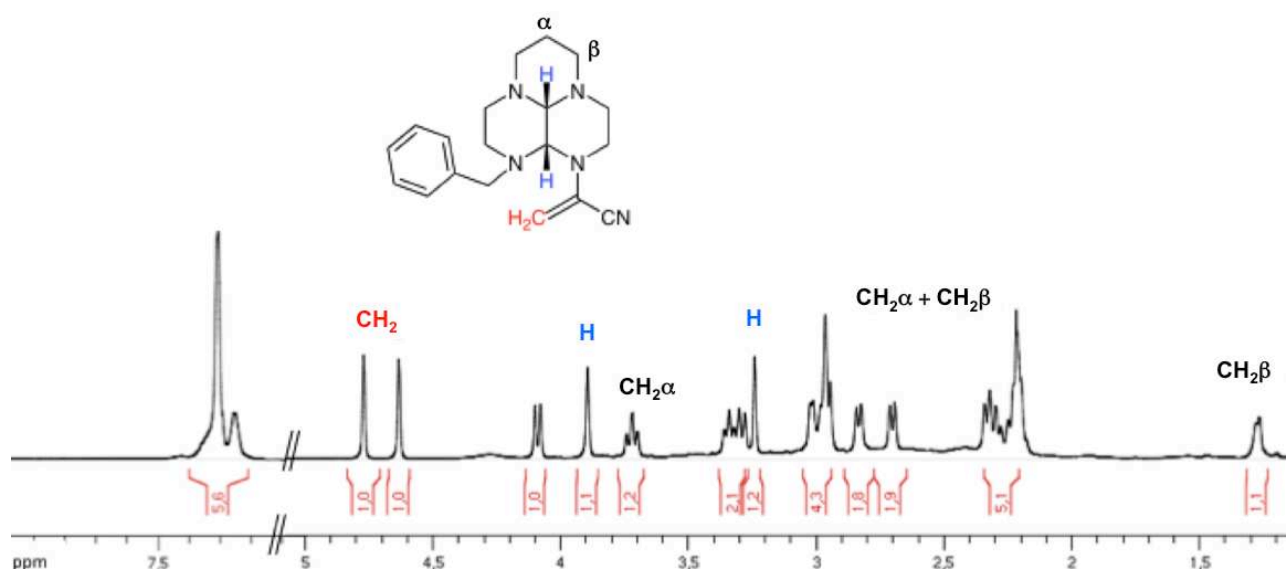
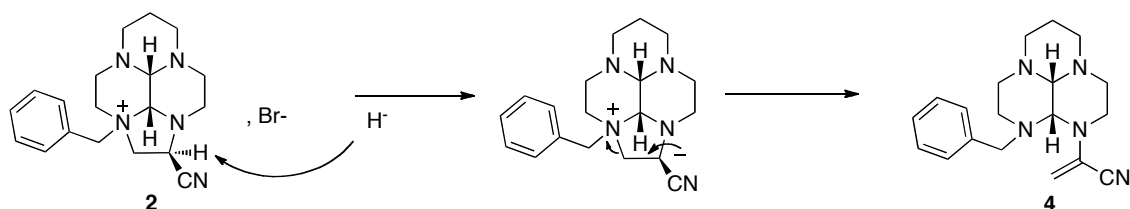


Figure II-12: <sup>1</sup>H NMR spectrum of compound **4** (220 K, 600 MHz, CDCl<sub>3</sub>).

<sup>13</sup>C NMR spectrum indicates the presence of a nitrile group ( $\delta = 116.1$  ppm) and confirms the presence of a double bond with a terminal CH<sub>2</sub> group ( $\delta = 99.2$  ppm). Moreover, analysis of the IR spectrum revealed an absorption band at 2230 cm<sup>-1</sup>, which is typical of the nitrile group. Another band is present at 1582 cm<sup>-1</sup>, which is characteristic of a conjugated carbon-carbon double bond.

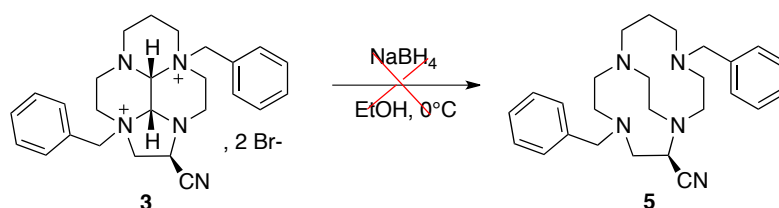
The formation of the acrylonitrile moiety could be explained by the removal of the acidic proton in alpha position of the nitrile by the hydride acting as a base, followed by the formation of the carbon-carbon double bond and the cleavage of the carbon-nitrogen bond (Scheme II-14).





Scheme II-14

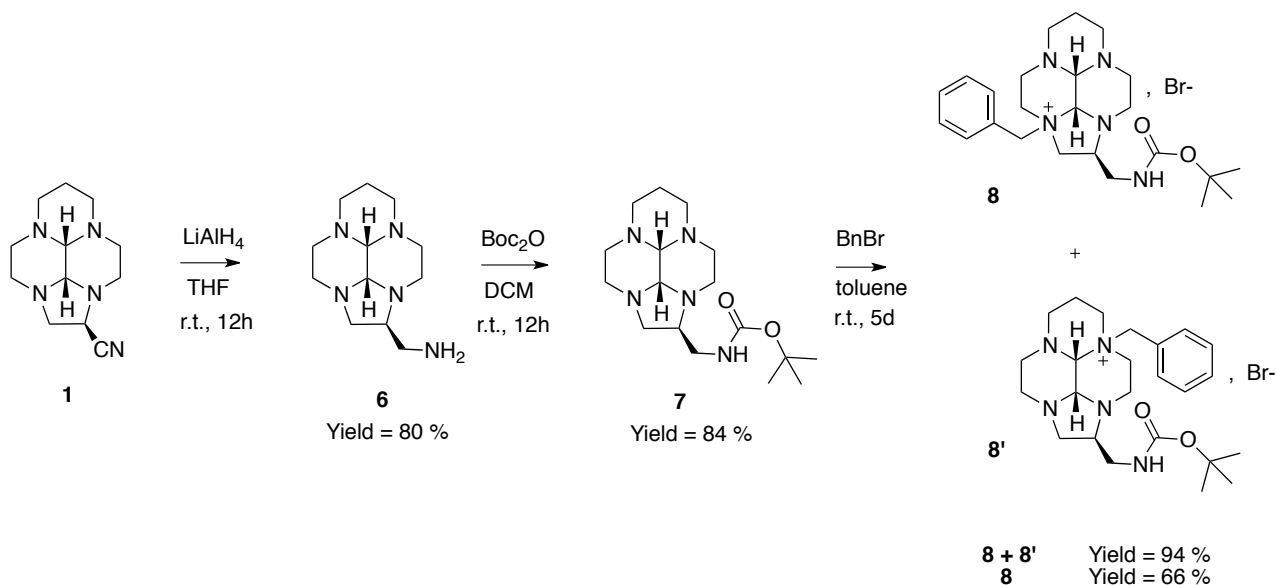
Unfortunately, the addition of a large excess of  $\text{NaBH}_4$  on **3** didn't yield the expected cross-bridged homocyclen **5**, but a mixture of products, which we were not able to separate and identify (Scheme II-15). To overcome these issues, we decided to reduce the nitrile group prior to quaternization reactions.



Scheme II-15

#### II.1.2.4 Reduction of the nitrile group, protection of the resulting amine and alkylation reactions

The nitrile group was easily reduced into primary amine using  $\text{LiAlH}_4$  to give compound **6** in 80 % yield (Scheme II-16). The primary amine was then protected by a Boc group leading to compound **7** in 84 % yield.



Scheme II-16

Monoalkylation of compound **7** was performed in toluene by reacting one equivalent of benzyl bromide. The resulting precipitate was isolated in 94 % yield and appeared to be a mixture of two regioisomers **8** and **8'** as determined by  $^1\text{H}$  NMR analysis in  $\text{D}_2\text{O}$  (Figure II-13). In both compounds, the two protons of the benzyl group ( $\text{H}_\text{a}/\text{H}_\text{b}$  for **8** and  $\text{H}'_\text{a}/\text{H}'_\text{b}$  for **8'**) are diastereotopic and constitute an AB-system appearing as a doublet of doublet around 5 ppm. The signals integration of  $\text{H}_\text{a}$  and  $\text{H}'_\text{a}$  on the  $^1\text{H}$  NMR spectrum of the crude indicates a ratio of 65/35 in favor of compound **8** (Figure II-14).

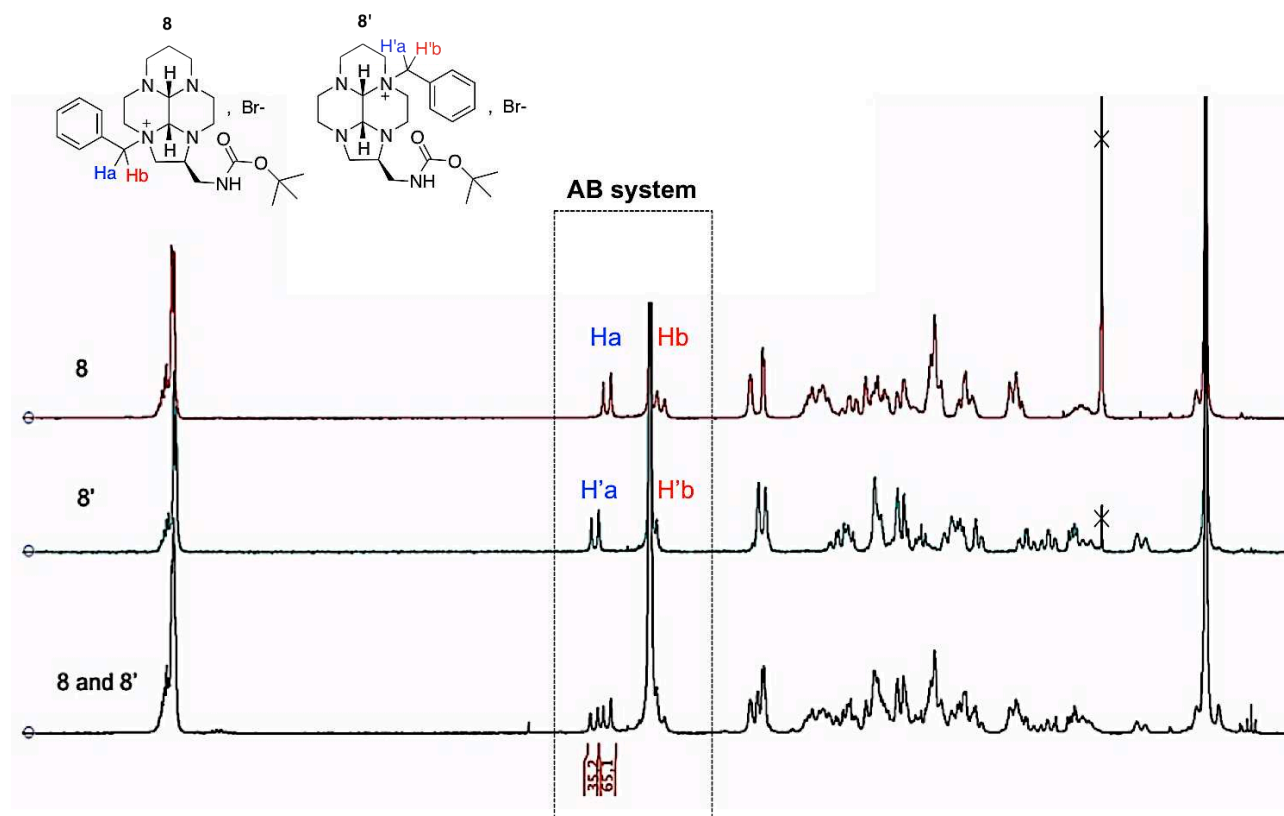


Figure II-13:  $^1\text{H}$  NMR spectrum of compound **8** and **8'** (300 K, 300 MHz,  $\text{D}_2\text{O}$ ).

The regioisomer **8** could be recrystallized in acetonitrile and its structure was established by X-Ray diffraction (Figure II-14). The structure revealed that the major product resulted from N1 alkylation, as in the case of compound **1**. However, in this case, the action of the electrophilic groupment on bis-aminal **7** is not 100 % regioselective and led to a mixture of N1 and N3 quaternized compounds **8** and **8'** (Scheme II-16). Modeling calculations were performed on compound **7**, showing a more pronounced nucleophilic character of N1 atom as in the case of compound **1**. However, steric hindrance around N1 atom due to the presence of the bulkier Boc protecting group when compared to the nitrile could explain the difference between **1** and **7**, and the formation of N3 quaternized bis-aminal **8'** in 28 % yield.

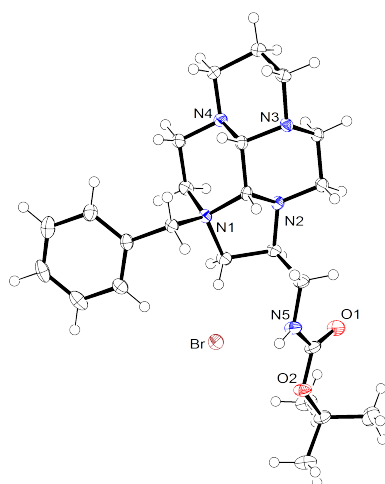
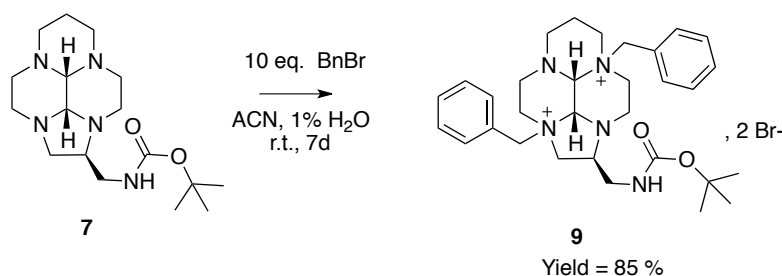


Figure II-14: ORTEP<sup>149</sup> view of compound **8**. Thermal ellipsoids are drawn at 50% probability. Solvent molecules are not shown for clarity.

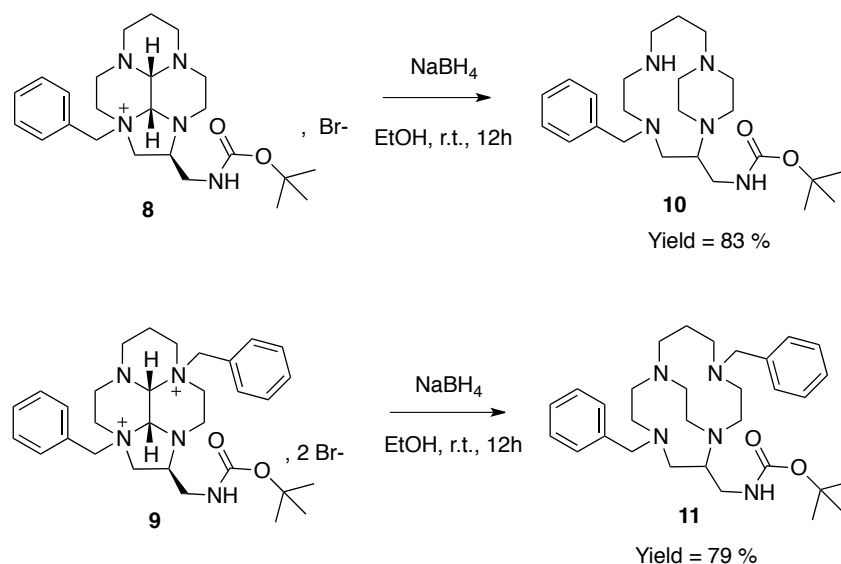
We also prepared the dialkylated ammonium salts by addition of a large excess of benzyl bromide on compound **7** in an acetonitrile/water mixture. The corresponding diquaternized bis-aminal **9** was isolated after seven days at room temperature in 85 % yield (Scheme II-17).



Scheme II-17

### II.1.2.5 Reductive ring opening with sodium borohydride

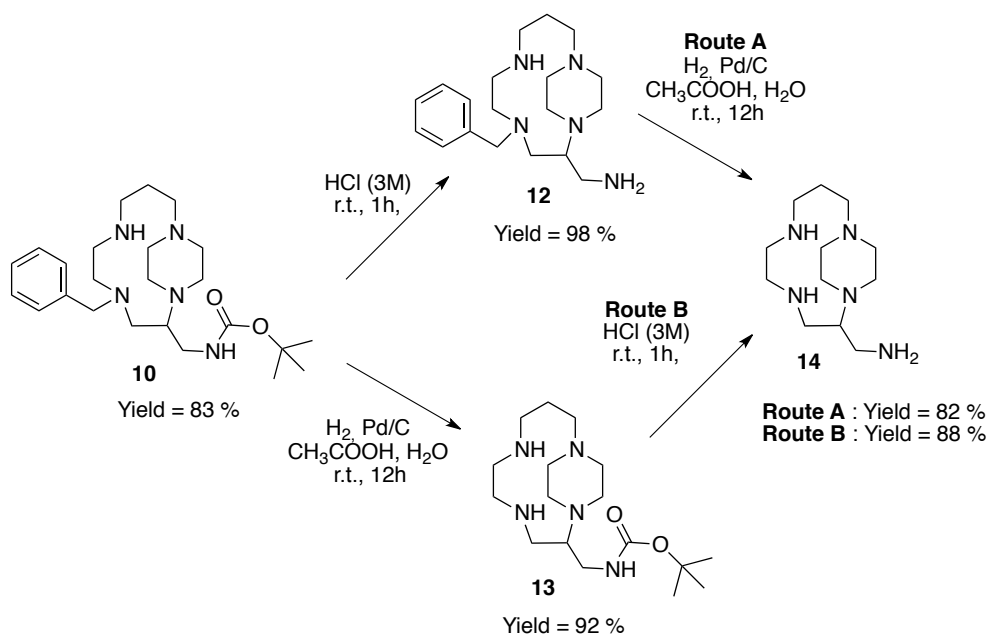
The addition of  $\text{NaBH}_4$  on compounds **8** and **9** in ethanol at room temperature led respectively to the expected protected side-bridged **10** and cross-bridged homocyclens **11** in 83 % and 79 % yield respectively (Scheme II-18).



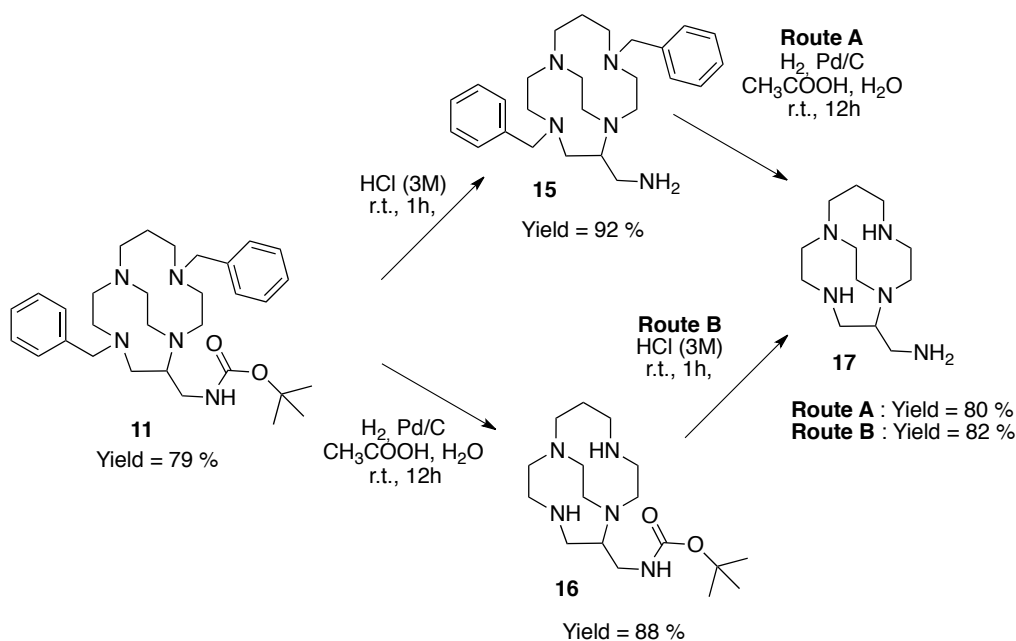
Scheme II-18

### II.1.2.6 Synthesis of new precursors of BFCAs based on constrained homocyclens

Selective deprotection reactions were performed in both side-bridged and cross-bridged series. Boc protecting group was cleaved in acidic condition to give compounds **12** and **15** in good yield, whereas benzyl groups were deprotected via catalytic hydrogenation to form compounds **13** and **16** (Scheme II-19, Scheme II-20). Such selective deprotection reactions allow nitrogen atoms discrimination and enable the selective introduction of various functional groups on the molecule. The preparation of partially functionalized macrocycles is of great interest since such derivatives are valuable bifunctional chelating agents precursors.



Scheme II-19



Scheme II-20

Compounds **13**, **15** and **16** are particularly promising building blocks for the synthesis of new BFCAs. In compounds **13** and **16**, a Boc group protects the pendant primary amine so that pendant coordinating arms can be selectively introduced on the secondary amines of the cycle. In case of compound **15**, the primary amine can be selectively functionalized in order to introduce a grafting function prior to debenzylation and introduction of pendant coordinating arms. After cleavage of the remaining protecting group, aminomethyl side-bridged **14** and cross-bridged **17** homocyclens were isolated in more than 80 % yield.

As a conclusion of this part, the method reported herein represents a very powerful route towards selectively functionalized constrained homocyclens. The method is highly regioselective and all regioisomers or diastereoisomers formed during the reaction can be easily separated by recrystallization in the appropriate solvent. These new aminomethyl constrained macrocycles can be further functionalized giving access to promising bifunctional chelating agents.

### II.1.3 Introduction of a grafting function

First attempts were performed to functionalize these new systems. Numerous grafting functions can be introduced on the macrocycles for allowing coupling with amino residues on biomolecules (Chapter I.II.1.3.2.2). We considered the preparation of systems bearing an isothiocyanate group.

Isothiocyanates can be formed by the reaction of an aromatic amine with thiophosgene. Thus, we investigated the introduction on a *p*-nitrophenyl group on the macrocyclic core that will be further modified. In Figure II-15 is represented the retrosynthetic route that we considered.

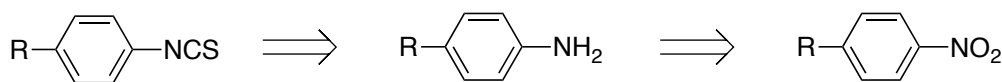
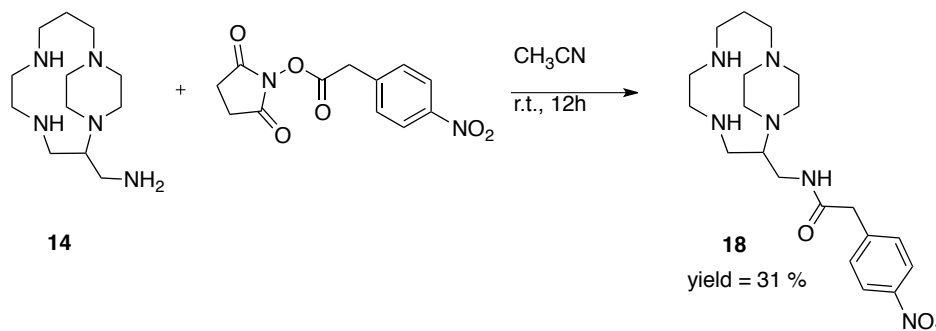


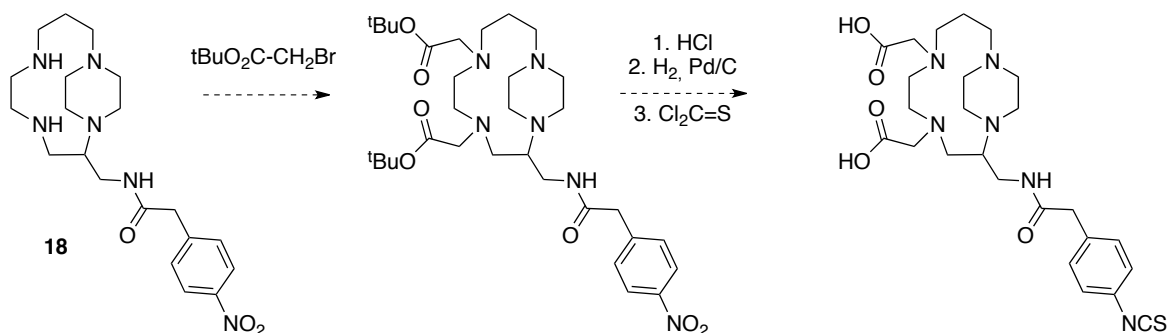
Figure II-15: Introduction of an isothiocyanate group.

The addition of one equivalent of *N*-succinimidyl-4-nitrophenylacetate on compound **14** in acetonitrile at room temperature resulted in the formation of **18** in 31 % yield (Scheme II-21). *N*-hydroxysuccinimide (NHS) ester-activated molecule is a useful tool for selective functionalization of primary amine yielding in stable amide bond. The reaction released NHS, which was easily removed by basic treatment.



Scheme II-21

The two secondary amine groups could be further functionalized with pendant coordinating arms such as *tert*-butylacetate (Scheme II-22). After deprotection of the ester groups in acidic solution, reduction of the nitro by hydrogenolysis, the desired grafting function will be introduced on the aniline by addition of thiophosgene.



Scheme II-22

### II.1.4 Conclusion

A new class of cross-bridged and side-bridged homocyclens bearing an aminomethyl pendant arm on the carbon skeleton has been prepared. These new polyazamacrocycles are valuable precursors of bifunctional chelating agents for applications in nuclear medicine. First attempts of functionalization are encouraging and further reactions are being investigated in our group, such as coupling with other activated esters or with acidic group in the presence of coupling reagents. Thus

the aminomethyl side-bridge system **14** has been successfully coupled to a fluorescent probe bearing a carboxylic acid residue within an undergoing PhD thesis in our group (D. Lhenry). Studies of the coordination properties of these new ligands are also being currently undertaken.

## **II.2 New synthetic methods of 1,4,7-triazacyclononane and its derivatives: towards TACN-based bifunctional chelating agents**

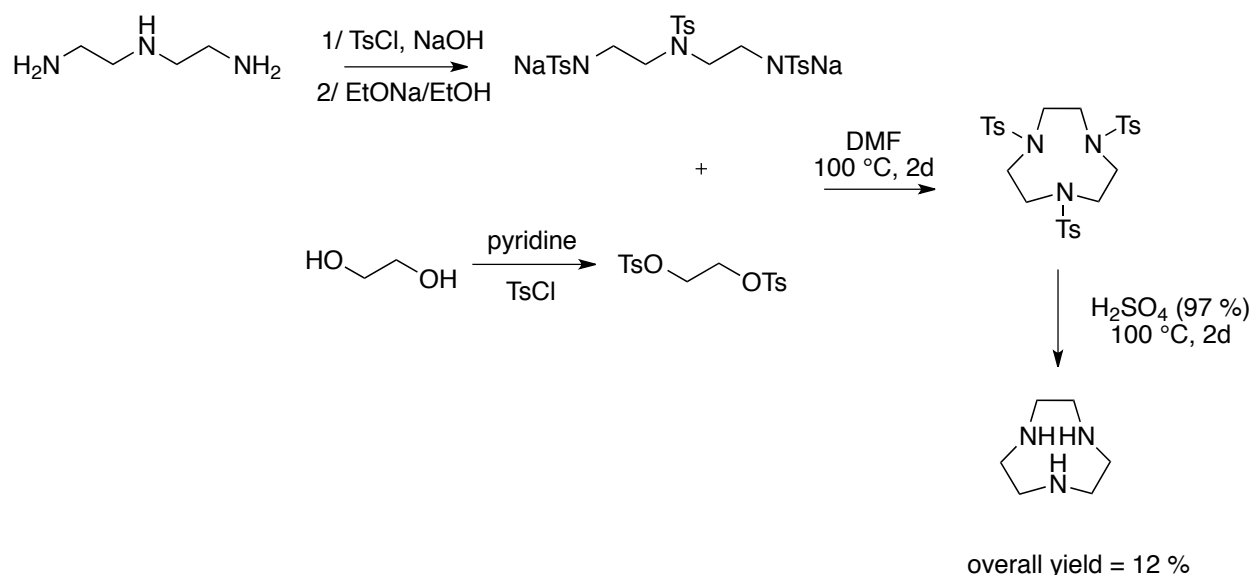
The interest in the synthesis of TACN and its derivatives has been maintained by the use of their metal complexes in a wide range of applications, such as molecular imaging (see chapter I) and catalysis. In thirty years, this class of compounds has appeared in more than 300 patents. Numerous metal complexes that have been prepared include Mn(II–V), Fe(II), Fe(III), Ru(II–IV and VI), Co(III), Ga(III) Cu(II) and Zn(II).<sup>150,151</sup> The ability of triazacyclononanes to stabilize high oxidation states of metal ions, in particular manganese, has led to the development of such complexes as oxidation catalysts. In particular, the ligand 1,4,7-trimethyl-1,4,7-triazacyclononane (METACN) has been the subject of many studies because of the catalytic activity of its binuclear manganese tris-oxo complex  $[(\text{METACN})_2\text{Mn}_2\text{O}_3]^{2+}$ .<sup>152,153</sup> Thus, METACN-Mn(IV) complexes have been used as bleaching agent in laundry formulations,<sup>153</sup> catalyst in olefin polymerization,<sup>154,155</sup> in olefin epoxidation with hydrogen peroxide in water<sup>156</sup> or organic solvents<sup>157</sup> and other oxidation processes.<sup>158,159</sup> Protein orientation at interfaces,<sup>160</sup> metalloenzyme biosite models,<sup>161</sup> magnet molecule clusters,<sup>162,163</sup> and diagnostical or therapeutical metal carriers<sup>59,164</sup> constitute other examples of domains in which the potentialities of TACN derivatives have been exploited.

Despite the above interest in triazacyclononane derivatives, there are few synthetic methodologies reported in the literature giving access to such systems.

### ***II.2.1 Synthetic routes towards TACN derivatives***

#### ***II.2.1.1 Synthesis of triazacyclononane***

The only reported synthesis of TACN follows the general procedure for the preparation of macrocyclic polyamines developed by Richman and Atkins.<sup>146,165</sup> This method is based on the reaction of a bis-*p*-toluenesulfonamide salt with a bis-tosylate or mesylate compound in anhydrous DMF (Scheme II-23). Tosyl groups contribute to preorganization of the intermediates and favor intramolecular cyclization.



Scheme II-23

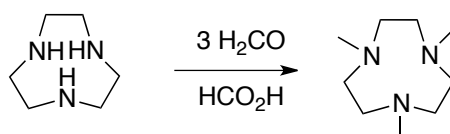
This method is not atom-economic, requires long reaction times and although the macrocyclization step is generally efficient, harsh conditions are required to remove the tosyl groups.

### II.2.1.2 Synthesis of *N*-functionalized TACN

Substitution on the nitrogen atoms is straightforward starting from the TACN intermediate. Selective functionalization reactions can be accomplished by discrimination of the amine functions of the macrocycle. One method consists in the introduction of a functional group before the cyclization step leading to *N*-alkylated derivatives at the end of the synthetic process.<sup>146,166,167</sup>

Selective protection of one or two nitrogen atoms of TACN was also performed by tosylation,<sup>168</sup> carbamation,<sup>169</sup> or pH controlled sulfomethylation,<sup>170</sup> including further purification and/or deprotection steps.

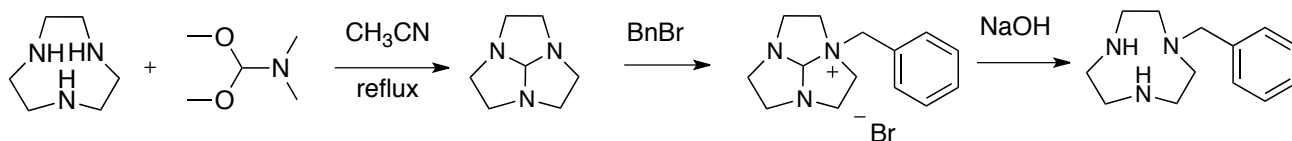
Another route toward *N*-functionalized TACN relies upon the introduction of a single *N*-formyl group masked as a tricyclic orthoamide and subsequent reaction of the orthoamide functional groups. Thus, meTACN was obtained by condensation of formaldehyde on TACN in the presence of formic acid (Scheme II-24).<sup>171</sup>



Scheme II-24

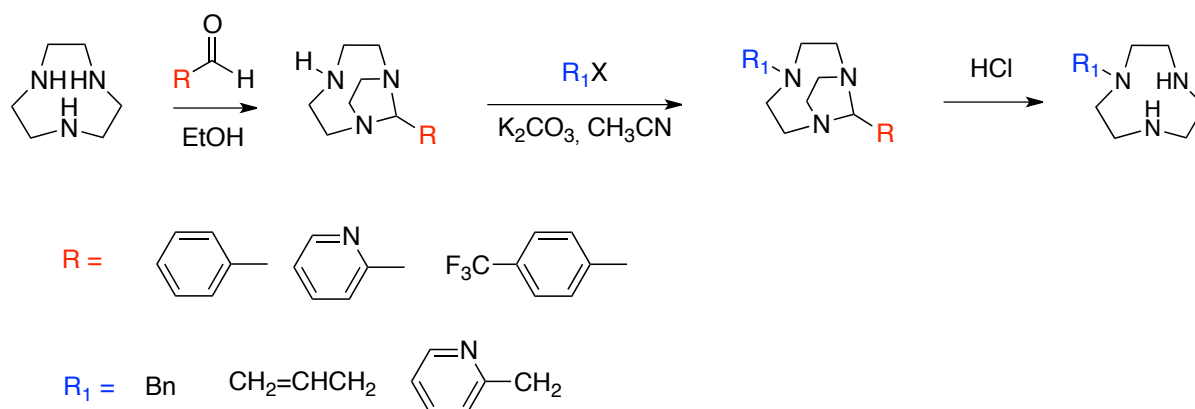


This method also allows the synthesis of selectively mono- or disubstituted compounds (Scheme II-25).<sup>172</sup> Thus, monobenzylTACN was synthesized after treatment of TACN with one equivalent of  $\text{Me}_2\text{NCH}(\text{OMe})_2$ , addition of one equivalent of benzylbromide and hydrolytic removal of the formyl group.



Scheme II-25

A recent route has been investigated by Tripiet and co-workers using mild and rapid conditions of aminal formation with substituted aromatic aldehydes (Scheme II-26).<sup>173</sup> The aminal function plays a protecting role that enables the functionalization with halogenoalkanes. Hydrolysis with hydrochloric acid easily resulted in various TACN derivatives bearing one pendant arm.

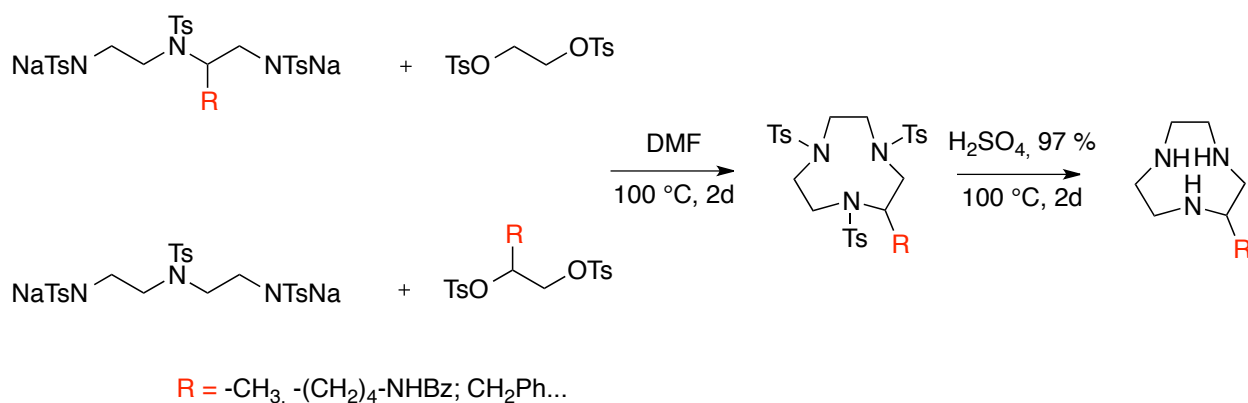


Scheme II-26

The different routes described above are complementary methods and offer choice in the nature of substituents on the nitrogen atoms.

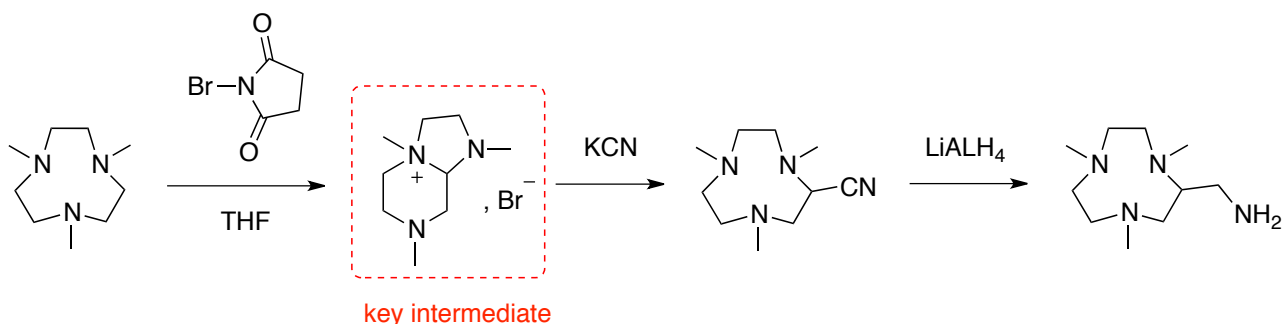
### II.2.1.3 Synthesis of C-functionalized TACN

The access to C-functionalized TACN is permitted through the use of Richman-Atkins conditions. This method requires the tedious preparation of a synthon functionalized on a carbon atom.<sup>174-178</sup>



Scheme II-27

An original method allowing functionalization of a carbon atom starting from meTACN has been reported in the literature (Scheme II-28).<sup>179</sup> Treatment of meTACN with *N*-bromosuccinimide in THF resulted in the oxidation of the macrocycle and in the formation of a bicyclic pyrazinium salt, which is the key intermediate of the synthesis. Addition of potassium cyanide led to the opening of the bicycle to form the expected 9-membered ring. The nitrile was then reduced by  $\text{LiAlH}_4$  in an amino group. Even though the method described reported herein is efficient, it requires the preliminary synthesis of meTACN and can be applied only to *N*-methylated TACN.



Scheme II-28

### II.2.2 Obtention of new TACN derivatives by using the « aminal tool »

Inspired by the previous work, a new methodology using the « aminal tool » was developed in the laboratory.<sup>180</sup> The objective was to mimic the synthetic route developed by Koek *et al*<sup>179</sup> by using well-known tools and the know-how of the laboratory.

The retrosynthesis that was considered is reported in Figure II-16. From the linear amine, we considered the synthesis of a non-substituted aminal followed by the functionalization of the secondary amines and the quaternization of the tertiary amine with adapted electrophiles.

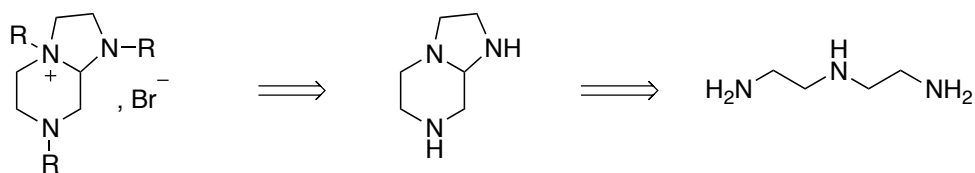
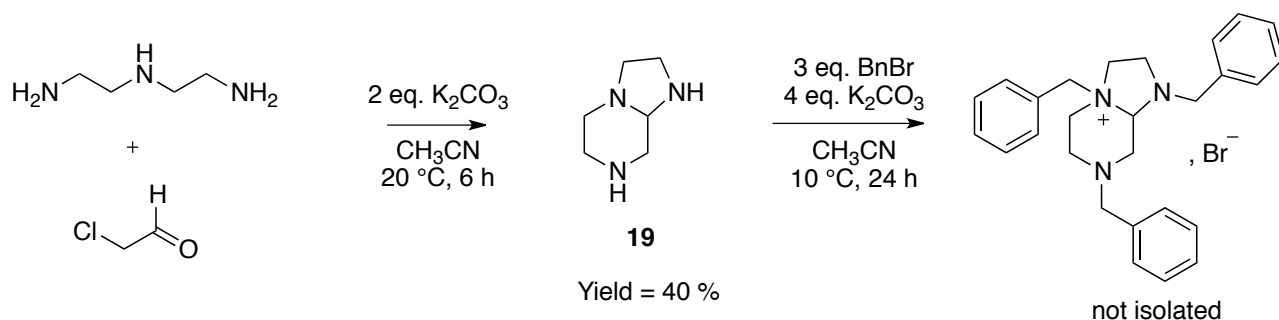


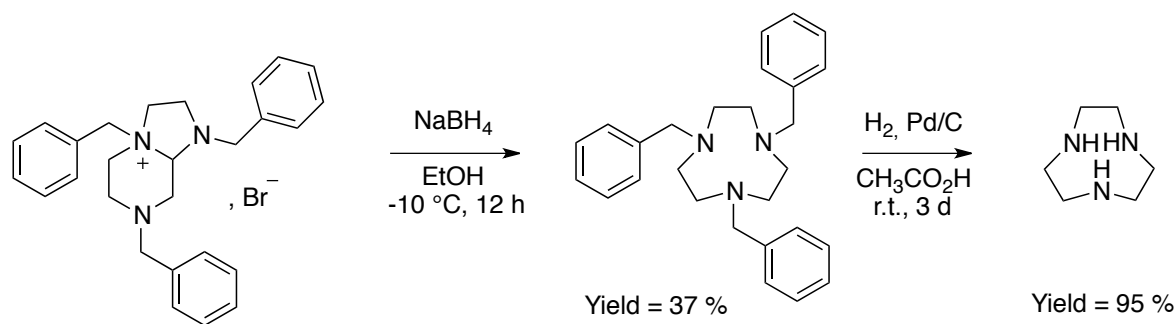
Figure II-16: Retrosynthetic scheme.

The synthetic route was originally developed by Yoann Rousselin.<sup>180</sup> The formation of the amina was performed by addition of chloroacetaldehyde on diethylenetriamine in the presence of potassium carbonate (Scheme II-29). This reaction gave access to the desired amina in 40 % yield and benzylbromide was added yielding the expected ammonium salt which was not isolated.



Scheme II-29

The ring opening of the ammonium salt was performed with hydride as nucleophilic agent (Scheme II-30). Thus, TACN was obtained in two steps from the quaternized compound after addition of NaBH<sub>4</sub> and deprotection of the benzyl group by hydrogenolysis. This synthesis is really efficient. It enables the preparation of TACN in large scale in 14 % yield from the starting linear amine.



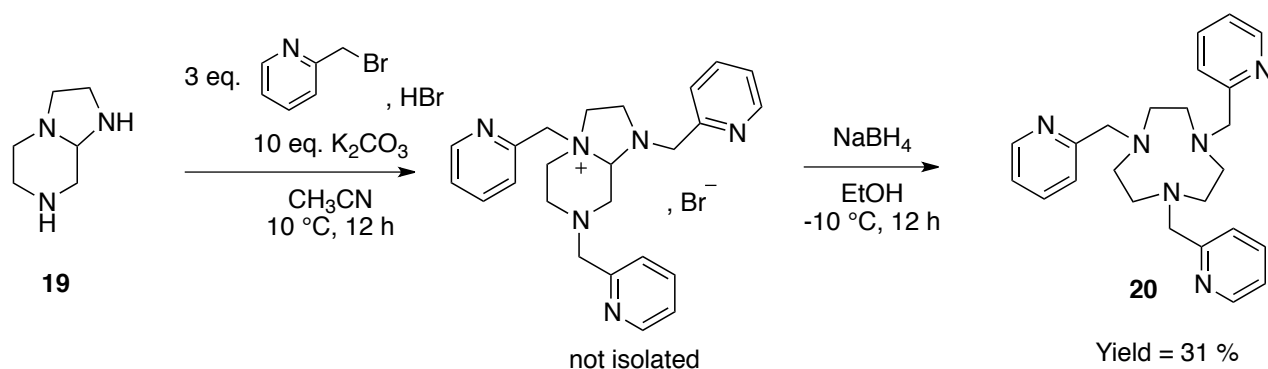
Scheme II-30

We further investigated the reactivity of amina **19** to check whether it was possible to use other electrophiles to build the quaternized ammonium salt.

### II.2.2.1 Functionalization of the aminoral with various electrophiles: towards *N*-functionalized TACN

#### II.2.2.1.1 Synthesis of trispyridineTACN

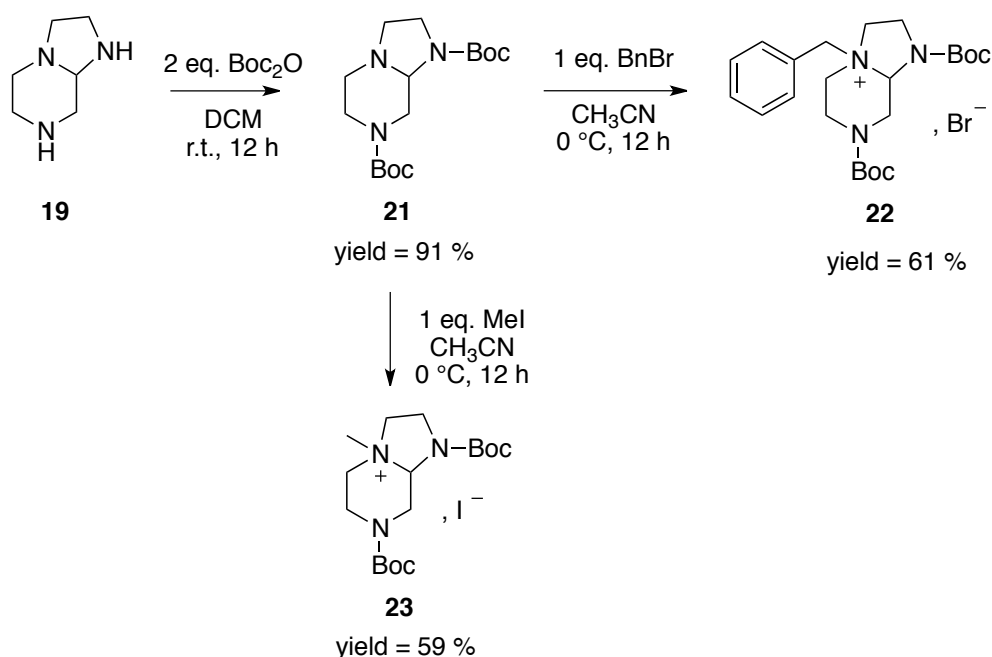
The addition of 2-(bromomethyl)pyridine on aminoral **19** followed by the ring-opening with  $\text{NaBH}_4$  led to the expected compound **20** in 31 % yield (Scheme II-31). Pyridine units are usually used as pendant coordinating arms in reported iron complexes. By this method, the final ligand can be directly obtained in three steps from the linear amine without any protection/deprotection step.



Scheme II-31

#### II.2.2.1.2 Selective *N*-functionalization

As mentioned previously, selective *N*-functionalized TACN is of major interest for the preparation of BFCAs. Such functionalization can be realized only by discriminating one nitrogen atom of the aminoral **19**. The presence of two different kinds of amine functions on **19** enabled the introduction of different groups. Thus, the secondary amines were protected by Boc groups to give compound **21** (Scheme II-32) in 91 % yield. The quaternization reaction was then performed with various electrophiles such as benzylbromide or methyl iodide yielding respectively compounds **22** and **23**.

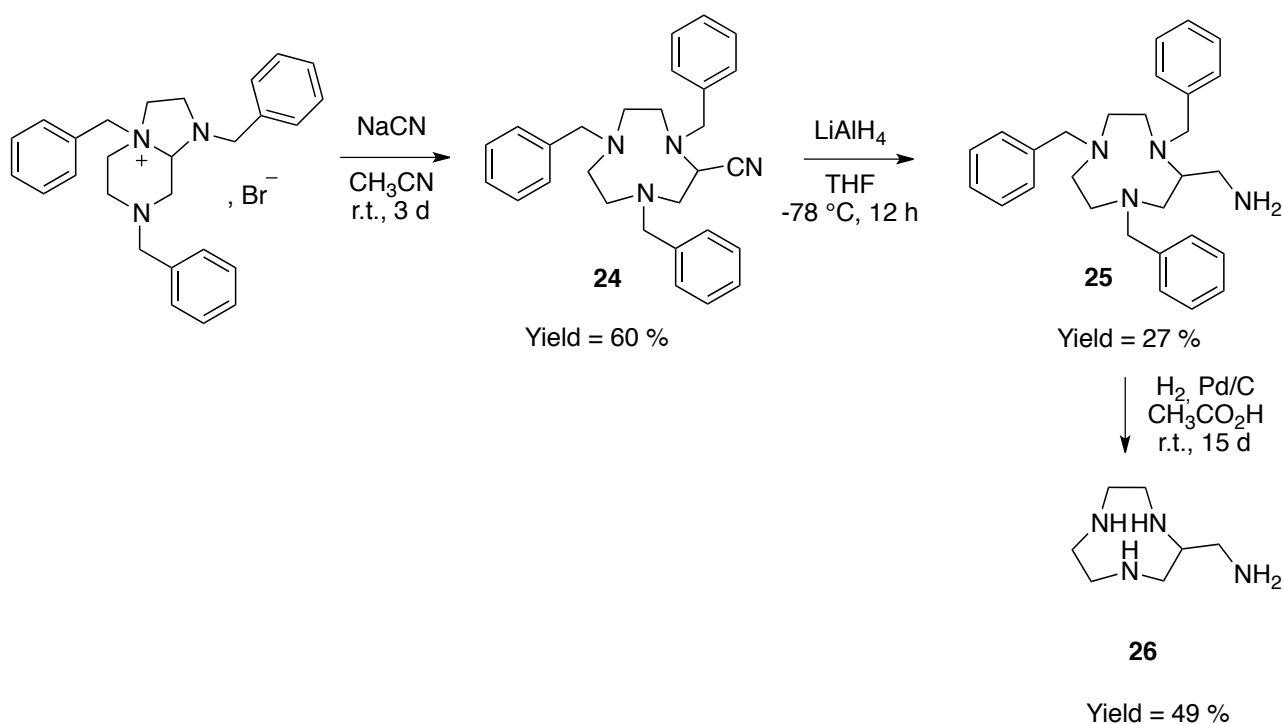


Scheme II-32

The addition of  $\text{NaBH}_4$  on compounds **22** and **23** didn't permit to open the ring even by varying solvent, temperature and number of equivalent. The addition of  $\text{LiAlH}_4$ , which is a stronger reducing agent, enabled the ring opening but also induced reduction of Boc groups in methyl. The reduction of Boc group by  $\text{LiAlH}_4$  has been previously reported. The formation of both  $\text{Me}_2\text{BnTACN}$  and  $\text{Me}_3\text{TACN}$  was attested by mass spectrometry. However, the desired products were obtained in a so low quantity that it was impossible to isolate them.

### II.2.2.2 Synthesis of C-functionalized TACN

In the previous part, ring opening was performed by using hydrides. The use of another nucleophile enabled the synthesis of new C-functionalized TACN. Thus, the addition of sodium cyanide on the quaternized ammonium salt yielded compound **24** which is a TACN derivative bearing a nitrile group (Scheme II-33).<sup>180</sup> The reduction of the nitrile was performed with  $\text{LiAlH}_4$  and the benzyl groups were then deprotected by hydrogenolysis, thus giving the C-aminomethyl TACN **26**.

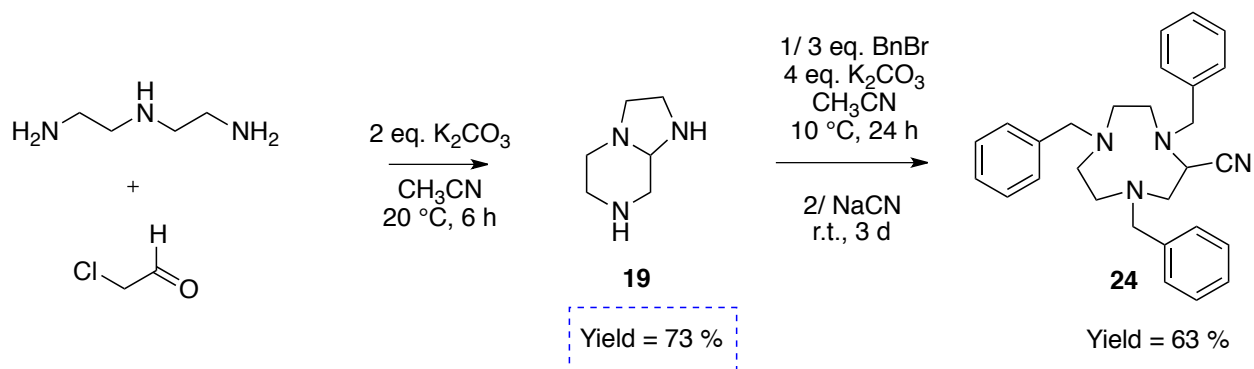


Scheme II-33

Such protected and non-protected aminomethyl TACN, **25** and **26** respectively, have never been reported in the literature. They are valuable precursors of a wide range of C-functionalized TACN-based BFCAs. However, the overall yield is low. Indeed, the fully deprotected TACN is obtained in 3 % yield in five steps from the linear amine. Moreover the method was not reproducible in large scale. The triprotected aminomethyl-derivative **25** was particularly difficult to isolate. These issues prompted us to optimize the synthetic procedure.

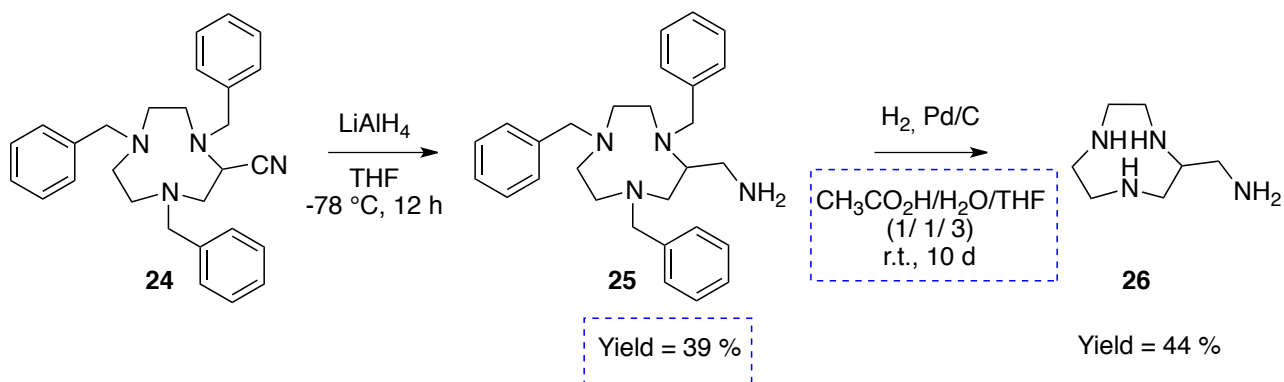
#### II.2.2.2.1 Optimization of the synthetic procedure

In the first step, cyclization reaction is in competition with polymerization reactions. By slowing down the addition process of chloroacetaldehyde on the linear amine, it was possible to synthesize aminal **19** in 73 % yield instead of 40 %.



Scheme II-34

As mentioned above, compound **25** was quite difficult to isolate (Scheme II-35). The process was optimized through several precipitation steps of the protonated species in a mixture of acetone/ethanol (1.5/0.5). The resulting powder was then recrystallized in water and after deprotonation, the desired product was isolated in 39 % yield. Even though this step remains delicate; the process is efficient and enabled the preparation of 160 g of compound **25**. It was also possible to shorten the reaction time of the debenzoylation step by using a mixture of acetic acid, water and THF.



Scheme II-35

The molecule **26** could be recrystallized in a 37 % HCl aqueous solution and its structure was elucidated by X-Ray diffraction. The crystal structure (Figure II-17) indicates that the compound is tetraprotonated.

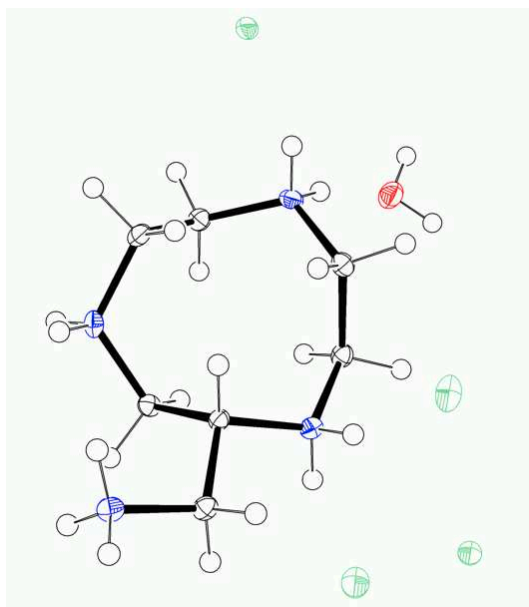


Figure II-17: ORTEP<sup>149</sup> view of compound **26**. Thermal ellipsoids are drawn at 50% probability.

By following this optimized procedure, we were able to synthesize compound **26** in 8 % yield from the linear amine. The synthetic method is reproducible and can be applied in large scale.

### ***II.2.3 Synthesis of new BFCAs based on C-functionalized TACN***

A wide range of new and promising BFCAs can be generated from the aminomethyl TACN-based precursors **25** and **26**. First attempts of functionalization were performed on the amino group to introduce various grafting functions. The introduction of original pendant coordinating arms was also considered. These two aspects will be presented in the two following parts.

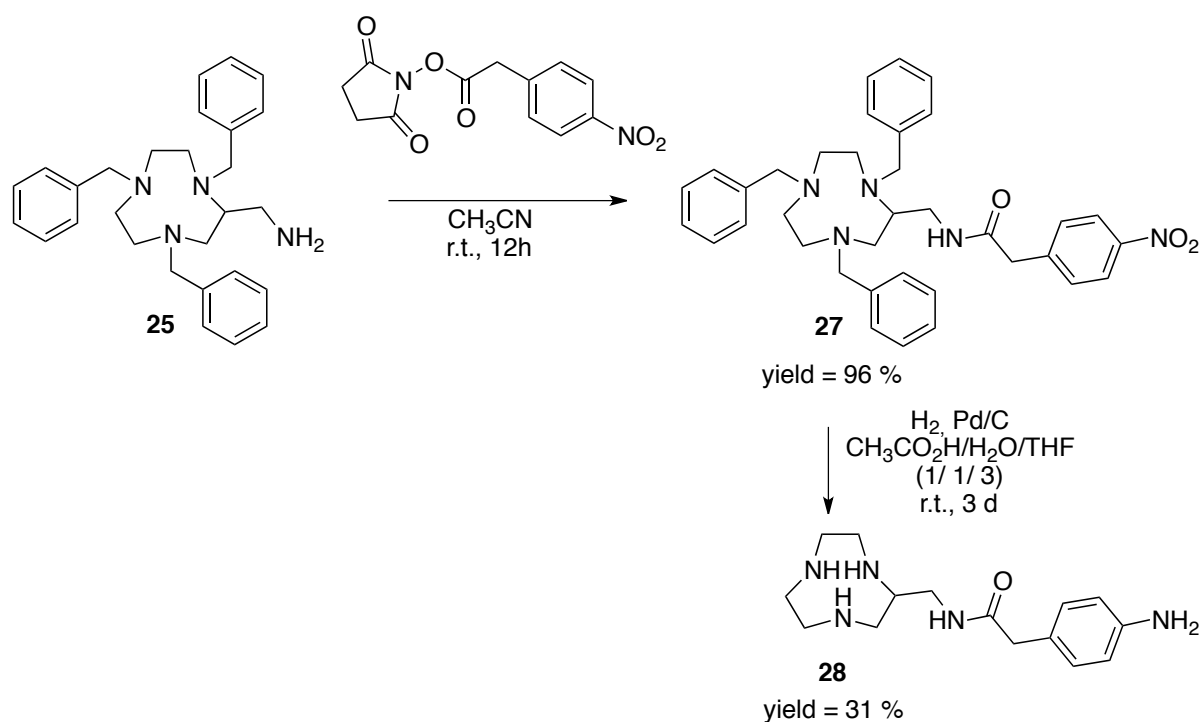
#### ***II.2.3.1 Choice of the grafting function***

Several grafting functions can be introduced on the macrocycle. Based on previous work on cyclen and homocyclen developed in the laboratory,<sup>148</sup> we considered the preparation of new chelating systems carrying either isothiocyanate, carboxylic acid or carboxylic anhydride function for coupling to lysine residues. The targeting vector can be also introduced by « click chemistry » reactions, involving alkyne and azide derivatives. Thus, we also investigated the synthesis of a C-functionalized TACN bearing a terminal triple bond.

##### **II.2.3.1.1 Introduction of an isothiocyanate function**

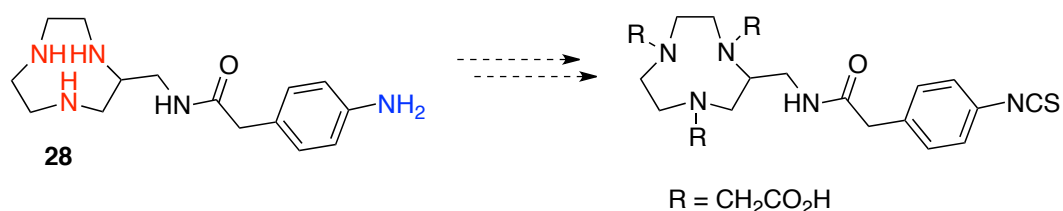
As described in chapter **II.1.3**, the synthesis of derivatives carrying an isothiocyanate function requires the preparation of a precursor possessing a *p*-nitrophenyl group. The addition of one equivalent of *N*-succinimidyl-4-nitrophenylacetate on compound **25** in acetonitrile at room temperature resulted in the formation of **27** in 96 % yield (Scheme II-36). The next step consisted in both reduction of the nitro group and deprotection of the benzyl groups. Thus, the desired compound **28** was isolated after 3 days.





Scheme II-36

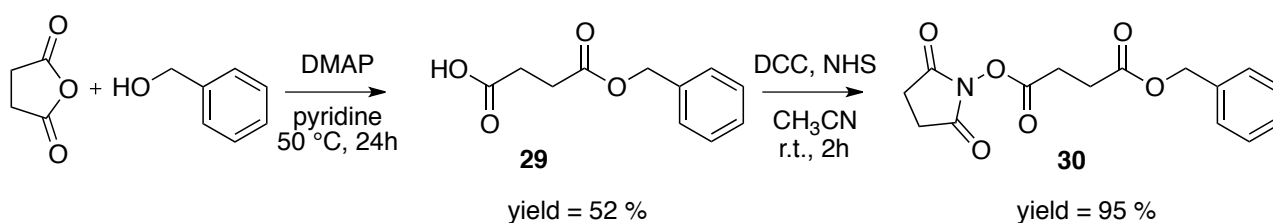
Compound **28** is a valuable building block that enables selective functionalization, aniline function being less reactive than secondary amines. The synthesis of a new class of BFCAs based on *C*-functionalized TACN is being currently undertaken from this precursor. The addition of the proper number of *tert*-butylbromoacetate equivalents on compound **28** should yield the expected trifunctionalized molecule. After cleavage of the ester groups in acidic conditions, the addition of thiophosgene will enable the introduction of the isothiocyanate function.



Scheme II-37

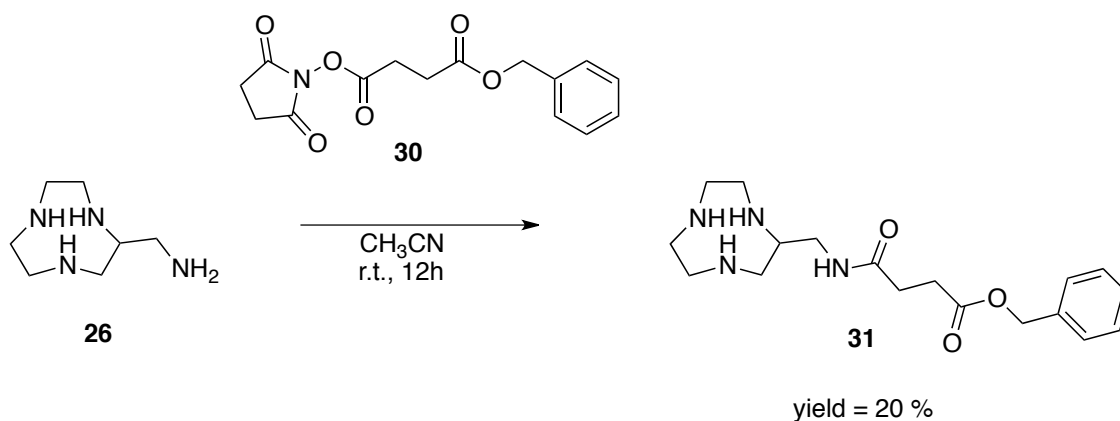
### II.2.3.1.2 Introduction of a carboxylic acid function

The synthetic route that was considered involved the preparation of an activated ester bearing a protected carboxylic function and the desired compound was successfully obtained.<sup>148</sup> This route was investigated in TACN series. Thus, the desired activated ester **30** was prepared in two steps from succinic anhydride and benzyl alcohol (Scheme II-38). Compound **30** possesses two acid functions: one is activated (NHS) for the coupling to the macrocycle, one is protected (OBn) for bioconjugation purposes.



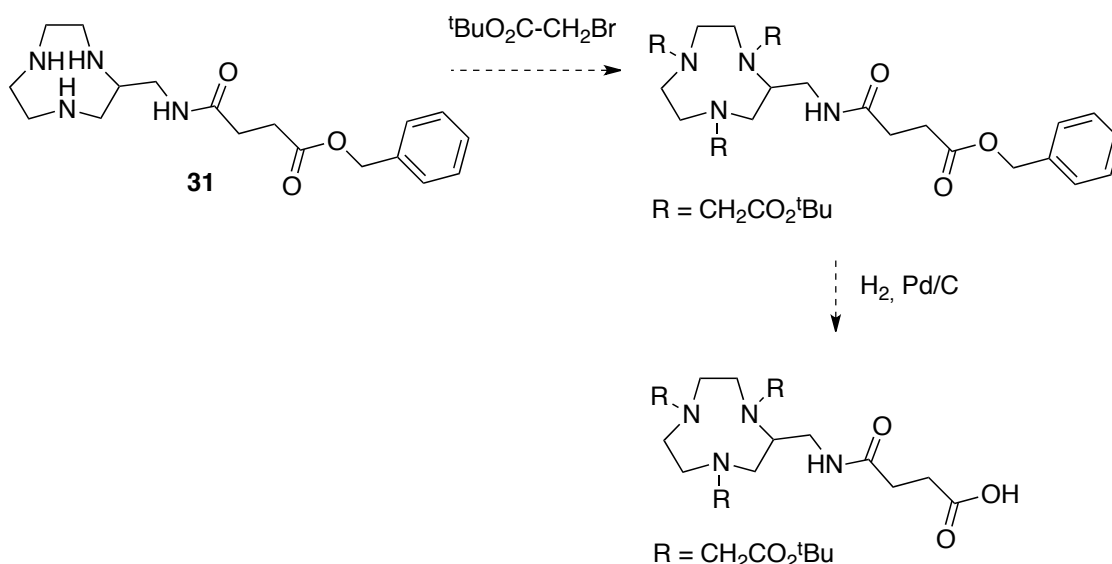
Scheme II-38

Primary amine being more reactive than secondary amine, activated ester **30** was directly added on macrocycle **26** and the reaction gave access to a mixture of compound **31** and NHS (Scheme II-39). Such by-product is usually removed by basic treatment. However, benzyl acetate functions are easily cleaved in such conditions and the use of base is, in this case, prohibited. Thus, compound **31** was purified by chromatography on reverse phase and isolated in 20 % yield.



Scheme II-39

Compound **31** needs to be further functionalized with pendant arms such as *tert*-butylacetate (Scheme II-40). The selective deprotection of the benzyl group by hydrogenolysis will release the carboxylic acid function, which allows selective covalent binding to the targeting vector.



Scheme II-40

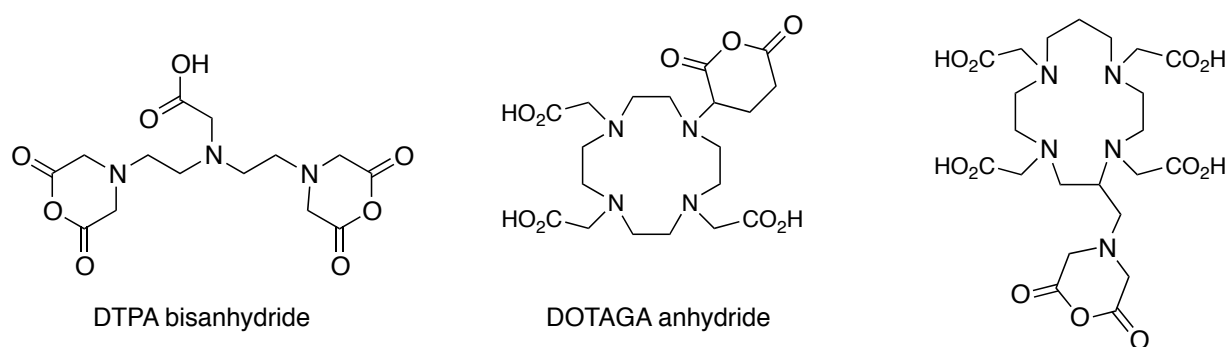
### II.2.3.1.3 Introduction of a carboxylic acid anhydride function

An alternative solution for attaching the macrocycle to the biomolecule is the use of a compound containing an acid anhydride functional group. The reaction with amines or other nucleophilic agents provides easy access to bifunctional chelating agents. Moreover, when compared to other activated acid derivatives, such as NHS or phenolic esters, the formation of the amide bond between the anhydride and the amine groups generates no side-product that need to be separated from the conjugate.

This approach has proved to be very efficient in the case of DTPA chelator. DTPA-bisanhydride has been used successfully for labeling antibodies (e.g. trastuzumab),<sup>181</sup> enzymes<sup>182</sup> or nanoparticles<sup>183</sup> for MRI and therapy (Scheme II-41).

Recently, the synthesis of a new DOTA bearing an anhydride function derivative, so-called DOTAGA-anhydride (Scheme II-41), was investigated in our group.<sup>184</sup> The use of this new bifunctional chelating agent represents a very convenient and attractive approach for the preparation of various bioconjugates for imaging and therapy. Thus, DOTAGA-anhydride was used to prepare ultrasmall nanoparticles decorated with DOTAGA units.<sup>185</sup> <sup>111</sup>In labeled DOTAGA-antibodies conjugates were also prepared in our group, showing the usefulness of the DOTAGA-anhydride for the efficient attachment of radiometal to a humanized mAb. A high specific tumor targeting was shown in a model of human breast tumors overexpressing HER2/neu antigen.<sup>186</sup> More generally, this building block can be used for the synthesis of a large variety of DOTA like compounds, such as bimodal agents for SPECT/Optical imaging.<sup>184</sup>

The method was also extended to prepare the equivalent in homocyclen series (Scheme II-41).<sup>148</sup>



Scheme II-41

Inspired by this previous work, we considered the introduction of a carboxylic acid anhydride function on a TACN core by functionalization of the primary amine (Figure II-18).

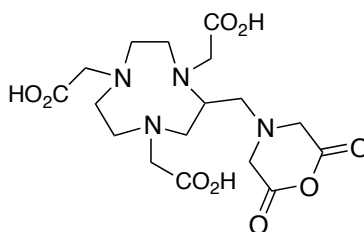
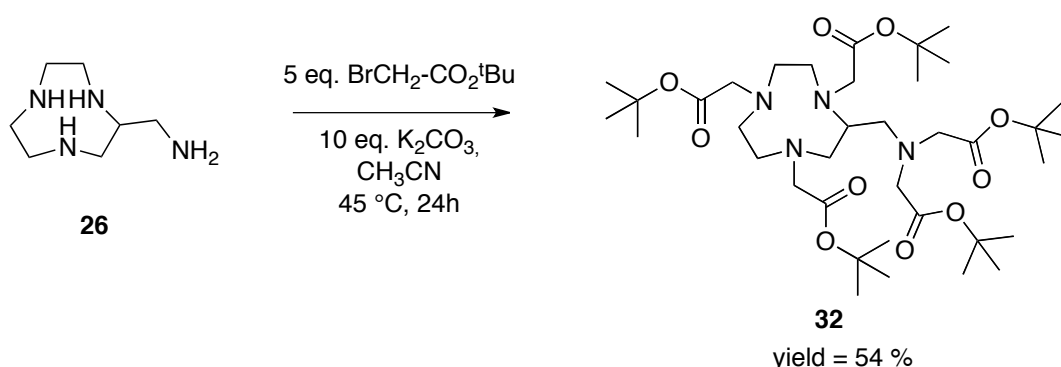


Figure II-18: Targeted building block.

The procedure developed by Claire Bernhard was followed to prepare the targeted molecule. Thus, five equivalents of *tert*-butylbromoacetate were added on compound **26** in the presence of K<sub>2</sub>CO<sub>3</sub> in acetonitrile (Scheme II-42). The analysis of the mass spectrum indicated the coexistence of two species, *i.e.* the desired compound **32** and the compound resulting from the addition of six arms on **26**. The purification process was not straightforward and required several successive chromatographic columns on aluminium oxide, thereby affording **32** in 54 % yield.



Scheme II-42

The <sup>13</sup>C{<sup>1</sup>H} NMR spectrum recorded in CDCl<sub>3</sub> (Figure II-19) confirmed the purity of compound **32**. It has to be noted that two *tert*-butylacetate arms being equivalent, only four signals

are expected for the ester carbonyl groups and for the quaternary carbon atoms of the *tert*-butyl groups.

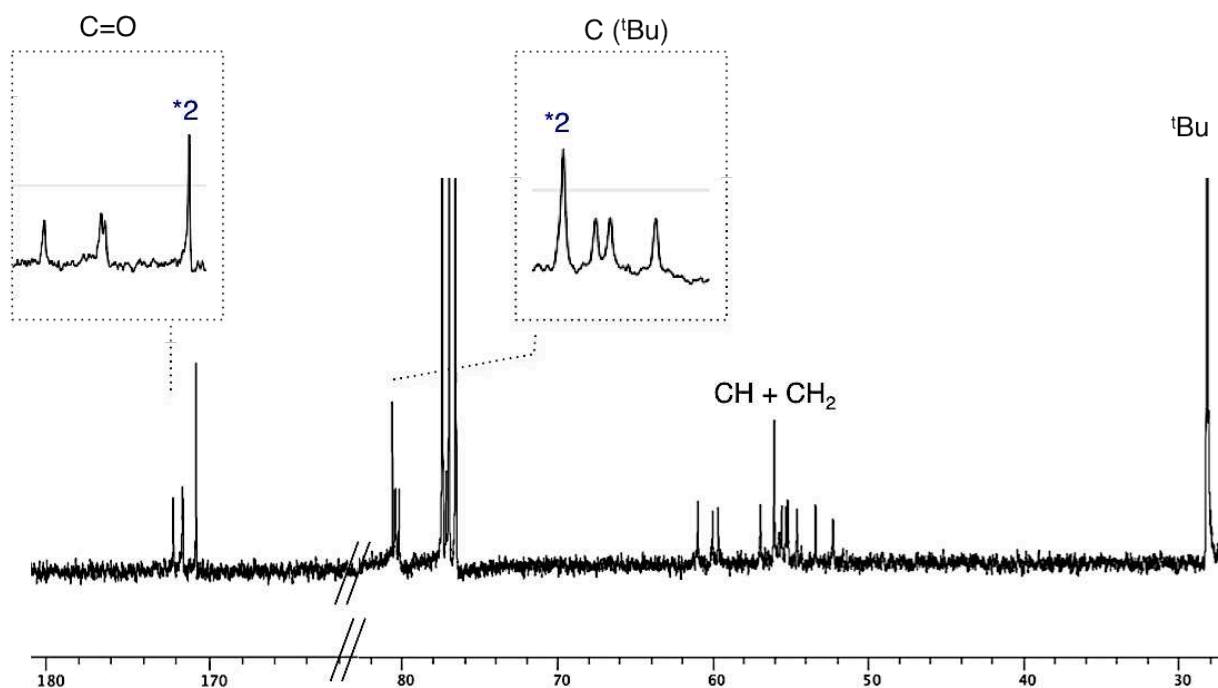
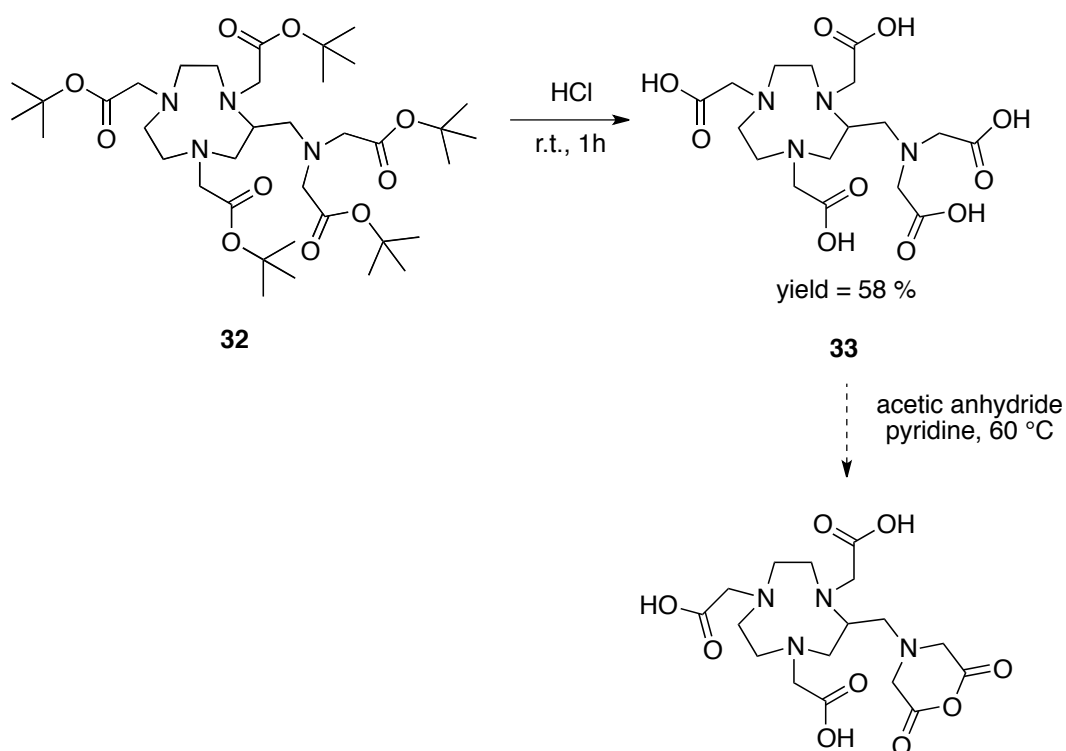


Figure II-19:  $^{13}\text{C}\{^1\text{H}\}$  NMR spectrum of compound **32** (300 MHz,  $\text{CDCl}_3$ , 300 K).

All *tert*-butylic ester functions were then deprotected in a concentrated HCl solution (Scheme II-43) to give **33** in 58 % yield. The cyclic anhydride should be generated after addition of acetic anhydride in the presence of pyridine at 60 °C. This reaction is being currently investigated in our group.

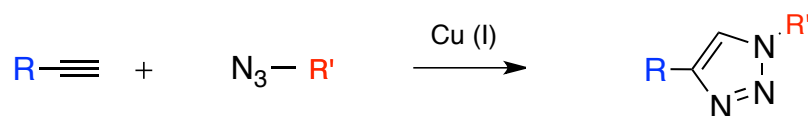


Scheme II-43

### II.2.3.1.4 Bioconjugation by « click chemistry »: preparation of a TACN-based derivative bearing a triple bond

#### II.2.3.1.4.1 « Click chemistry » reaction

One particularly advantageous approach for chemical conjugation is the use of so-called « click chemistry », which has received remarkable attention over the past several years for use in numerous applications in bioconjugate chemistry.<sup>187-191</sup> The most-widely used click reaction, first described by Huisgen, is based on a [3+2] cycloaddition reactions between azides and alkynes to form triazoles (Scheme II-44). Copper (I) catalyzed variants of this cycloaddition have been subsequently developed that lead to triazole products in high yields under mild conditions.<sup>192</sup>



Scheme II-44

The use of the Cu(I)-catalyzed cycloaddition of azides and terminal alkynes has only very recently found applications in the design of probes for molecular imaging.<sup>89,189,191,193</sup> Such cycloaddition gives high chemical yields under mild reaction conditions even in aqueous media. The reactions are regiospecific (resulting exclusively in the formation of 1,4-bifunctionalized 1,2,3-triazole products). Moreover the reagents are compatible with biologically relevant motifs and the resultant triazole can play a potential role in the coordination chemistry of the final complex.<sup>90,193,194</sup>

Very few publications have reported the use of copper catalyzed click reactions for the coupling of metal chelators to bioactive molecules.<sup>88,190,194-196</sup> This is primarily due to the affinity of the Cu catalyst for the macrocyclic chelator moiety; which results in copper sequestration and decreases the efficiency of the catalyst. Recently, however, Lebedev *et al.*, described the facile preparation of CB-TE2A-peptide conjugates by Cu(I) catalyzed azide-alkyne click chemistry (Figure II-20).<sup>197</sup> Copper was removed from the bioconjugated chelators by precipitation with sodium sulfide Na<sub>2</sub>S and this work represents a promising route for preparation of bioactive radiolabeled agents. Recently, Martin *et al.* have recently developed a method to conjugate a DOTA derivative to a neuropeptide using copper-free click chemistry.<sup>91</sup>

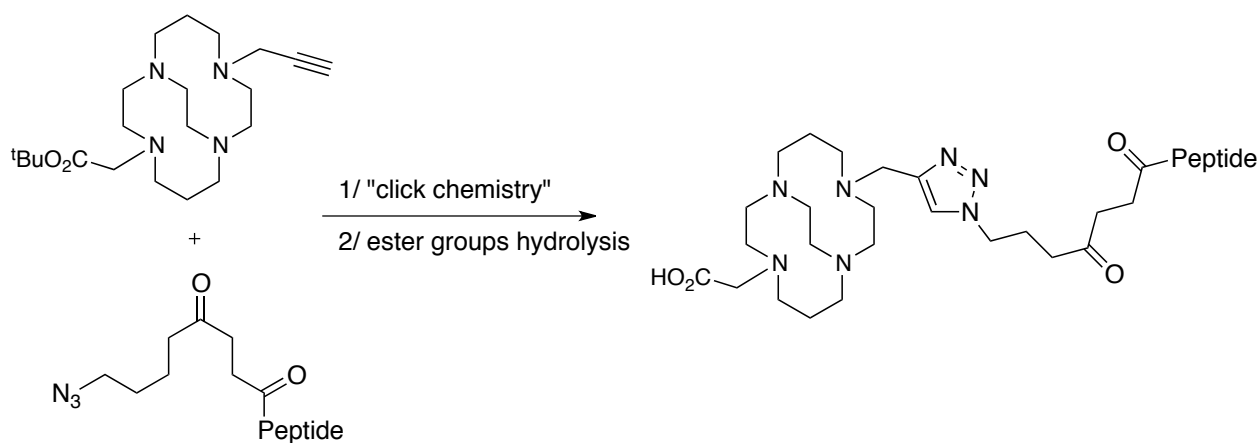
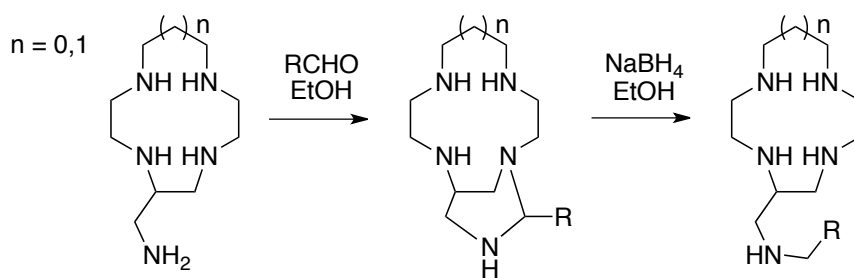


Figure II-20: « Click » conjugation on a model peptide.<sup>197</sup>

Thus, the « click chemistry » approach offers an attractive complement to more traditional methods of conjugating macrocyclic chelators to peptides. In this context, we considered the synthesis of a TACN-based precursor allowing « click » reactions.

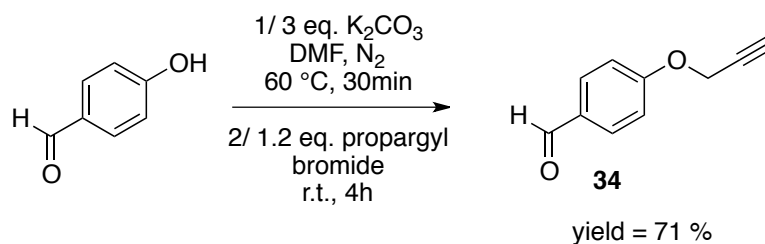
#### II.2.3.1.4.2 Synthesis of a new C-functionalized TACN bearing an alkyne group

The triple bond will be introduced by functionalization of the primary amine by following a synthetic procedure developed in the laboratory (Scheme II-45).<sup>124,180</sup> This procedure is based on the peculiar reactivity of C-aminomethyl macrocycles with aldehydes, resulting in the highly regioselective N-functionalization of the pendant primary amine group. The addition of one equivalent of aldehyde on such macrocycles resulted in the formation of a six-membered exocyclic amination in around 80 % yield, which after reduction yields exclusively the compound N-functionalized on the exocyclic nitrogen atom (Scheme II-45).



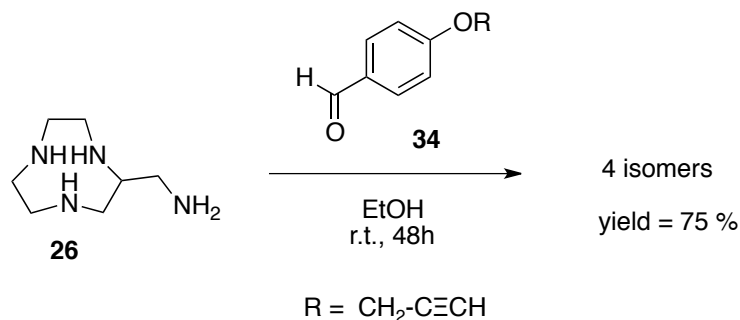
Scheme II-45

We first prepared a synthon carrying both an aldehyde and an alkyne group.<sup>198</sup> Thus, compound **34** was obtained after addition of propargylbromide on 4-hydroxybenzaldehyde in basic conditions (Scheme II-46).



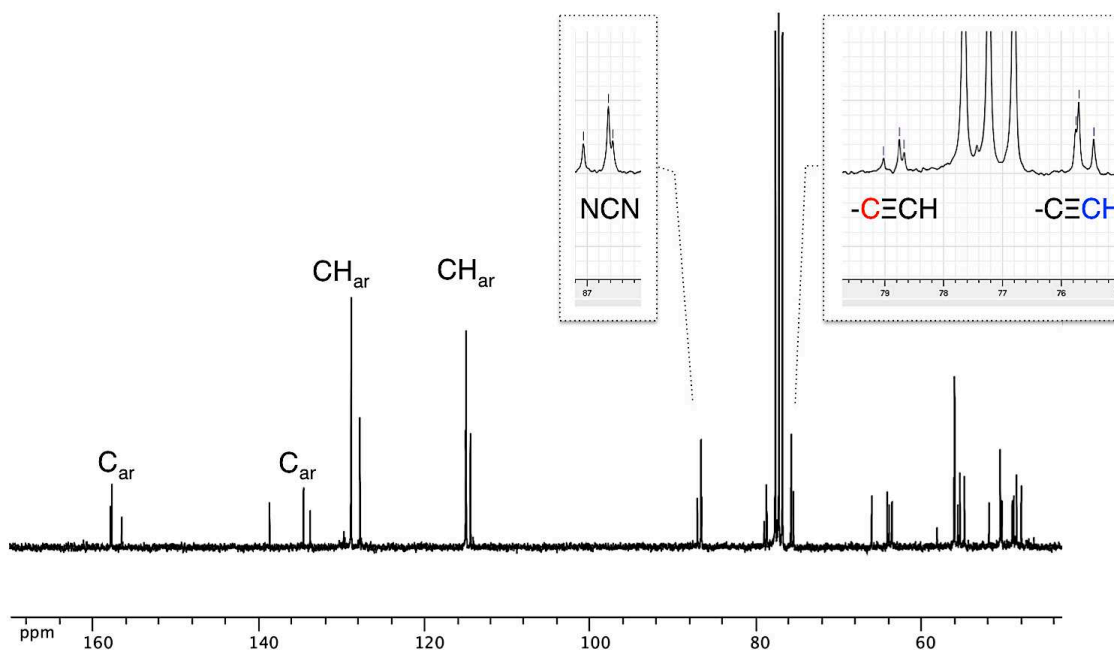
Scheme II-46

Surprisingly, treatment of compound **26** with aldehyde **34** resulted in a mixture of four compounds as attested by NMR spectroscopy (Scheme II-47, Figure II-21).



Scheme II-47

The  $^{13}\text{C}\{^1\text{H}\}$  spectrum shows the absence of the signal characteristic of an imine bond indicating that all the species are aminal compounds. This is confirmed by the presence of at least three signals around 86 ppm, that are typical of aminal carbon.

Figure II-21:  $^{13}\text{C}\{^1\text{H}\}$  NMR spectrum of **35** and **35'** (125 MHz,  $\text{CDCl}_3$ , 300 K).



The coexistence of several aминаl derivatives indicates that the reaction is not regioselective as in case of cyclen and homocyclen.<sup>124,148,180</sup> Unfortunately, we were not able to separate them by precipitation or recrystallization.

The formation of thermodynamically stable five- or six-membered ring аминаl derivatives is of course favored. Figure II-22 lists all аминаl derivatives that can be formed during the reaction. All compounds possess two chiral centers, *i.e.* the аминаl carbon and the carbon atom bearing the аминomethyl arm. Thus, several stereoisomers are expected.

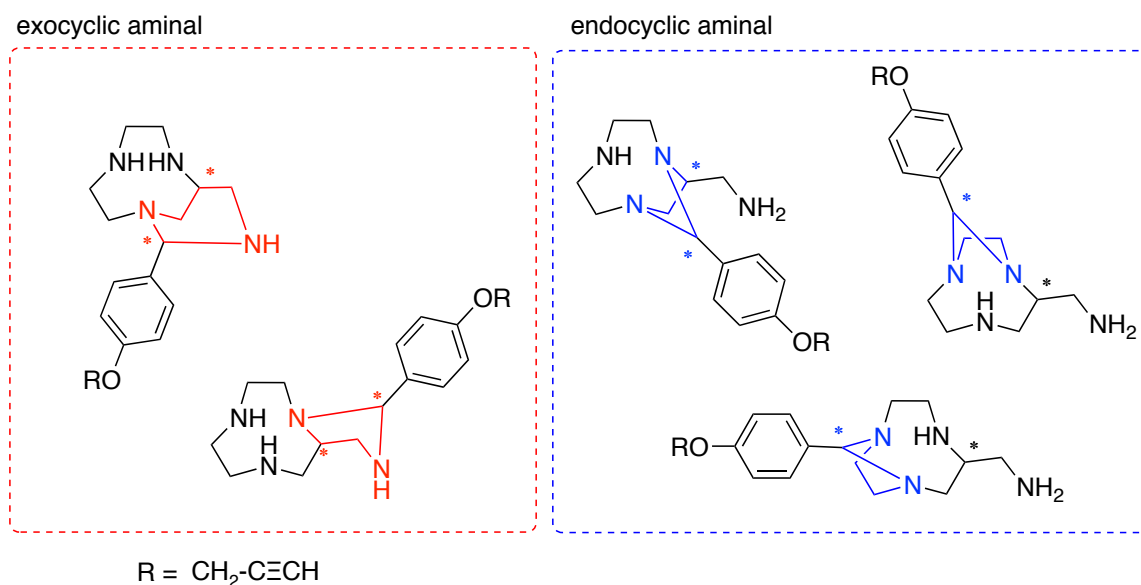
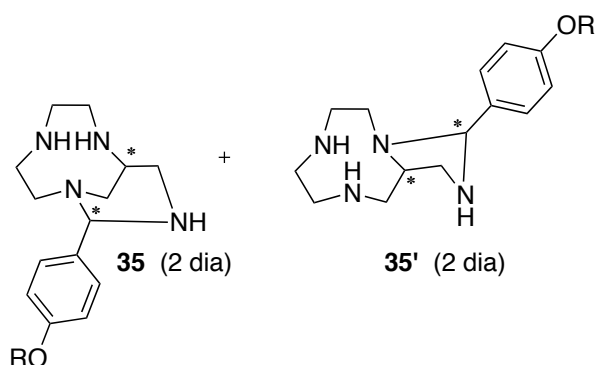


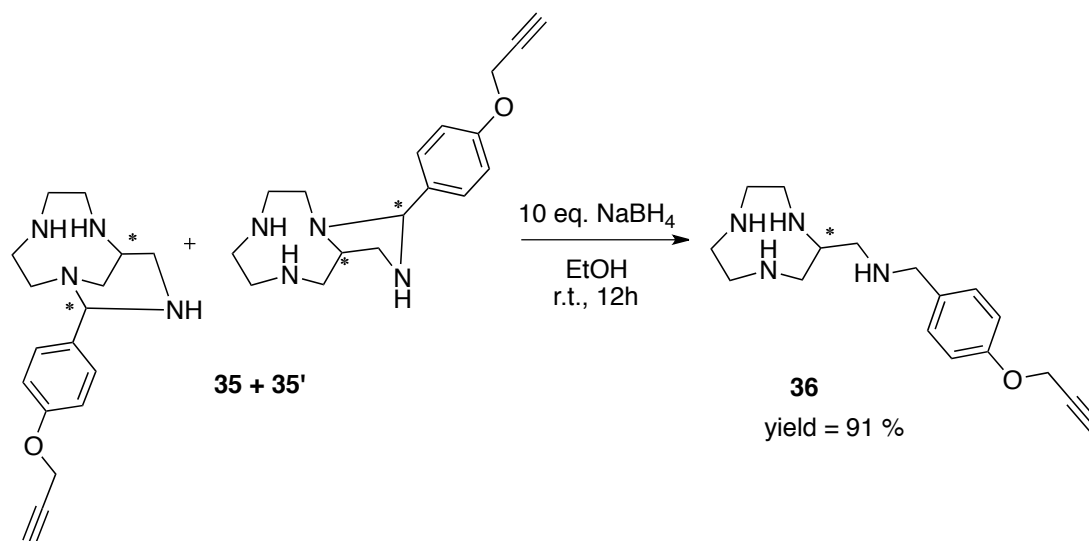
Figure II-22: Thermodynamically stable аминаl derivatives that can be formed by reaction of compound **26** with aldehyde **34**.

Primary аmine being more reactive than secondary аmine, we can suppose that the formation of exocyclic аминаls is favored. This behavior has been previously demonstrated in cyclen and homocyclen series.<sup>148,180,199</sup> In this case, we obtained a mixture of two regioisomers **35** and **35'**. Compounds **35** and **35'** are both a mixture of diastereoisomers.



Scheme II-48

The addition of  $\text{NaBH}_4$  on the mixture of **35** and **35'** resulted in the formation of a sole product **36** in 91 % yield (Scheme II-49). Further studies are being currently investigated to confirm the structure of compounds **35** and **35'**.



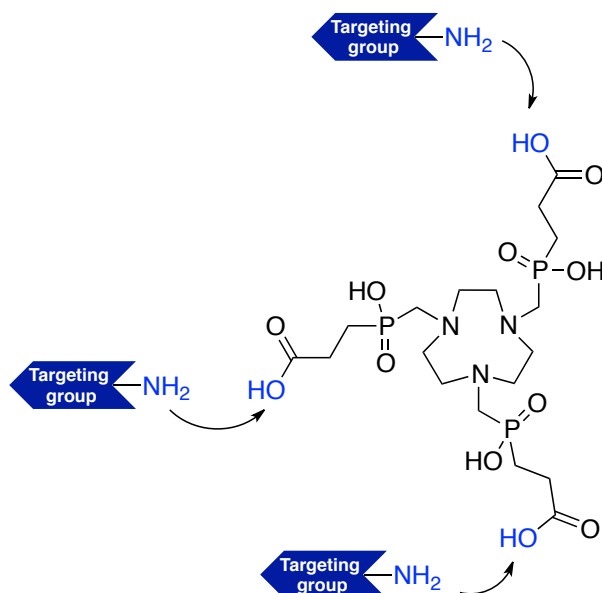
Scheme II-49

### II.2.3.2 Synthesis of new TACN-based bifunctional phosphinate ligands

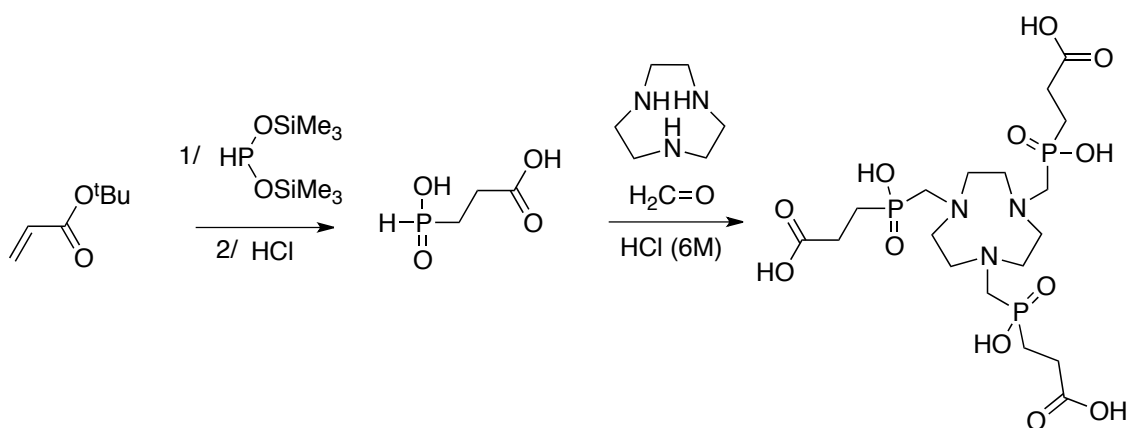
In the previous part, the synthesis of new TACN-based systems carrying various grafting functions was described. Such macrocyclic ligands were functionalized with acetate pendant arms to optimize metal chelation. Recently, several groups have reported the promising properties towards metal chelation of polyazamacrocycles bearing phosphonate and phosphinate arms.<sup>63-65,200-202</sup> In the next part, we will be particularly interested in the new TACN-based bifunctional phosphinate ligands reported in the literature. We will then present the synthesis of new C-functionalized analogues prepared in the laboratory.

#### II.2.3.2.1 Reported work on new triphosphinic acid TACN and synthetic tools

Notni and co-workers reported the synthesis of a novel bifunctional triphosphinic acid chelator based on TACN, so-called TRAP. This chelator complexed  $^{68}\text{Ga}$  much more efficiently than the established BFCAs (Figure II-23), *i.e.* it allows fast complex formation in mild labeling conditions.<sup>65</sup> Such system constitutes an ideal framework for the preparation of multimeric bioconjugates.<sup>64,66,67</sup> Indeed, phosphinic acid and carboxylic groups exhibiting different reactivity, the carboxylate functions can be functionalized without having to protect the phosphinate moieties.<sup>63</sup>

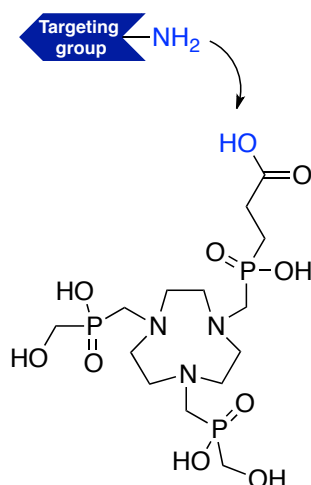
Figure II-23: Structure of TRAP.<sup>63</sup>

TRAP was synthesized via a Mannich-type reaction using a phosphorous precursor, formaldehyde and TACN.<sup>63</sup> The phosphorus precursor was obtained in two steps (Scheme II-50). After reaction between *tert*-butylacrylate and bis(trimethylsilyl)hydrophosphite, which was generated *in situ*, the mixture was hydrolyzed in acidic conditions. The resulting species was then added to TACN in the presence of formaldehyde and the desired trifunctionalized TACN was isolated in 55 % yield. Carboxylate groups were then used as conjugation sites and coupled with many targeting molecules.<sup>64,67</sup>



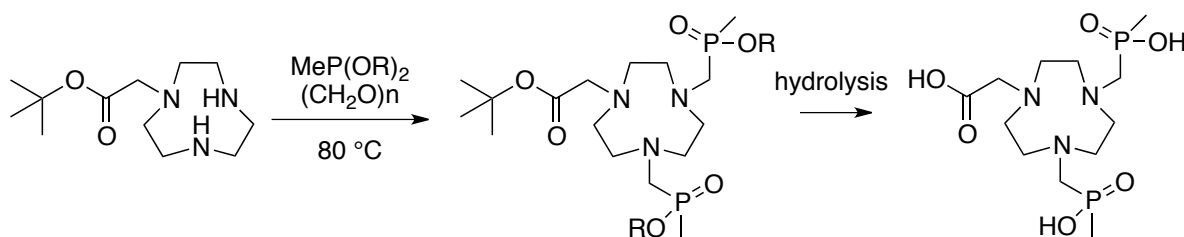
Scheme II-50

Pursuing this approach, Notni and co-workers developed the synthesis of a TRAP derivative, so-called NOPO, which possesses only one site for bioconjugation (Figure II-24A).<sup>66</sup>

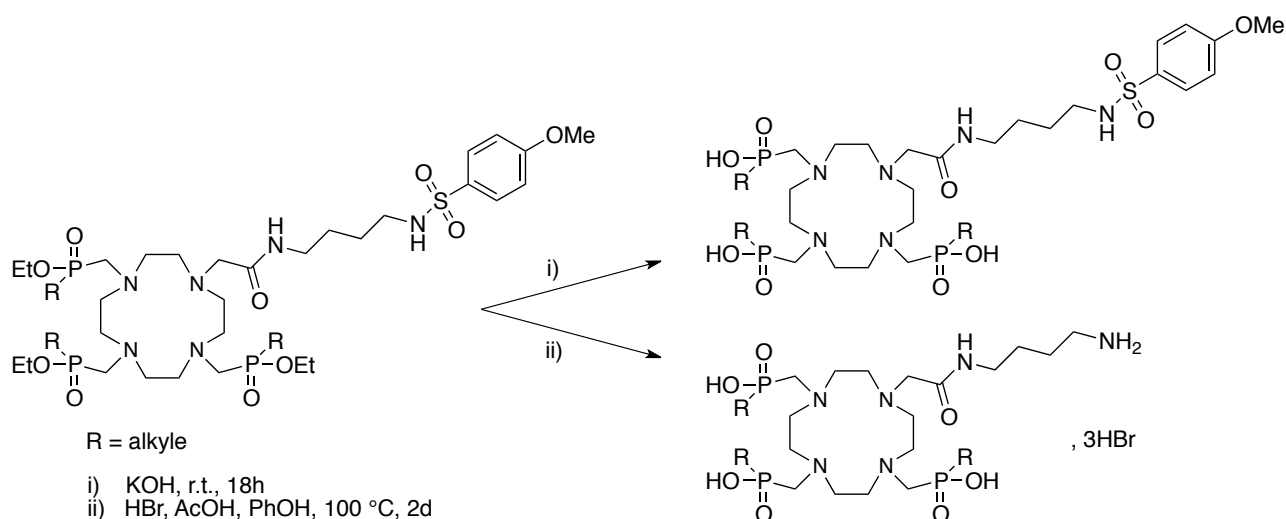
Figure II-24: Structure of the NOPO chelator.<sup>66</sup>

Notni and co-workers worked out a powerful route towards phosphinate derivatives. However, the reaction conditions are particularly harsh. The use of concentrated acidic solution under heat is indeed not compatible with several organic functions. Milder conditions were previously reported by Huskens and co-workers (Scheme II-51).<sup>203</sup> Thus, this procedure enabled the synthesis of various ligands containing acetate and methylphosphinate side chains in good yield in short synthetic sequences.<sup>200,202,204</sup>

The method is based on the condensation of paraformaldehyde on a TACN unit leading to the formation of iminium species. These species are then trapped by the appropriate alkyl dialkoxyposphine to yield the corresponding di-phosphinate esters after rearrangement.<sup>205</sup> The hydrolysis of phosphinate ester was performed either in acidic or basic conditions.<sup>200,202,204-206</sup>

Scheme II-51<sup>203</sup>

Moreover, the selective deprotection of phosphinate esters was possible in presence of sensitive functions such as amide or sulfonamide (Scheme II-52).<sup>205</sup>

Scheme II-52: Selective hydrolysis of phosphinate esters.<sup>205</sup>

All these data prompted us to investigate the synthesis of new *C*-functionalized TACN carrying both a grafting function and phosphinate arms.

### II.2.3.2.2 Synthesis

We aimed at synthesizing a *C*-functionalized TACN bearing a grafting function on the exocyclic amine and three phosphinate arms on the amines involved in the macrocyclic ring (Figure II-25). Several synthetic routes were considered. Among them, the retrosynthesis presented in Figure II-25 seemed to be the easiest and the fastest way to prepare the targeted molecule. This method is based on the use of a TACN-based synthon carrying the desired grafting function, *i.e.* a carboxylic acid group. The functionalization using Huskens conditions will be directly performed on this synthon.

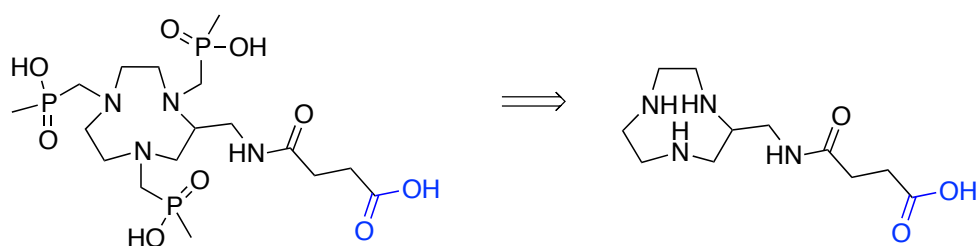
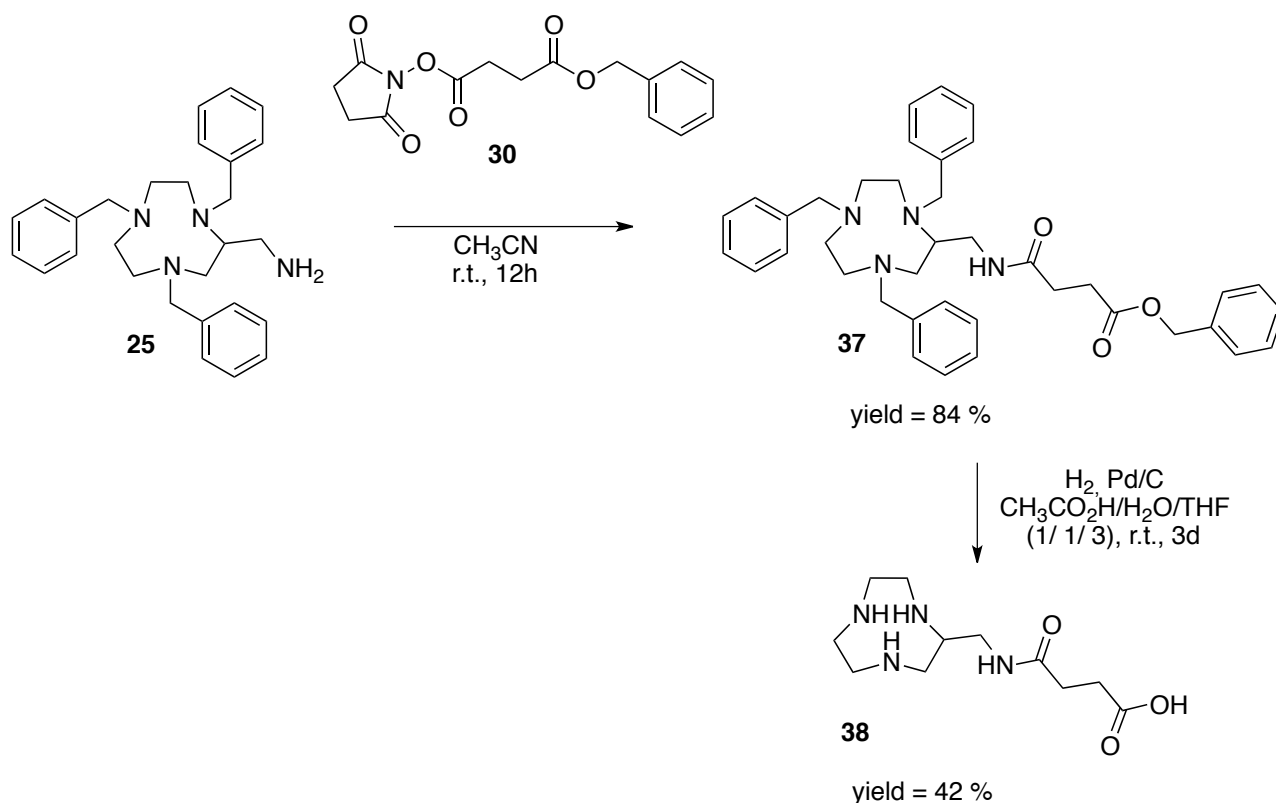


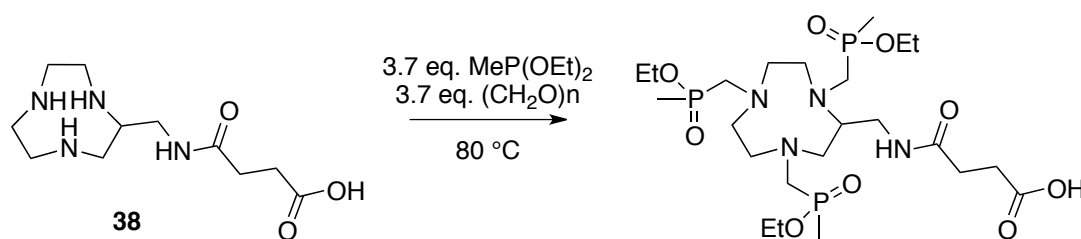
Figure II-25: Retrosynthesis considered.

The desired synthon could be synthesized through many ways. We chose to use the precursors already available in the laboratory, *i.e.* compounds **25** and **30**. Compound **37** was isolated in 84 % yield after functionalization of the primary amine of compound **25** with activated ester **30**. The benzyl groups were then removed by hydrogenolysis with palladium giving access to compound **38** in 42 % yield (Scheme II-53).



Scheme II-53

Compound **38** was heated at 80 °C in the presence of paraformaldehyde and methyldiethoxyphosphine (Scheme II-54). The presence of the desired compound in the crude was detected by mass spectrometry, however we were not able to isolate it. Indeed, the reaction yielded a mixture of mono-, di-, tri-phosphinate products and of several *N*-methylated species resulting from side reactions.



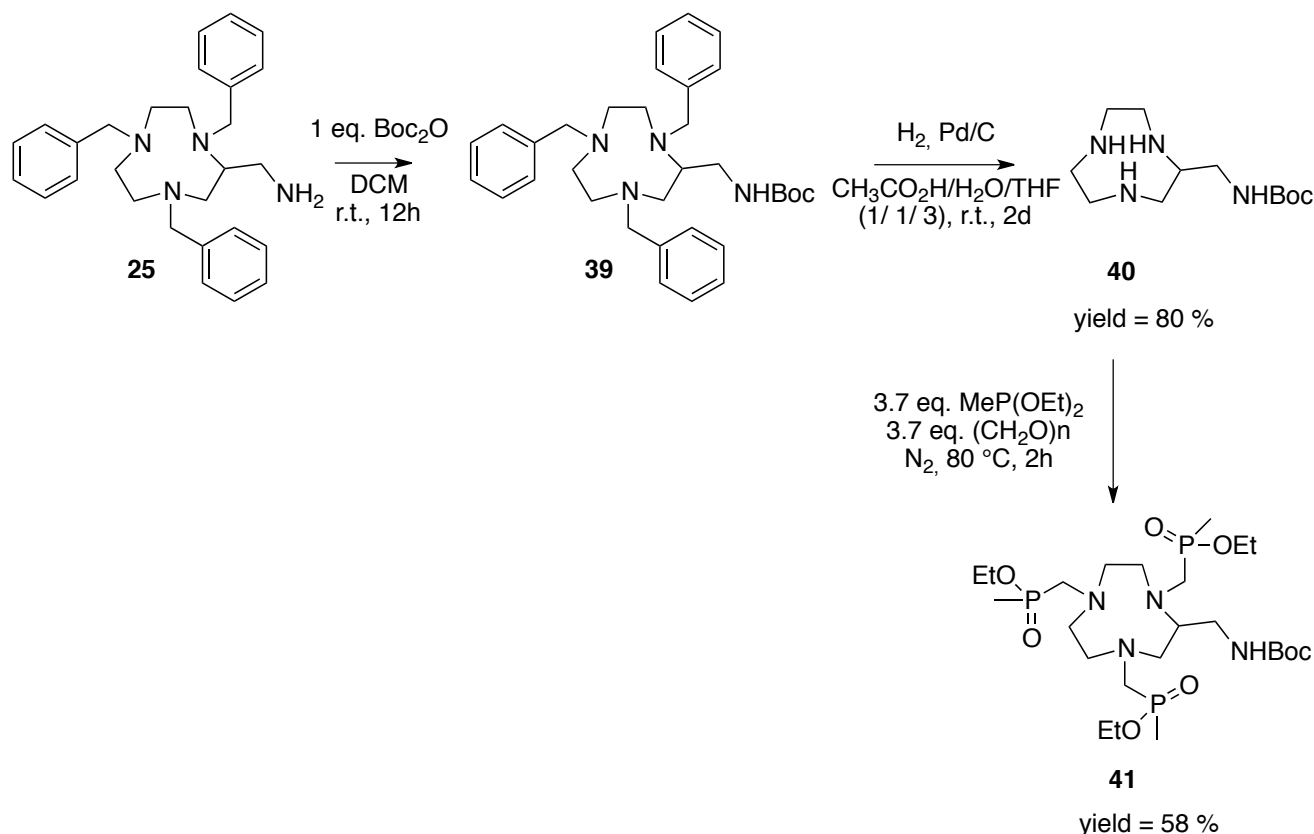
Scheme II-54

Moreover, the formation of several stereoisomers was expected due to the presence of stereogenic centers on phosphonate derivatives. The expected compound possesses 4 chiral atoms, *i.e.* the phosphorous atoms and the carbon atom bearing the grafting function. In principle, for this compound 32 stereoisomers are possible, existing as 16 NMR-indistinguishable enantiomer pairs. The following of the purification process by  $^1\text{H}$  and  $^{31}\text{P}$  NMR analyses was particularly difficult due to the presence of all diastereoisomers.

To allow an easier following of the reaction and purification process, we considered the synthesis of a new synthon, bearing a functional group used both as a protecting group and as probe

for NMR analyses. Boc group, exhibiting a characteristic singlet around 1.5 ppm, was an ideal choice for such purpose.

The addition of one equivalent of  $\text{Boc}_2\text{O}$  on **25** followed by the selective removal of the benzyl groups gave access to compound **40** in good yield (Scheme II-55). Functionalization of compound **40** was then performed by using Huskens conditions and resulted in the formation of **41**.



Scheme II-55

The reaction mixture was treated and the resulting product was analyzed by mass spectrometry, which confirmed the formation of compound **41**. The spectrum also revealed the presence of various by-products, such as di-substituted species. However in this case,  $^1\text{H}$  NMR analysis enabled identification of several species that clearly helped us in the purification process.

The  $^1\text{H}$  NMR spectrum exhibits characteristic signals in defined areas (Figure II-26). The pseudo-singlet around 5.8 ppm is typical of an amide proton. The usual quartet of a  $\text{CH}_2$  coupling with a  $\text{CH}_3$  is splitted into a doublet of quartets by the presence of the phosphorous atom.<sup>203,205</sup> The triplet around 1.3 ppm is characteristic of the corresponding  $\text{CH}_3$  group coupling with  $\text{CH}_2$ . In the area around 1.5 ppm can be found signals corresponding to the P-coupled methyl groups. All P- $\text{CH}_3$  groups are non-equivalent. However, it has to be noted that the complexity of this area is particularly enhanced because of the coexistence of numerous regioisomers and diastereoisomers. Finally, two singlets of high intensity around 1.4 ppm can be attributed to Boc groups.

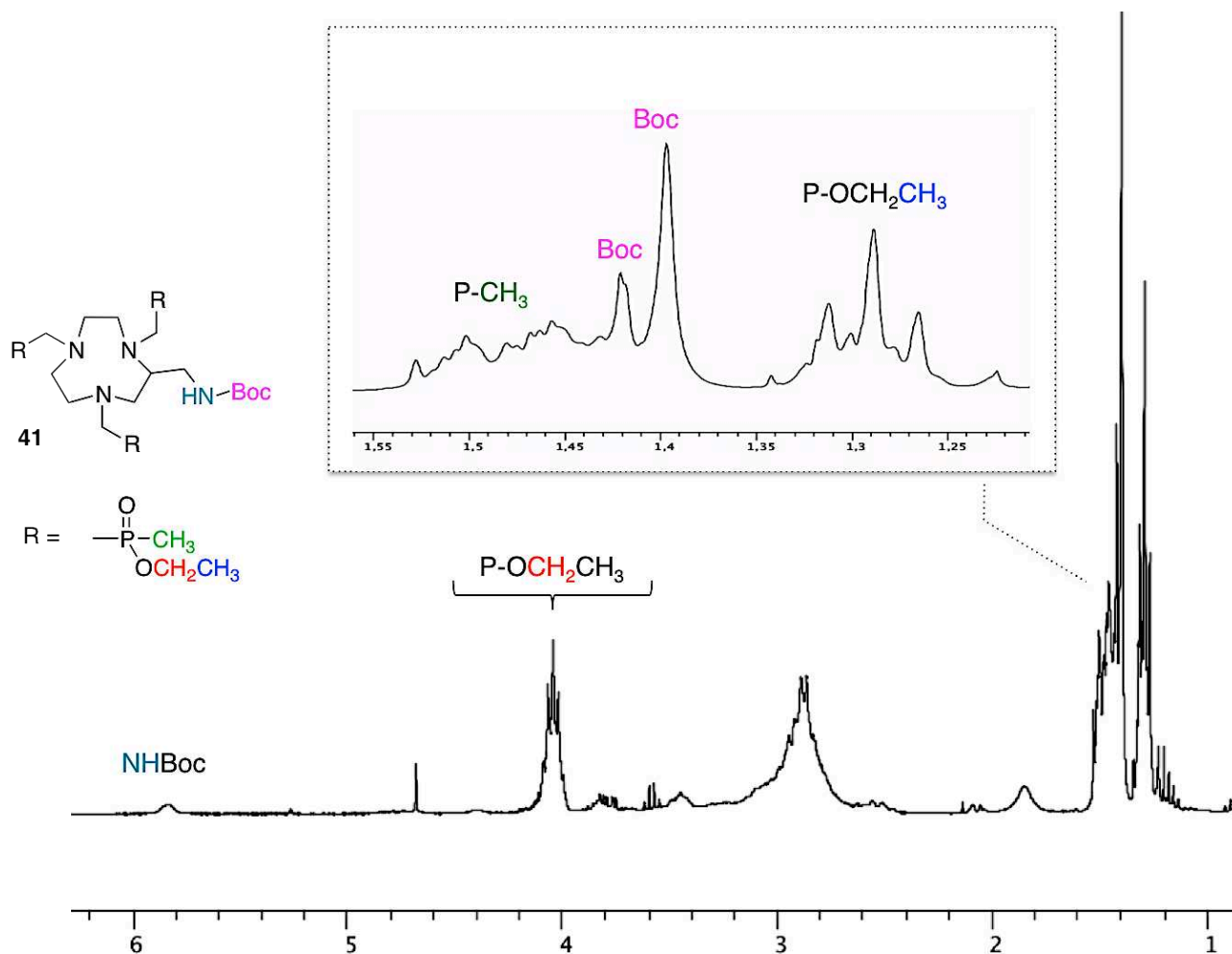


Figure II-26:  $^1\text{H}$  NMR spectrum of compound **41** before purification by chromatography (300 MHz,  $\text{CDCl}_3$ , 300 K).

We were able to separate different species by flash chromatography on silica gel and to isolate di-phosphinate species from tri-phosphinate derivatives. A zoom of the  $^1\text{H}$  NMR spectrum between 1.2 and 1.6 ppm of different column fractions is reported in Figure II-27. Attribution of signals indicates that F1 contains only disubstituted compounds, whereas F3 and F4 contain trisubstituted species. These results were confirmed by mass spectrometry.



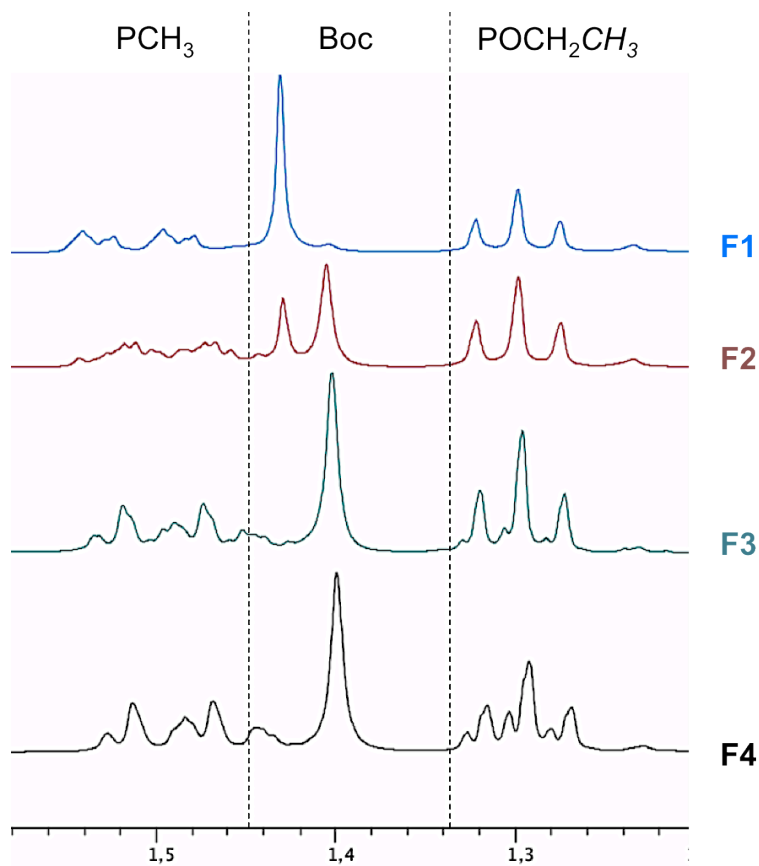


Figure II-27: Following of the purification process of compound **41** by  $^1\text{H}$  NMR spectroscopy (300 MHz,  $\text{CDCl}_3$ , 300 K).

Comparison of  $^1\text{H}$  NMR spectra indicates that the chemical shift of *tert*-butyl signal of Boc groups of tri-substituted derivatives is lower than the one of di-substituted species. The complexity of the area corresponding to P- $\text{CH}_3$  signals on the  $^1\text{H}$  NMR spectra of F1, F3 and F4 proves the coexistence of several diastereoisomers. Furthermore, F3 and F4 contain diastereoisomers in different proportions as reveals the signal shape of the  $\text{CH}_3$  of -POEt group. Moreover, it has to be noted that the secondary amines of compound **40** are non-equivalent. We can expect the formation of a mixture of di-substituted regioisomers in case of F1 (Figure II-28).

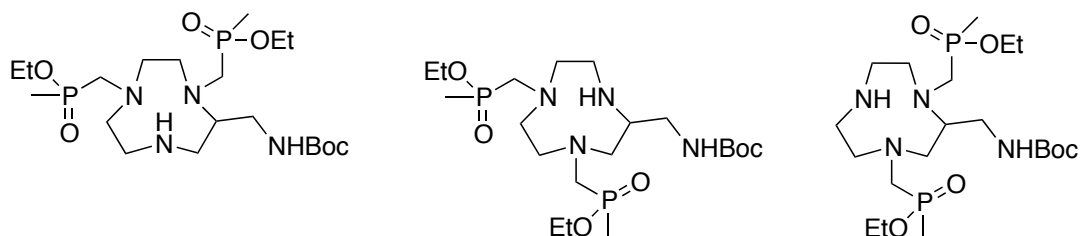
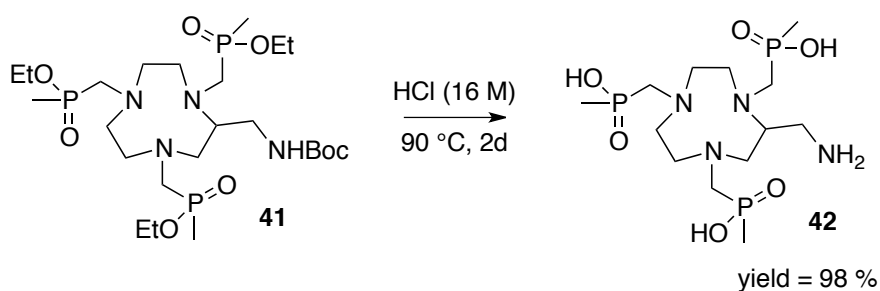


Figure II-28: Structures of the various regioisomers resulting from the di-substitution of compound **40**.

Hydrolysis of Boc and phosphinate esters of the trisubstituted species at 90 °C in a concentrated HCl solution gave access to compound **42** in 98 % yield (Scheme II-56).



Scheme II-56

The deprotection of the phosphinate ester groups resulted in an obvious simplification of the  $^{31}\text{P}\{^1\text{H}\}$  NMR spectrum (Figure II-29), which exhibited only three signals left. The phosphinic acid units being non equivalent, each signal can be attributed to one phosphorous atom, indicating that a molecular process is affecting the chiral centers of compound **41**.

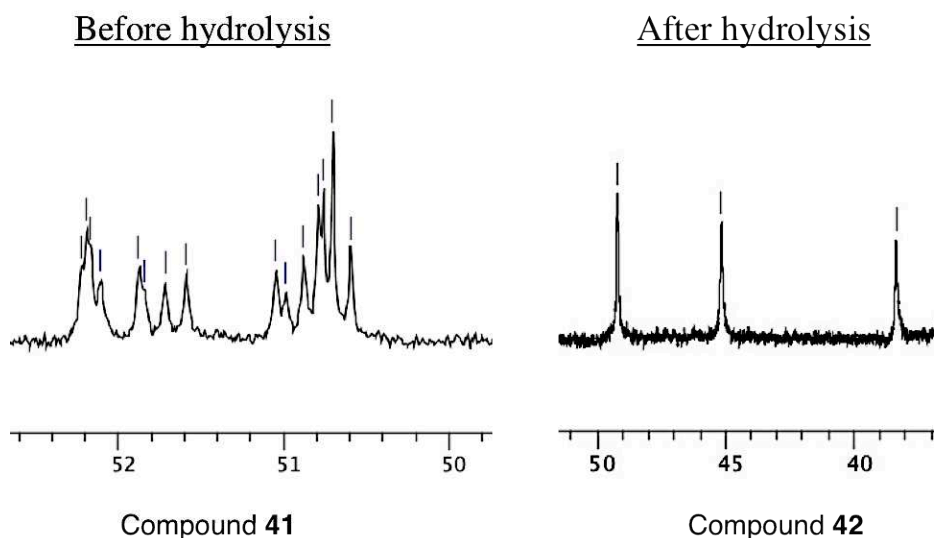
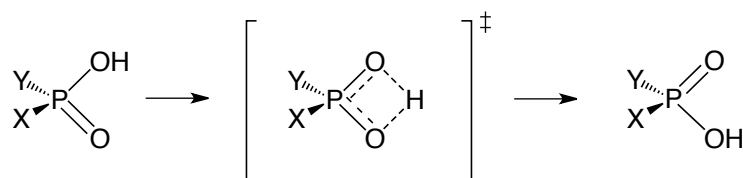


Figure II-29:  $^{31}\text{P}\{^1\text{H}\}$  NMR spectra of compound **41** (F4) (202 MHz,  $\text{CDCl}_3$ , 300 K) and compound **42** (202 MHz,  $\text{D}_2\text{O}$ , 300 K, pD = 1).

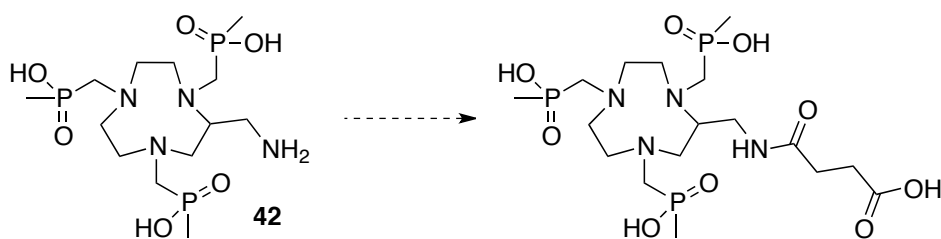
This phenomenon can be explained by proton transfers producing an inversion of the chirality of the phosphorous atoms at the NMR-acquisition time scale (Scheme II-57).<sup>207</sup> Such behavior has been previously reported with other polyphosphinates macrocycles.<sup>203,205,206</sup>



Scheme II-57: Schematic representation of the proton transfer process in phosphinic acid.

The last step of the route towards a new TACN-based BFCA is based on the introduction of the grafting function on the primary amine. First attempts of ring-opening of succinic anhydride in the presence of a base are being currently investigated in the laboratory. The access towards dimeric

systems will be also possible from compound **42**, by introducing two acetate arms on the primary amine.



Scheme II-58

To conclude, by using synthetic procedures developed in our group combined with functionalization methods reported in the literature, we can generate a new family of TACN-based chelators with high potential for Ga chelation.

## II.2.4 Conclusion

Using a synthetic route previously developed in our group, we were able to facilitate the synthesis of *N*-functionalized TACN by reducing step number. Moreover, optimization of the reaction conditions enables the preparation of aminomethylTACN at a 100 grams scale. This compound is a valuable precursor of a new family of *C*-functionalized TACN derivatives. By varying the grafting functions and the pendant coordinating arms, we could generate really promising BFCAs for copper and gallium chelation.

## II.3 Synthesis of new cyclen-based cryptands

A way for binding selectively metal cations is the use of specific cages featuring highly pre-organized sets of donors and inner cavities of appropriate dimension to encapsulate selected metal cations<sup>208</sup>. “Crown” ethers and later “cryptands” were discovered and found to have a remarkable affinity for alkali and alkaline earth metal ions.<sup>209-212</sup> There has been much current interest in the development of new macrobicyclic ligands containing appropriate binding sites and cavities of suitable size and shape for copper chelation. The cyclic frameworks of polyazacycloalkanes make them valuable precursors of such macrobicyclic systems and this aspect will be discussed in the following part.

### II.3.1 Cryptands based on tetraazacycloalkanes

Numerous studies on cage-type polyazamacrobicycles have shown the influence of parameters such as ligand rigidity, type of donor atoms and their disposition on the selectivity for metal

coordination.<sup>209,213-222</sup> Some highly preorganized molecules based on tetraazacycloalkanes have already been synthesized. These bowl-shaped ligands generally adopt conformation having all four nitrogen lone pairs pointing inside the cavity for complexation, which determine the formation of highly stable metal complexes (Figure II-30). As mentioned in chapter II.1, cross-bridged and side bridged systems particularly favor the coordination of  $\text{Cu}^{2+}$  metal ion. However, the main drawback of such constrained macrocycles remains their slow kinetic complexation. In this context, research have been focused on the synthesis of new constrained derivatives using unusual and longer bridges, the bridge being added either on two carbon atoms or on two adjacent or non-adjacent nitrogen atoms.

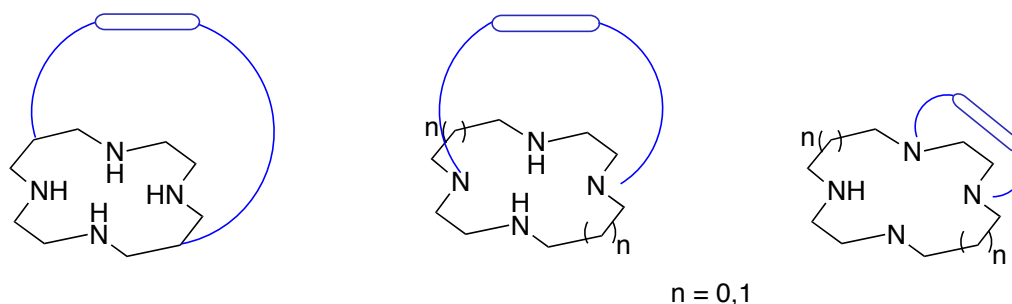


Figure II-30: Examples of cage ligands based on tetraazacycloalkanes.

### II.3.1.1 Sarcophagines: efficient cryptands for copper chelation

Sargeson and Smith have developed a new type of BFC based on sarcophagine (Sar) for preparation of new radiopharmaceuticals (Figure II-31).<sup>215,223-226</sup> Such derivatives coordinate particularly  $\text{Cu}^{2+}$  within the multiple macrocyclic rings comprising the Sar cage structure, yielding extraordinarily stable complexes that are inert to the dissociation of metal ion.<sup>75</sup> The cage-like BFC Sar ligands are unique in their ability to selectively label  $^{64}\text{Cu}^{2+}$  rapidly over a wider range of pH value under mild conditions.<sup>215,224</sup>

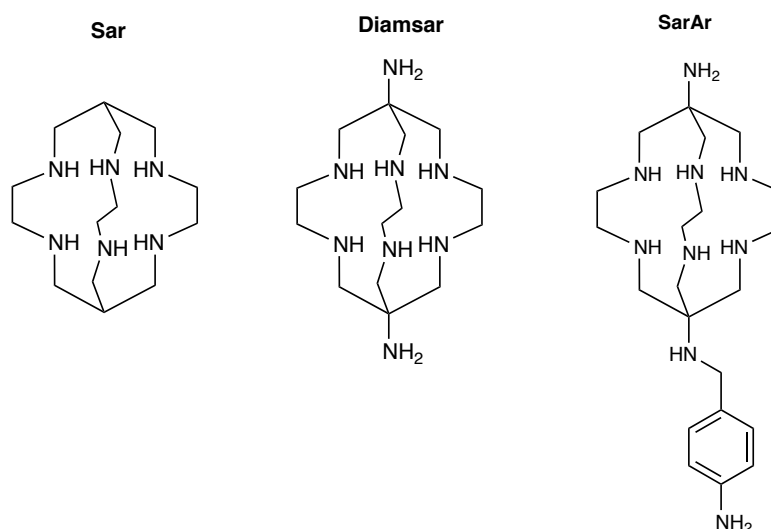


Figure II-31: Hexaaza cages Sar, Diamsar and SarAr.

These sexadentate macrobicyclic ligands are obtained by using a cobalt(III) ion as a template to hold the reacting organic fragments.<sup>225,226</sup> Treatment of the cobalt(II) cage with cyanide anions led to the metal free sarcophagine which is isolated and can encapsulate other metal ions.

### II.3.1.2 Other examples of cryptands

There are numerous examples of cryptands based on tetraazacycloalkanes carrying the bridge between two nitrogen atoms. Adamanzanes of short bridge (ethane and propane) adopt a conformation where two protons can be involved in a network of strong  $-^+N-H\cdots N$  hydrogen bonds. Such species are called « proton sponge ».<sup>137,140,141,144,217-221,227-230</sup>

Springwork and co-workers reported the synthesis of a bowl tetraamine [2<sup>4</sup>.3<sup>1</sup>]adamanzane (1,4,7,10-tetraazabicyclo[5.3.3]pentadecane) (Figure II-32),<sup>217-221</sup> which behaves as a proton-sponge. This species couldn't be completely deprotonated in aqueous solution, preventing copper complexation in such media. Larger derivatives were prepared and for example [3<sup>5</sup>]adamanzane (Figure II-32) could form copper complexes in aqueous solution.<sup>214,230</sup>

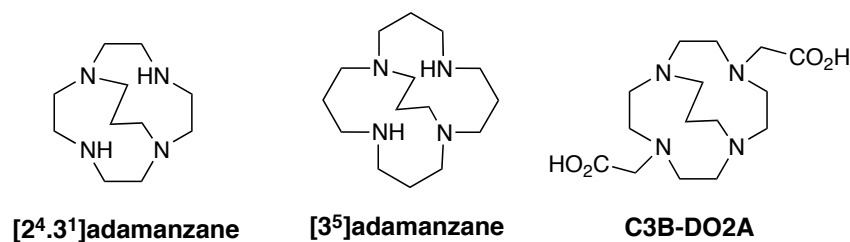
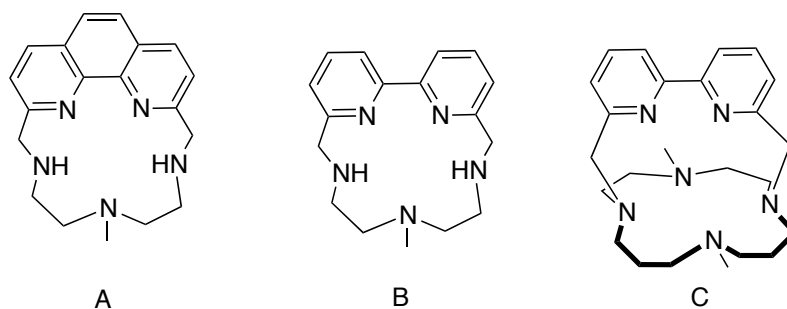


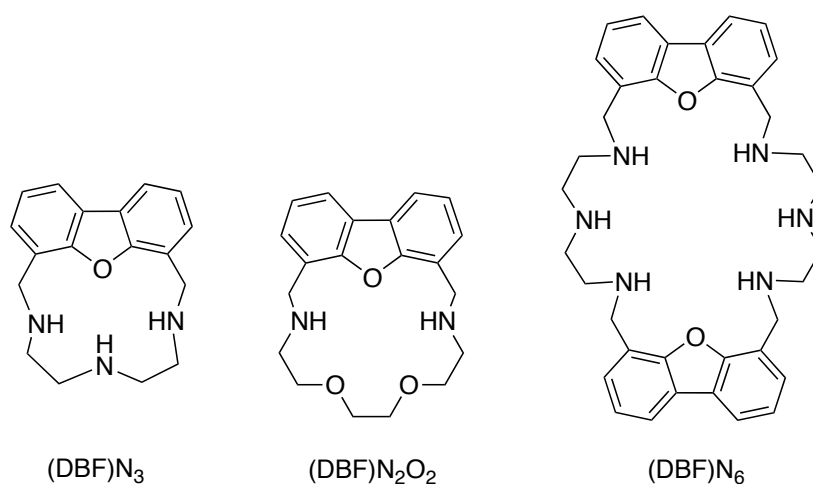
Figure II-32: Examples of adamanzanes.<sup>214</sup>

From these results, Odendaal and co-workers investigated the synthesis of pendant-armed derivatives.<sup>82</sup> The bis-carboxymethyl pendant-armed cyclen with a trimethylene cross-bridged so-called C3B-DO2A especially demonstrated excellent properties towards copper chelation (Figure II-32). Indeed the resulting <sup>64</sup>Cu complex was remarkably inert, even if biodistribution studies indicated a very slow *in vivo* clearance.

New macrocyclic structures incorporating longer bridge with heteroaromatic subunits such as phenanthroline or 2,2'-dipyridine were reported in the literature (Figure II-33A and B).<sup>227,231,232</sup> These units are rather rigid, and, at the same time, provide two aromatic nitrogens whose unshared electron pairs may act cooperatively in binding cations. The presence of such rigid aromatic systems gives particular coordination properties to the macrocyclic ligands defining particular preorganized binding sites for the metal ions. The cryptand **C** (Figure II-33) behave as a proton sponge behavior, however, **C** was able to encapsulate Cu(II) in aqueous solution.<sup>227</sup>

Figure II-33: New macrocyclic structures with heteroaromatic subunits.<sup>227</sup>

Delgado and co-workers developed simple synthetic methods to prepare polyaza- or polyoxopolyaza-macrocyclic compound having rigid 4,6-dibenzofuran (DBF) units and flexible spacers able to recognize metal ions or organic substrates (Figure II-34).<sup>233</sup> All the prepared macrocycles displayed an important structural feature with one or two DBF coupled at the 4 and 6 position. (DBF) $N_3$  was found in a few amount as a side product of the synthesis of (DBF) $N_6$ . It was isolated from the mother solution as a copper(II) complex by addition of  $CuSO_4$ . Further studies on metal coordination are being currently investigated.

Figure II-34: New polyaza- and polyoxopolyaza-macrocyclic.<sup>233</sup>

In this context, our group decided to prepare a new cryptand resulting from the addition of such DBF derivatives on a cyclen moiety (Figure II-35).<sup>234,235</sup> We also considered the synthesis of a more flexible cryptand carrying a diphenylether (DPE) unit as a bridge.

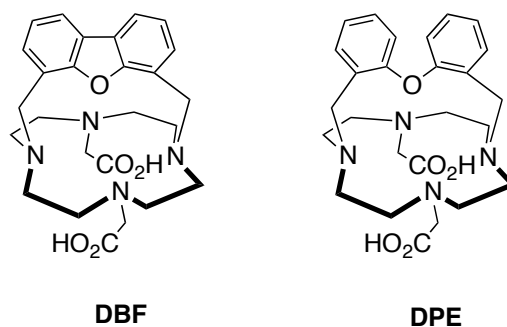
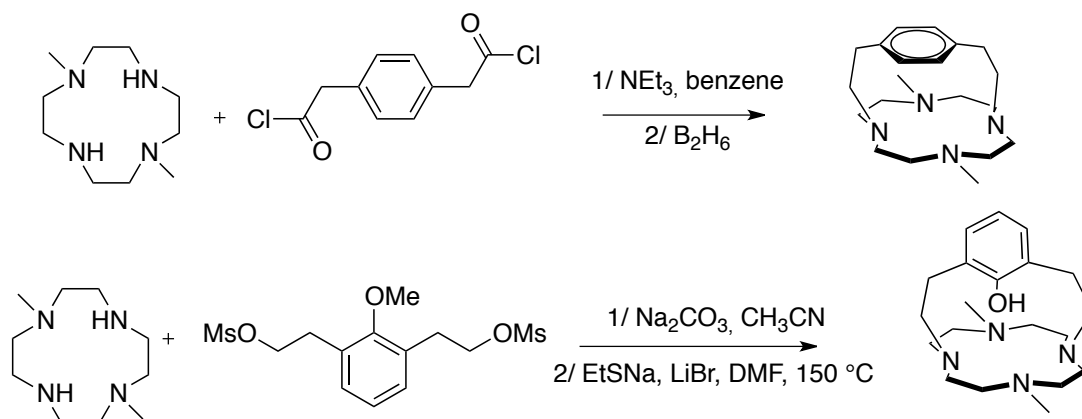


Figure II-35: New cryptands based on cyclen.

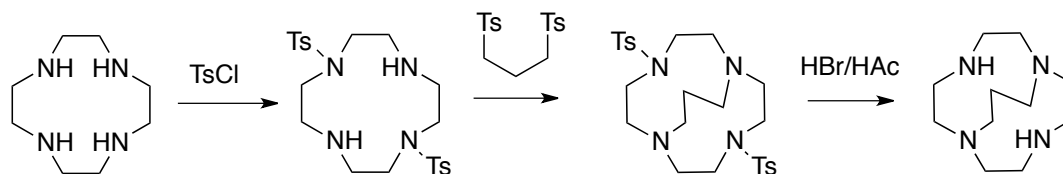
### II.3.2 Synthetic pathways toward macrobicyclic systems.

Numerous synthetic pathways have been elaborated to prepare cyclen-based cryptands that allow the production of a large range of ligands starting from 1,7-dimethyl-cyclen or 1,7-bis(*p*-toluenesulfonyl)-cyclen. Most macrobicycles and macrotricycles have been prepared according to a multi-step reaction scheme involving trans-di-protection of tetraazacycloalkanes, using methyl,<sup>236-239</sup> tosyl<sup>218</sup> or Boc<sup>240,241</sup> as protective groups. When methyl is used as protecting agent, the deprotection is impossible and methylated macrocycles generally exhibit lower affinity toward transition metals than unprotected one (Scheme II-59).<sup>238,239</sup>



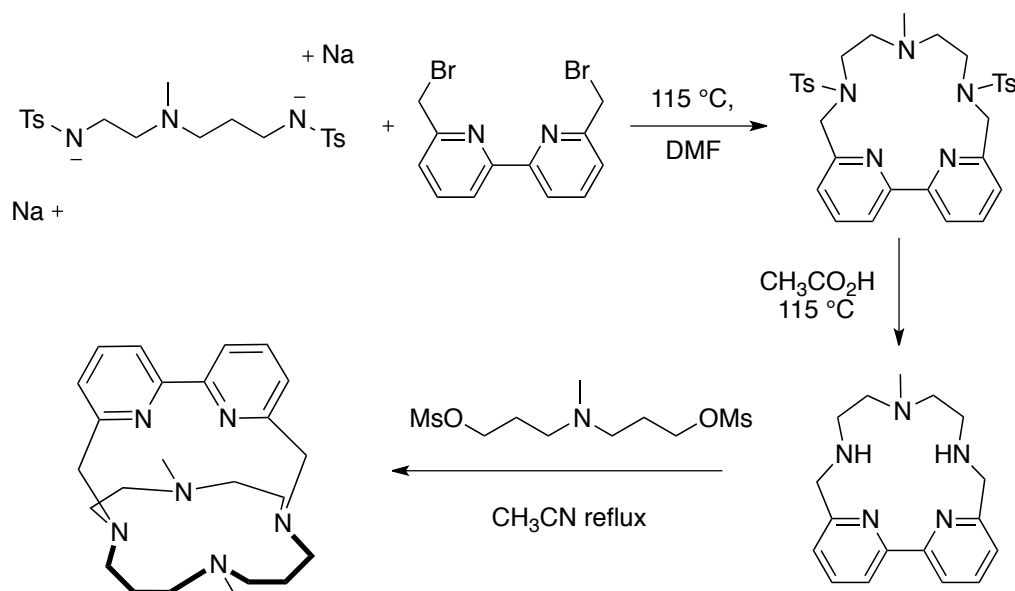
Scheme II-59

For *N*-tosyl and *N*-carbamate derivatives, the protection reaction isn't selective and leads to a mixture of mono-, di-, tri- and tetra-protected macrocycles (Scheme II-60).<sup>218</sup> These synthetic routes impart tedious multi-step syntheses, implying multiple protection/deprotection sequences.

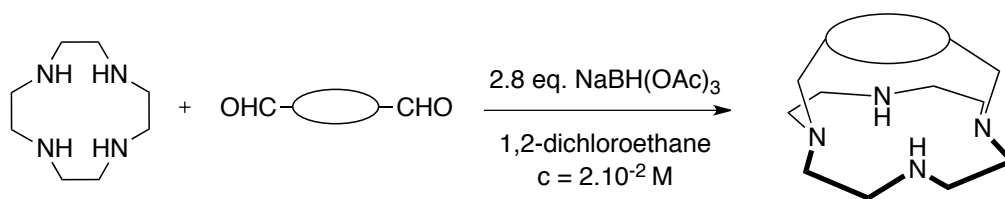


Scheme II-60

Another route consists in preparing selectively protected linear amines that can be further condensed on dibrominated species according to Richman Atkins cyclization conditions (Scheme II-61).<sup>146,227</sup> As mentioned previously, this methodology is far from optimal, as many chemical functions cannot survive the harsh conditions required in the detosylation step.

Scheme II-61<sup>227</sup>

An efficient route for the synthesis of selectively 1,7-difunctionalized cyclens was developed in the laboratory by reacting two equivalents of various aldehydes with cyclen under reductive amination conditions (Scheme II-62).<sup>234,235</sup> In such reactions, the reducing agent must be selective enough to reduce the imine or iminium species formed *in situ*, without reacting with the starting aldehyde. Among the different reducing agents, sodium tri-acetoxyborohydride ( $\text{NaBH}(\text{OAc})_3$ ) has been widely used.<sup>242-245</sup> Several aldehydes were added on cyclen in the presence of 2.8 equimolar amounts of reductant in 1,2-dichloroethane (0.02 M) at room temperature.<sup>234,235</sup> The method described herein is also a powerful tool for the synthesis of cryptands incorporating a cyclen. Cryptands can be prepared in high yields by a one-pot reaction using dialdehydes as starting materials.



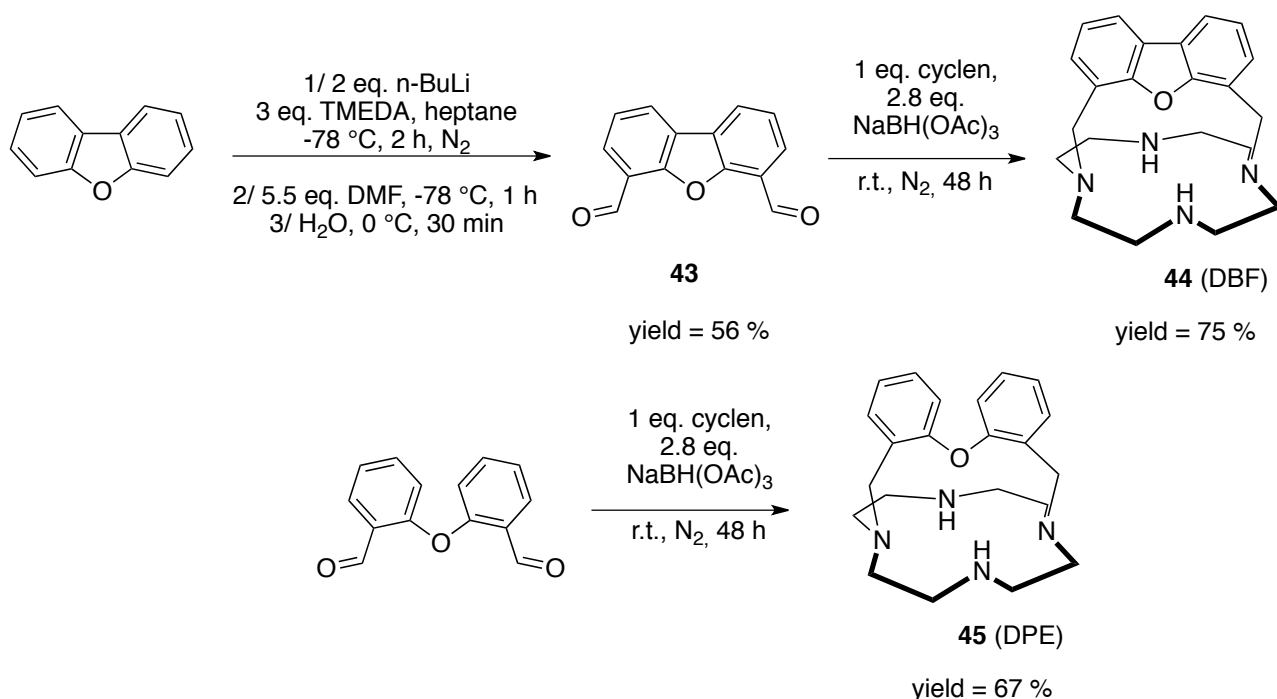
Scheme II-62

### II.3.3 New cyclen-based systems bearing a diphenylether or a dibenzofuran unit

The procedure described above enabled the synthesis of cryptands featuring a dibenzofuran or a diphenylether unit connecting the nitrogen atoms in 1,7 position of the tetraaza moiety (Scheme II-63). The dialdehyde **43** was prepared by a reported method,<sup>233,246,247</sup> involving treatment of dimethyldibenzofuran with an excess of both TMEDA and *n*-BuLi, heating at 60 °C for 2 hours and addition of 5.5 eq. of DMF at -78 °C. Cryptand **44** was obtained by addition of compound **43** on



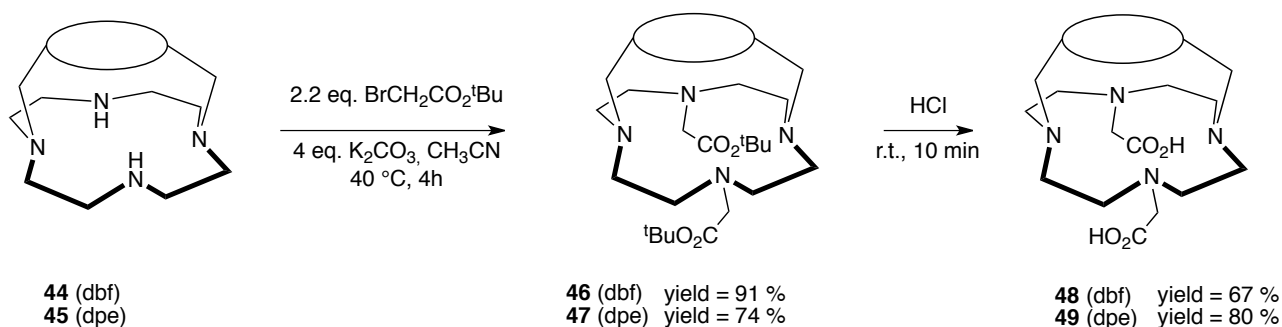
cyclen in reductive amination conditions described above.<sup>234,235</sup> The same reaction conditions enabled the preparation of compound **45** from bis(2-formylphenyl)ether.



Scheme II-63

Studies of macrobicycles **44** and **45** indicated that they both display a rigid molecular architecture, characterized by a small inner cavity and a pre-organized disposition of the set of donor atoms.<sup>248</sup> These structural features strongly affect both protonation and metal binding characteristics of the two cryptands. In fact, the ammonium groups formed upon ligand protonation give rise to an inner-cavity hydrogen bonding network, which stabilized the protonated forms of the cryptands. Ligand rigidity, small cavity dimension and/or high basicity make Cu<sup>2+</sup> and Zn<sup>2+</sup> complexes difficult to form. Indeed, they could not be prepared in aqueous solution but in acetonitrile.

In order to change the metal complexation behavior of such compounds, we decided to introduce pendant coordinating arms such as acetate groups. Thus, both cryptands **44** and **45** were functionalized in acetonitrile using 2.2 eq. of *tert*-butylbromoacetate in the presence of potassium carbonate (Scheme II-64). The desired compounds **46** and **47** were isolated in good yield, 91 % and 74 % respectively.



Scheme II-64

$^1\text{H}$  NMR spectra of both compounds **46** and **47** in  $\text{CDCl}_3$  indicated the presence of an inner cavity hydrogen ( $\delta$  around 8.5 ppm), which is typical of a species exhibiting a « proton sponge » behavior. The proton is indeed stabilized by cooperative intramolecular hydrogen bonds. The addition of a few amount of  $\text{D}_2\text{O}$  in the corresponding NMR tubes led to the disappearance of such signal (Figure II-36) due to an exchange phenomenon with a deuterium atom.

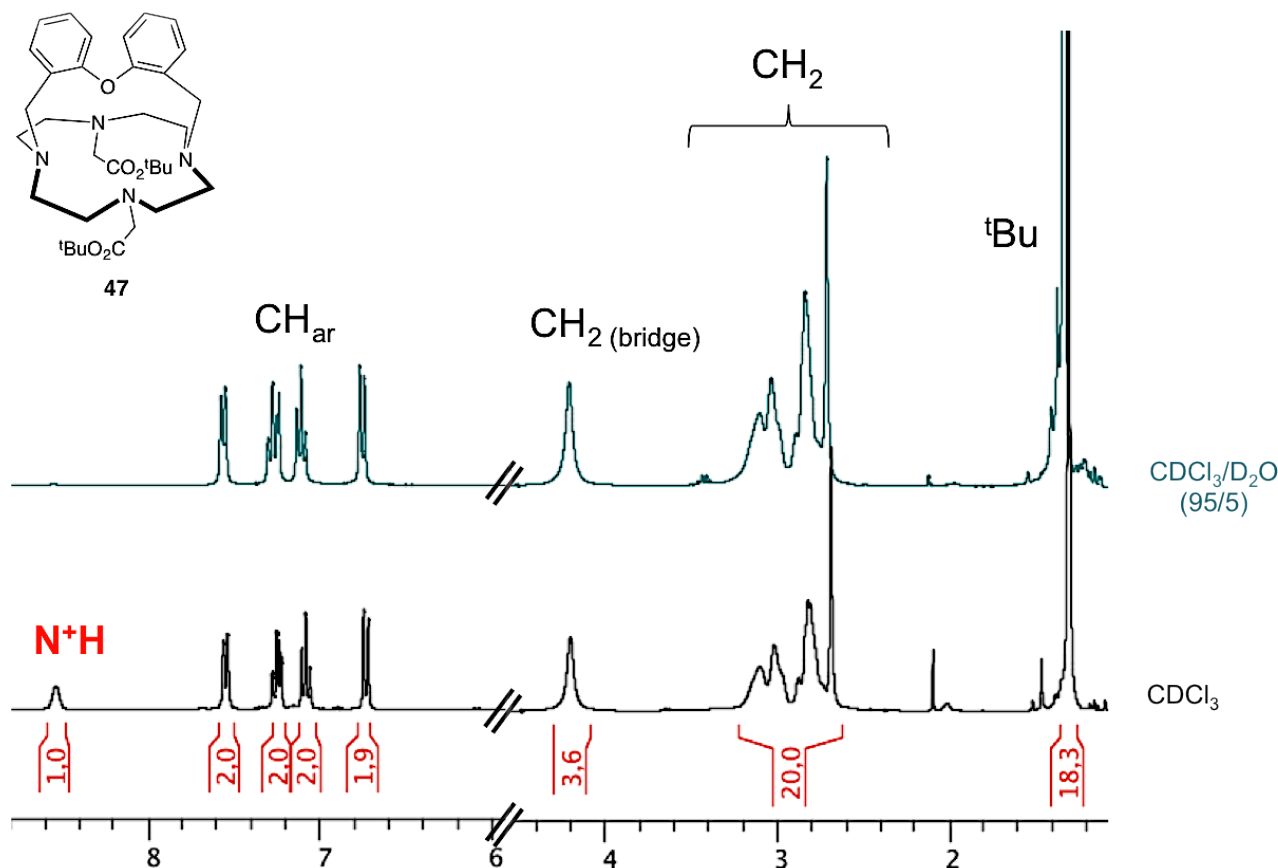


Figure II-36: Comparison of  $^1\text{H}$  NMR spectra of compound **47** in different solvents (300 K, 300 MHz).

Compound **46** and **47** were then dissolved in a concentrated acidic solution to hydrolyze the *tert*-butylic esters (Scheme II-64). As their parent ligand, both cryptands **48** and **49** exhibited an extremely high basic center, indicating them as « proton sponges ». Preliminary NMR studies of both

compounds revealed the presence of several species at pD = 1 (Figure II-37). The addition of NaOD until pD = 14 resulted in the diminution of the number of signals that indicates the coexistence of different protonated species. Further protonation studies are being currently investigated in the group of Pr. Rita Delgado.

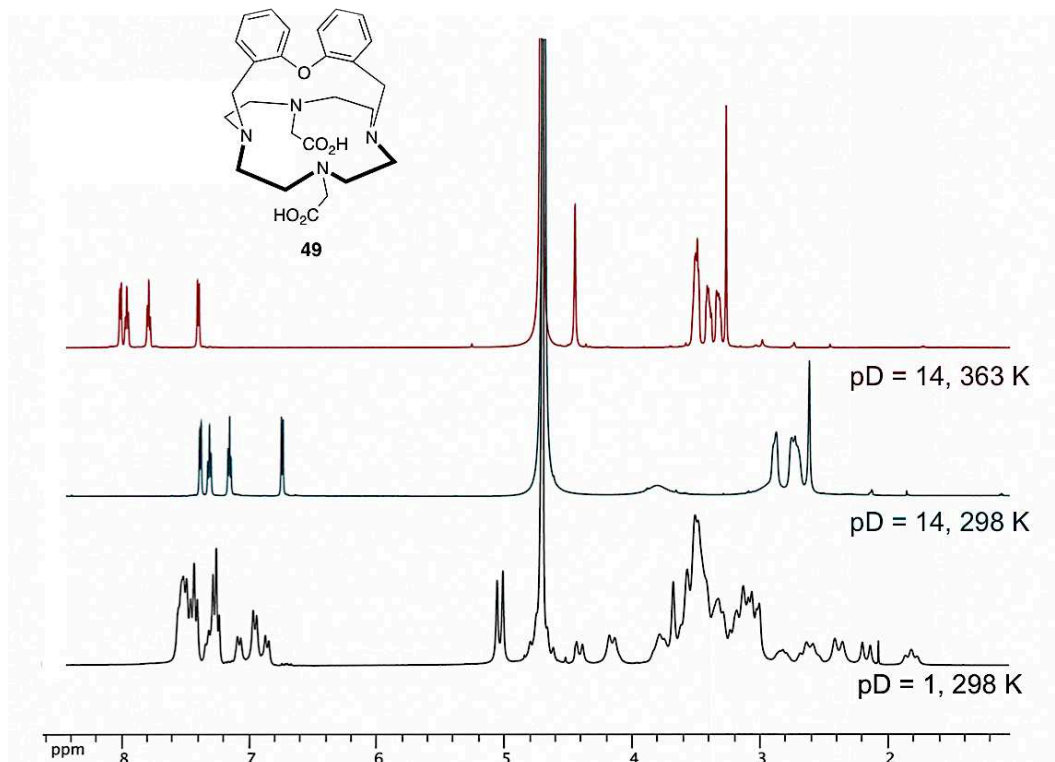
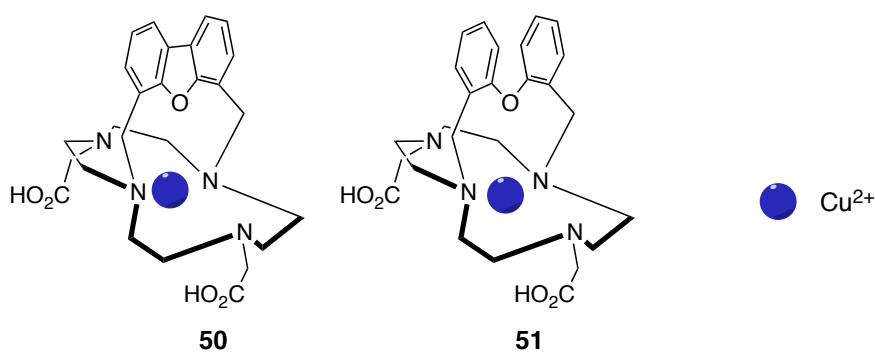


Figure II-37:  $^1\text{H}$  NMR spectrum of **49** at acid and basic pD at different temperature (300 MHz,  $\text{D}_2\text{O}$ ).

The capacity of **48** and **49** to form thermodynamic and kinetically stable metal complexes was also investigated by the group of Pr Rita Delgado. Studies revealed that the two chelators are selective for copper(II), forming thermodynamically very stable complexes. The kinetic inertness of these copper complexes was evaluated at  $5 \text{ mol}\cdot\text{dm}^{-3}$   $\text{HClO}_4$  (or  $\text{HCl}$ ) aqueous solution at 298.2 K. At 363.2 K the half-life of the complex was estimated at about 3.1 h for **50**, and at about 4.6 days for **51** (Scheme II-65). These values place the complexes studied in this work amongst the most inert copper(II) complexes of tetraazamacrocyclic *N*-acetate derivatives known so far, at the best of our knowledge.



Scheme II-65

Single crystals of **50** were obtained after very slow evaporation of a very acidic aqueous solution from the complex dissociation experiment with  $\text{HClO}_4$ . The molecular structure of the complex is built up from a symmetric unit composed of two disordered  $\text{ClO}_4^-$  as counterions. The resulting structure is reported in Figure II-38. The ligand acts as a hexadentate ligand. The copper(II) ion is in a distorted octahedral environment with the four nitrogen atoms, the O(3) oxygen of a pendant carboxylic arm and the O(5) oxygen of the dibenzofuran unit. The distance Cu-O(5) is shorter than the one reported for copper-dibenzofuran bond of macrocyclic systems<sup>233,249</sup> probably due to the rigidity of the ligand. This distance is however similar to the one observed in the copper(II) complex with the parent ligand **44** published by Bazzicalupi *et al.*<sup>248</sup>

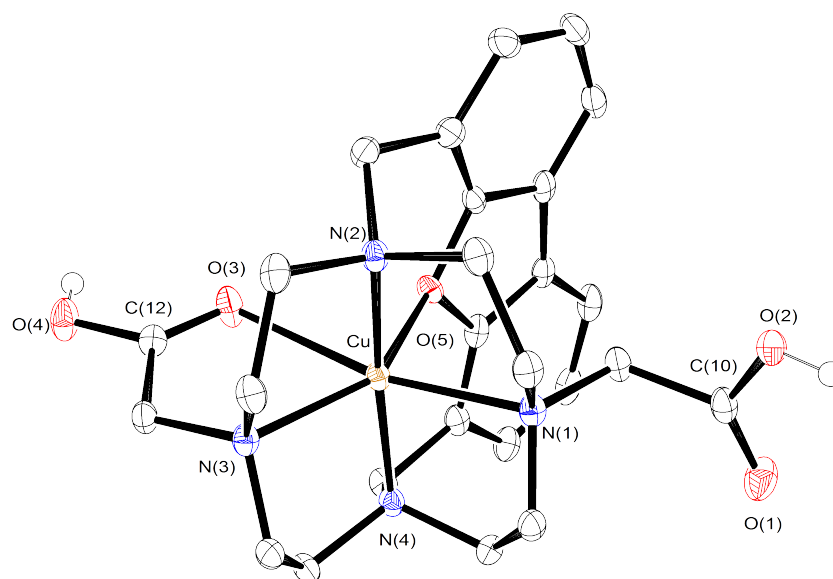


Figure II-38: ORTEP<sup>149</sup> view of **50** showing thermal ellipsoids at the 50 % probability level. Hydrogen atoms on carbon atoms have been omitted for clarity.

In this part, we presented the synthesis of new DO2A-based cryptands bearing dibenzofuran or diphenylether unit in good yield. The presence of two acetate arms enabled the preparation of highly thermodynamic stable and kinetically inert complexes with  $\text{Cu}^{2+}$  in aqueous media. Even though, the resulting complexes were very slow to form, it would be of great interest to evaluate their potential as copper chelate for radioimaging applications. The use of such cryptands in the field of molecular imaging requires the introduction of a targeting vector on the macrobicyclic core. This core could be further functionalized by addition of a double arm on a nitrogen atom of the cyclen subunit (Figure II-39A). We can also work on the bridge unit by using the methodology developed in the lab to prepare new cryptands. For example, we can consider the synthesis of a new macrobicyclic core with a phenanthroline moiety acting as the bridge (Figure II-39B).

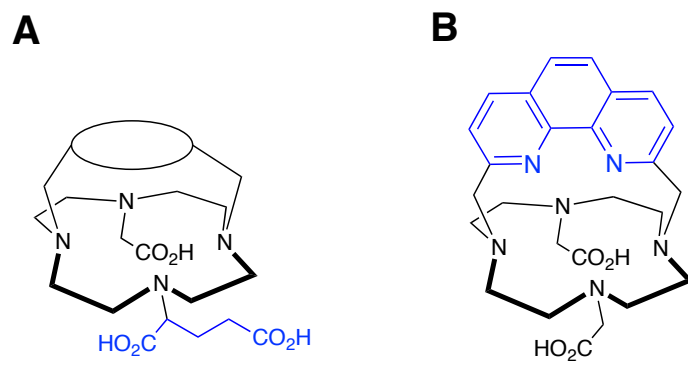


Figure II-39

## II.4 Conclusion

The objective of this thesis work was to explore new ligand systems intended for nuclear medicine applications. Several fundamental criteria in the design of bifunctional chelating agents were critical to consider for optimizing the coordination properties of the chelator:

- Matching the metal ion with the cavity size.
- Tuning the rigidity of the ligand.
- Providing donor binding atoms to complete the coordination sphere of the metal.

The tuning of these parameters enabled the synthesis of a wide range of new macrocyclic scaffolds (Figure II-40). Varying the cavity size (9-, 12- and 13-membered rings), the nature of the pendant coordinating arms (carboxylate or phosphinate) and the rigidity of the systems (by bridging two nitrogen atoms), we aimed at building optimized systems for copper and gallium chelation.

Lastly, we incorporated handles for bioconjugation reactions onto the chelators by using the C-functionalization approach. The breadth of choices of conjugation reactive functional groups enabled the preparation of a wide series of potential BFCAs.

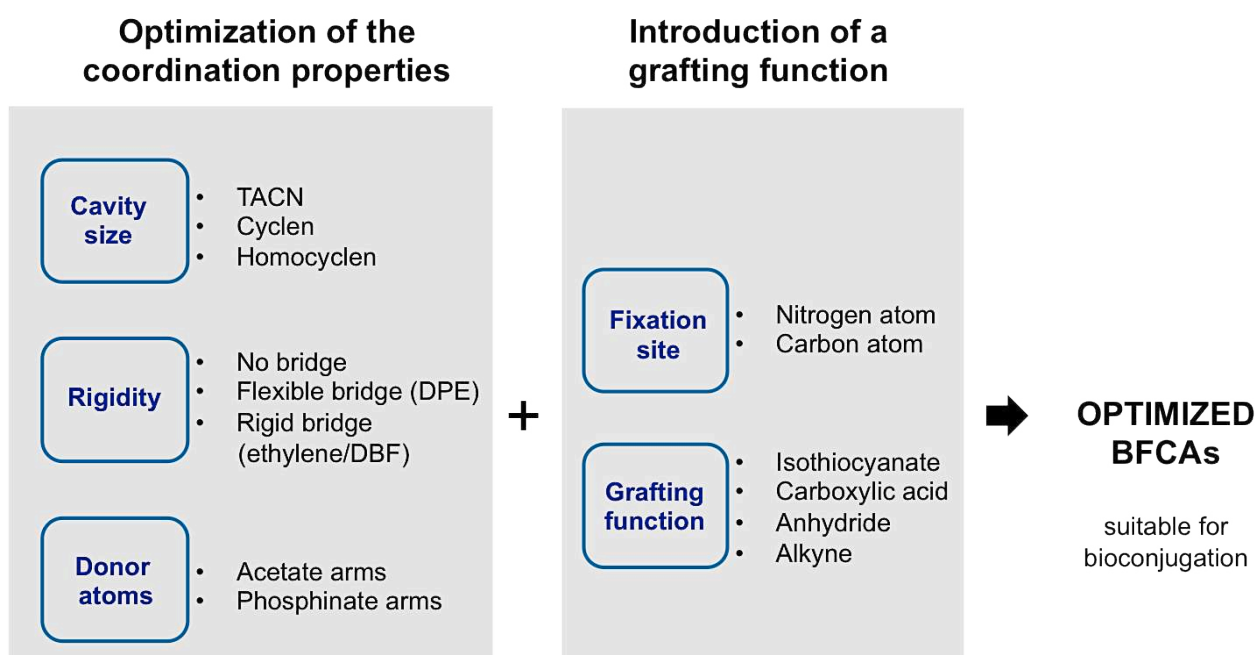


Figure II-40: Development of new BFCAs.



**III. New imaging agents for targeting chemokine  
receptor CXCR4**





### III. New imaging agents for targeting chemokine receptor CXCR4

The development of imaging agents for targeting CXCR4 is a rapidly expanding research field where a number of different chemical strategies are being pursued (Chapter I.II). To image CXCR4 expression in tumors, several research groups used the ability of the cyclam function of AMD3100 and AMD3465 to form strong complexes with metal ions (Figure III-1).<sup>4</sup> Recently, it was found that these CXCR4 targeting moieties also provide versatile platforms for the preparation of imaging agents. Thus, the phenyl ring of AMD3100 has been replaced by anthracene<sup>115</sup> and Khan *et al.* has replaced one of the cyclam with a fluorescent tag.<sup>114</sup>

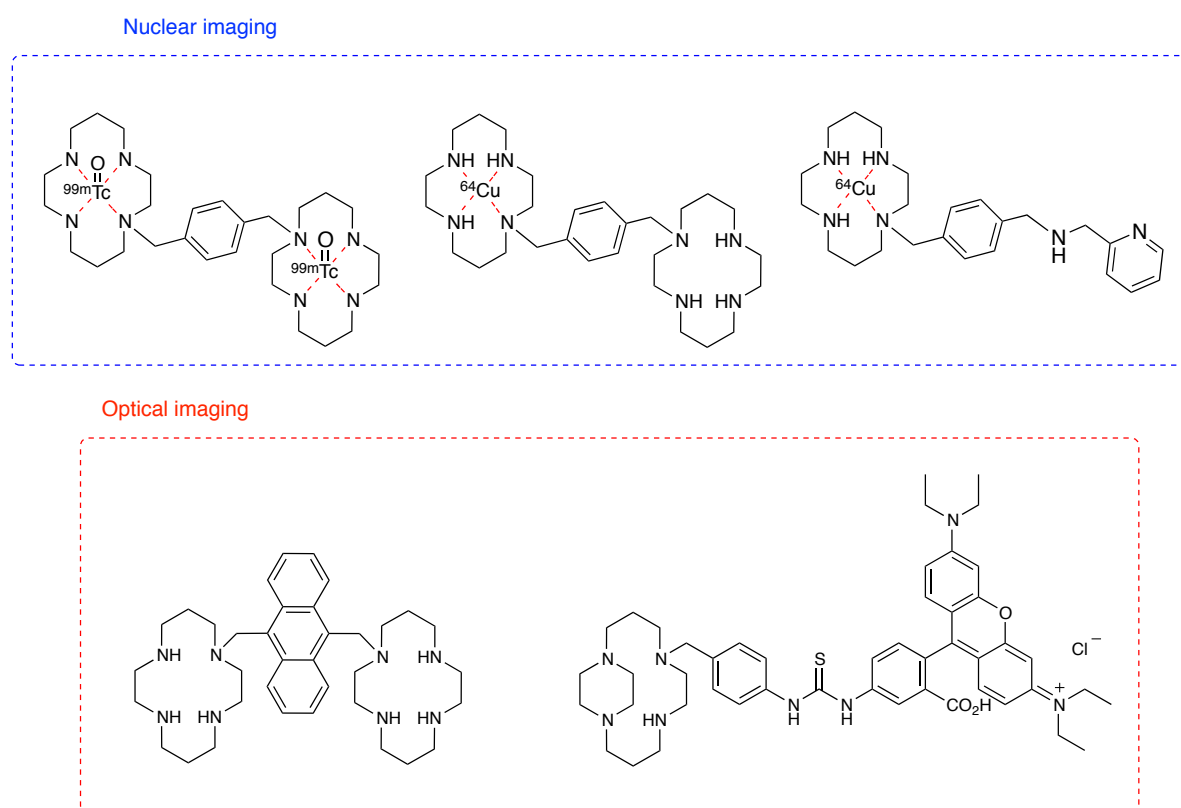


Figure III-1: Examples of CXCR4-targeting imaging agent based on cyclam.<sup>4</sup>

As part of our ongoing effort to prepare high affinity CXCR4 binding ligands for molecular imaging purposes, we were interested in generating a new family of imaging agents based on AMD3100 and AMD3465. We aimed at building general macrobicyclic platforms that enable the introduction of various probes, the AMD-like moiety serving as a carrier for specific delivery of a radioactive or fluorescent tag to cancer tissues (Figure III-2).



Figure III-2: Schematic representation of new imaging agents based on AMD3100 and AMD3465 for targeting CXCR4.

Thus, we considered the preparation of building blocks in both AMD3100 and AMD3465 series for targeting CXCR4. On the AMD cores, we aimed at introducing a spacer carrying a reactive function, *i.e.* a primary amine that enables the attachment of the desired tag (Figure III-3).

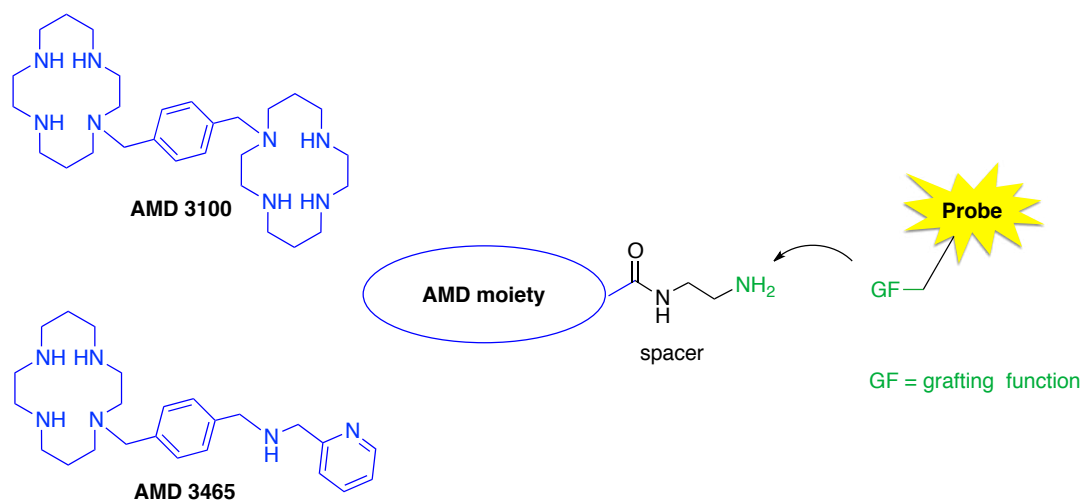


Figure III-3: Schematic representation of the building blocks.

This kind of approach using bismacrocycles based imaging agents has been previously used to detect and diagnose a wide variety of medical conditions characterized by dying cells.<sup>250-252</sup> A series of mono-, di-, and tetrameric cyclen ligands were synthesized, labeled with  $Zn^{2+}$  and used as carriers of fluorescent or radioactive probes for cell death *in vitro* and *in vivo* imaging (Figure III-4). The bis-zinc complex specifically targets phosphatidylserine, which is a phospholipid component abnormally exposed on the surface of apoptotic cells.<sup>250,253</sup>

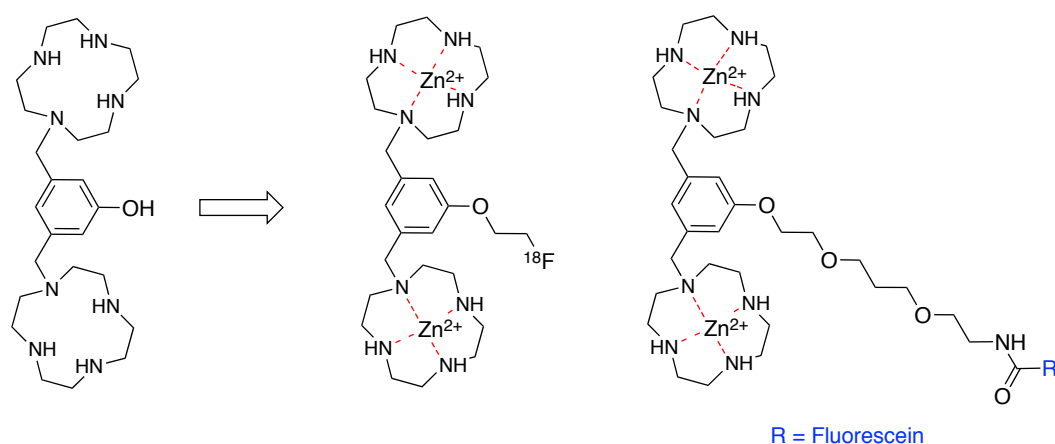
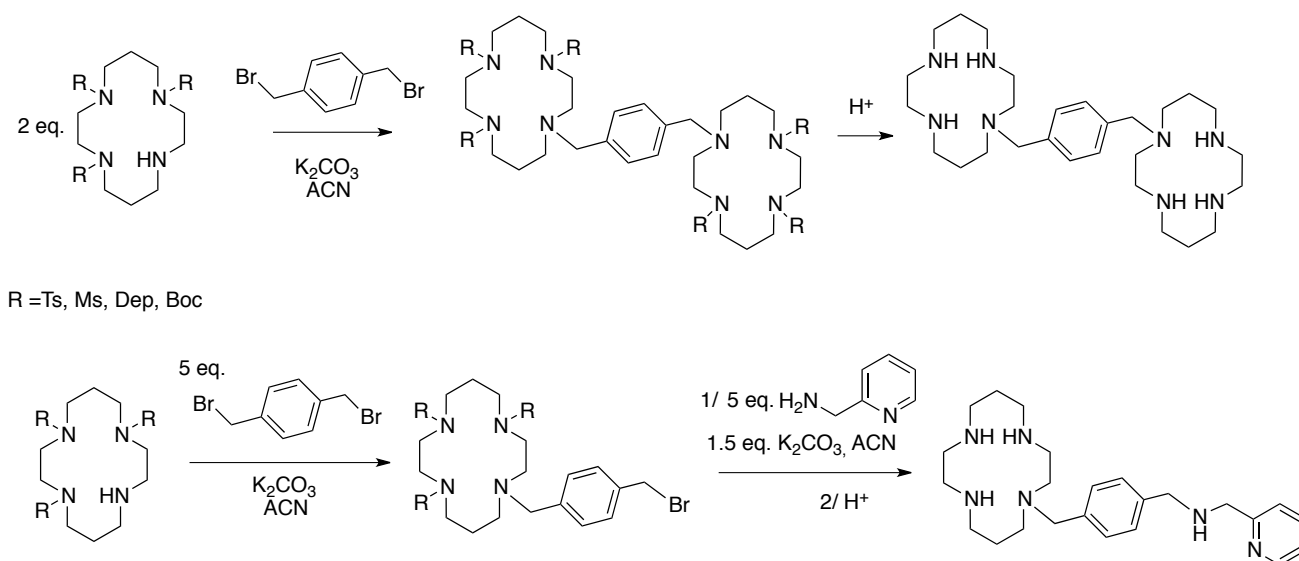


Figure III-4: Chemical structures of zinc complexes designed for apoptosis imaging.<sup>250</sup>

In the following chapter, we will present the synthetic routes towards AMD3100 and AMD3465 and their functionalized derivatives that are reported in the literature. We will describe the synthetic pathways for the obtention of new AMD-based building blocks. Finally, the synthesis of new imaging agents based on these building blocks will be presented.

### III.1 Synthesis of new AMD3100- and AMD3465-based building blocks

Several synthetic routes towards AMD3100 and AMD3465 are reported in the literature.<sup>128,254-258</sup> Most of them are based on the reaction of selectively protected cyclam rings with  $\alpha,\alpha$ -dibromo-*p*-xylene in acetonitrile containing potassium carbonate (Scheme III-1). AMD3100 can be generated in two steps from cyclam protected with tosyl, mesityl, diethylphosphoramidate (Dep) or Boc groups. Monofunctionalization of the dibromo species by using an excess of dibromo spacer followed by the reaction of the resulting bromide with an excess of aminomethylpyridine and deprotection in acidic conditions give access to AMD3465.



Scheme III-1: General synthesis scheme of AMD3100 and AMD3465.

In order to introduce an additional group, functionalized analogues were synthesized using the methodologies reported above and are reported in Figure III-5. Thus, AMD3100 was functionalized on a nitrogen atom of cyclam ring by a quinoline group<sup>259</sup> or azidothymidine.<sup>258</sup> There are only two examples of functionalized AMD3465 derivatives reported in the literature, with a methyl<sup>257</sup> or methylpyridine group<sup>260</sup> on the nitrogen atom bearing the pyridine moiety.

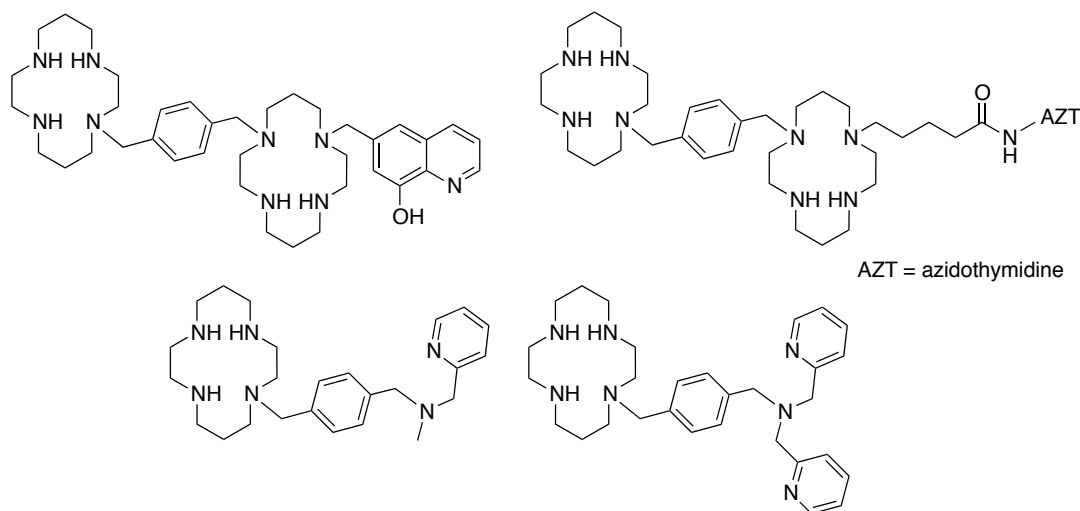


Figure III-5: Examples of functionalized AMD3100 and AMD3465 derivatives.

We investigated the synthesis of two building blocks carrying a primary amine in AMD3100 and AMD3465 series (Figure III-6). The anchor point choice of the spacer in both series will be discussed in the following part.

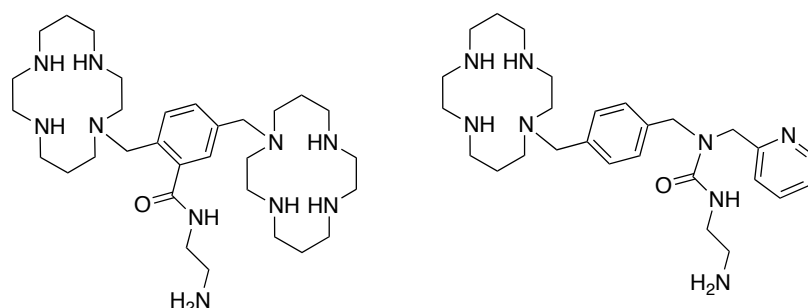


Figure III-6: Building blocks in AMD3100 and AMD3465 series.

### III.1.1.1 AMD3100 series

We first considered the introduction of the spacer on the aromatic moiety in AMD3100 series (Figure III-7). The formation of such compound requires the preliminary synthesis of a dibromo aromatic spacer bearing an ester group. The resulting substituted *p*-dibromoxylyl group can be further functionalized with tris(Boc)cyclam and the grafting function can be introduced by nucleophilic substitution on the ester group.

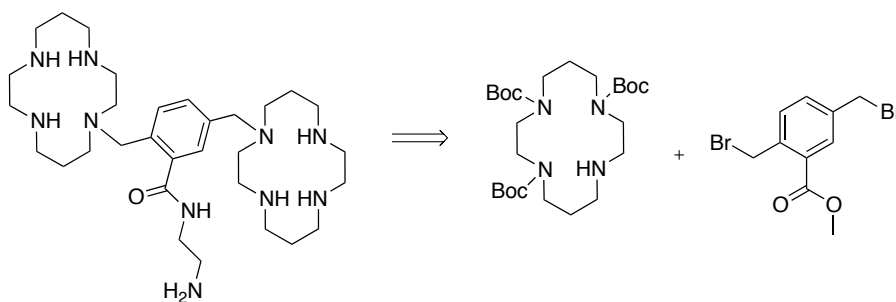
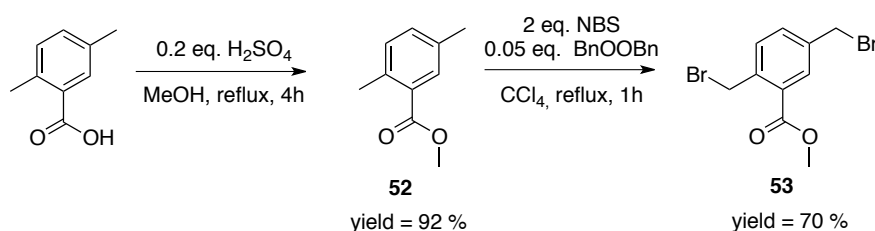


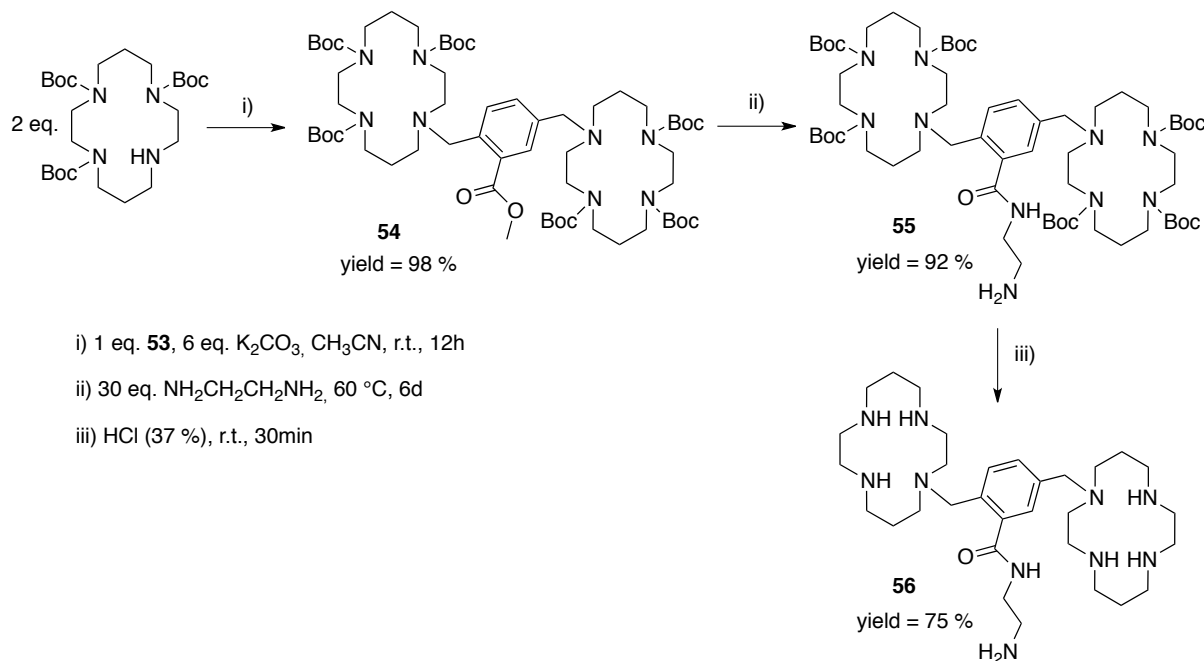
Figure III-7: Retrosynthesis towards AMD3100-based building block.

The aromatic core was obtained in two steps from the commercial products (Scheme III-2).<sup>261</sup> Esterification with methanol using sulfuric acid as catalyst yielded compound **52** in 92 % yield. Compound **53** was finally prepared through NBS-based bis-bromination of the aryl methyl groups of compound **52**.



Scheme III-2

The AMD3100 structure was then built through condensation of two equivalents of tris(Boc)cyclam on compound **53** in the presence of a base (Scheme III-3). The resulting compound **54** was isolated in 98 % yield. The nucleophilic attack of ethylenediamine on the ester function of **54** gave access to **55** after 6 days at 60 °C. Boc groups were then deprotected in acidic condition yielding the desired building block **56** in 75 % yield.



Scheme III-3

The  $^1\text{H}$  NMR spectrum of compound **56** attested the deprotection of the Boc groups (Figure III-8). The signals of the  $\text{CH}_2\text{a}$  and  $\text{CH}_2\text{a}'$  appear upfield, *i.e.* around 4.5 ppm.

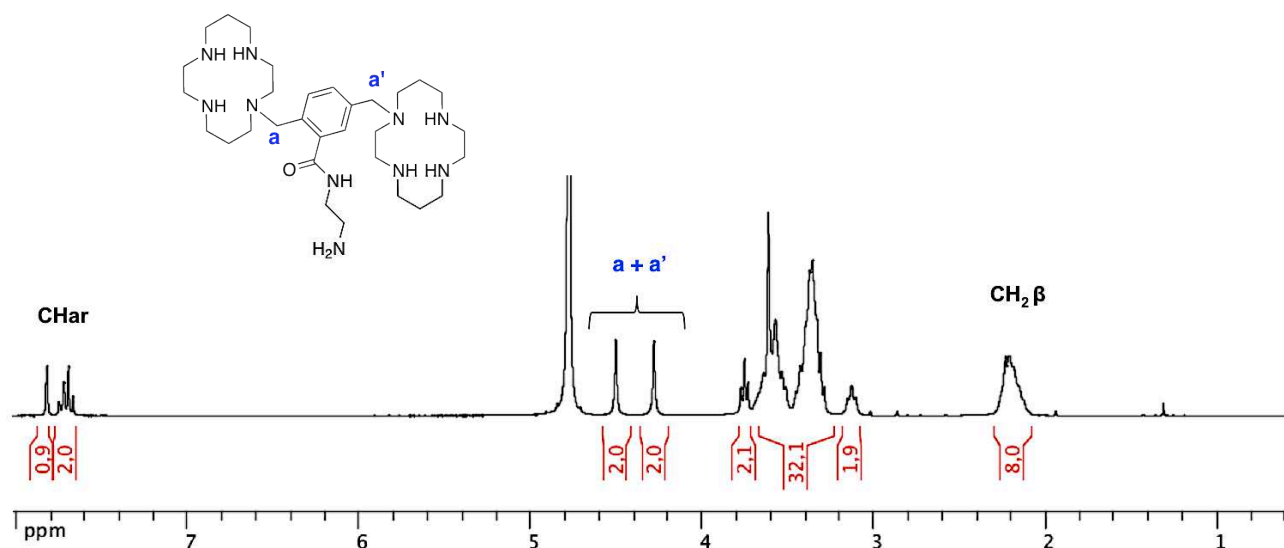
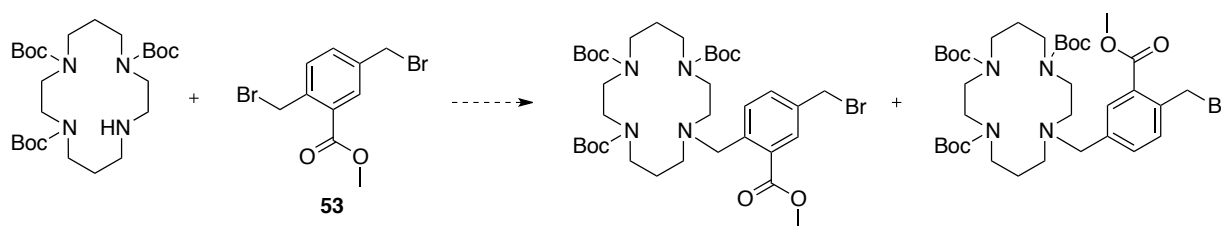


Figure III-8:  $^1\text{H}$  NMR spectrum of compound **56** (300 MHz,  $\text{D}_2\text{O}$ , 300 K).

### III.1.1.2 AMD3465 series

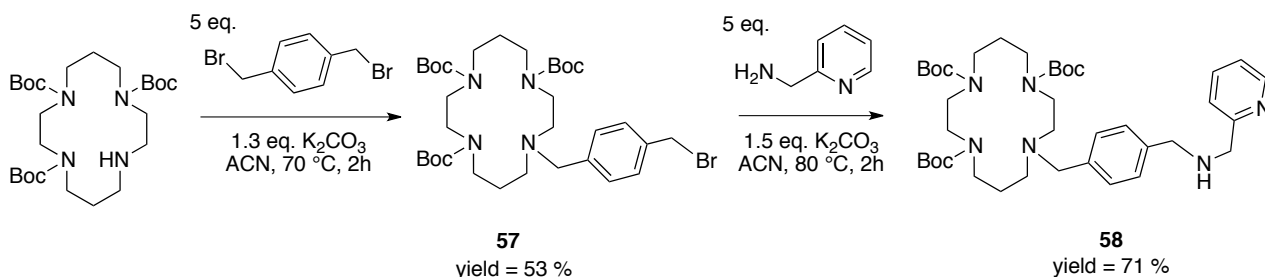
Another strategy was investigated to prepare AMD3465 derivatives. Indeed, the aromatic spacer **53** being asymmetrical, the addition of tris(Boc)cyclam would result in two regioisomers hardly separable (Scheme III-4).



Scheme III-4

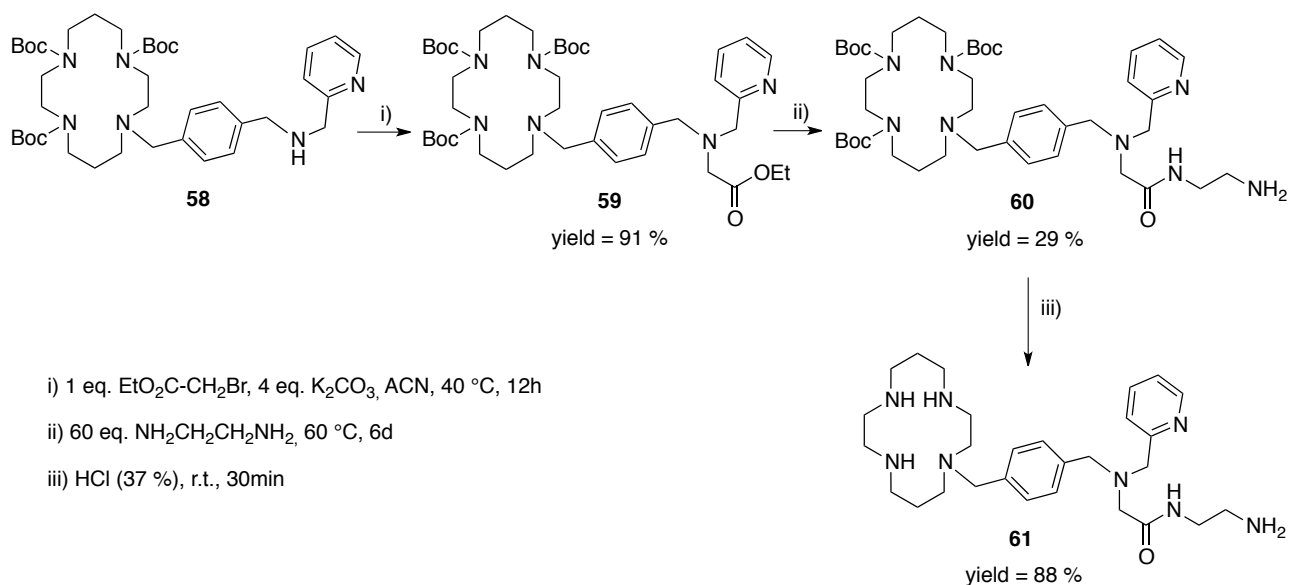
Thus, we decided to build the AMD3465 scaffold and to further introduce the linker on the amino group of the aminomethylpyridine moiety.

The addition of five equivalents of  $\alpha,\alpha$ -dibromo-*p*-xylene on tris(Boc)cyclam resulted in the formation of compound **57** in 53 % yield. Compound **58** was obtained after nucleophilic substitution of the bromide by aminomethylpyridine.



Scheme III-5

The secondary amine of compound **58** was then alkylated by using ethylbromoacetate in acetonitrile in the presence of potassium carbonate (Scheme III-6). Compound **59** was isolated in 91 % yield and added to a large excess of ethylenediamine yielding compound **60**. Several successive chromatographic columns on silica gel were necessary to purify this compound, which was finally obtained in 29 % yield. Finally, the acidic hydrolysis of the Boc groups gave access to the desired building block **61**.



Scheme III-6

The synthesis of building block **61** was realized in 5 steps from tris(Boc)cyclam in 9 % yield. This overall yield was not satisfying and moreover the purification process of compound **60** was particularly tedious. These issues prompted us to develop a new synthetic procedure.

We considered the preparation of an analogue of compound **60** bearing a protective group on the primary amine function (Figure III-9). The resulting compound being less polar, its purification should be easier by column chromatography. This compound could be synthesized by following the retrosynthesis reported in Figure III-9, which is based on the peptidic coupling between a monoprotected diamine and an AMD3465 derivative carrying a carboxylic acid function.



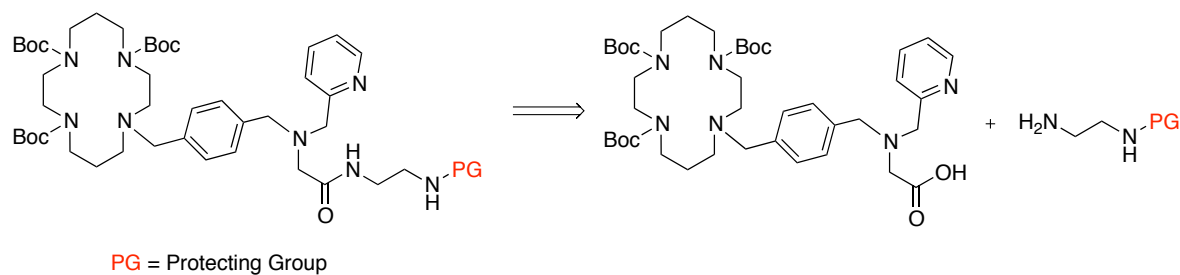
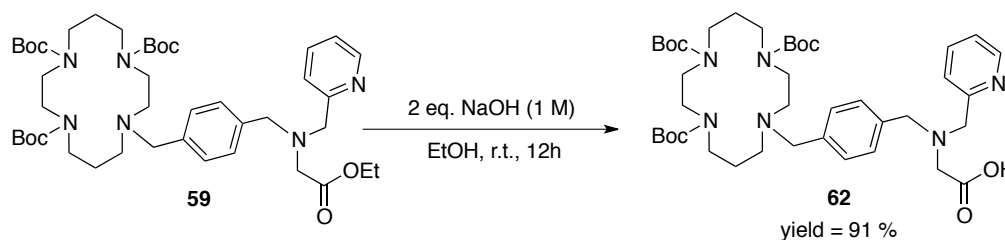


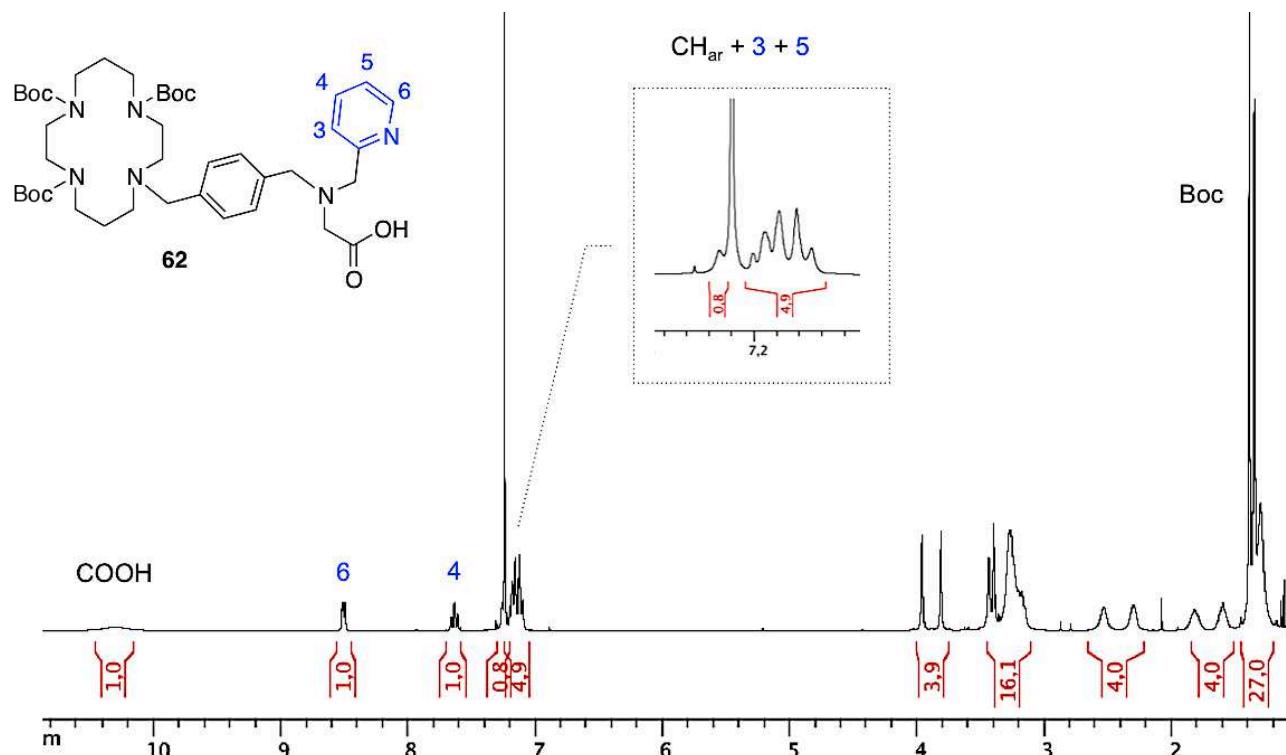
Figure III-9

We were able to selectively deprotect the ethylic ester function of compound **59** by using two equivalents of NaOH in ethanol (Scheme III-7).<sup>262</sup> The resulting compound was purified by simple extraction and isolated in 91 % yield.

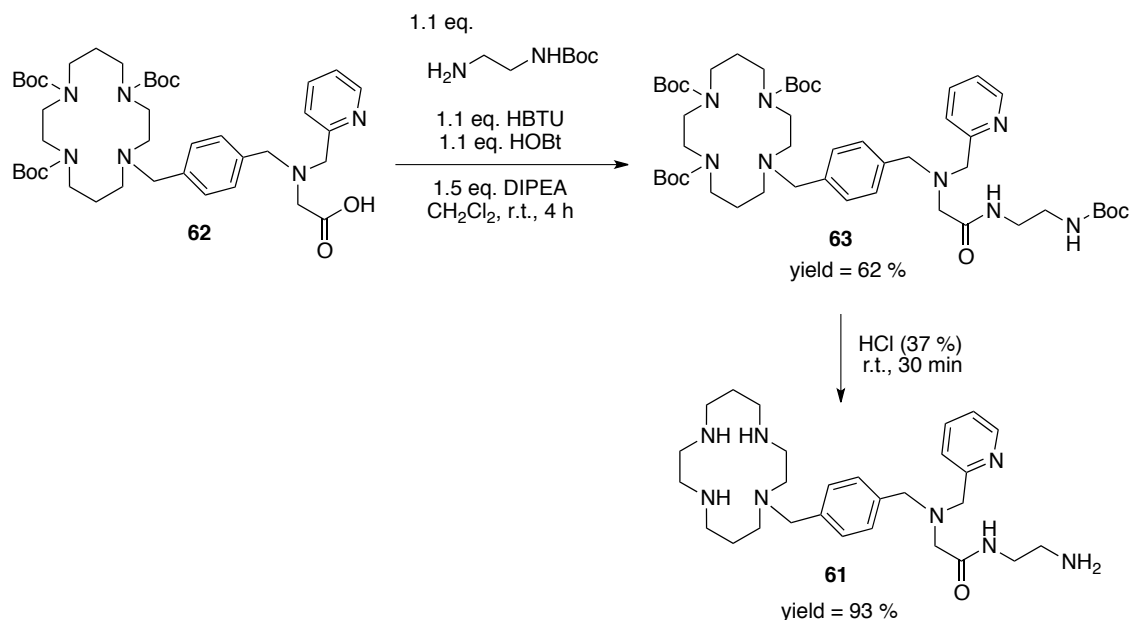


Scheme III-7

<sup>1</sup>H NMR spectrum of compound **62** indicates the presence of the Boc groups and confirms the saponification of the ester function (Figure III-10). Indeed, the large signal at 10.31 ppm is typical of a carboxylic acid proton.

Figure III-10: <sup>1</sup>H NMR spectrum of compound **62** (300 MHz, CDCl<sub>3</sub>, 300 K).

Compound **62** was then engaged in a coupling reaction with *tert*-butyl(2-aminoethyl)carbamate in the presence of base (Scheme III-8). Such process is based on the activation of the carboxylic acid moiety in the presence of coupling reagents, *i.e.* HOBt and HBTU, yielding compound **63** in 62 % yield after purification by flash chromatography. Final step consisted in the acidic hydrolysis of Boc groups resulting in the formation of **61** in 93 % yield.



Scheme III-8

The synthetic pathway described above enabled the obtention of product **61** in a higher overall yield compared to the method reported in Scheme III-6 (15 % instead of 9 %). Even though the process involves one step more, the syntheses are faster, the reaction conditions are milder and purifications are easier and reproducible.

To conclude, we developed efficient syntheses towards functionalized AMD3100 and AMD3465 derivatives. With the building blocks in hand, we sought to add a probe by using coupling reactions with carboxylic acid, active ester or anhydride (Figure III-11). The advantage of this approach is the possibility to introduce at this stage any kind of probes, such as a fluorescent dye or a macrocyclic chelating agent.

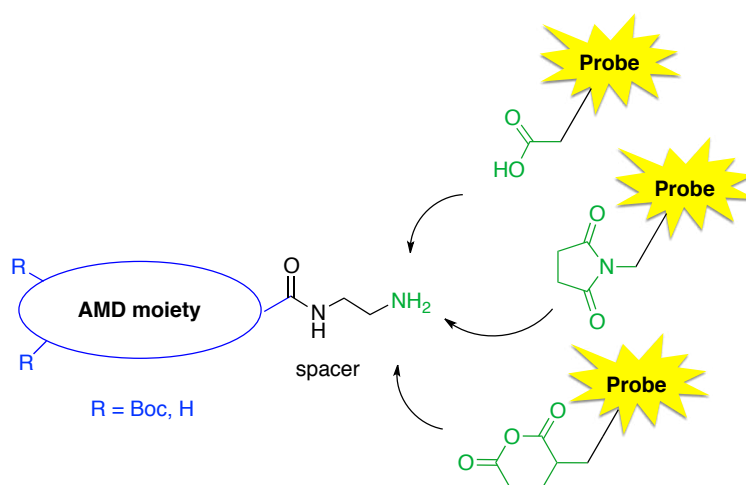


Figure III-11: General procedure to introduce the desired tag on the building blocks.

## III.2 New imaging agents for targeting CXCR4

### III.2.1 Introduction of a fluorescent tag

Among the fluorescent probes, the borodipyromethene family (4,4-difluoro-4-borata-3a-azonia-4a-aza-s-indacene, abbreviated as Bodipy<sup>®</sup>) has gained recognition as being one of the most versatile fluorophores and this dye has steadily increased in popularity over the past two decades due to their excellent properties (Figure III-12).<sup>118,263-268</sup> They exhibit high stability, high extinction coefficients, sharp emission bands and high fluorescence quantum yields.<sup>269-271</sup> They are soluble in most organic solvents and recently water soluble dyes were obtained by functionalization with oligo(ethyleneglycol) residues<sup>272</sup> or addition of sulfonic acid,<sup>273-275</sup> carboxylic acid<sup>276</sup> or quaternary ammonium moieties.<sup>274</sup>

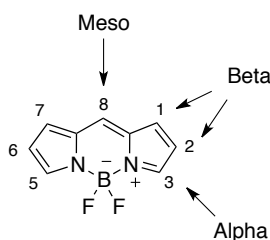


Figure III-12: Generic structure of Bodipy.

The photophysical characteristics of synthetically modified Bodipys vary with respect to the number, nature, as well as the position of the attached substituents.<sup>271</sup> Conjugation of the  $\pi$ -electrons runs along the organic backbone and can be extended by condensation of suitable groups onto the periphery or by attachment of conjugated units to one or both pyrrole fragments. Such extended delocalization pathway lead to Bodipy dyes emitting in the near-IR regions of the spectrum, which is of great interest for *in vivo* applications.<sup>272,273</sup>

All these attractive properties prompted us to introduce a Bodipy dye on the AMDs-based building blocks. This work requires the preparation of a Bodipy scaffold carrying a grafting function. Many synthetic methodologies have been reported in the literature to build and functionalize the Bodipy core. Our group optimized the reaction conditions of a *meso*-substituted Bodipy bearing a carboxylic acid function and the resulting compound was activated and added on various macrocyclic units (Figure III-13).<sup>148,276</sup> The incorporation of macrocyclic moieties on the Bodipy core did not impact the photophysical properties of the dye and made it soluble in water. All compounds exhibited the spectral characteristics of the parent molecule, such as absorption maxima in the range of 520-530 nm, with high molar absorption coefficients from 30,000 to 75,000 M<sup>-1</sup>cm<sup>-1</sup>. The emission maxima of the molecules were in the range of 520-525 nm with high quantum yield (from 50 % to 72 %).

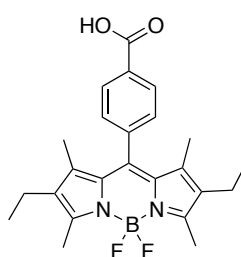
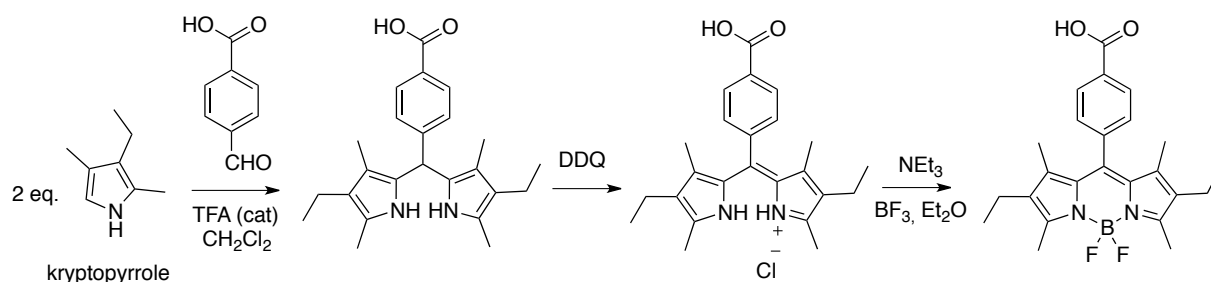


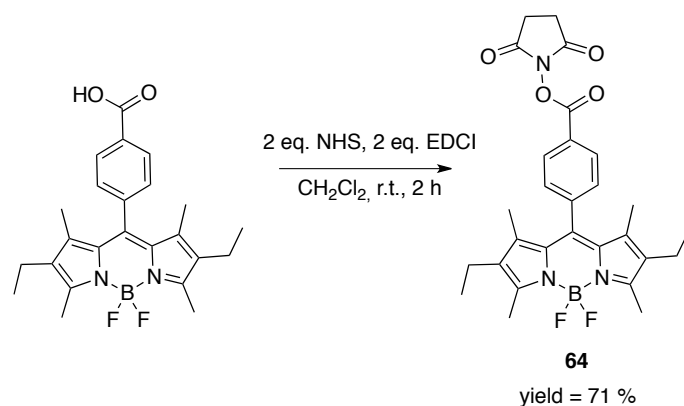
Figure III-13: *Meso*-substituted Bodipy.

The precursor is obtained in a classical « one-pot » synthesis approach involving acid catalyzed condensation of 4-carboxybenzaldehyde and kryptopyrroles generating a dipyrromethane species (Scheme III-9).<sup>148,277</sup> The use of DDQ enables the oxidation of the resulting dipyrromethane to dipyrromethene, which is then converted to Bodipy by action of a tertiary amine and BF<sub>3</sub>.OEt<sub>2</sub>.



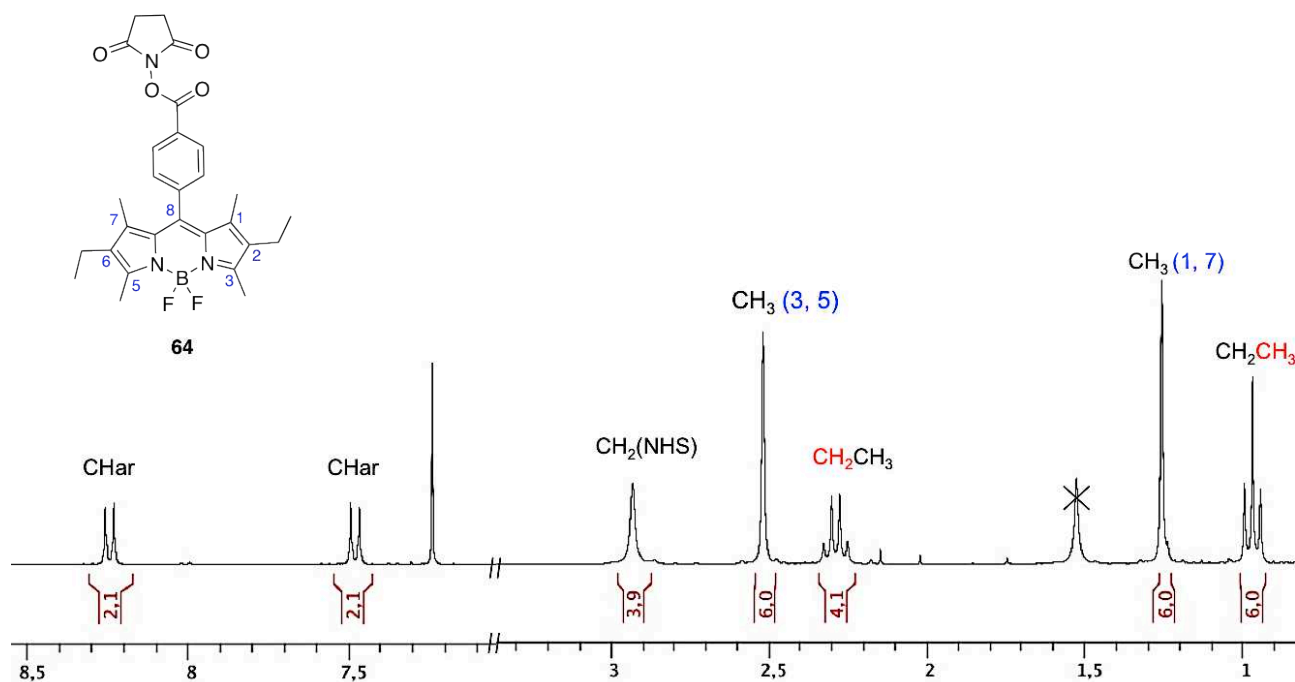
Scheme III-9

This key intermediate was converted to the corresponding *N*-hydroxysuccinimidyl ester **64** in 71% yield, upon reaction with NHS in the presence of EDCI in dichloromethane at room temperature (Scheme III-10).<sup>276,277</sup> Compound **64** is particularly stable and can be easily purified by column chromatography on silica gel.

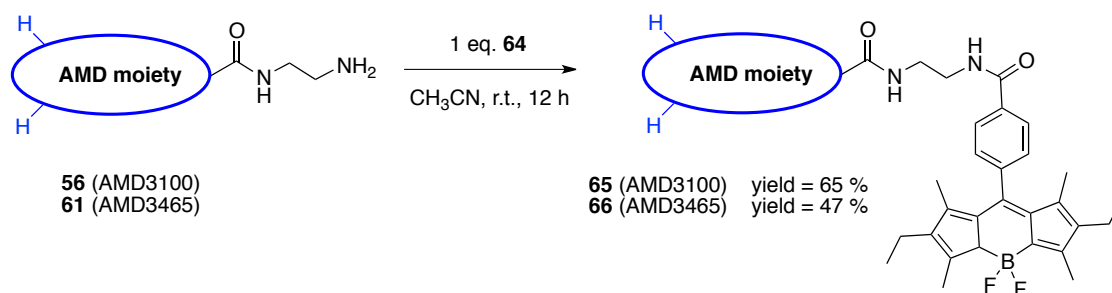


Scheme III-10

Compound **64** was analyzed by NMR spectroscopy in  $\text{CDCl}_3$ . Well-resolved  $^1\text{H}$  NMR spectrum of **64** shows a peak at around 2.92 ppm due to the  $\text{CH}_2$  protons of the *N*-hydroxysuccinimidyl moiety (Figure III-14). The ethyl group signals consist of a triplet at 0.97 ppm and a quartet at 2.27 ppm. The singlet at 1.26 ppm is attributed to the six protons of the methyl groups in position 1 and 7. The methyl groups in position 3 and 5 are affected by the presence of the nitrogen atom and appear downshifted at 2.51 ppm.

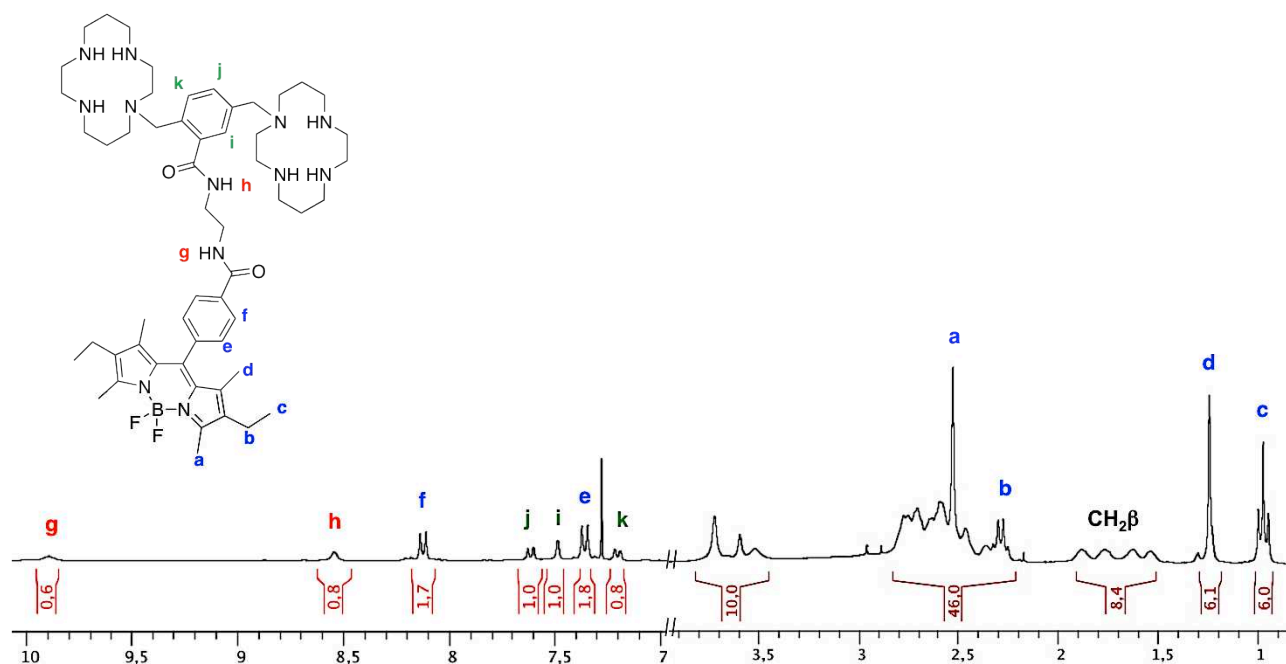
Figure III-14:  $^1\text{H}$  NMR spectrum of compound **64** (300 MHz,  $\text{CDCl}_3$ , 300 K).

The subsequent coupling of the activated ester **64** with the building blocks in both series AMD3100 and AMD3465 series yielded compounds **65** and **66** in 65 % and 47 % yield respectively. Both compounds were isolated after column chromatography. It has to be noted that **65** and **66** are both soluble in various organic solvents (DMF, acetonitrile, dichloromethane) and also in water. This behavior has been previously reported in Bodipy-DOTA derivatives.<sup>276</sup>



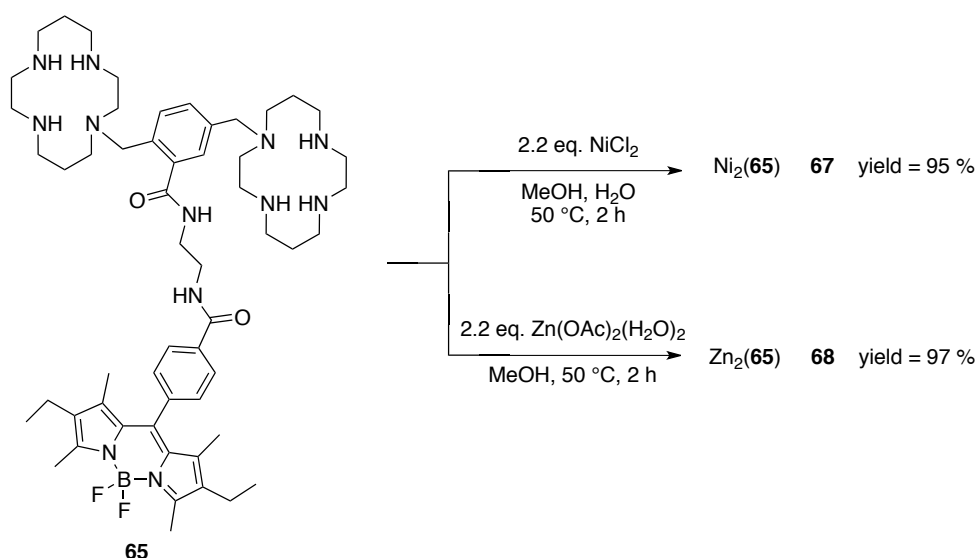
Scheme III-11

The NMR spectrum of compound **65** in  $\text{CDCl}_3$  is reported in Figure III-15. The formation of the desired compound was attested by the presence of a signal characteristic of an amide proton at 9.9 ppm. The aromatic signals were attributed with COSY  $\{^1\text{H}-^1\text{H}\}$  analysis.

Figure III-15:  $^1\text{H}$  NMR spectrum of compound **65** (300 MHz,  $\text{CDCl}_3$ , 300 K).

It has been previously demonstrated that incorporation of metal ions such as  $\text{Zn}^{2+}$  and  $\text{Ni}^{2+}$  into the cyclam rings led to the enhancement of the binding affinity to CXCR4. Thus, from the free ligand **65** and **66** were prepared a series of transition metal complexes.

Compound **65** was labeled with  $\text{Ni}^{2+}$  and  $\text{Zn}^{2+}$  (Scheme III-12) by adding two equivalents of metal salts. Both complexes were isolated in good yield and are water-soluble. The formation of the resulting complexes **67** and **68** was attested by mass spectrometry.



Scheme III-12

As an example, the HR-MS spectrum of the biszinc complex in AMD3100 is reported in Figure III-16. The spectrum exhibits a peak corresponding to the molecular ion  $[\text{M}-3\text{OAc}-\text{H}]^{2+}$ .

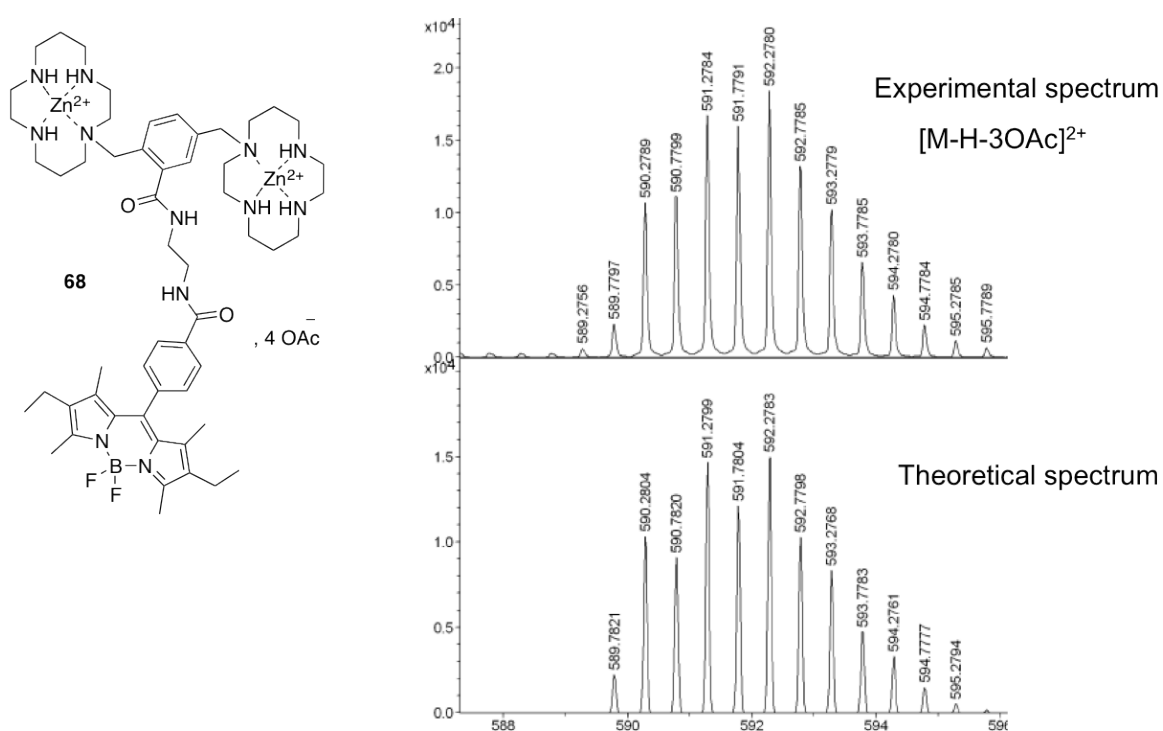
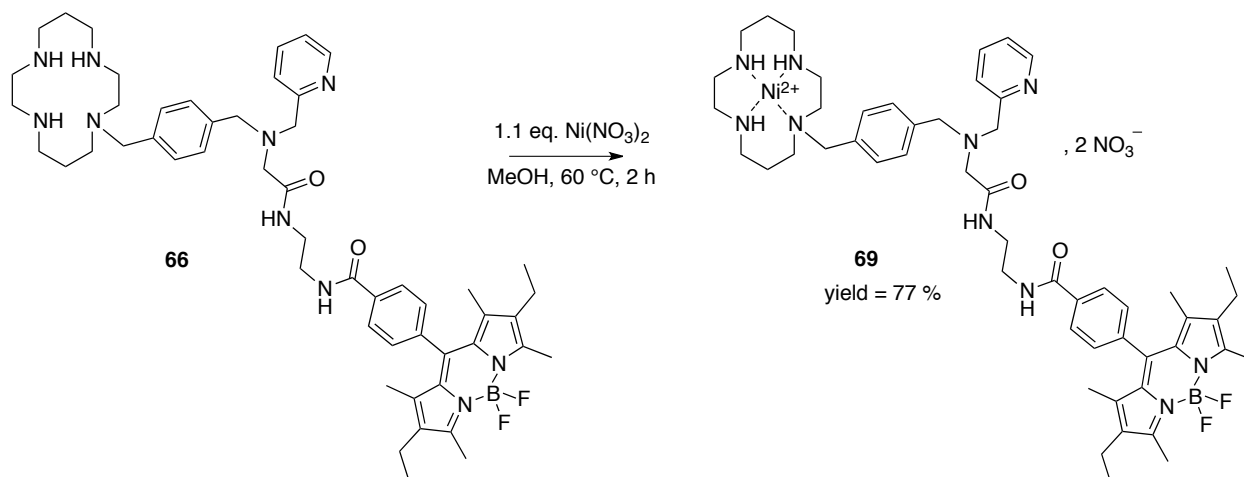


Figure III-16: HR-MS spectrum of compound **68**. Comparison between experimental spectrum and theoretical spectrum ( $\Delta(\text{ppm}) = 2.4$ ).

We also prepared the Ni(II) complex in AMD3465 series from the free ligand **66**. The addition of 1.1 equivalent of  $\text{Ni}(\text{NO}_3)_2$  in methanol resulted in the formation of the desired compound in 77% yield (Scheme III-13). Compound **69** is also soluble in water.



Scheme III-13

To conclude, a fluorescent dye was successfully added on the AMD3100 and AMD3465 scaffolds. Five new systems, either metalated and non-metalated, were obtained in good yields and are water-soluble, thus enabling the use of such agents for *in vivo* optical imaging. Photophysical and biological studies are being currently investigated on each compound and the results will be of great importance to validate the proof-of-concept of this project. The addition of a bulky group on the AMD core can cause steric hindrance, resulting in diminution of the binding affinity and specificity to the receptor. From the biological results, we will be able to tune the AMD scaffold to get the system with the highest potential, by introducing a longer spacer or modifying the spacer anchor point.

### III.2.2 Introduction of a macrocyclic chelating agent

We then investigate the synthesis of new imaging agents for nuclear imaging applications by introducing a chosen chelate on the building blocks. The general procedure giving access to these new systems is reported in Figure III-17. We will first concentrate on the introduction of a macrocyclic chelating agent (DOTA or NODAGA) on the building blocks previously prepared. In a second part, we will present the strategy based on the protection of the cyclam rings with a chosen metal to allow the selective radiolabeling of DOTA or NODAGA moiety.



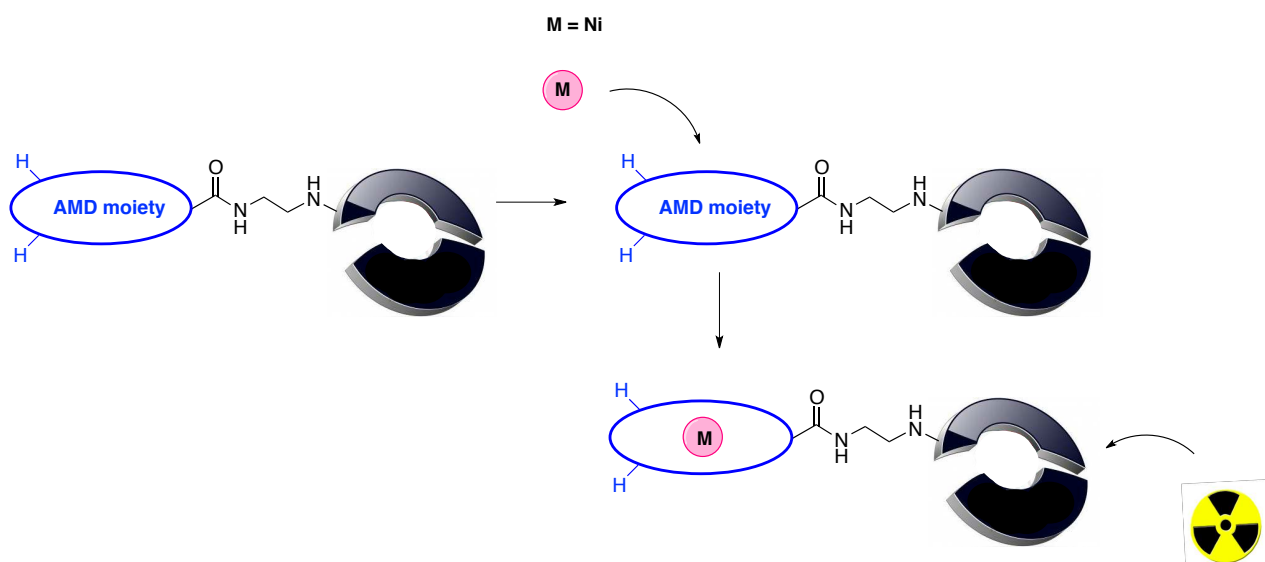


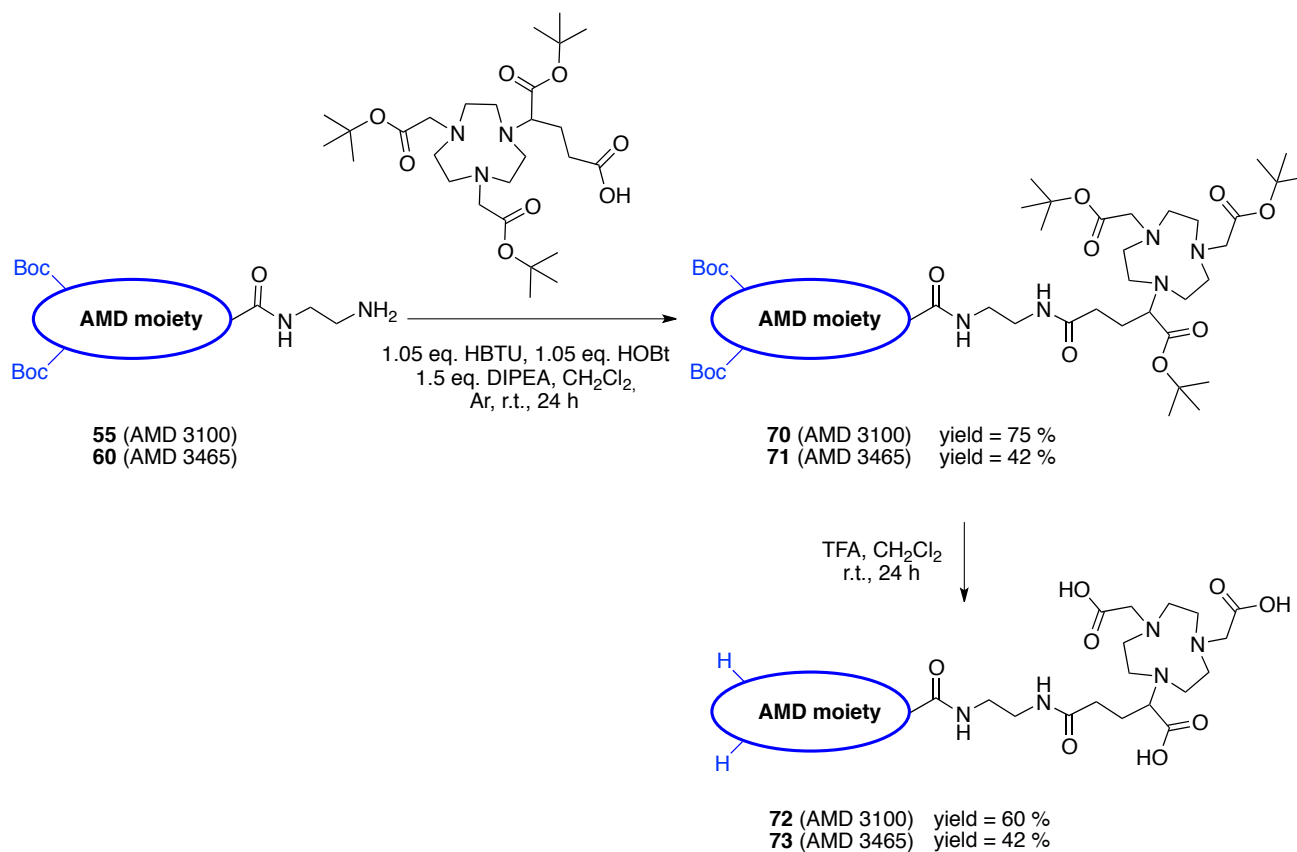
Figure III-17: Protection of the AMD moiety by using a metal cation that enables selective radiolabeling.

### III.2.2.1 Choice of the radiochelate

We considered the synthesis of AMD3100 and AMD3465 analogues carrying a NODAGA moiety that is adapted for Cu(II) and Ga(III) and a DOTA moiety for In(III) chelation. We started from the Boc protected building blocks (**55** and **60**) for synthetic purposes: after coupling, the purification process will be easy by chromatography on normal phase.

#### III.2.2.1.1 Introduction of a NODAGA moiety

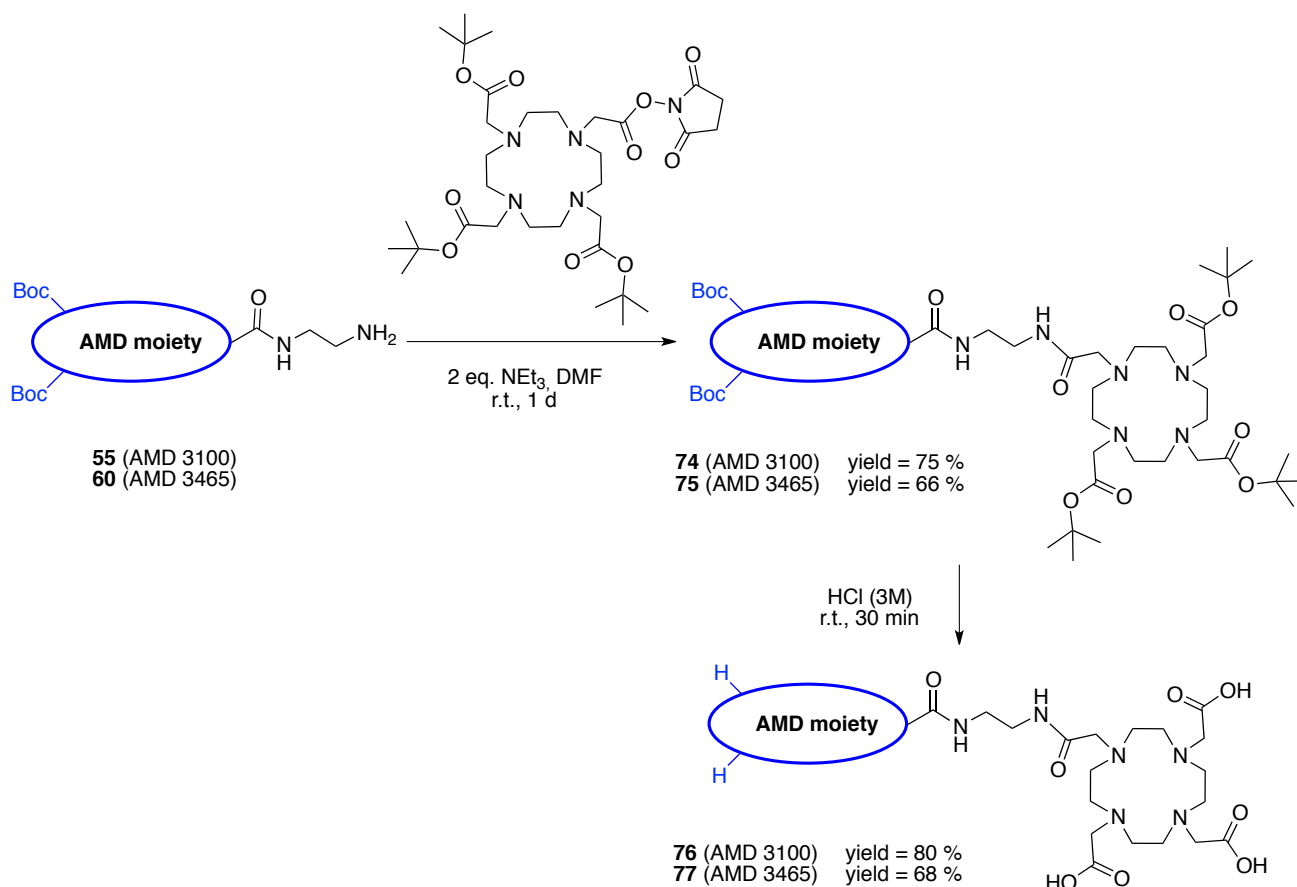
The addition of NODAGA-tris(<sup>t</sup>Bu) in the presence of DIPEA and coupling agents on compounds **55** and **60** resulted respectively in the formation of **70** and **71**, which were easily purified by chromatography on silicate. After deprotection of the Boc and ester groups in acidic conditions, the corresponding tris-macrocycle **72** and bis-macrocycle **73** were isolated in 60 % and 42 % yield.



Scheme III-14

### III.2.2.1.2 Introduction of a DOTA moiety

The addition of one equivalent of DOTA-tris(<sup>t</sup>Bu)ester NHS on **55** and **60** in the presence of a base resulted in the formation of the expected tris- and bis-macrocycle, respectively **74** and **75** (Scheme III-15). Both compounds **74** and **75** were purified by flash chromatography on normal phase and isolated in quite good yields. The deprotection of both Boc and ester groups in acidic conditions gave access to compound **76** and **77**.



Scheme III-15

To observe the amide protons resonance, NMR analyses of compound **76** and **77** were performed in DMSO. The resulting  $^1\text{H}$  NMR spectrum of compound **77** at 365 K is reported in Figure III-19. The spectrum exhibits characteristic signals such as the multiplet around 2.2 ppm corresponding to the  $\text{CH}_2\beta$ . From  $^1\text{H}$ - $^1\text{H}$  COSY experiment, the signals at  $\delta = 8.57$  ppm and  $\delta = 8.69$  ppm were assigned to amide protons. The crosspeaks on the COSY spectrum indicates the correlation between the amide protons and  $\text{CH}_2$  protons. The corresponding spectrum also enabled the assignments of phenyl and pyridine protons. The multiplet around 7.5 ppm is attributed to the aryl protons and the protons of the pyridine moiety appear downfield.

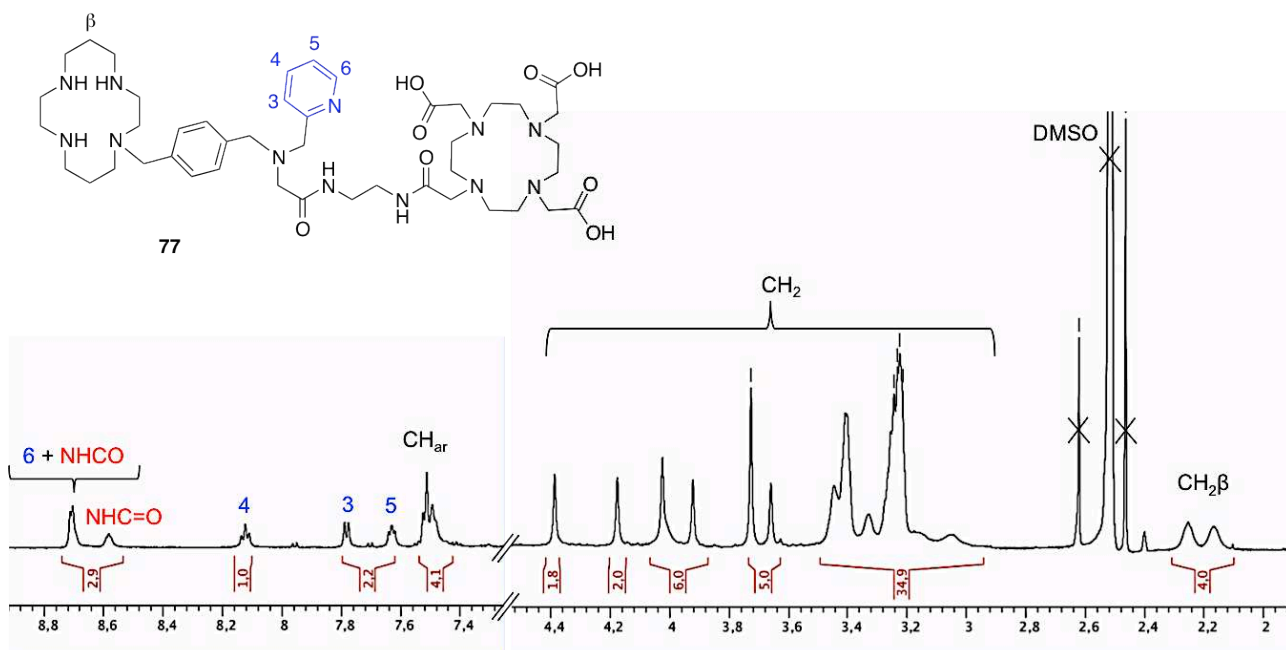


Figure III-18:  $^1\text{H}$  NMR spectrum of compound **77** (600 MHz, DMSO, 365 K).

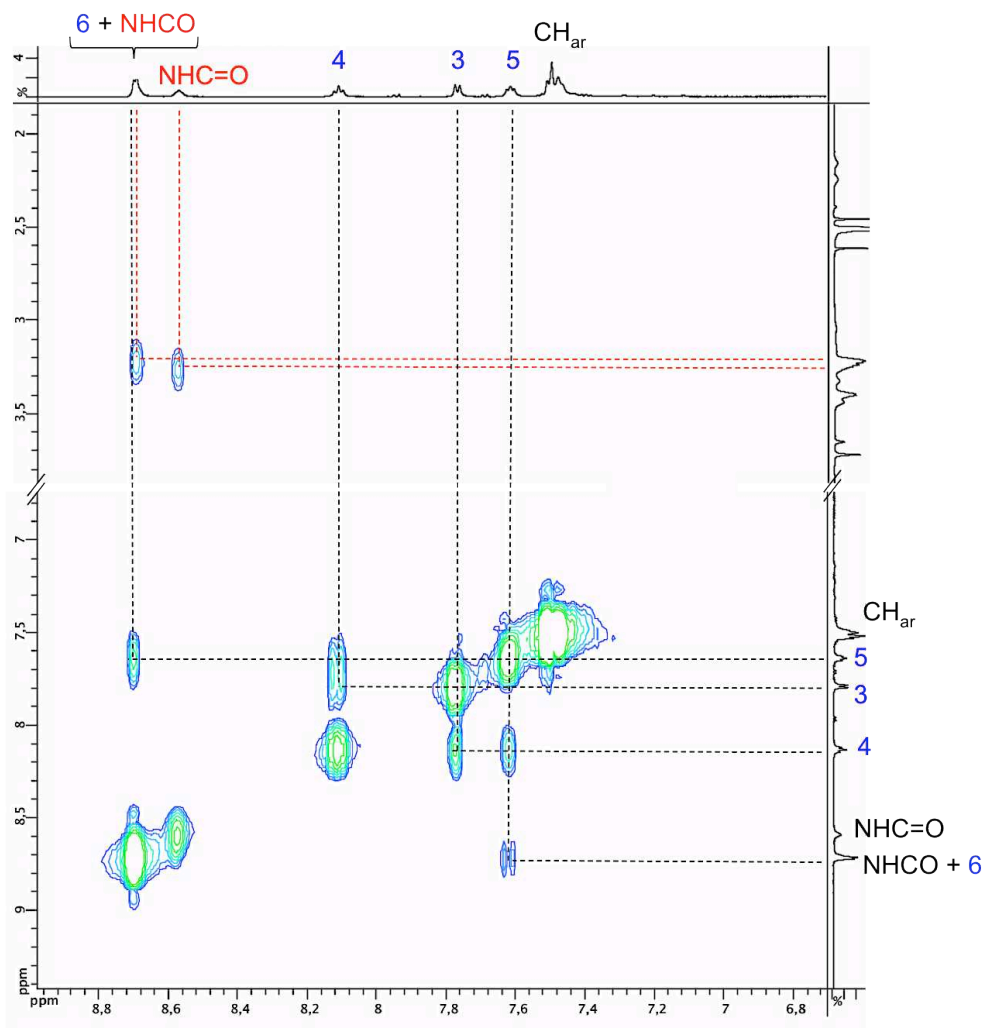
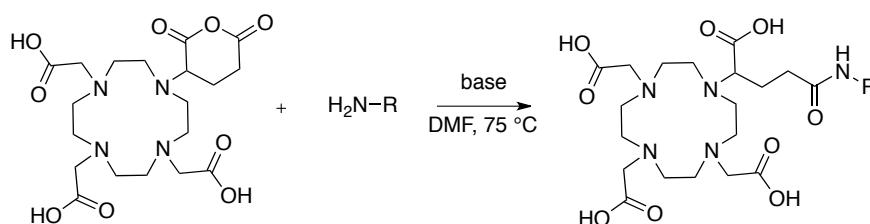


Figure III-19: Parts of the COSY  $\{^1\text{H}-^1\text{H}\}$  NMR spectrum of compound **77** (600 MHz, DMSO, 365 K). Correlations are indicated by dashed lines.

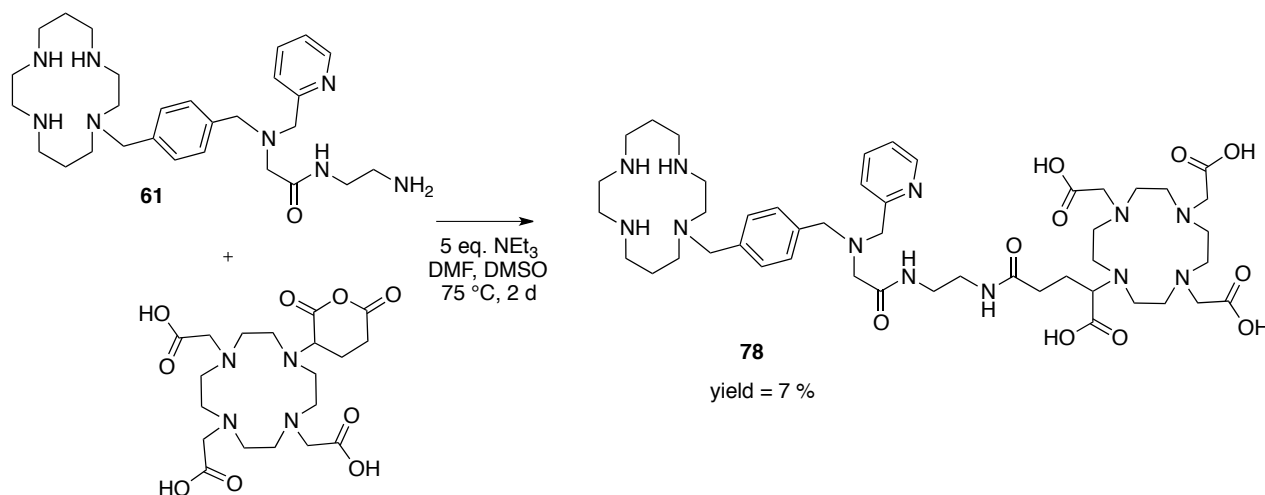
## III.2.2.1.3 Introduction of a DOTAGA moiety

In the previous case, the attachment of the DOTA-fragment onto the building blocks has involved one of the coordinating acetate pendant arms thereby leading to DOTA-monoamide units. The transformation of one of the carboxylic acid group into a carboxamide can decrease the stability of the complex. Thus, we decided to introduce a DOTAGA derivative on our building blocks by using a convenient approach developed in our group based on the ring opening of the anhydride function of the DOTAGA-anhydride.<sup>148,184,186</sup> The regioselectivity of the reaction has been previously elucidated and the reaction with amines or other nucleophilic agents a sole product (Scheme III-16).<sup>184</sup>



Scheme III-16: Selective ring opening of DOTAGA-anhydride

Compound **61** was reacted with DOTAGA-anhydride in DMF at 75 °C in the presence of NEt<sub>3</sub> (Scheme III-17). After one day, we didn't observe the formation of the expected compound, probably because of the poor solubility of the anhydride species in the mixture. The addition of DMSO enabled the obtention of compound **78**. After purification by column chromatography on a C18-reverse phase column, **78** was isolated in 7 % yield.



Scheme III-17

The reaction conditions need to be optimized, however this approach is of great interest. Indeed in comparison with other activated acid derivatives such as NHS esters, the formation of the amide bond generates no side-products that need to be separated from the conjugate. Moreover, in this case four acetate arms are available for metal chelation.

### III.2.2.1.4 Conclusion

Five new systems were synthesized in few steps from the AMD-based precursors. The building blocks developed in the laboratory offer a convenient and attractive approach to generate various imaging agents for radiometal chelation.

### III.2.2.2 Protection of the cyclam rings

It has been previously demonstrated that incorporation of metal ions such as  $Zn^{2+}$ ,  $Cu^{2+}$  and  $Ni^{2+}$  into the cyclam rings led to the enhancement of the binding affinity to CXCR4. Taking this advantage, we considered the protection of the cyclam rings by using such ions (Figure III-20). The choice of the metal is of great importance to prevent any transchelation or transmetalation phenomena in intramolecular or intermolecular level during synthesis or radiolabeling.

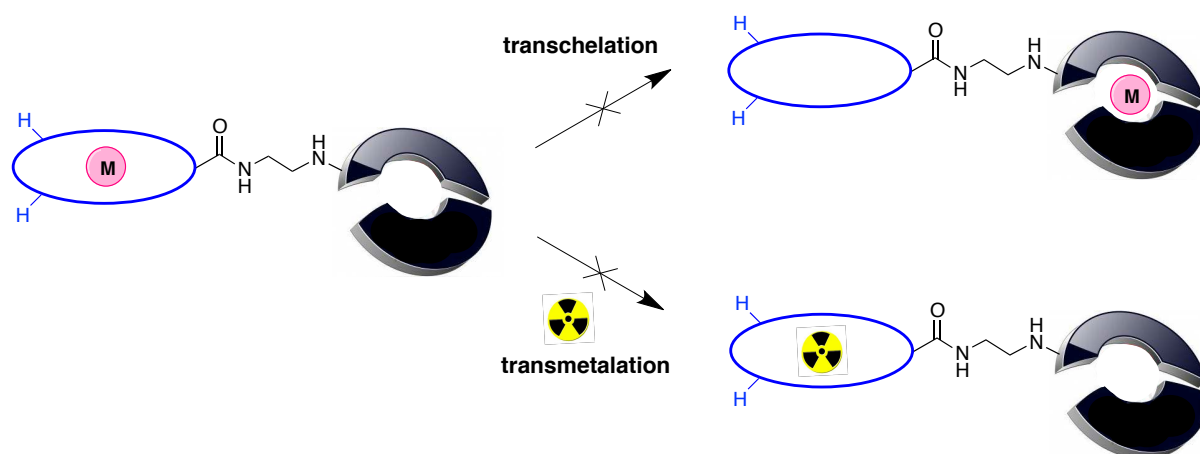


Figure III-20: Transchelation and transmetalation phenomena that can occur during the labeling and radiolabeling processes.

$Ni^{2+}$ -cyclam complexes are known to be particularly inert,<sup>278</sup> the complexes persisting almost indefinitely even in strongly acidic solutions.<sup>279,280</sup> The only reported method to remove  $Ni^{2+}$  from cyclam ring uses extremely drastic conditions involving cyanide at high temperature.<sup>279,281,282</sup> A heterodimetallic platform containing a tripodal tetraamine subunit and a cyclam subunit covalently linked through nitrogen atoms by a 1,4-xylyl spacer was reported by Amendola *et al* (Figure III-21).<sup>278,283</sup> The addition of one equivalent of  $Ni^{2+}$  on ligand A resulted in the sole labeling of the cyclam ring. The resulting complex was then reacted with copper(II) at room temperature. Even if  $Cu^{2+}$  gives with cyclam a more stable complex than  $Ni^{2+}$ , the inertness imparted by the ligand prevented metal replacement.

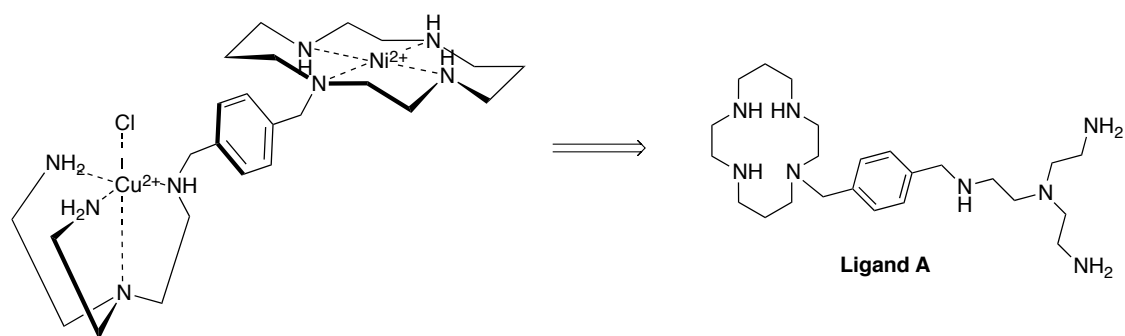


Figure III-21: Heterodimetallic platform obtained by successive labeling of ligand A with Ni(II) and Cu(II).<sup>278</sup>

This previous work prompted us to investigate the synthesis of a heterotrimetallic complex based on AMD3100 (Figure III-22). We first tried to introduce Ni(II) selectively in the cyclam rings.

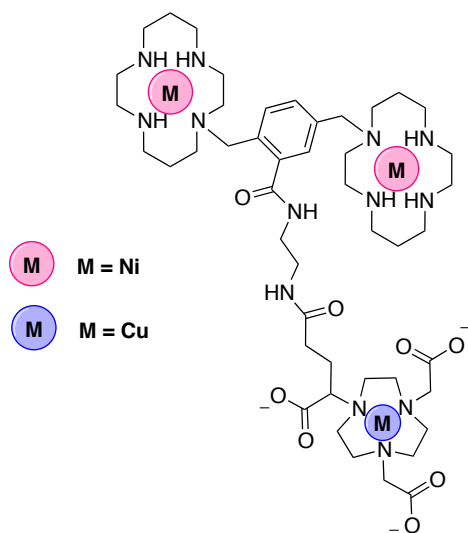
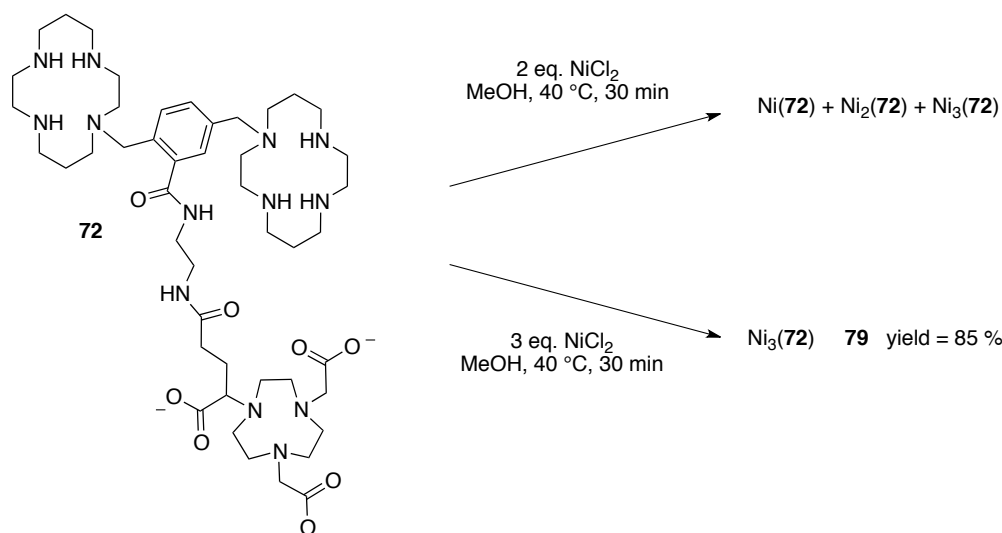


Figure III-22

First attempts of complexation with Ni<sup>2+</sup> were performed on compound **72** (Scheme III-18). Two equivalents of NiCl<sub>2</sub> were added on a solution of **72** in methanol. The mixture was heated at 40 °C during 30 min. The analysis of the mass spectrum of the crude indicated the coexistence of the mono-, bis- and tris-nickel complexes in solution that we were not able to separate. The reaction being non selective towards cyclam rings metalation, we decided to prepare deliberately the tris-nickel species by adding 3 equivalents of NiCl<sub>2</sub>.



Scheme III-18

The formation of compound **79** was attested by mass spectrometry. The HR-MS spectrum of **79** is represented in Figure III-23 and demonstrated the presence of the  $[M-3Cl]^{3+}$  species.

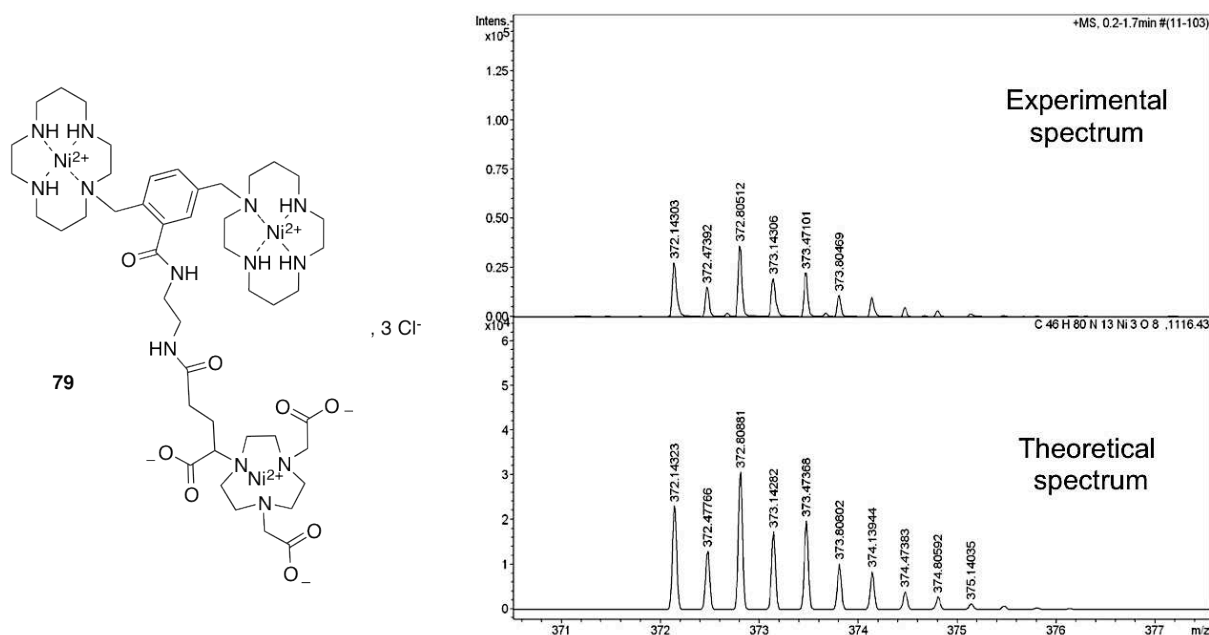


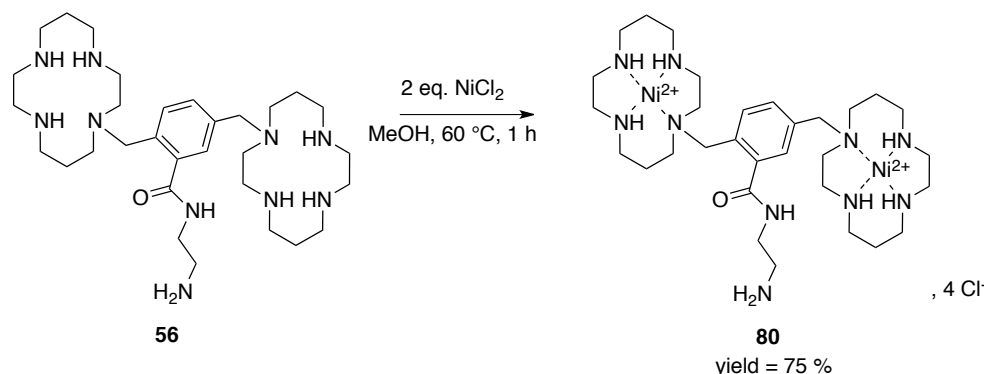
Figure III-23: HR-MS spectrum of compound **79**. Comparison between experimental spectrum and theoretical spectrum.

We tried to selectively remove Ni from the NOTA moiety by using acid at different concentrations varying the temperature, but it only resulted in the rupture of the amide bonds. The complexes were particularly inert towards demetalation by strong acids. Moreover, the addition of Cu(NO<sub>3</sub>)<sub>2</sub> in the mixture didn't yield any transmetalation phenomenon as attested by mass spectrometry indicating that both Ni(II)-cyclam and Ni(II)-NOTA complexes are particularly inert.

As it is impossible to selectively label the cyclam rings in the presence of a NODAGA moiety, we decided to introduce Ni<sup>2+</sup> directly on the building block **56** and to further functionalize the

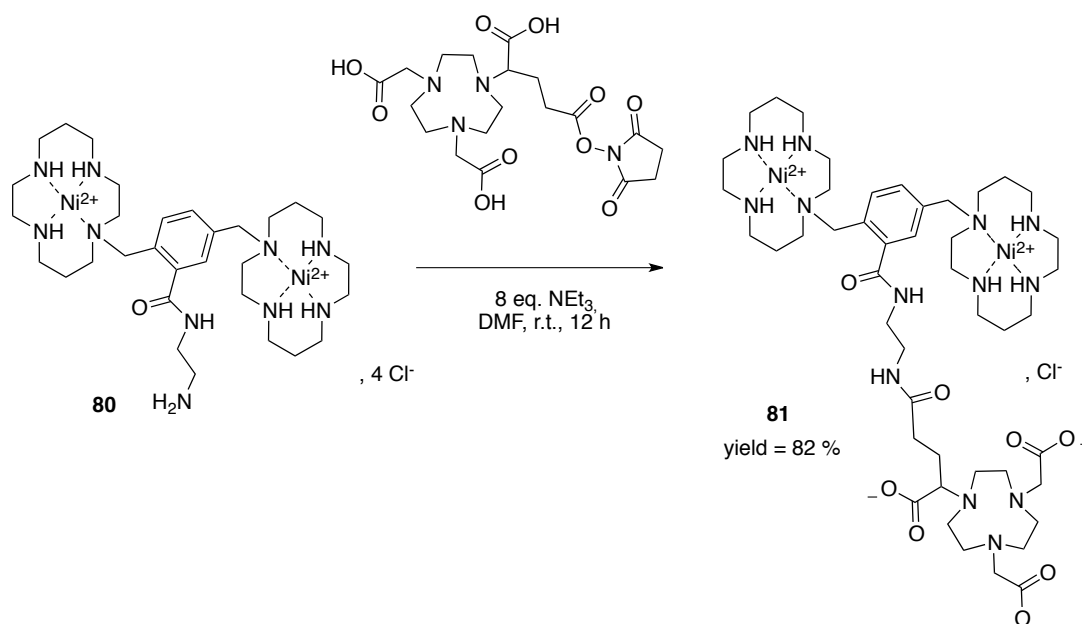


resulting complex with the third macrocycle. Thus, two equivalents of  $\text{NiCl}_2$  were added on a solution of compound **56** in methanol at  $60^\circ\text{C}$  during one hour (Scheme III-19). The resulting complex **80** was isolated in 75 % yield after purification by flash chromatography on reverse phase. This purification step is of great importance to remove any trace of free  $\text{Ni(II)}$  in the product.



Scheme III-19

Compound **80** was then engaged in a coupling reaction with NODAGA-NHS (Scheme III-20). The deprotonation of the primary amine was ensured by a large excess of base. Such coupling reaction generates NHS as by-products, and we were able to purify the desired compound **81** by using a steric exclusion column.



Scheme III-20

The HR-MS spectrum of **81** is represented in Figure III-24 and the peak at  $m/z = 530.75$  was identified as the molecular specie  $[\text{M}+\text{H}-\text{Cl}]^{2+}$  showing the formation of the expected compound as the sole product. The mass spectrum indicated that there was no trace of mono- and tris-nickel species. These data demonstrated that nickel atoms are still included in the cyclam rings. Indeed, if a transchelation phenomenon from cyclam to NODAGA occurred in solution, we should observe the coexistence of mono-, bis- and tris-nickel species.

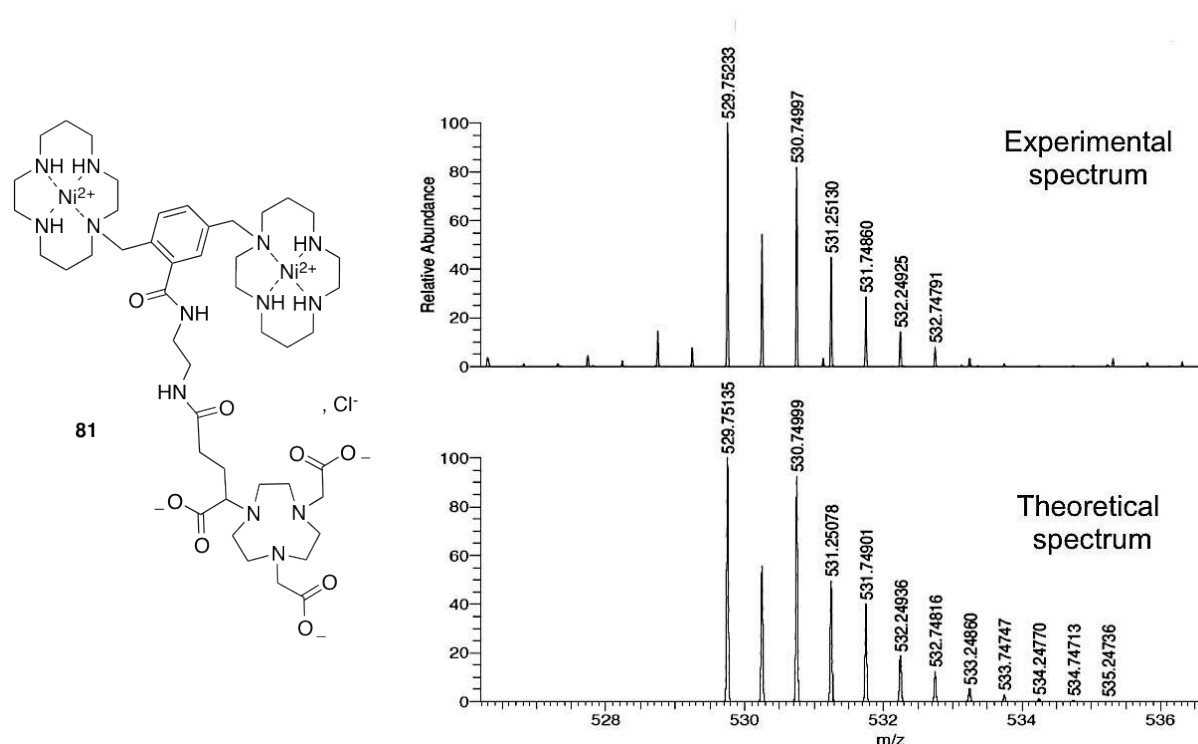
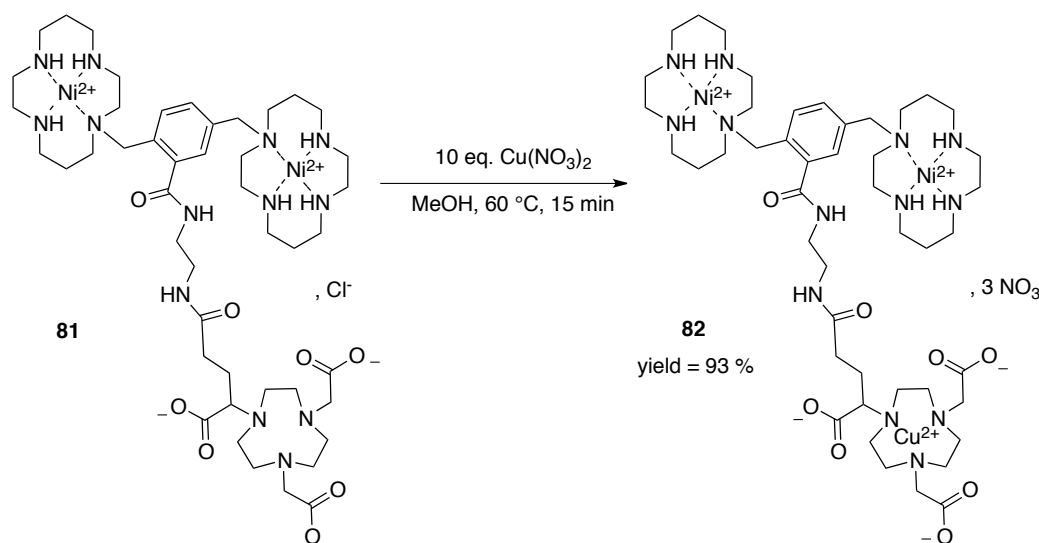


Figure III-24: HR-MS spectrum of compound **81**. Comparison between experimental spectrum and theoretical spectrum.

We then tried to introduce copper selectively in the NODAGA ring. Ten equivalents of  $\text{Cu}(\text{NO}_3)_2$  were added to compound **81** in MeOH and the resulting mixture was heated at  $60^\circ\text{C}$  during 15 min (Scheme III-21). The formation of a complex containing one copper and two nickel atoms was attested by the presence of the molecular ion  $[\text{M}-3(\text{NO}_3)-\text{H}]^{2+}$  peak at 560.21 in the mass spectrum (Figure III-25). Even though a large excess of copper was used, we didn't observe the formation of species with two or three copper atoms, indicating that Ni-cyclam complexes were inert towards transmetalation.



Scheme III-21

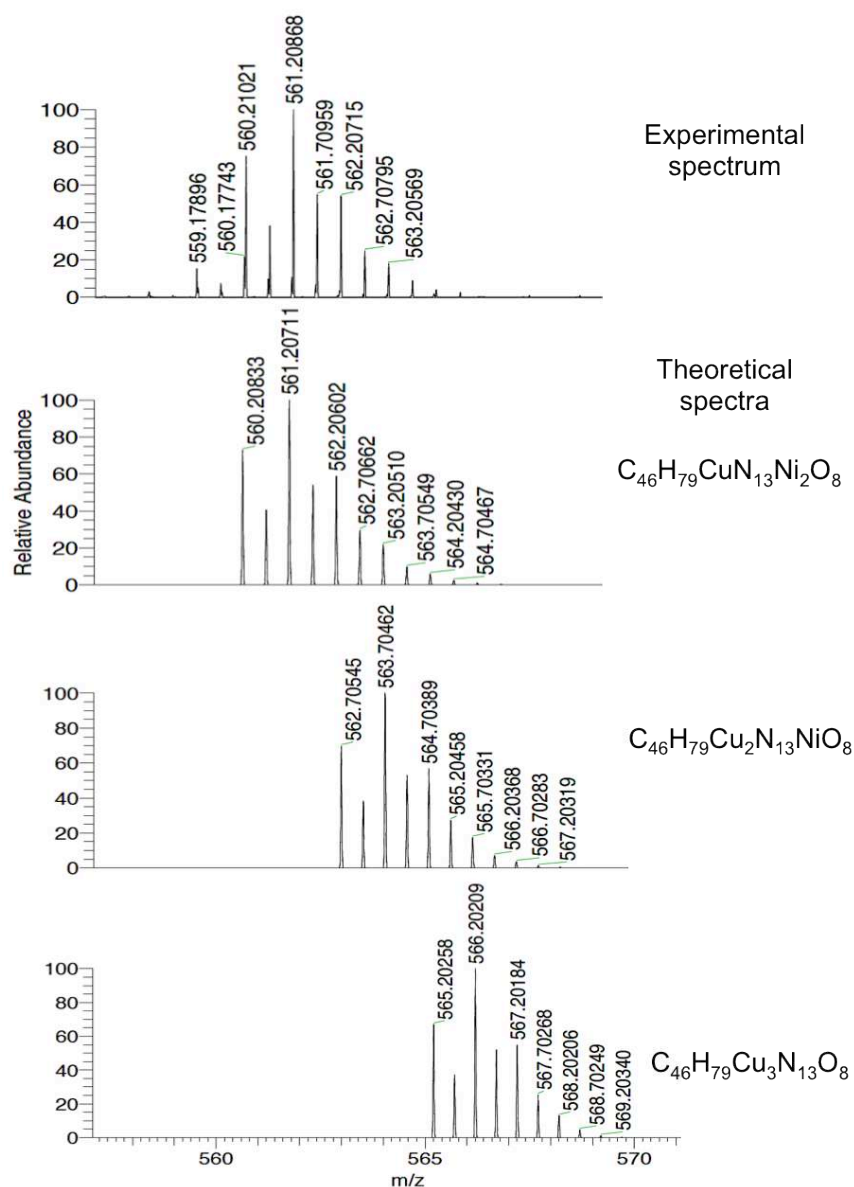


Figure III-25: HR-MS spectrum of compound **82**. Comparison between experimental spectrum and theoretical spectra of trimetallic complexes.

First attempts of metalation are encouraging, however some UV and EPR analyses are being currently investigated in our group to gain further insight into the location of Cu(II) in the molecule.

The same strategy can be applied in AMD3465 series and the synthesis of metalated derivatives of AMD3465 series is part of an undergoing PhD work.

### III.3 Conclusion

The objective of this thesis work was to develop new imaging agents for targeting CXCR4 based on AMDs scaffolds. The access towards these agents has first required the preparation of original building blocks in AMD3100 and AMD3465 series.

The conjugation of such platforms onto a chosen probe enabled the synthesis of various imaging agents. The advantage of this approach is the possibility to introduce at this stage any kind of probes, such as a fluorescent dye or a macrocyclic system. Several systems carrying a Bodipy dye were prepared and their solubility in water ensure their use for *in vivo* optical applications. Regarding the introduction of macrocyclic chelates, it has been demonstrated in AMD3100 series that the order of moieties incorporation is essential to synthesis success. Indeed, metalation of the building blocks prior to introduction of the macrocycle enabled the protection of the cyclam rings and as such allowed the selective radiolabeling of the NODAGA moiety. Further studies are being currently undertaken to ensure that no transmetalation or transchelation phenomena occur in the heterotrimetallic complex.

There are several areas where we need to extend this thesis work. The steric hindrance caused by the probe can result in diminution of the binding affinity and loss of specificity for the receptor. Thus, biological results will be essential to determine the efficiency of our systems. We can tune the AMDs scaffolds to optimize the efficiency by modifying the spacer length or the spacer anchor point. Thus, we can consider the introduction of the spacer either on a carbon atom of a cyclam ring or of the pyridine moiety (Figure III-26).

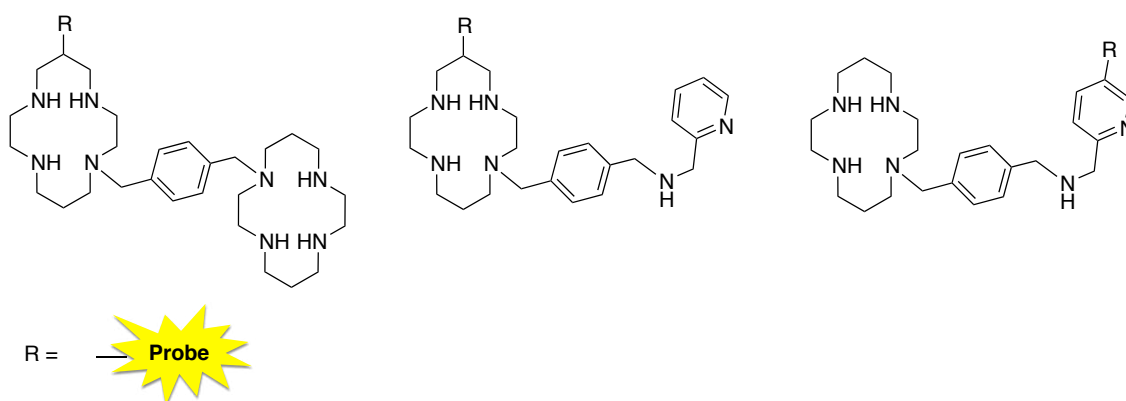


Figure III-26: Tuning of the AMDs scaffolds.

The incorporation of others probes can also be considered. For example, addition of a prosthetic group for  $^{18}\text{F}$  labeling is being currently undertaken in our group. A second generation of imaging agents can be also generated by combining on the same molecule a fluorescent dye and a radioisotope. The resulting systems would be capable of simultaneous optical imaging and PET or SPECT scintigraphy.



## **Conclusion**



The increasing knowledge in molecular biology has led to the identification of several cancer biomarkers. Among them, CXCR4 has been considered as a potential target for *in vivo* molecular imaging and/or therapeutic purposes. The validation and potential of interest of such target have been intensively studied, and the identification and design of high-affinity antagonists have been - and remains - an area of intense research.

The objective of this thesis work was to develop CXCR4-targeted tools to localize and treat cancer at an early stage. In this line, we investigated the synthesis of new target-specific radiopharmaceuticals. The work focused on two main axes, *i.e.* the chelating agent and the carrier, by using the know-how and the expertise of our group in polyazacycloalkanes synthesis and functionalization.

Thus, we developed new macrocyclic scaffolds that provide versatile platforms to the obtention of new bifunctional chelating agents adapted for copper and gallium chelation. Several parameters were tuned such as the cavity size of the chelate and the coordinating arms to ensure the stability of the resulting complexes. By varying the grafting function, we were able to create a wide library of potential BFCAs suitable for conjugation purposes. Moreover, such scaffolds could be easily modified to adjust the *in vivo* behavior and pharmacokinetics of the future imaging agents.

Simultaneously, we worked on CXCR4-specific carriers. By using well-known CXCR4 antagonists, *i.e.* AMD3100 and AMD3465, we investigated the synthesis of new platforms that enabled the introduction of various chelates. The method was also extended towards optical imaging applications and the resulting fluorescent compounds are valuable tools for preclinical studies. There is no such an easy task that one can simply attach a tag onto the selected targeting vector without significantly changing its receptor binding affinity and biodistribution characteristics. Biological studies will be determinant to validate the proof-of-concept of our project.

To conclude, developing new generation of target-specific imaging agents aims at satisfying the unmet medical need for early detection of diseases or radiotherapy of cancers. The less obvious role, then, becomes imaging's involvement in the discovery process. While perhaps less obvious, it is also potentially the point of greatest impact on any drug discovery program that is establishing the validity and relevance of novel biological targets. So, non-invasive imaging represents a unique powerful method of establishing the validity of novel therapeutic intervention. In this context, theragnostic radiopharmaceuticals have the power to drive advances in personalized medicine that will offer better-targeted diagnosis and treatments. Using this approach, it would be possible to envision a future where treatments are tailored to individual patients' specific disease parameters and where imaging data could be analyzed in real-time and in advance to predict likely effectiveness of therapy.





## **Experimental Section**



## I. Instrumentation

### NUCLEAR MAGNETIC RESONANCE SPECTROSCOPY

NMR spectra were recorded on a Bruker 300, 500 or 600 spectrometer (300 MHz, 500 MHz or 600 MHz for  $^1\text{H}$ ; 75 MHz, 125 MHz or 150 MHz for  $^{13}\text{C}$ ). All chemical shifts were referenced to the solvent peak. The following abbreviations are used: s: singlet, d: doublet, t: triplet, q: quartet, m: multiplet, bs: broad signal.

### MASS SPECTROMETRY

Mass spectra were obtained by MALDI-TOF (Matrix Assisted Laser Desorption Ionization - Time Of Flight) with a Bruker DALTONICS Ultraflex II spectrometer.

Electrospray mass measurements were carried out using a Bruker microTOF-Q<sup>TM</sup> ESI-TOF (ElectroSpray Ionization - Time Of Flight) mass spectrometer and a THERMO LTQ Orbitrap XL mass spectrometer coupled with an HPLC Ultimate 3000 DIONEX.

### ELEMENTAL ANALYSIS

Elemental analyses were performed with a Fisons EA CHNS instrument.

### UV-VISIBLE SPECTROSCOPY

Absorption spectra were recorded on a JASCO Bio-spectrophotometer UV-Vis V-630Bio.

### INFRARED SPECTROSCOPY

InfraRed spectra were recorded on a Bruker vector 22 in ATR mode and with a Bruker IFS 66v with 1 % sample mixed with potassium bromide.

### CHROMATOGRAPHIC TECHNIQUES

Flash Chromatography was performed using the Automatic Reveleris<sup>®</sup> Flash Chromatography System (GRACE) equipped with a multiple channel detection (UV (254 nm and/or 215 nm) and ELSD (Evaporative Light Scattering Detection)). Reveleris<sup>®</sup> 4, 12, 24 g Silica Flash Cartridges and Reveleris<sup>®</sup> C18 RP 4, 12, 40, 80 g Cartridges were used for normal and reversed phase silica gel chromatography respectively.

### REAGENTS AND SOLVENTS

All commercially available reagents (Fluka, Aldrich, Acros) were used without any further purification, except for ethylenediamine which was first distilled. TriBocyclam, NODA-GA-tris (tBu), DOTA-tris(tBu) ester NHS and DOTA-GA anhydride were obtained from CheMatech<sup>®</sup> and used without further purification. Technical solvents were used without any purification.

## X-RAY DIFFRACTION

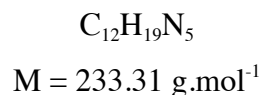
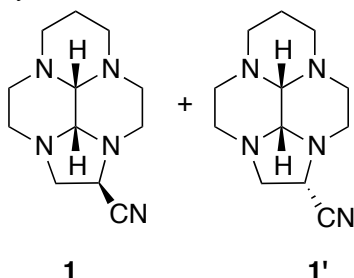
Diffraction data were collected on a Nonius Kappa Apex-II or Nonius Kappa CCD diffractometer equipped with a nitrogen jet stream low-temperature system (Oxford Cryosystems). The X-ray source was graphite-monochromated Mo- $K_{\alpha}$  radiation ( $\lambda = 0.71073 \text{ \AA}$ ) from a sealed tube. The lattice parameters were obtained by least-squares fit to the optimized setting angles of the entire set of collected reflections. No significant temperature drift was observed during the data collections. Data were reduced by using DENZO<sup>284</sup> software, with applying multi-scan absorption corrections.<sup>285</sup> The structure was solved by direct methods using the SIR92<sup>286</sup> program. Refinements were carried out by full-matrix least-squares on  $F^2$  using the SHELXL97<sup>287,288</sup> program on the complete set of reflections. Anisotropic thermal parameters were used for non-hydrogen atoms. All H atoms, on carbon atom, were placed at calculated positions using a riding model with C-H = 0.95  $\text{\AA}$  (aromatic), C-H = 0.99  $\text{\AA}$  (methylene) or 0.98  $\text{\AA}$  (methyl) with  $U_{\text{iso}}(\text{H}) = 1.2U_{\text{eq}}(\text{CH})$ ,  $U_{\text{iso}}(\text{H}) = 1.2U_{\text{eq}}(\text{CH}_2)$  or  $U_{\text{iso}}(\text{H}) = 1.5U_{\text{eq}}(\text{CH}_3)$ . Hydrogen atoms, in water molecules or hydroxyl group from methanol were found on the difference Fourier maps. The different pictures of X-Ray diffraction were generated by ORTEP III and Mercury programs

## COMPUTATIONAL METHOD

Structures of **1**, **2a-h** and **7** were computed by using hybrid density functional theory (B3LYP) and the 6-31G\*\* basic set, as implemented in Jaguar 5.5, release 16.5.

## II. Experimental part Chapter II

### 1 *cis-decahydro-1H-2a,4a,7a,9a-tetraazacyclopenta[cd]phenalene-2-carbonitrile*



A solution of 40 % glyoxal in water (169.5 g, 1.17 mol) in ethanol (0.7 L) was added to a solution of *N,N*-bis(aminoethyl)propane-1,3-diamine (187.2 g, 1.17 mol) in ethanol (2 L) at 0 °C. After stirring at this temperature for 2 h, the solvent was evaporated and the colorless oil was dissolved in ethanol (300 mL) and acetonitrile (3.8 L). 139.3 g of benzotriazole (1.17 mol, 1 equivalent) and 161.7 g of  $\text{K}_2\text{CO}_3$  (1.17 mol, 1 eq.) were added. A solution of 50 % chloroacetaldehyde in water (183.7 g, 1.17 mol, 1 equivalent) was slowly added at 0 °C and the resulting mixture was stirred for 2 h. 49.0 g of NaCN (1.17 mol, 1 equivalent) were then added. The mixture was stirred overnight at room temperature. The solution was filtered on celite and the solid was washed with acetonitrile (500 mL). The filtrate was evaporated, and the resulting solid was taken in 1 L of dichloromethane. After filtration, the organic phase was washed with a 3 M solution of sodium hydroxide (2\*600 mL), dried over  $\text{MgSO}_4$  and the solvent was evaporated. The residual brown solid was purified by aluminium oxide chromatography (eluent:  $\text{CH}_2\text{Cl}_2$ ) to give a mixture of **1** and **1'** as a white powder ( $m = 114.5 \text{ g}$ , yield = 42 %, Mp: 71 +/-2 °C).

**1** and **1'** ESI-MS:  $m/z = 234.17 [\text{M}+\text{H}]^+$ .

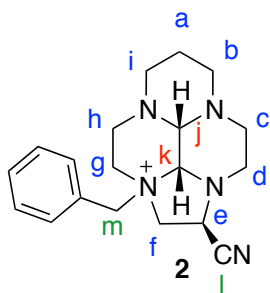
HRMS-ESI:  $m/z =$  calculated for  $\text{C}_{12}\text{H}_{19}\text{N}_5+\text{H}$ : 234.1713 obtained 234.1718.

The diastereoisomer **1** was recrystallized in cyclohexane.

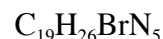
$^1\text{H}$  NMR (600 MHz,  $\text{D}_2\text{O}$ , 300 K)  $\delta$  (ppm): 1.20-1.25 (m, 1H), 2.08-3.52 (m, 17H), 3.95-3.97 (m, 1H).

$^{13}\text{C}\{^1\text{H}\}$  NMR (150 MHz,  $\text{CDCl}_3$ , 250 K)  $\delta$  (ppm): 19.8 ( $\text{CH}_2\beta$ ), 44.9, 46.2, 49.0, 49.5, 52.0, 52.8, 54.8 ( $\text{CH}_2$ ), 57.5 (CH), 75.2, 75.4 (NCN), 117.3 (CN).

Elemental analysis:  $\text{C}_{12}\text{H}_{19}\text{N}_5$ . Calculated: C (61.77 %), H (8.21 %), N (30.02 %). Obtained: C (61.80 %), H (8.31 %), N (29.64 %).

**2** *cis-9a-benzyl-2-cyanododecahydro-2a,4a,7a,9a-tetraazacyclopenta[cd]phenalene-9a-ium bromide*

, Br-



$$M = 403.35 \text{ g}\cdot\text{mol}^{-1}$$

146 mg of benzyl bromide (0.85 mmol) were added to a solution of **1** (200 mg, 0.85 mmol) in acetonitrile (3 mL). After 24 h, the resulting precipitate was filtered, washed with 30 mL of  $\text{CH}_3\text{CN}$  and recrystallized in methanol to give **2** as a white powder ( $m = 290 \text{ mg}$ , yield = 85 %, Mp (decomposition):  $190 \pm 1 \text{ }^\circ\text{C}$ ).

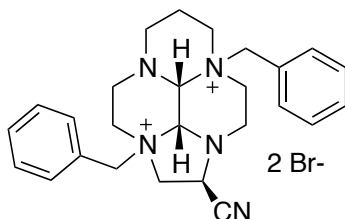
$^1\text{H}$  NMR (600 MHz,  $\text{D}_2\text{O}$ , 300 K)  $\delta$  (ppm): 1.53-1.55 (m, 1H,  $\text{C}^{\text{a}}\text{H}_2$ ), 2.18-2.26 (m, 1H,  $\text{C}^{\text{a}}\text{H}_2$ ), 2.60-2.65 (m, 1H,  $\text{C}^{\text{i}}\text{H}_2$ ), 2.69-2.73 (m, 1H,  $\text{C}^{\text{c}}\text{H}_2$ ), 2.75-2.81 (m, 1H,  $\text{C}^{\text{d}}\text{H}_2$ ), 2.90-2.95 (m, 1H,  $\text{C}^{\text{h}}\text{H}_2$ ), 3.08-3.16 (m, 4H,  $\text{C}^{\text{h}}\text{H}_2$ ,  $\text{C}^{\text{i}}\text{H}_2$ ,  $\text{C}^{\text{b}}\text{H}_2$ ,  $\text{C}^{\text{b}}\text{H}_2$ ), 3.29-3.32 (m, 1H,  $\text{C}^{\text{d}}\text{H}_2$ ), 3.49-3.54 (m, 1H,  $\text{C}^{\text{c}}\text{H}_2$ ), 3.65-3.70 (m, 1H,  $\text{C}^{\text{s}}\text{H}_2$ ), 3.72-3.78 (m, 1H,  $\text{C}^{\text{s}}\text{H}_2$ ), 4.00-4.08 (m, 2H,  $\text{C}^{\text{k}}\text{H}$ ,  $\text{C}^{\text{f}}\text{H}_2$ ), 4.25-4.26 (m, 1H,  $\text{C}^{\text{i}}\text{H}$ ), 4.48 (dd, 1H,  $^2\text{J} = 13.4 \text{ Hz}$ ,  $^3\text{J} = 3.3 \text{ Hz}$ ,  $\text{C}^{\text{f}}\text{H}_2$ ), 4.90 (dd, 1H,  $^2\text{J} = 8.3 \text{ Hz}$ ,  $^3\text{J} = 3.3 \text{ Hz}$ ,  $\text{C}^{\text{e}}\text{H}$ ), 4.98 (d, 1H,  $^2\text{J} = 13.4 \text{ Hz}$ ,  $\text{C}^{\text{m}}\text{H}_2$ ), 5.02 (d, 1H,  $^2\text{J} = 13.4 \text{ Hz}$ ,  $\text{C}^{\text{m}}\text{H}_2$ ), 7.59-7.68 (m, 5H, CHar).

$^{13}\text{C}\{^1\text{H}\}$  NMR (150 MHz,  $\text{D}_2\text{O}$ , 300 K)  $\delta$  (ppm): 18.6 ( $\text{C}^{\text{a}}\text{H}_2$ ), 42.2 ( $\text{C}^{\text{c}}$ ), 46.3 ( $\text{C}^{\text{d}}\text{H}_2$ ), 46.9 ( $\text{C}^{\text{h}}\text{H}_2$ ), 50.1 ( $\text{C}^{\text{e}}\text{H}$ ), 51.4 ( $\text{C}^{\text{b}}\text{H}_2$ ), 53.4 ( $\text{C}^{\text{i}}\text{H}_2$ ), 57.6 ( $\text{C}^{\text{s}}\text{H}_2$ ), 61.6 ( $\text{C}^{\text{m}}\text{H}_2$ ), 62.8 ( $\text{C}^{\text{f}}\text{H}_2$ ), 70.6 ( $\text{C}^{\text{j}}\text{H}_2$ ), 78.8 ( $\text{C}^{\text{k}}\text{H}_2$ ), 114.0 ( $\text{C}^{\text{l}}\text{N}$ ), 126.0 (CHar), 129.9 (\*2) (CHar), 131.5 (Car), 132.7 (\*2) (CHar).

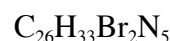
ESI-MS:  $m/z = 324.22$  [ $\text{M}-\text{Br}$ ] $^+$ .

HRMS-ESI:  $m/z =$  calculated for  $\text{C}_{19}\text{H}_{26}\text{N}_5$ : 324.2182 obtained 324.2179.

Elemental analysis:  $\text{C}_{19}\text{H}_{26}\text{BrN}_5$ . Calculated C (56.44 %), H (6.48 %), N (17.32 %). Obtained: C (56.12 %), H (6.43 %), N (17.16 %).

**3** *cis-4a,9a-dibenzyl-2-cyanododecahydro-1H-2a,4a,7a,9a-tetraazacyclopenta[cd]phenalene-4a,9a-diiium bromide*

2 Br-



$$M = 575.38 \text{ g}\cdot\text{mol}^{-1}$$

4.4 g of benzyl bromide (25.7 mmol) were added to a solution of **1** (600 mg, 2.57 mmol) in acetonitrile (9 mL). The solution was stirred at room temperature during 10 days. The precipitate,

which was formed during the reaction was filtered, washed with 30 mL of CH<sub>3</sub>CN and recrystallized in water to give **3** as a white solid (m = 1.12 g, yield = 76 %, Mp (decomposition): 120 +/- 1 °C).

<sup>1</sup>H NMR (300 MHz, D<sub>2</sub>O, 300 K) δ (ppm): 1.80-1.95 (m, 1H), 2.18-2.34 (m, 1H), 2.66-2.83 (m, 1H), 3.10-3.30 (m, 2H), 3.34-3.57 (m, 4H), 3.66-3.96 (m, 4H), 4.08-4.20 (m, 1H), 4.53-4.67 (m, 2H), 4.72-4.73 (m, 1H), 4.89-5.03 (m, 2H), 5.05-5.24 (m, 3H), 5.41-5.44 (m, 1H), 7.52-7.69 (m, 10H).

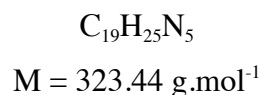
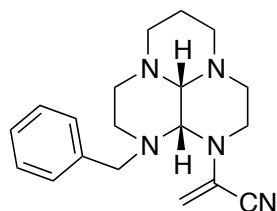
<sup>13</sup>C{<sup>1</sup>H} NMR (75 MHz, D<sub>2</sub>O, 300 K) δ (ppm): 21.0 (CH<sub>2</sub>β), 42.8, 49.0, 49.7 (CH<sub>2</sub>), 50.5 (CH), 53.2, 55.0, 63.4, 63.7, 63.8, 65.1 (CH<sub>2</sub>), 77.5, 80.6 (NCN), 116.8 (CN), 127.1, 127.8 (Car), 132.1 (\*2), 132.4 (\*2) (CHar), 134.0, 134.2 (Car), 134.8 (\*2), 135.8 (\*2) (CHar).

ESI-MS: *m/z* = 414.12 [M-2Br-H]<sup>+</sup>, 496.19 [M-Br]<sup>+</sup>.

HRMS-ESI: *m/z* = calculated for C<sub>26</sub>H<sub>33</sub>N<sub>5</sub>-H: 414.2652 obtained 414.2650.

Elemental analysis for C<sub>26</sub>H<sub>33</sub>Br<sub>2</sub>N<sub>5</sub>•3H<sub>2</sub>O•3CH<sub>3</sub>OH. Calculated: C (49.03 %), H (6.55 %), N (10.59 %). Obtained: C (49.37 %), H (6.42 %), N (11.08 %).

**4** 2-((3*a*'*R*,9*a**S*)-1-benzylhexahydro-1*H*-1,3*a*,6*a*,9-tetraazaphenalen-9(3*a*'*H*,4*H*,9*a**H*)-yl)acrylonitrile



280 mg (7.42 mmol) of NaBH<sub>4</sub> were added to a suspension of **2** (200 mg, 0.495 mmol) in 5 mL of ethanol/water (95:5). The solution was stirred at 0 °C overnight. The solvent was evaporated to give a white solid. CH<sub>2</sub>Cl<sub>2</sub> was added (10 mL) and the insoluble salts were removed by filtration. The solvent was evaporated to give **4** as a colorless oil (m = 152 mg, yield = 95 %, Mp (decomposition): 85 +/- 1 °C).

<sup>1</sup>H NMR (600 MHz, CDCl<sub>3</sub>, 220 K) δ (ppm): 1.21 (m, 1H, CH<sub>2</sub>β), 2.06-2.30 (m, 5H), 2.61-2.67 (m, 2H), 2.74-2.80 (m, 2H), 2.86-2.98 (m, 2H), 3.18-3.19 (m, 1H, N-CH-N), 3.20-3.33 (m, 2H), 3.61-3.71 (m, 1H), 3.84-3.86 (m, 1H, N-CH-N), 4.05 (m, 1H), 4.57 (d, 1H, C=CH<sub>2</sub>, <sup>2</sup>J = 2.1 Hz), 4.71 (d, 1H, C=CH<sub>2</sub>, <sup>2</sup>J = 2.1 Hz), 7.14-7.33 (m, 5H, CHar).

<sup>13</sup>C{<sup>1</sup>H} NMR (150 MHz, CDCl<sub>3</sub>, 220 K) δ(ppm): 19.3 (CH<sub>2</sub>β), 40.9, 44.5, 50.7, 51.8, 52.2, 56.4, 56.8 (CH<sub>2</sub>), 74.1, 75.9 (NCN), 99.2 (C=CH<sub>2</sub>), 116.1 (CN), 127.1 (C=CH<sub>2</sub>), 127.2 (CHar), 128.5 (\*2) (CHar), 129.5 (\*2) (CHar), 137.5 (Car).

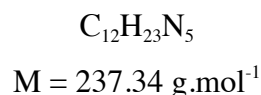
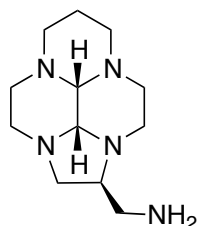


ESI-MS:  $m/z = 324.22$   $[M+H]^+$ .

HRMS-ESI:  $m/z =$  calculated for  $C_{19}H_{25}N_5+H$ : 324.2182, obtained 324.2177.

IR  $\nu$  ( $cm^{-1}$ ): 1582 (C=C), 2230 (CN).

**6** bisaminal-glyoxal-(1,4,7,10-tetraazacyclotridecan-5-yl)methanamine



A solution of **1** (90.2 g, 0.39 mmol) in dry THF (300 mL) was slowly added to a suspension of 15.3 g of  $LiAlH_4$  (0.43 mol, 1.1 equivalent) in THF (1 L) under nitrogen at  $-78^\circ C$ . The resulting mixture was stirred overnight. Water was carefully added at  $-78^\circ C$  in order to neutralize the excess of  $LiAlH_4$ . After evaporation of the solvent,  $CHCl_3$  was added (2\*500 mL) and insoluble impurities were eliminated by filtration. Pure **6** was obtained as a colorless oil ( $m = 74.1$  g, yield = 80 %).

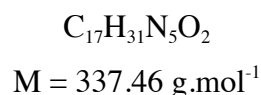
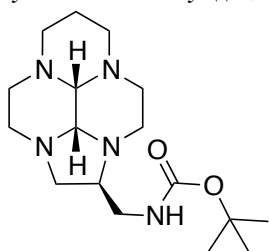
$^1H$  NMR (300 MHz,  $CDCl_3$ , 300 K)  $\delta$  (ppm): 1.01-1.27 (m, 3H), 1.49-1.57 (m, 1H), 1.94-2.17 (m, 4H), 2.22-2.55 (m, 5H), 2.63-2.68 (m, 6H), 2.89-2.98 (m, 1H), 3.15-3.19 (m, 1H), 3.22-3.32 (m, 2H).

$^{13}C\{^1H\}$  NMR (75 MHz,  $CDCl_3$ , 300 K)  $\delta$ (ppm): 20.2 ( $CH_2\beta$ ), 45.8, 46.0, 50.4, 51.5, 52.4, 53.3, 55.2 (\*2) ( $CH_2$ ), 67.6 (CH), 75.8, 76.4 (NCN).

MALDI-TOF:  $m/z = 235.19$   $[M-2H]^+$ .

HRMS-ESI:  $m/z =$  calculated for  $C_{12}H_{23}N_5+Na$ : 260.1846, obtained: 260.1834.

**7** bisaminal-glyoxal-tert-butyl((1,4,7,10-tetraazacyclotridecan-5-yl)methyl)carbamate



A solution of  $Boc_2O$  (84.4 g, 0.39 mol) in  $CH_2Cl_2$  (3 L) was slowly added to a solution of **6** ( $m = 91.8$  g, 0.39 mol) in  $CH_2Cl_2$  (0.9 L). The solution was stirred overnight at room temperature.

After evaporation of the solvent, the residual oil was purified by aluminium oxide chromatography (eluent:  $\text{CH}_2\text{Cl}_2$ ) to give **7** as a yellow oil ( $m = 105.2$  g, yield = 80 %).

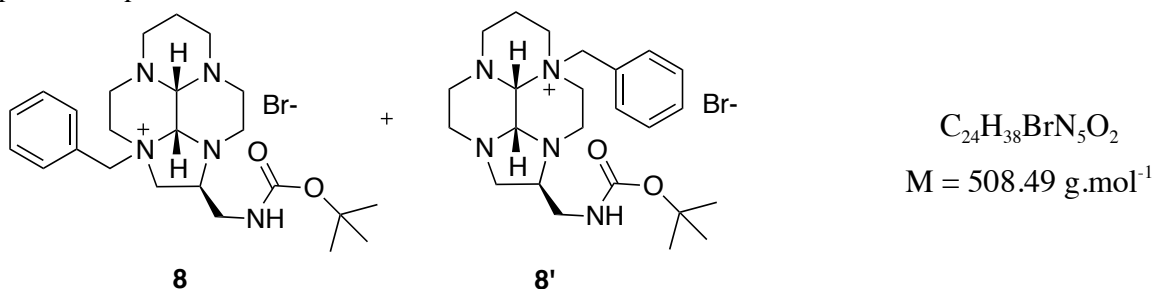
$^1\text{H}$  NMR (500 MHz,  $\text{CDCl}_3$ , 300 K)  $\delta$ (ppm): 1.18-1.24 (m, 1H,  $\text{CH}_2\beta$ ), 1.40 (s, 9H,  $\text{CH}_3$ ), 1.62-1.72 (m, 1H), 1.98-2.28 (m, 4H), 2.36-2.42 (m, 1H), 2.50-2.57 (m, 1H), 2.58-2.62 (m, 1H), 2.77-2.84 (m, 1H), 2.80 (d, 1H,  $^3J = 2.5$  Hz, N-CH-N), 2.86-3.01 (m, 5H), 3.02-3.09 (m, 1H), 3.10-3.20 (m, 1H), 3.27 (d, 1H,  $^3J = 2.5$  Hz, N-CH-N), 3.33-3.43 (m, 2H), 5.00 (bs, 1H,  $\text{NHC=O}$ ).

$^{13}\text{C}\{^1\text{H}\}$  NMR (125 MHz,  $\text{CDCl}_3$ , 300 K)  $\delta$ (ppm): 20.3 ( $\text{CH}_2\beta$ ), 28.6 (\*3) ( $\text{CH}_3$ ), 43.9, 45.9, 50.4, 51.3, 52.5, 53.4, 54.7, 55.3 ( $\text{CH}_2$ ), 64.4 (CH), 76.3, 76.4 (NCN), 79.3 (C), 156.2 (C=O).

ESI-MS:  $m/z = 338.25$   $[\text{M}+\text{H}]^+$ , 360.23  $[\text{M}+\text{Na}]^+$ .

HRMS-ESI:  $m/z =$  calculated for  $\text{C}_{17}\text{H}_{31}\text{N}_5\text{O}_2+\text{H}$ : 338.2551 obtained 338.2553.

**8** *cis-9a-benzyl-2-((tert-butoxycarbonyl)amino)methyl)dodecahydro-2a,4a,7a,9a-tetraazacyclopenta[cd]phenalen-9a-ium bromide*



30.8 g of benzyl bromide (0.18 mol) were added to a solution of **7** (62.1 g, 0.18 mol) in toluene (615 mL). The solution was stirred at room temperature during 5 days. The precipitate which was formed during the reaction was filtered, washed with 300 mL of toluene and 300 mL of ether to give a mixture of **8** and **8'** as a white solid ( $m = 86.0$  g, yield = 94 %).

ESI-MS:  $m/z = 428.32$   $[\text{M}-\text{Br}]^+$ .

HRMS-ESI:  $m/z =$  calculated for  $\text{C}_{24}\text{H}_{38}\text{N}_5\text{O}_2$ : 428.3020 obtained 428.3013.

The regioisomers **8** and **8'** can be separated by recrystallization in acetonitrile.

### Compound 8

Mp (decomposition): 146 +/- 2 °C.

$^1\text{H}$  NMR (300 MHz,  $\text{D}_2\text{O}$ , 300 K)  $\delta$  (ppm): 1.49 (s, 9H,  $\text{CH}_3$ ), 1.52-1.56 (m, 1H,  $\text{CH}_2\beta$ ), 2.18-2.32 (m, 1H), 2.58-2.68 (m, 2H), 2.86-2.97 (m, 2H), 3.05-3.87 (m, 13H), 4.11-4.12 (m, 1H), 4.19 (s,

1H), 4.72 (d, 1H,  $^2J = 13.2$  Hz, CH<sub>2</sub>Ph), 5.04 (d, 1H,  $^2J = 13.2$  Hz, CH<sub>2</sub>Ph), 7.60-7.62 (m, 5H, CHar).

<sup>13</sup>C{<sup>1</sup>H} NMR (75 MHz, D<sub>2</sub>O, 300 K) δ(ppm): 18.6 (CH<sub>2</sub>β), 27.7 (\*3) (CH<sub>3</sub>), 39.1, 42.9, 43.8, 46.5, 51.3, 53.3, 53.9 (CH<sub>2</sub>), 54.6 (CH), 61.1, 63.2 (CH<sub>2</sub>), 70.8, 79.6 (NCN), 81.6 (C), 126.3 (Car), 129.6 (\*2), 131.2, 132.5 (\*2) (CHar), 158.1 (C=O).

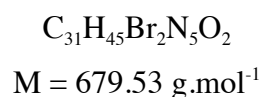
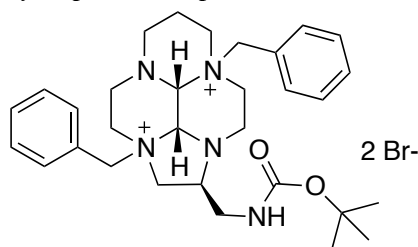
### Compound 8'

Mp (decomposition): 151 +/- 2 °C.

<sup>1</sup>H NMR (300 MHz, D<sub>2</sub>O, 300 K) δ(ppm): 1.49 (s, 9H, CH<sub>3</sub>), 1.84-1.90 (m, 1H, CH<sub>2</sub>β), 2.13-2.30 (m, 2H), 2.38-2.47 (m, 1H), 2.50-2.60 (m, 1H), 2.81-2.85 (m, 1H), 2.92-3.47 (m, 10H), 3.58-3.72 (m, 2H), 4.10-4.14 (m, 3H), 4.76 (d, 1H,  $^2J = 13.3$  Hz, CH<sub>2</sub>Ph), 5.11 (d, 1H,  $^2J = 13.3$  Hz, CH<sub>2</sub>Ph), 7.59-7.68 (m, 5H, CHar).

<sup>13</sup>C{<sup>1</sup>H} NMR (150 MHz, D<sub>2</sub>O, 300 K) δ(ppm): 18.4 (CH<sub>2</sub>β), 27.2 (\*3) (CH<sub>3</sub>), 42.4, 43.0, 47.7, 49.6, 50.6, 52.0, 52.1, 59.4, 62.7 (CH<sub>2</sub>), 63.2 (CH), 68.7 (NCN), 80.8 (C), 81.4 (NCN), 125.1 (Car), 128.9 (\*2), 130.7, 132.9 (\*2) (CHar), 157.8 (C=O).

### 9 *cis-4a,9a-dibenzyl-2-(((tert-butoxycarbonyl)amino)methyl)dodecahydro-1H-2a,4a,7a,9a-tetraazacyclopenta[cd]phenalene-4a,9a-dium bromide*



34.6 g of benzyl bromide (0.20 mol) were added to a solution of **7** (6.8 g, 20.3 mmol) in acetonitrile (200 mL) and water (10 mL). The solution was stirred at room temperature during 7 days. The precipitate formed during the reaction was filtered, washed with 150 mL of acetonitrile and 150 mL of ether to give compound **9** as a white solid (m = 4.98 g, yield = 95 %, Mp: 123 +/- 1 °C).

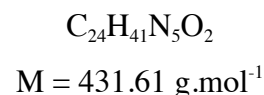
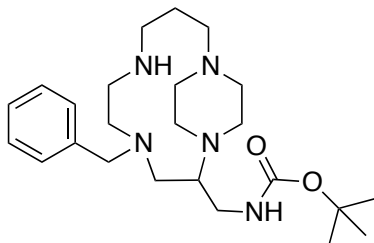
<sup>1</sup>H NMR (300 MHz, D<sub>2</sub>O, 300 K) δ (ppm): 1.32 (s, 9H, CH<sub>3</sub>), 1.83-1.90 (m, 1H, CH<sub>2</sub>β), 2.21-2.26 (m, 1H, CH<sub>2</sub>β), 2.68-2.77 (m, 1H), 3.10-4.00 (m, 16H), 4.26-4.35 (m, 1H), 4.57-4.60 (m, 1H), 4.76-4.84 (m, 2H), 4.93-5.04 (m, 2H), 7.53-7.63 (m, 10H, CHar).

<sup>13</sup>C{<sup>1</sup>H} NMR (125 MHz, D<sub>2</sub>O, 300 K) δ(ppm): 18.6 (CH<sub>2</sub>β), 27.6 (\*3) (CH<sub>3</sub>), 39.1, 39.8, 46.1, 47.5, 50.7, 51.7 (CH<sub>2</sub>), 55.7 (CH), 60.5, 60.6, 62.2, 62.8 (CH<sub>2</sub>), 75.1, 78.5 (NCN), 81.7 (C), 124.8, 125.7 (Car), 129.5 (\*2), 129.8 (\*2) 131.4, 131.6, 132.4 (\*2), 133.3 (\*2) (CHar), 157.9 (C=O).

ESI-MS:  $m/z = [M-2Br]^{2+}$ .

HRMS-ESI:  $m/z =$  calculated for  $C_{31}H_{45}N_5O_2$ : 259.6781 obtained 259.6780.

**10** *tert-butyl ((4-benzyl-1,4,7,11-tetraazabicyclo[9.2.2]pentadecan-2-yl)methyl)carbamate*



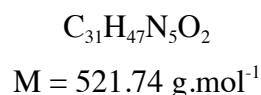
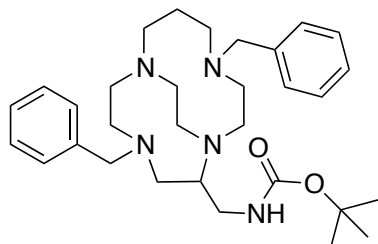
8.75 g (0.23 mol) of  $\text{NaBH}_4$  were added to a solution of **8** (11.76 g, 23.12 mmol) in 300 mL of ethanol. The solution was stirred at room temperature overnight. The solvent was evaporated to give a white solid.  $\text{CH}_2\text{Cl}_2$  was added (500 mL) and the insoluble salts were removed by filtration. After evaporation of the solvent, the residue was washed with 10 mL of a 3 M NaOH solution. After extraction with chloroform (2\*200 mL), the organic phase was dried over  $\text{MgSO}_4$ . The solvent was then evaporated, the resulting oil was purified by aluminium oxide chromatography (eluent:  $\text{CH}_2\text{Cl}_2/\text{MeOH}$ : 85/15) and the compound **10** was obtained as a colorless oil ( $m = 8.09$  g, yield = 81 %).

$^1\text{H}$  NMR (300 MHz,  $\text{CDCl}_3$ , 300 K)  $\delta$  (ppm): 1.43 (m, 9H,  $\text{CH}_3$ ), 1.61-1.75 (m, 2H,  $\text{CH}_2\beta$ ), 2.32-3.08 (m, 21H), 3.49 (d, 1H,  $^2J = 13.8$  Hz,  $\text{CH}_2\text{Ph}$ ), 3.55-3.65 (m, 1H), 3.80 (d, 1H,  $^2J = 13.8$  Hz,  $\text{CH}_2\text{Ph}$ ), 4.98 (s, 1H,  $\text{NHC=O}$ ), 7.21-7.33 (m, 5H,  $\text{CHar}$ ).

$^{13}\text{C}\{^1\text{H}\}$  NMR (75 MHz,  $\text{CDCl}_3$ , 300 K)  $\delta$ (ppm): 26.0 ( $\text{CH}_2\beta$ ), 28.6 (\*3) ( $\text{CH}_3$ ), 40.7, 41.2, 48.6, 49.8, 49.9, 50.7, 51.3, 54.8, 55.4, 56.3, 58.8 ( $\text{CH}_2$ ), 59.1 ( $\text{CH}$ ), 79.3 (C), 127.4, 128.4 (\*2), 129.8 (\*2) ( $\text{CHar}$ ), 136.3 (Car), 156.1 (C=O).

ESI-MS:  $m/z = 432.35 [M+H]^+$ , 454.32  $[M+Na]^+$ .

HRMS-ESI:  $m/z =$  calculated for  $C_{24}H_{41}N_5O_2+H$ : 432.3333 obtained 432.3315.

**11** *tert-butyl ((4,11-dibenzyl-1,4,8,11-tetraazabicyclo[6.5.2]pentadecan-13-yl)methyl)carbamate*

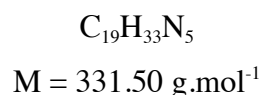
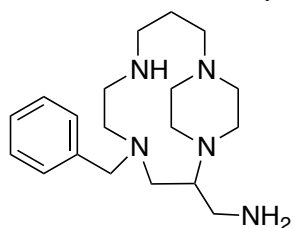
2.32 g (61.2 mmol) of  $\text{NaBH}_4$  were added to a solution of **9** (8.32 g, 12.2 mmol) in 120 mL of ethanol. The solution was stirred at room temperature overnight. The solvent was evaporated to give a white solid.  $\text{CH}_2\text{Cl}_2$  was added (300 mL) and the insoluble salts were removed by filtration. After evaporation of the solvent, the residue was washed with 20 mL of a 3 M NaOH solution, extracted with chloroform (2\*100mL) and dried over  $\text{MgSO}_4$ . After evaporation of the solvent, the residual oil was purified by aluminium oxide chromatography (eluent:  $\text{CH}_2\text{Cl}_2/\text{MeOH}$ : 90/10) to give **11** as a yellow oil (m = 6.36 g, yield = 79 %).

$^1\text{H}$  NMR (300 MHz,  $\text{CDCl}_3$ , 300 K)  $\delta$  (ppm): 1.39 (s, 9H,  $\text{CH}_3$ ), 1.47-1.57 (m, 1H,  $\text{CH}_2\beta$ ), 1.87-2.02 (m, 2H), 2.20-2.32 (m, 2H), 2.47-2.76 (m, 5H), 2.87-3.35 (m, 13H), 3.78-4.04 (m, 4H, ( $\text{CH}_2\text{Ph}$ ), 5.27-5.34 (m, 1H,  $\text{NHC=O}$ ), 7.18-7.25 (m, 10H,  $\text{CHar}$ ), 11.15 (bs, 1H,  $\text{N}^+\text{H}$ ).

$^{13}\text{C}\{^1\text{H}\}$  NMR (150 MHz,  $\text{CDCl}_3$ , 300 K)  $\delta$  (ppm): 21.8 ( $\text{CH}_2\beta$ ), 28.7 (\*3) ( $\text{CH}_3$ ), 40.4, 43.0, 48.6, 49.7, 49.8, 50.9, 54.0, 55.4, 55.5, 56.3, 58.2, 60.0 ( $\text{CH}_2$ ), 64.4 ( $\text{CH}$ ), 79.6, (C), 127.9, 128.2, 128.7 (\*4), 129.9 (\*2), 130.4 (\*2) ( $\text{CHar}$ ), 134.6, 136.4 (Car), 156.5 ( $\text{C=O}$ ).

ESI-MS:  $m/z = 522.38$  [ $\text{M}+\text{H}$ ] $^+$ .

HRMS-ESI:  $m/z =$  calculated for  $\text{C}_{31}\text{H}_{47}\text{N}_5\text{O}_2+\text{H}$ : 522.3803 obtained 522.3802.

**12** *(4-benzyl-1,4,7,11-tetraazabicyclo[9.2.2]pentadecan-2-yl)methanamine*

8.09 g (18.7 mmol) of compound **10** were dissolved in 30 mL of a 37 % HCl solution. The mixture was stirred for 30 min at room temperature. 250 mL of acetone were added and a precipitate was formed immediately. The precipitate was filtered, washed with acetone, ether, and dried under vacuum to give **12** (+ 5 HCl) as a white solid. The solid was dissolved in a 16 M NaOH solution until pH = 14. After extraction with chloroform (2\*150 mL), the organic phase was dried over  $\text{MgSO}_4$  and the solvent was evaporated. Pure **12** was obtained as a colorless oil (m = 5.41 g, yield = 87 %).

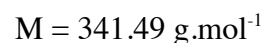
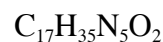
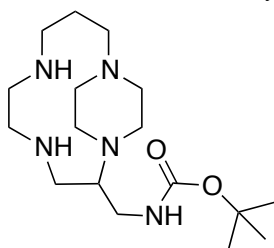
$^1\text{H}$  NMR (500 MHz,  $\text{CDCl}_3$ , 300 K)  $\delta$  (ppm): 1.67-1.78 (m, 2H,  $\text{CH}_2\beta$ ), 2.38-3.05 (m, 23 H), 3.52 (d, 1H,  $^2J = 13.6$  Hz,  $\text{CH}_2\text{Ph}$ ), 3.60-3.65 (m, 1H), 3.86 (d, 1H,  $^2J = 13.6$  Hz,  $\text{CH}_2\text{Ph}$ ), 7.25-7.34 (m, 5H, CHar).

$^{13}\text{C}\{^1\text{H}\}$  NMR (125 MHz,  $\text{CDCl}_3$ , 300 K)  $\delta$ (ppm): 26.5 ( $\text{CH}_2\beta$ ), 41.3, 42.4, 48.5, 49.8, 50.5, 50.7, 51.8, 55.4, 55.7, 56.5, 58.4 ( $\text{CH}_2$ ), 62.1 (CHC), 127.2 (CHar), 128.2 (\*2) (CHar), 129.6 (\*2) (CHar), 138.4 (Car).

ESI-MS:  $m/z = 332.28$   $[\text{M}+\text{H}]^+$ .

HRMS-ESI:  $m/z =$  calculated for  $\text{C}_{19}\text{H}_{33}\text{N}_5+\text{H}$ : 332.2809 obtained 332.2809.

**13** *tert-butyl (1,4,7,11-tetraazabicyclo[9.2.2]pentadecan-2-ylmethyl)carbamate*



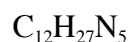
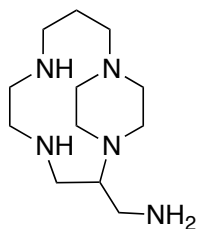
Compound **10** (5.55 g, 12.9 mmol) was dissolved in a mixture of acetic acid (43 mL) and water (4 mL) and 550 mg of 10 % Pd/C (0.5 mmol) were added under  $\text{H}_2$ . After consumption of hydrogen, the mixture was filtered to remove palladium. After evaporation of the solvent, the residue was dissolved in acetone (100 mL). 5 mL of a 3 M HCl solution were added and the resulting precipitate was filtered after 1 hour, washed with acetone (20 mL) and dried under vacuum to give a white powder. The resulting precipitate was then dissolved in a 3 M NaOH solution until  $\text{pH} = 12$ . After extraction with chloroform (2\*50 mL), the organic phase was dried over  $\text{MgSO}_4$  and the solvent was evaporated to give **13** as a yellow oil ( $m = 2.52$  g, yield = 57 %).

$^1\text{H}$  NMR (300 MHz,  $\text{CDCl}_3$ , 300 K)  $\delta$  (ppm): 1.41 (s, 9H,  $\text{CH}_3$ ), 1.60-1.68 (m, 2H,  $\text{CH}_2\beta$ ), 2.14-2.26 (m, 2H), 2.42-3.35 (m, 21H), 4.81 (s, 1H,  $\text{NHC=O}$ ).

$^{13}\text{C}\{^1\text{H}\}$  NMR (125 MHz,  $\text{CDCl}_3$ , 300 K)  $\delta$ (ppm): 25.3 ( $\text{CH}_2\beta$ ), 28.5 (\*3) ( $\text{CH}_3$ ), 39.0, 41.9, 46.2, 47.9, 49.7 (\*2), 50.7, 51.0, 51.1, 54.1 ( $\text{CH}_2$ ), 63.8 (CH), 79.1 (C), 157.8 (C=O).

ESI-MS:  $m/z = 342.29$   $[\text{M}+\text{H}]^+$ .

HRMS-ESI:  $m/z =$  calculated for  $\text{C}_{17}\text{H}_{35}\text{N}_5\text{O}_2+\text{H}$ : 342.2864 obtained 342.2864.

**14** 1,4,7,11-tetraazabicyclo[9.2.2]pentadecan-2-ylmethanamine

$$M = 241.38 \text{ g}\cdot\text{mol}^{-1}$$

*Route A:* **12** (2.83 g, 8.3 mmol) was dissolved in a mixture of acetic acid (30 mL) and water (3 mL) and 350 mg of 10 % Pd/C (0.3 mmol) were added under H<sub>2</sub>. After consumption of hydrogen, the mixture was filtered to remove palladium. After evaporation of the solvent, the residue was dissolved in acetone (75 mL). 3 mL of a 37 % HCl solution were added and the resulting precipitate was filtered after 1 hour, washed with acetone (20 mL) and dried under vacuum to give a white powder. The resulting precipitate was then dissolved in a 16 M NaOH solution until pH = 14. After extraction with chloroform (2\*50 mL), the organic phase was dried over MgSO<sub>4</sub> and the solvent was evaporated to give **14** as a yellow oil (m = 1.76 g, yield = 88 %).

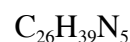
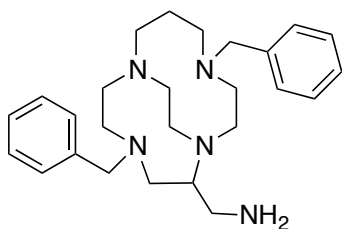
*Route B:* 2.0 g (6.0 mmol) of **13** were dissolved in 10 mL of a 37 % HCl solution. The mixture was stirred for 30 min at room temperature. 50 mL of acetone were added and a precipitate was formed immediately. The precipitate was filtered, washed with acetone, ether, and dried under vacuum to give **14** (+ 5 HCl) as a white solid. The solid was dissolved in a solution of 16 M NaOH until pH = 14. After extraction with chloroform (3\*100 mL), the organic phase was dried over MgSO<sub>4</sub> and the solvent was evaporated. The compound **14** was obtained as a colorless oil (m = 1.45 g, yield = 82 %).

<sup>1</sup>H NMR (300 MHz, CDCl<sub>3</sub>, 300 K) δ (ppm): 1.57-1.67 (m, 2H), 2.11-2.19 (m, 2H), 2.39-2.97 (m, 21H), 3.09-3.14 (m, 1H), 3.30-3.35 (m, 1H).

<sup>13</sup>C{<sup>1</sup>H} NMR (125 MHz, CDCl<sub>3</sub>, 300 K) δ (ppm): 25.3 (CH<sub>2</sub>β), 38.8, 44.0, 45.9, 47.7, 49.5, 49.6, 51.0, 51.1, 51.6, 53.9 (CH<sub>2</sub>), 67.6 (CH).

ESI-MS:  $m/z = 242.23$  [M+H]<sup>+</sup>.

HRMS-ESI:  $m/z =$  calculated for C<sub>12</sub>H<sub>27</sub>N<sub>5</sub>+H: 242.2339 obtained 242.2344.

**15** (4,11-dibenzyl-1,4,8,11-tetraazabicyclo[6.5.2]pentadecan-13-yl)methanamine

$$M = 421.62 \text{ g}\cdot\text{mol}^{-1}$$

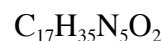
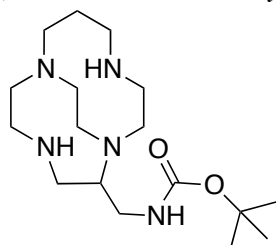
2 g (3.83 mmol) of compound **11** were dissolved in 10 mL of a 37 % HCl solution. The mixture was stirred for 30 min at room temperature. 150 mL of acetone were added and a precipitate was formed immediately. The precipitate was filtered, washed with acetone, ether, and dried under vacuum. The white solid was dissolved in a solution of sodium hydroxide 16 M until pH = 14. After extraction with chloroform (2\*100 mL), the organic phase was dried over MgSO<sub>4</sub> and the solvent was evaporated. **15** was obtained as a colorless oil (m = 1.49 g, yield = 92 %).

<sup>1</sup>H NMR (500 MHz, CDCl<sub>3</sub>, 300 K) δ(ppm): 1.19-1.33 (m, 2H, CH<sub>2</sub>β), 1.58-1.85 (m, 6H), 2.06-2.14 (m, 1H), 2.38-2.44 (m, 1H), 2.47-2.55 (m, 1H), 2.61-2.74 (m, 3H), 2.80-2.89 (m, 4H), 2.92-2.98 (m, 1H), 3.05-3.10 (m, 1H), 3.14-3.22 (m, 2H), 3.26-3.62 (m, 2H), 3.77 (d, 1H, <sup>2</sup>J = 13.8 Hz, CH<sub>2</sub>Ph), 3.89 (d, 1H, <sup>2</sup>J = 13.8 Hz, CH<sub>2</sub>Ph), 3.91 (d, 1H, <sup>2</sup>J = 13.8 Hz, CH<sub>2</sub>Ph), 3.96 (d, 1H, <sup>2</sup>J = 13.8 Hz, CH<sub>2</sub>Ph), 7.23-7.36 (m, 10H, CHar), 10.99 (bs, 1H, N<sup>+</sup>H).

<sup>13</sup>C{<sup>1</sup>H} NMR (125 MHz, CDCl<sub>3</sub>, 300 K) δ(ppm): 21.9 (CH<sub>2</sub>β), 41.7, 43.1, 48.6, 50.0, 50.4, 50.8, 53.9, 55.7, 56.3, 56.5, 58.4, 60.4 (CH<sub>2</sub>), 68.1 (CH), 128.0, 128.2, 128.8 (\*4), 129.8 (\*2), 130.2 (\*2) (CHar), 134.8, 136.5 (Car).

ESI-MS:  $m/z = 422.32$  [M+H]<sup>+</sup>.

HRMS-ESI:  $m/z =$  calculated for C<sub>26</sub>H<sub>39</sub>N<sub>5</sub>+H: 422.3278 obtained 422.3271.

**16** tert-butyl (1,4,8,11-tetraazabicyclo[6.5.2]pentadecan-13-ylmethyl)carbamate

$$M = 341.49 \text{ g}\cdot\text{mol}^{-1}$$

**11** (2 g, 3.83 mmol) was dissolved in a mixture of acetic acid (13 mL) and water (1 mL) and 163 mg of 10 % Pd/C (0.15 mmol, 0.04 equivalent) were added under H<sub>2</sub>. After consumption of hydrogen, the mixture was filtered to remove palladium. After evaporation of the solvent, the residue was dissolved in acetone (50 mL). 7 mL of a 3 M HCl solution were added and the resulting precipitate was filtered after 1 hour, washed with acetone (100 mL) and dried under vacuum to give a white powder. The resulting precipitate was then dissolved in a 3 M NaOH solution until pH = 12.



After extraction with chloroform (2\*100 mL), the organic phase was dried over MgSO<sub>4</sub> and the solvent was evaporated to give **16** as a yellow oil (m = 1.15 g, yield = 88 %).

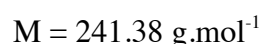
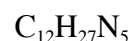
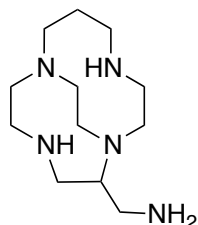
<sup>1</sup>H NMR (500 MHz, CDCl<sub>3</sub>, 330 K) δ (ppm): 1.21-1.32 (m, 2H), 1.42 (s, 9H, CH<sub>3</sub>), 1.56-1.67 (m, 1H), 1.89-2.00 (m, 2H), 2.08-2.16 (m, 1H), 2.32-2.39 (m, 1H), 2.43-2.49 (m, 1H), 2.57-3.37 (m, 17H), 4.56 (s, 1H, NHC=O).

<sup>13</sup>C{<sup>1</sup>H} NMR (150 MHz, CDCl<sub>3</sub>, 300 K) δ(ppm): 22.3 (CH<sub>2</sub>β), 28.7 (\*3) (CH<sub>3</sub>), 29.9, 41.1, 44.1, 44.2, 45.4, 45.5, 46.7, 50.7, 53.0, 55.6, 64.4 (CH), 79.7 (C), 156.0 (C=O).

ESI-MS:  $m/z = 342.29$  [M+H]<sup>+</sup>.

HRMS-ESI:  $m/z =$  calculated for C<sub>17</sub>H<sub>35</sub>N<sub>5</sub>O<sub>2</sub>+H: 342.2864 obtained 342.2860.

### **17** 1,4,8,11-tetraazabicyclo[6.5.2]pentadecan-13-ylmethanamine



*Route A:* **15** (1.0 g, 3.06 mmol) was dissolved in a mixture of acetic acid (1 mL) and water (10 mL) and 130 mg of 10 % Pd/C (0.12 mmol, 0.04 equivalent) were added under H<sub>2</sub>. After consumption of hydrogen, the mixture was filtered to remove palladium. After evaporation of the solvent, the residue was dissolved in acetone (80 mL). 5 mL of a 37 % HCl solution were added and the resulting precipitate was filtered after 1 hour, washed with acetone (20 mL) and dried under vacuum to give a white powder. The resulting precipitate was then dissolved in a 16 M NaOH solution until pH = 14. After extraction with chloroform (2\*60 mL), the organic phase was dried over MgSO<sub>4</sub> and the solvent was evaporated to give **17** as a yellow oil (m = 0.90 g, yield = 82 %).

*Route B:* 1.0 g (2.37 mmol) of **16** were dissolved in 10 mL of a 37 % HCl solution. The mixture was stirred for 30 min at room temperature. 100 mL of acetone were added and a precipitate was formed immediately. The precipitate was filtered, washed with acetone, ether, and dried under vacuum to give **17** (+ 5 HCl) as a white solid. The solid was dissolved in a solution of sodium hydroxide 16 M until pH = 14. After extraction with chloroform (2\*100 mL), the organic phase was dried over MgSO<sub>4</sub> and the solvent was evaporated. The compound **17** was obtained as a colorless oil (m = 0.46 g, yield = 80 %).

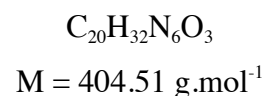
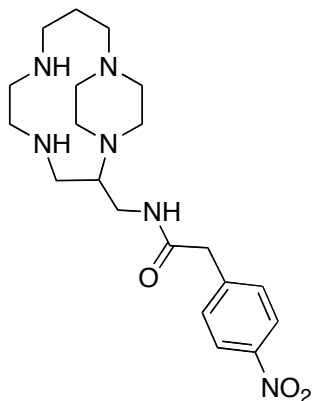
<sup>1</sup>H NMR (300 MHz, D<sub>2</sub>O, 300 K) δ(ppm): 1.74-1.79 (m, 1H), 2.24-2.50 (m, 2H), 2.69-3.74 (m, 20H).

$^{13}\text{C}\{^1\text{H}\}$  NMR (150 MHz,  $\text{D}_2\text{O}$ , 300 K)  $\delta$ (ppm): 18.9 ( $\text{CH}_2\beta$ ), 37.8, 43.1, 43.2, 45.7, 46.5, 47.3, 48.9, 51.7, 52.6, 55.2 ( $\text{CH}_2$ ), 60.4 ( $\text{CH}$ ).

ESI-MS:  $m/z = 242.23$  [ $\text{M}+\text{H}$ ] $^+$ .

HRMS-ESI:  $m/z =$  calculated for  $\text{C}_{12}\text{H}_{27}\text{N}_5+\text{H}$ : 242.2339 obtained 242.2333.

**18** *N*-(1,4,7,11-tetraazabicyclo[9.2.2]pentadecan-2-ylmethyl)-2-(4-nitrophenyl)acetamide



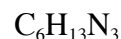
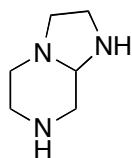
153 mg of *N*-succinimidyl-4-nitrophenylacetate (0.55 mmol) were added to a solution of **14** (133 mg, 0.55 mmol) in acetonitrile (10 mL). The reaction mixture was stirred overnight at room temperature. After evaporation of the solvent, the resulting oil was taken up in dichloromethane (15 mL), washed with a 8 M NaOH solution until pH = 14. The organic layer was dried over  $\text{MgSO}_4$  and concentrated in vacuo. The resulting oil was then purified by chromatography on aluminium oxide (eluent:  $\text{CH}_2\text{Cl}_2/\text{MeOH}$  95:5) to give compound **18** as a yellow oil ( $m = 67$  mg, yield = 31 %).

$^1\text{H}$  NMR (300 MHz,  $\text{CDCl}_3$ , 300 K)  $\delta$  (ppm): 1.60-1.69 (m, 2H), 2.09-2.18 (m, 2H), 2.42-3.35 (m, 21H), 3.62 (s, 2H), 6.18 (bs, 1H,  $\text{NHCO}$ ), 7.45 (d, 2H,  $^2J = 8.8$  Hz), 8.17 (d, 2H,  $^2J = 8.8$  Hz).

$^{13}\text{C}\{^1\text{H}\}$  NMR (75 MHz,  $\text{CDCl}_3$ , 300 K)  $\delta$ (ppm): 25.4, 39.3, 40.8, 43.6, 46.8, 48.0, 49.7, 50.1, 50.6, 50.9, 51.3, 54.7, 63.2 ( $\text{CH}_2+\text{CH}$ ), 124.0 (\*2), 130.5 (\*2) ( $\text{CHar}$ ), 143.1, 147.4 ( $\text{Car}$ ), 169.3 ( $\text{C}=\text{O}$ ).

ESI-MS:  $m/z = 405.26$  [ $\text{M}+\text{H}$ ] $^+$ .

HRMS-ESI:  $m/z =$  calculated for  $\text{C}_{20}\text{H}_{32}\text{N}_6\text{O}_3+\text{H}$ : 405.2609, obtained 405.2602.

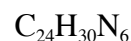
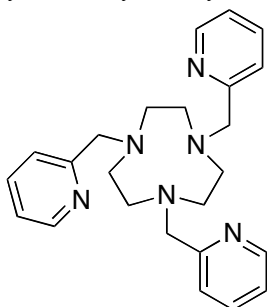
**19** Octahydroimidazol[1,2-a]pyrazine

M = 127.19 g.mol<sup>-1</sup>

A solution of chloroacetaldehyde (50 % in water, 111.8 g, 0.71 mol) in 500 mL of acetonitrile was added at 20 °C to a solution of diethylenetriamine (73.3 g, 0.71 mol) and 196.8 g of K<sub>2</sub>CO<sub>3</sub> (1.42 mol, 2 eq) in 1 L of acetonitrile. The mixture was stirred at this temperature for 6 h. After filtration on celite, the solvent was evaporated. The oily residue was taken up in diethylether (800 mL), insoluble impurities were removed by filtration. After evaporation of the solvent, compound **19** was isolated as a yellow oil (m = 64.3 g, yield = 71 %).

<sup>1</sup>H NMR (300 MHz, CDCl<sub>3</sub>, 298 K) δ (ppm): 1.60-1.81 (bs, 2H, NH), 1.93-2.04 (m, 2H), 2.23 (m, 1H, <sup>2</sup>J = 11.6, <sup>3</sup>J = 8.0 Hz, CH<sub>2</sub>CH), 2.43-2.45 (m, 2H), 2.56-2.63 (m, 3H), 2.73-2.77 (m, 2H), 2.87 (dd, 1H, <sup>2</sup>J = 11.6, <sup>3</sup>J = 2.6 Hz, CH<sub>2</sub>CH).

<sup>13</sup>C{<sup>1</sup>H} NMR (75 MHz, CDCl<sub>3</sub>, 298 K) δ (ppm): 42.1, 44.3, 48.4, 50.2, 51.6 (CH<sub>2</sub>α), 75.7 (CH).

**20** 1,4,7-tris(pyridin-2-ylmethyl)-1,4,7-triazacyclononane

M = 402.54 g.mol<sup>-1</sup>

9.85 g of 2-(bromomethyl)pyridine hydrobromide (39.0 mmol, 3 eq) were slowly added at 10 °C to a solution of **19** (1.62 g, 13.0 mmol) and K<sub>2</sub>CO<sub>3</sub> (45.5 g, 330.0 mmol) in 90 mL of acetonitrile. The mixture was stirred at room temperature overnight. After filtration on celite, the solvent was removed. The oily residue was taken up overnight in diethylether (200 mL) and the resulting precipitate was filtered, washed with diethylether (2\*20 mL) and dried in vacuo to give 12.96 g of intermediate. 5.0 g of the obtained intermediate (10.3 mmol) were then placed in dry ethanol (45 mL) and 3.9 g of NaBH<sub>4</sub> (103.0 mmol) were added at - 10 °C to the solution. After 12 h, the solvent was evaporated in vacuo and the resulting mixture was taken up in 50 mL of diethylether. Insoluble impurities were removed by filtration. After evaporation of the solvent, the compound **20** was obtained as an orange oil (m = 1.62 g, yield = 31 %).

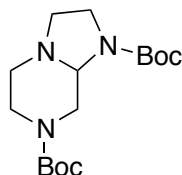
<sup>1</sup>H NMR (300 MHz, CDCl<sub>3</sub>, 298 K) δ (ppm): 3.06 (s, 12H), 4.34 (s, 6H), 7.80-7.84 (m, 3H), 7.92-7.95 (m, 3H), 8.33-8.39 (m, 3H), 8.64-8.66 (m, 3H).

$^{13}\text{C}\{^1\text{H}\}$  NMR (75 MHz,  $\text{CDCl}_3$ , 298K)  $\delta$  (ppm): 49.3 (\*6), 56.3 (\*3), 126.4 (\*3), 127.3 (\*3), 143.5 (\*3), 145.6 (\*3), 150.3 (\*3).

ESI-MS:  $m/z = 403.26$   $[\text{M}+\text{H}]^+$ .

HRMS-ESI:  $m/z =$  calculated for  $\text{C}_{24}\text{H}_{30}\text{N}_6+\text{H}$ : 403.2605, obtained 403.2594.

**21** di-tert-butyl hexahydroimidazo[1,2-a]pyrazine-1,7-dicarboxylate



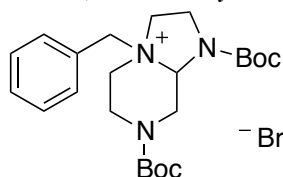
$$M = 327.42 \text{ g}\cdot\text{mol}^{-1}$$

A solution of  $\text{Boc}_2\text{O}$  (5.79 g, 26.6 mol) in dichloromethane (30 mL) was added dropwise to a solution of **19** (1.69 g, 13.3 mmol) in dichloromethane (30 mL). The mixture was stirred overnight at room temperature. After evaporation of the solvent, the resulting product was taken up in diethylether (50 mL). Impurities were removed by filtration on celite and compound **21** was isolated as a brown powder ( $m = 3.98$  g, yield = 91 %).

$^1\text{H}$  NMR (300 MHz,  $\text{CDCl}_3$ , 298 K)  $\delta$ (ppm): 3.32-3.39 (m, 18H), 4.37-4.67 (m, 2H), 4.73-5.98 (m, 8H), 6.44 (m, 1H).

ESI-MS:  $m/z = 328.15$   $[\text{M}+\text{H}]^+$ .

**22** 4-benzyl-1,7-bis(tert-butoxycarbonyl)octahydro-1H-imidazo[1,2-a]pyrazin-4-ium bromide



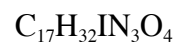
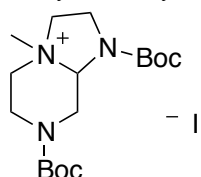
$$M = 498.45 \text{ g}\cdot\text{mol}^{-1}$$

A solution of benzylbromide (742 mg, 4.3 mmol) in acetonitrile (5 mL) was added dropwise at 0 °C to a solution of **21** (1.45 g, 4.34 mmol) in acetonitrile (10 mL). The mixture was stirred overnight at room temperature. After evaporation of the solvent, the resulting oil was taken up in diethylether (20 mL). After filtration, the precipitate was washed twice with diethylether (10 mL) and dried in vacuo to give compound **22** as a beige solid ( $m = 1.31$  g, yield = 61 %).

$^1\text{H}$  NMR (500 MHz,  $\text{CDCl}_3$ , 320 K)  $\delta$ (ppm): 1.35 (s, 9H), 1.51 (s, 9H), 3.58-3.66 (m, 2H), 3.70-3.78 (m, 1H), 3.81-3.93 (m, 3H), 4.13-4.20 (m, 1H), 4.46 (m, 1H), 4.56-4.65 (m, 1H), 4.75 (d, 1H,  $^2\text{J} = 12.3$  Hz), 4.83 (m, 1H), 5.19 (m, 1H), 5.46 (d, 1H,  $^2\text{J} = 12.3$  Hz), 7.45-7.51 (m, 3H), 7.59 (d, 2H,  $^3\text{J} = 7.1$  Hz).

ESI-MS:  $m/z = 418.27 [M-Br]^+$ .

**23** 1,7-bis(tert-butoxycarbonyl)-4-methyloctahydro-1H-imidazo[1,2-a]pyrazin-4-ium iodide



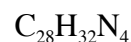
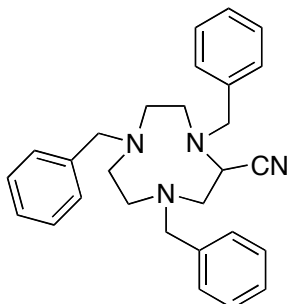
$$M = 469.36 \text{ g}\cdot\text{mol}^{-1}$$

A solution of iodomethane (0.92 mg, 6.5 mmol) in acetonitrile (5 mL) was added dropwise at 0 °C to a solution of **21** (2.12 g, 6.5 mmol) in acetonitrile (10 mL). The mixture was stirred overnight at room temperature. After evaporation of the solvent, the resulting oil was taken up in diethylether (30 mL). After filtration, the precipitate was washed twice with diethylether (10 mL) and dried in vacuo. Compound **23** was obtained as a yellow solid ( $m = 1.78 \text{ g}$ , yield = 59 %).

$^1\text{H NMR}$  (300 MHz,  $\text{CDCl}_3$ , 298 K)  $\delta$ (ppm): 1.40-1.48 (m, 21H), 3.70-4.74 (m, 10H), 5.0 (m, 1H).

ESI-MS:  $m/z = 230.12 [M-I-2^t\text{Bu} + 2\text{H}]^+$ , 286.19  $[M-I-^t\text{Bu} + \text{H}]^+$ , 342.25  $[M-I]^+$ .

**24** 1,4,7-tribenzyl-1,4,7-triazacyclononane-2-carbonitrile



$$M = 424.58 \text{ g}\cdot\text{mol}^{-1}$$

259.3 g of benzyl bromide (1.5 mol) were slowly added to a solution of **19** (64.3 g, 0.5 mol) and  $\text{K}_2\text{CO}_3$  (278.8 g, 2.0 mol) in 1.1 L of acetonitrile at 10 °C. Then 24.76 g of sodium cyanide (0.5 mol) were carefully added. The mixture was stirred at room temperature for four days. After filtration on celite, the solvent was evaporated in vacuo and the residual oil was taken up in diethylether (3 L). Insoluble impurities were removed by filtration. After evaporation of the solvent, compound **24** was obtained as a brown oil (137.2 g, yield = 63 %).

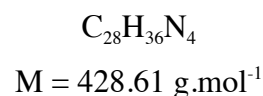
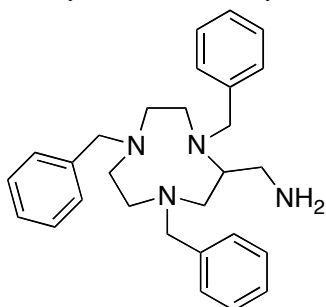
$^1\text{H NMR}$  (300 MHz,  $\text{CDCl}_3$ , 298 K)  $\delta$ (ppm): 1.53-1.78 (m, 1H), 2.43-2.56 (m, 4H), 2.66-2.74 (m, 1H), 2.82-2.88 (m, 2H), 2.95-2.99 (m, 1H), 3.14-3.22 (m, 1H), 3.42-3.53 (m, 1H), 3.63-3.84 (m, 6H), 7.19-7.33 (m, 15H).

$^{13}\text{C}\{^1\text{H}\}$  NMR (75 MHz,  $\text{CDCl}_3$ , 298 K)  $\delta$  (ppm): 54.7 (CH), 55.5, 56.4, 57.4, 58.8, 61.4, 62.1, 63.5, 65.9 ( $\text{CH}_2$ ), 118.0 (CN), 126.8, 127.1, 127.7, 128.0, 128.1, 128.2, 128.3, 128.4, 128.6, 128.8, 129.0, 129.1 (\*2), 129.2, 129.4 (CHar) 138.2, 139.3, 139.9 (Car).

ESI-MS:  $m/z = 425.25$   $[\text{M}+\text{H}]^+$ .

IR ( $\text{cm}^{-1}$ ): 2250 (CN).

**25** (1,4,7-tribenzyl-1,4,7-triazacyclononan-2-yl)methanamine



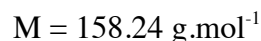
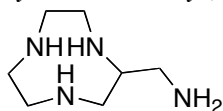
A solution of **24** (112.7 g, 0.27 mol) in THF (450 mL) was slowly added at  $-78\text{ }^\circ\text{C}$  to a suspension of 11.5 g of  $\text{LiAlH}_4$  (0.32 mol, 1.2 eq) in THF (450 mL) under nitrogen. An emission of fumes was observed. The resulting mixture was stirred overnight. 100 mL of water were carefully added. After removal of the solvent, the residual green solid was taken up in chloroform (1 L), the solution was dried over  $\text{MgSO}_4$ , insoluble impurities were removed by filtration on celite. The residual brown oil was placed in acetone (200 mL), and a solution of 37 % HCl (200 mL) was carefully added. The white precipitate formed was filtered and recrystallized in water to give **25** (+ 3 HCl) as a white solid. The resulting crystals were then dissolved in a 16 M NaOH solution until  $\text{pH} = 14$ . After extraction with chloroform (2\*500 mL), the organic phase was dried over  $\text{MgSO}_4$  and the solvent was evaporated to give **25** as a yellow oil (45.3 g, yield = 39 %).

$^1\text{H}$  NMR (300 MHz,  $\text{CDCl}_3$ , 298 K)  $\delta$ (ppm): 1.45 (bs, 2H), 2.39-2.86 (m, 10H), 3.03-3.11 (m, 1H), 3.35-3.75 (m, 7H), 3.85 (bs, 1H), 7.24-7.44 (15H).

$^{13}\text{C}\{^1\text{H}\}$  NMR (75 MHz,  $\text{CDCl}_3$ , 298 K)  $\delta$  (ppm): 42.5, 51.1, 52.8, 55.1, 55.6, 57.9, 58.2 ( $\text{CH}_2$ ), 62.8 (CH), 63.5, 64.3 ( $\text{CH}_2$ ) 126.7, 127.0, 127.1, 128.3 (\*9), 128.8, 129.2, 129.5 (CHar), 140.2, 140.4, 141.2 (Car).

ESI-MS:  $m/z = 429.31$   $[\text{M}+\text{H}]^+$ .

HRMS-ESI:  $m/z =$  calculated for  $\text{C}_{28}\text{H}_{36}\text{N}_4+\text{H}$ : 429.3012 obtained 429.3060.

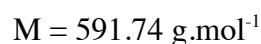
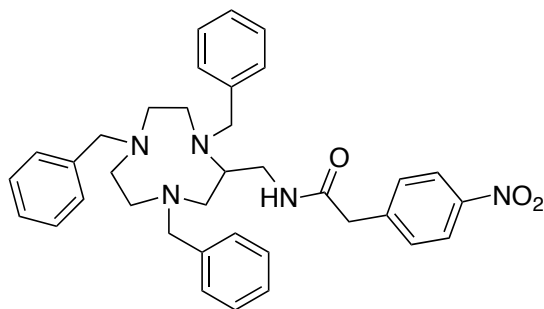
**26** (1,4,7-triazacyclononan-2-yl)methanamine

5.0 g of compound **25** (11.7 mol) were dissolved in a mixture of acetic acid (29 mL), water (29 mL) and THF (98 mL) and 500 mg of 10 % Pd/C (0.47 mmol, 0.04 equivalent) were added under H<sub>2</sub>. After consumption of hydrogen, the mixture was filtered to remove palladium. After evaporation of the solvent, the residue was dissolved in ethanol (100 mL). 5 mL of a 37 % HCl solution were added and the resulting precipitate was filtered after 1 h, washed with acetone (20 mL) and dried under vacuum to give a white powder. The resulting precipitate was recrystallized in water. The white crystals were dissolved in a 16 M NaOH solution until pH = 14. After extraction with chloroform (2\*50 mL), the organic phase was dried over MgSO<sub>4</sub> and the solvent was evaporated in vacuo to give **26** as a yellow oil (m = 0.79 g, yield = 44 %).

<sup>1</sup>H NMR (300 MHz, CDCl<sub>3</sub>, 298 K) δ(ppm): (m, 13 H) 2,98 - 3,58.

<sup>13</sup>C{<sup>1</sup>H} NMR (150 MHz, CDCl<sub>3</sub>, 298 K) δ(ppm): 40.9, 42.0, 42.9, 45.2, 46.2, 47.2 (CH<sub>2</sub>α) 50.6 (CH).

ESI-MS: m/z = 159.16 [M+H]<sup>+</sup>.

**27** 2-(4-nitrophenyl)-N-((1,4,7-tribenzyl-1,4,7-triazacyclononan-2-yl)methyl)acetamide

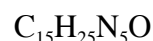
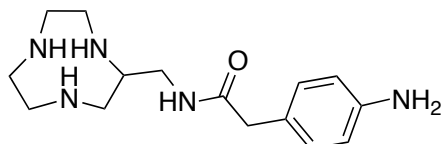
0.69 g of N-succinimidyl-4-nitrophenylacetate (2.5 mmol) were added to a solution of **25** (1.06 g, 2.5 mmol) in CH<sub>2</sub>Cl<sub>2</sub> (10 mL) and the resulting mixture was stirred overnight at room temperature. After evaporation of the solvent, the residue was washed with 30 mL of 1 M NaOH solution, the organic phase was extracted with dichloromethane and dried over MgSO<sub>4</sub>. After evaporation, compound **27** was obtained as a pink foam (m = 1.42 g, yield = 96 %).

<sup>1</sup>H NMR (300 MHz, CDCl<sub>3</sub>, 298 K) δ(ppm): 2.29-2.80 (m, 9H), 2.95 (t, 1H, J<sub>app</sub> = 12.3 Hz), 3.15 (d, 1H, J = 13.8 Hz), 3.36-3.71 (m, 9H), 4.37-4.38 (m, 1H), 6.14-6.16 (m, 1H, NHC=O), 6.79-6.81 (m, 2H, CH<sub>ar</sub><sub>NO<sub>2</sub></sub>), 7.14-7.37 (m, 15H, CH<sub>ar</sub>), 8.04 (d, 2H, J = 8.6 Hz, CH<sub>ar</sub><sub>NO<sub>2</sub></sub>).

$^{13}\text{C}\{^1\text{H}\}$  NMR (75 MHz,  $\text{CDCl}_3$ , 298K)  $\delta$  (ppm): 39.2, 43.6, 50.2, 51.6, 53.6, 55.7, 55.8, 57.0, 58.0, 59.1 ( $\text{CH}_2$ ), 64.6 (CH), 124.0 (\*2) ( $\text{CHar}_{\text{NO}_2}$ ), 127.0, 127.2, 127.3, 128.3 (\*3), 128.4 (\*2), 128.5 (\*2), 129.1 (\*2), 129.5 (\*2) ( $\text{CHar}$ ), 130.5 (\*2) ( $\text{CHar}_{\text{NO}_2}$ ), 139.8, 139.9, 140.0 (Car), 142.6, 147.1 ( $\text{Car}_{\text{NO}_2}$ ), 168.7 (C=O).

ESI-MS:  $m/z = 592.33$   $[\text{M}+\text{H}]^+$ .

**28** *N-((1,4,7-triazacyclononan-2-yl)methyl)-2-(4-aminophenyl)acetamide*



$$M = 291.39 \text{ g}\cdot\text{mol}^{-1}$$

1.33 g of compound **27** (2.3 mmol) were dissolved in a mixture of acetic acid (16 mL), water (16 mL) and THF (49 mL) and 96 mg of 10 % Pd/C (0.1 mmol, 0.04 equivalent) were added under  $\text{H}_2$ . After consumption of hydrogen, the mixture was filtered to remove palladium. After evaporation of the solvent, the residue was dissolved in ethanol (100 mL). 5 mL of a 37 % HCl solution were added and the resulting precipitate was filtered after 1 h, washed with acetone (20 mL) and dried under vacuum to give a white powder. The resulting precipitate was then dissolved in a 16 M NaOH solution until pH = 14. After extraction with chloroform (2\*25 mL), the organic phase was dried over  $\text{MgSO}_4$  and the solvent was evaporated in vacuo to give **28** as a yellow oil ( $m = 0.20$  mg, yield = 31 %).

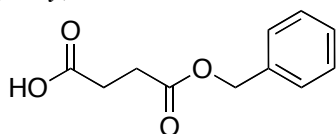
$^1\text{H}$  NMR (300 MHz,  $\text{CDCl}_3$ , 298 K)  $\delta$ (ppm): 1.90-2.13 (bs, 4H), 2.27-2.42 (m, 2H), 2.53-2.88 (m, 10H), 3.20-3.27 (m, 1H), 3.50-3.78 (m, 3H), 6.24-6.28 (m, 1H,  $\text{NHC}=\text{O}$ ), 6.60 (d, 2H,  $^3J = 8.2$  Hz,  $\text{CHar}_{\text{NH}_2}$ ), 6.97 (d, 2H,  $^3J = 8.2$  Hz,  $\text{CHar}_{\text{NH}_2}$ ).

$^{13}\text{C}\{^1\text{H}\}$  NMR (75 MHz,  $\text{CDCl}_3$ , 298K)  $\delta$  (ppm): 43.2, 43.5, 46.5, 46.7, 47.0, 47.4, 48.9 ( $\text{CH}_2$ ), 54.9 (CH), 115.6 (\*2) ( $\text{CHar}_{\text{NH}_2}$ ), 124.8 ( $\text{Car}_{\text{NH}_2}$ ), 130.5 (\*2) ( $\text{CHar}_{\text{NH}_2}$ ), 145.8 ( $\text{Car}_{\text{NH}_2}$ ), 172.2 (C=O).

ESI-MS:  $m/z = 292.21$   $[\text{M}+\text{H}]^+$ , 314.19  $[\text{M}+\text{Na}]^+$ .

HRMS-ESI:  $m/z =$  calculated for  $\text{C}_{24}\text{H}_{30}\text{N}_6+\text{H}$ : 592.3282, obtained 592.3315.

**29** *4-(benzyloxy)-4-oxobutanoic acid*



$$M = 208.07 \text{ g}\cdot\text{mol}^{-1}$$

2.0 g of succinic acid anhydride (20.0 mmol) were dissolved in dried pyridine (10 mL). Benzyl alcohol (2.2 g, 20.3 mmol) and 4-dimethylaminopyridine (10 mg, 0.08 mmol) were added

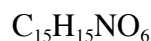
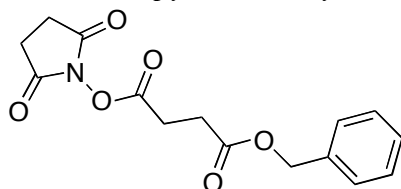


and the mixture was heated to 50 °C during 24 h. After evaporation, CH<sub>2</sub>Cl<sub>2</sub> was added and the product was extracted with a saturated solution of sodium bicarbonate. The aqueous phase was washed with dichloromethane and then acidified with a 2 M HCl solution until pH = 4. The white precipitate was extracted with ethyl acetate and evaporation of the solvent give compound **29** as a white solid (m = 2.2 g, yield = 52 %).

<sup>1</sup>H NMR (300 MHz, CDCl<sub>3</sub>, 298 K) δ(ppm): 2.61 (m, 4H), 5.07 (s, 2H, CH<sub>2</sub>Ph), 7.22-7.33 (m, 5H), 7.59-10.20 (bs, 1H, COOH).

<sup>13</sup>C{<sup>1</sup>H} NMR (75 MHz, CDCl<sub>3</sub>, 298 K) δ(ppm): 29.0, 29.1 (CH<sub>2</sub>), 66.9 (CH<sub>2</sub>Ph), 128.4 (\*2), 128.5, 128.7 (\*2) (CHar), 135.8 (Car), 172.2, 178.5 (C=O).

**30** *benzyl (2,5-dioxopyrrolidin-1-yl) succinate*



$$M = 305.09 \text{ g}\cdot\text{mol}^{-1}$$

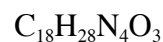
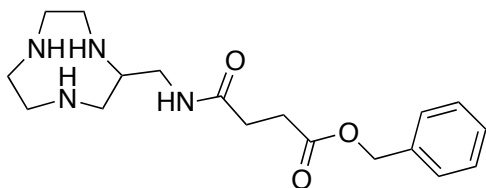
1.0 g of compound **29** (4.8 mmol), DCC (990 mg, 4.8 mmol) and NHS (550 mg, 4.8 mmol) were dissolved in CH<sub>3</sub>CN (20 mL). The solution was stirred at room temperature for 2 h. The precipitate which was formed during the reaction was removed by filtration. The solvent was evaporated and the resulting colorless oil was placed in the fridge to give **30** as a white solid (m = 1.4 g, yield = 95 %).

<sup>1</sup>H NMR (300 MHz, CDCl<sub>3</sub>, 298 K) δ(ppm): 2.68-2.78 (m, 6H), 2.90 (t, 2H, <sup>3</sup>J = 7.0 Hz), 5.08 (s, 2H, CH<sub>2</sub>Ph), 7.22-7.35 (m, 5H).

<sup>13</sup>C{<sup>1</sup>H} NMR (75 MHz, CDCl<sub>3</sub>, 298 K) δ(ppm): 25.4 (\*2), 26.1, 28.4 (CH<sub>2</sub>), 66.6 (CH<sub>2</sub>Ph), 128.3, 128.4 (\*2), 128.6 (\*2) (CHar), 135.6 (Car), 167.7, 169.1 (\*2), 170.8 (C=O).

ESI-MS: m/z = 328.08 [M+Na]<sup>+</sup>.

HRMS-ESI: m/z = calculated for C<sub>15</sub>H<sub>15</sub>NO<sub>6</sub>+Na: 328.0792 obtained, 328.0793.

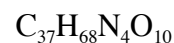
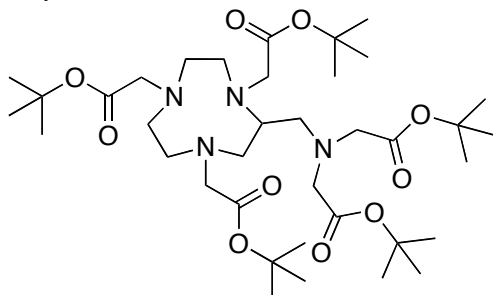
**31** benzyl 4-(((1,4,7-triazacyclononan-2-yl)methyl)amino)-4-oxobutanoate

$$M = 348.44 \text{ g}\cdot\text{mol}^{-1}$$

231 mg of compound **30** (0.76 mmol) were added on a solution of compound **26** (120 mg, 0.76 mmol) in acetonitrile. The mixture was stirred at room temperature for 12 h. Solvent was evaporated and the mixture was taken up in diethylether. Impurities were removed by filtration, the solvent was evaporated and the resulting oil was purified by flash chromatography on reverse phase (A: HCOOH/H<sub>2</sub>O (0.01 mol.L<sup>-1</sup>), B: CH<sub>3</sub>CN, B 80 → 100). Compound **31** was isolated as a colorless oil (m = 53 mg, yield = 20 %).

<sup>1</sup>H NMR (300 MHz, D<sub>2</sub>O, 298 K) δ(ppm): 2.59-2.66 (m, 1H), 2.76-3.86 (m, 16H), 5.22 (s, 2H, CH<sub>2</sub>Bn), 7.42-7.55 (m, 5H).

ESI-MS: m/z = 349.24 [M+H]<sup>+</sup>.

**32** tri-tert-butyl-2,2',2''-(2-((bis(2-(tert-butoxy)-2-oxoethyl)amino)methyl)-1,4,7-triazacyclononan-1,4,7-triyl) triacetate

$$M = 728.96 \text{ g}\cdot\text{mol}^{-1}$$

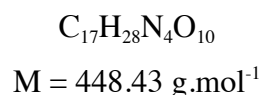
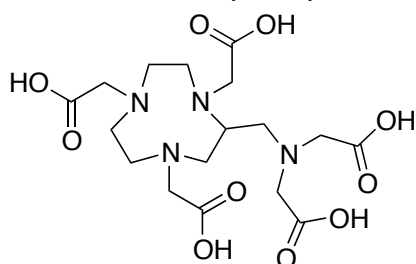
A solution of *tert*-butylbromoacetate (4.66 g, 23.89 mmol) was added to a solution of **25** (756 mg, 4.79 mmol) and K<sub>2</sub>CO<sub>3</sub> (6.61 g, 47.89 mmol) in acetonitrile (16 mL). The resulting mixture was heated at 45 °C for 24 h. After cooling, the solution was filtered on celite. The solvent was evaporated and the resulting oil was taken up in diethylether. The impurities were removed by filtration, solvent was evaporated and the residue was purified by several successive chromatographies on aluminium oxide (eluent: CH<sub>2</sub>Cl<sub>2</sub>/MeOH 99:1) to give pure **32** as a yellow oil (m = 1.89 g, yield = 54 %).

<sup>1</sup>H NMR (300 MHz, CDCl<sub>3</sub>, 298 K) δ (ppm): 1.38-1.41 (m, 45H, CH<sub>3</sub>), 2.43 (dd, 1H, J = 13.2, 7.7 Hz), 2.60-3.11 (m, 11H), 3.19-3.45 (m, 10 H), 4.02-4.13 (m, 1H).

$^{13}\text{C}\{^1\text{H}\}$  NMR (75 MHz,  $\text{CDCl}_3$ , 298K)  $\delta$  (ppm): 28.4 (\*15) ( $\text{CH}_3$ ), 52.5, 53.6, 54.8, 55.4, 55.5, 55.8, 56.3 (\*2), 59.9, 60.2 ( $\text{CH}_2$ ), 61.2 (CH), 80.4, 80.6, 80.7, 80.8 (\*2) (C), 171.0 (\*2), 171.7, 171.8, 172.3 (C=O).

ESI-MS:  $m/z = 729.5$  [ $\text{M}+\text{H}$ ] $^+$ , 751.5 [ $\text{M}+\text{Na}$ ] $^+$ .

**33** 2,2',2''-(2-((bis(carboxymethyl)amino)methyl)-1,4,7-triazacyclononane-1,4,7-triyl)triacetic acid



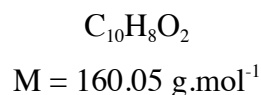
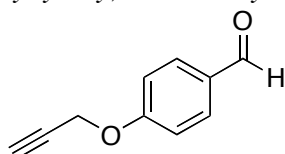
10 mL of a 37 % HCl aqueous solution were added on 50 mg of compound **32** (0.07 mmol). The mixture was stirred 1 hour at room temperature. After evaporation, the resulting precipitate was washed with acetone (50 mL). After filtration, compound **33** was isolated as a white powder ( $m = 360$  mg, yield = 58 %).

$^1\text{H}$  NMR (300 MHz,  $\text{CDCl}_3$ , 298 K)  $\delta$  (ppm): 2.76-2.87 (m, 1H), 3.02-3.91 (m, 12H), 4.35-4.31 (m, 10H).

ESI-MS:  $m/z = 449.3$  [ $\text{M}+\text{H}$ ] $^+$ , 471.2 [ $\text{M}+\text{Na}$ ] $^+$ , 493.2 [ $\text{M}+2\text{Na}-\text{H}$ ] $^+$ .

HRMS-ESI:  $m/z =$  calculated for  $\text{C}_{17}\text{H}_{28}\text{N}_4\text{O}_{10}+\text{H}$ : 449.1878, obtained 449.1858.

**34** 3-(Prop-2-ynoxy)benzaldehyde

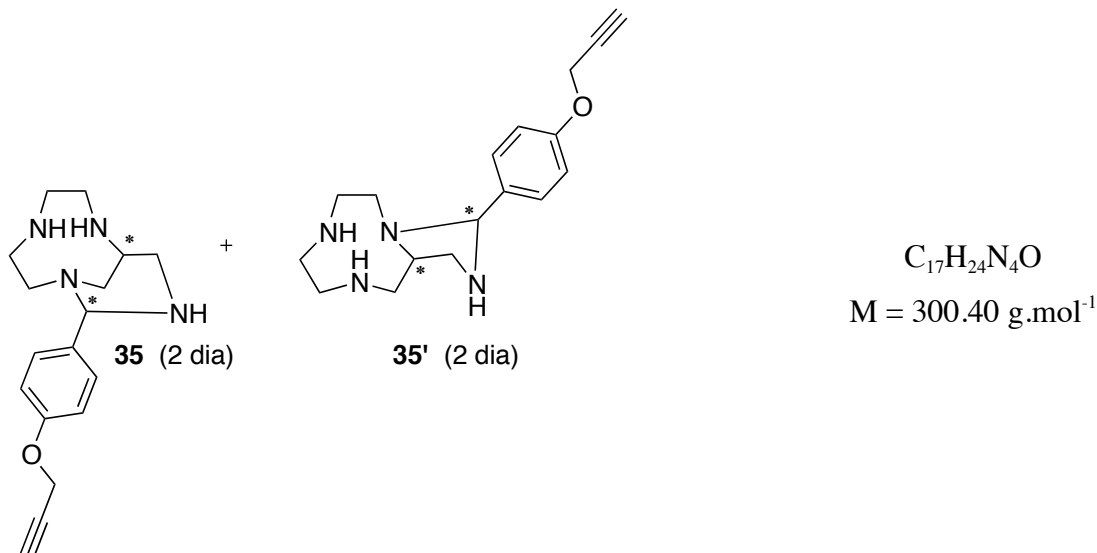


A mixture of 4-hydroxybenzaldehyde (4.0 g, 0.032 mol) and  $\text{K}_2\text{CO}_3$  (13.5 g, 0.098 mol) in dry DMF (75 mL) was heated to 55-60 °C for 30 min under  $\text{N}_2$ . After cooling at room temperature, 5.8 g of propargyl bromide (0.039 mol) were added through septum using syringe. The mixture was stirred for 4 h at room temperature and poured in ice water with stirring. Stirring continued for 10 min, the solid formed was filtered and dried under vacuum to give the desired compound **34** as a white solid ( $m = 3.6$  g, yield = 71 %).

$^1\text{H}$  NMR (300 MHz,  $\text{CDCl}_3$ , 300 K)  $\delta$  (ppm): 2.54 (t, 1H,  $^4\text{J} = 2.3$  Hz,  $\text{C}\equiv\text{CH}$ ), 4.75 (d, 2H,  $^4\text{J} = 2.3$  Hz,  $\text{CH}_2-\text{C}\equiv\text{CH}$ ), 7.07 (d, 2H,  $^3\text{J} = 8.2$  Hz), 7.83 (d, 2H,  $^3\text{J} = 8.2$  Hz), 9.86 (s, 1H, CHO).

$^{13}\text{C}\{^1\text{H}\}$  NMR (75 MHz,  $\text{CDCl}_3$ , 300 K)  $\delta$  (ppm): 55.9 ( $\text{CH}_2$ ), 76.4 ( $\text{C}\equiv\text{CH}$ ), 78.7 ( $\text{C}\equiv\text{CH}$ ), 115.2 (\*2) (CHar), 130.5 (Car), 131.9 (\*2) (CHar), 162.5 (Car), 190.8 ( $\text{C}=\text{O}$ ).

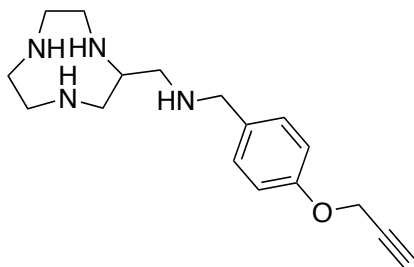
**35 + 35'** 11-(4-(prop-2-yn-1-yloxy)phenyl)-1,4,7,10-tetraazabicyclo[6.3.1]dodecane



1.20 g of compound **34** (7.5 mmol) were added to a solution of **26** (1.19 mg, 7.5 mmol) in ethanol (25 mL) and the mixture was stirred at room temperature for 48 h. The solvent was evaporated to dryness, and the residual oil was taken up in diethylether (25 mL). After stirring during 12 h, the insoluble impurities were removed by filtration. After evaporation of the solvent, a mixture of 4 isomers **35** (2 diastereoisomers) and **35'** (2 diastereoisomers) was obtained as a yellow foam ( $m = 1.40 \text{ g}$ , yield = 75 %).

$^{13}\text{C}\{^1\text{H}\}$  NMR (75 MHz,  $\text{CDCl}_3$ , 298K)  $\delta$  (ppm): 47.9 (\*2), 48.5 (\*2), 48.8 (\*2), 49.0 (\*2), 50.2 (\*2), 50.3 (\*2), 50.4 (\*2), 50.5 (\*2), 51.8 (\*2), 54.8 (\*2), 55.3 (\*2), 55.6 (\*2), 56.0 (\*4), 56.1 (\*2), 58.1 (\*2) ( $\text{CH}_2$ ), 63.5, 63.9, 64.1, 66.0 (CH), 75.5, 75.7 (\*2), 75.8 ( $\text{C}\equiv\text{CH}$ ), 78.7, 78.8 (\*2), 79.0 ( $\text{C}\equiv\text{CH}$ ), 86.6, 86.7 (\*2), 87.1 (NCN), 114.5 (\*2), 114.9 (\*4), 115.0 (\*2), 127.8 (\*2), 128.8 (\*4), 129.0 (\*2) (CHar), 133.8, 134.6 (\*2), 138.7, 156.6, 157.8 (\*2), 157.9 (Car).

ESI-MS:  $m/z = 301.21 [\text{M}+\text{H}]^+$ ,  $339.22 [\text{M}+\text{Na}]^+$ .

**36** *N-((1,4,7-triazacyclononan-2-yl)methyl)-1-(4-(prop-2-yn-1-yloxy)phenyl)methanamine*

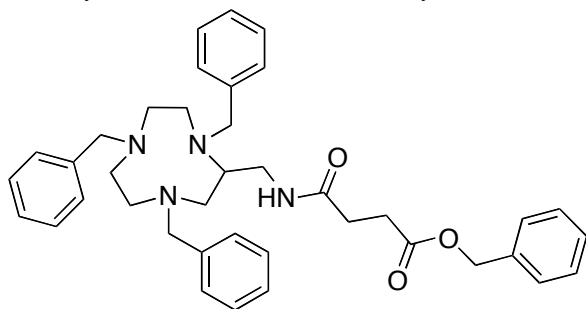
$$M = 302.41 \text{ g}\cdot\text{mol}^{-1}$$

250 mg of  $\text{NaBH}_4$  (6.7 mmol) were added on a solution of compounds **35** and **35'** (201 mg, 0.67 mmol) in ethanol (10 mL) at 0 °C. The mixture was stirred overnight at room temperature. The solvent was evaporated, the resulting solid was dissolved in dichloromethane (25 mL). After filtration of the insoluble impurities, the solution was washed with a 3 M NaOH solution (10 mL), dried over  $\text{MgSO}_4$  and the solvent was evaporated to give **36** as a very hygroscopic white foam (m = 135 mg, yield = 68 %).

$^1\text{H}$  NMR (300 MHz,  $\text{CDCl}_3$ , 298 K)  $\delta$  (ppm): 1.10-1.60 (m, 3H), 2.30-2.90 (m, 15H), 3.65 (s, 2H), 4.61 (d, 2H,  $^4J = 2.3$  Hz,  $\text{CH}_2\text{C}\equiv\text{CH}$ ), 6.86 (d, 2H,  $^3J = 8.7$  Hz), 7.18 (d, 2H,  $^3J = 8.7$  Hz).

$^{13}\text{C}\{^1\text{H}\}$  NMR (75 MHz,  $\text{CDCl}_3$ , 298K)  $\delta$  (ppm): 46.0, 46.4, 47.0, 47.2, 47.3, 49.9, 53.6, 55.6, 55.9, 75.6 ( $\text{CH}_2\text{C}\equiv\text{CH}$ ), 78.8 ( $\text{CH}_2\text{C}\equiv\text{CH}$ ), 114.8 (\*2), 129.3 (\*2), 130.1, 156.6.

ESI-MS:  $m/z = 303.22$  [ $\text{M}+\text{H}$ ] $^+$ .

**37** *benzyl 4-oxo-4-(((1,4,7-tribenzyl-1,4,7-triazacyclononan-2-yl)methyl)amino)butanoate*

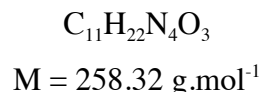
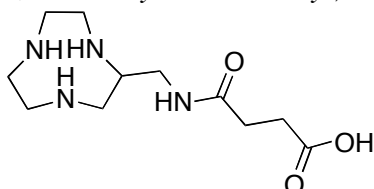
$$M = 618.81 \text{ g}\cdot\text{mol}^{-1}$$

3.01 g (7.02 mmol) of **25** and 2.14 g of **30** (7.02 mmol) were dissolved in  $\text{CH}_3\text{CN}$  (25 mL). The mixture was stirred at room temperature for 12 h. Solvent was evaporated and the mixture was taken up in diethylether. Impurities were removed by filtration and the solvent was evaporated to give the compound **37** as a yellow oil (m = 3.65 g, yield = 84 %).

$^1\text{H}$  NMR (500 MHz,  $\text{CDCl}_3$ , 298 K)  $\delta$ (ppm): 2.26-2.32 (m, 3H), 2.40-2.66 (m, 9H), 2.79 (t, 1H,  $^3J = 11.5$  Hz), 2.95 (t, 1H,  $^3J = 11.5$  Hz), 3.22-3.37 (m, 3H), 3.41-3.59 (m, 5H), 4.05 (s, 1H), 5.00 (s, 2H,  $\text{CH}_2\text{Ph}$ ), 5.96 (s, 1H, NH), 7.06-7.27 (m, 20H).

$^{13}\text{C}\{^1\text{H}\}$  NMR (125 MHz,  $\text{CDCl}_3$ , 298 K): 29.8 ( $\text{CH}_2\text{CO}_2\text{Bn}$ ), 31.1( $\text{CH}_2\text{CONH}$ ), 39.3, 50.5, 52.8, 55.5, 55.9 ( $\text{CH}_2$ ), 57.7 ( $\text{CH}$ ), 57.9, 58.3, 63.9, 64.2 ( $\text{CH}_2$ ), 66.5 ( $\text{OCH}_2\text{Ph}$ ), 126.9, 127.0, 127.2, 128.2 (\*2), 128.3 (\*3), 128.4 (\*3), 128.5 (\*2), 128.6, 128.8 (\*2), 129.1 (\*2), 129.5 (\*2) ( $\text{CHar}$ ), 136.0, 140.0, 140.1, 140.5 ( $\text{Car}$ ), 170.9, 172.8 ( $\text{C=O}$ ).

**38** 4-(((1,4,7-triazacyclononan-2-yl)methyl)amino)-4-oxobutanoic acid

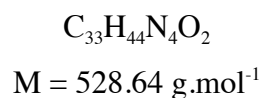
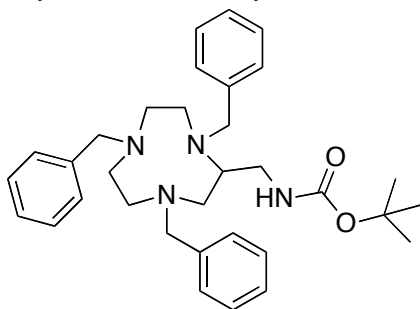


Compound **37** (3.65 g, 5.90 mmol) was dissolved in a mixture of acetic acid (7 mL), water (7 mL) and THF (20 mL) and 260 mg of 10 % Pd/C (0.26 mmol) were added under  $\text{H}_2$ . After consumption of hydrogen, the mixture was filtered to remove palladium and the solvent was evaporated to give **38** as a yellow oil ( $m = 0.64 \text{ g}$ , yield = 42 %).

$^{13}\text{C}\{^1\text{H}\}$  NMR (150 MHz,  $\text{D}_2\text{O}$ , 298 K)  $\delta(\text{ppm})$ : 32.2, 32.8, 39.4 (\*2), 40.3, 42.0 (\*2), 44.2, 45.4 ( $\text{CH}_2$ ), 52.5 ( $\text{CH}$ ), 176.8 ( $\text{C=O}$ ).

ESI-MS:  $m/z = 259.22$  [ $\text{M}+\text{H}$ ] $^+$ .

**39** tert-butyl ((1,4,7-tribenzyl-1,4,7-triazacyclononan-2-yl)methyl)carbamate



A solution of  $\text{Boc}_2\text{O}$  (4.20 g, 19.2 mmol) in  $\text{CH}_2\text{Cl}_2$  (100 mL) was slowly added to a solution of **25** (8.24 g, 19.2 mmol) in  $\text{CH}_2\text{Cl}_2$  (150 mL). The solution was stirred overnight at room temperature. After evaporation of the solvent, the residual oil was purified by aluminium oxide chromatography (eluent:  $\text{CH}_2\text{Cl}_2$ ) to give **39** as a yellow oil ( $m = 7.38 \text{ g}$ , yield = 73 %).

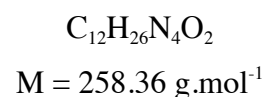
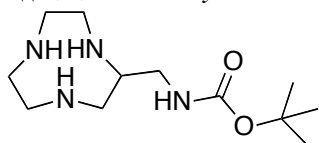
$^1\text{H}$  NMR (300 MHz,  $\text{CDCl}_3$ , 298 K)  $\delta(\text{ppm})$ : 1.42 (s, 9H,  $\text{CH}_3$ ), 2.34-2.67 (m, 8H), 2.83-2.92 (m, 1H), 2.97-3.16 (m, 2H), 3.35-3.65 (m, 7H), 4.05 (m, 1H), 4.94 (m, 1H), 7.15-7.33 (m, 15H).

$^{13}\text{C}\{^1\text{H}\}$  NMR (150 MHz,  $\text{CDCl}_3$ , 298 K)  $\delta$ (ppm): 28.7 (\*3) ( $\text{CH}_3$ ), 40.7, 50.6, 53.2, 55.3, 56.2, 57.9, 58.1 ( $\text{CH}_2$ ), 58.5 (CH), 63.8, 64.2 ( $\text{CH}_2$ ), 79.0 (C), 126.8, 127.0, 127.2, 128.4 (\*6), 129.0 (\*2), 129.2 (\*2), 129.5 (\*2) (CHar), 140.1, 140.3, 140.7 (Car), 156.3 (C=O).

ESI-MS:  $m/z = 529.35$  [ $\text{M}+\text{H}$ ] $^+$ .

HRMS-ESI:  $m/z =$  calculated for  $\text{C}_{33}\text{H}_{44}\text{N}_4\text{O}_2+\text{H}$ : 529.3537 obtained 529.3528.

**40** *tert*-butyl ((1,4,7-triazacyclononan-2-yl)methyl)carbamate



Compound **39** (3.33 g, 6.30 mmol) was dissolved in a mixture of acetic acid (20 mL), water (20 mL) and THF (60 mL) and 266 mg of 10 % Pd/C (0.25 mmol) were added under  $\text{H}_2$ . After consumption of hydrogen, the mixture was filtered to remove palladium. After evaporation of the solvent, the residue was dissolved in ethanol (100 mL). 5 mL of a 3 M HCl solution were added and the resulting precipitate was filtered after 1 hour, washed with ethanol (20 mL) and dried under vacuum to give a white powder. The resulting precipitate was then dissolved in a 3 M NaOH solution until  $\text{pH} = 12$ . After extraction with chloroform (2\*50 mL), the organic phase was dried over  $\text{MgSO}_4$  and the solvent was evaporated to give **40** as a yellow oil ( $m = 1.30$  g, yield = 80 %).

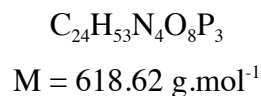
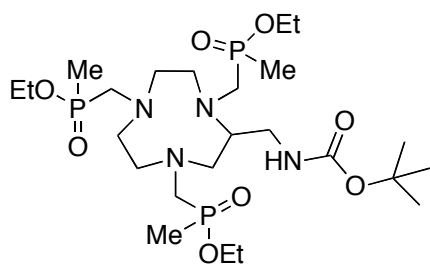
$^1\text{H}$  NMR (300 MHz,  $\text{CDCl}_3$ , 298 K)  $\delta$ (ppm): 1.39 (s, 9H,  $\text{CH}_3$ ), 2.35-3.24 (m, 13H), 4.28-4.55 (m, 3H, NH), 5.83 (s, 1H,  $\text{NHC}=\text{O}$ ).

$^{13}\text{C}\{^1\text{H}\}$  NMR (150 MHz,  $\text{CDCl}_3$ , 298 K)  $\delta$ (ppm): 28.6 (\*3) ( $\text{CH}_3$ ), 43.1, 44.0, 44.6, 45.6, 45.8, 45.9 ( $\text{CH}_2$ ), 46.8 (CH), 79.5 (C), 156.8 (C=O).

ESI-MS:  $m/z = 203.15$  [ $\text{M}-^t\text{Bu}+2\text{H}$ ] $^+$ , 259.15 [ $\text{M}+\text{H}$ ] $^+$ .

HRMS-ESI:  $m/z =$  calculated for  $\text{C}_{12}\text{H}_{26}\text{N}_4\text{O}_2+\text{H}$ : 259.2129 obtained 259.2116.

**41** *tert-butyl((1,4,7-tris((ethoxy(methyl)phosphoryl)methyl)-1,4,7-triazacyclononan-2-yl)ethyl) carbamate*

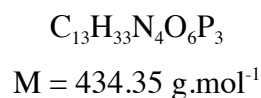
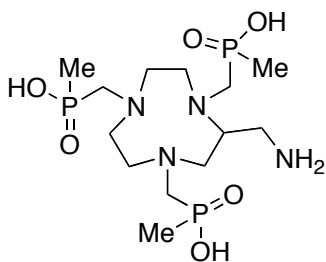


A mixture of **40** (420 mg, 1.12 mmol) and diethoxymethylphosphine (818 mg, 6.01 mmol), was prepared using the phosphine as the solvent. Nitrogen was bubbled into the flask for 5 min, after which the mixture was heated to 80 °C. Paraformaldehyde (189 mg, 6.01 mmol) was added, and the mixture was stirred for 2 h at 80 °C. After cooling to room temperature, water was added and the pH lowered to 5 with a 3 M HCl solution. The solution was washed twice with diethylether (30 mL). The pH was raised to 13 with a 3 M NaOH solution. The aqueous layer was extracted twice with chloroform (2\*50 mL). The organic layers were dried over MgSO<sub>4</sub>. After evaporation of the solvent, the residual oil was purified by flash chromatography (eluent: CH<sub>2</sub>Cl<sub>2</sub>/MeOH 70:30) to give **41** as a yellow oil (m = 360 mg, yield = 58 %).

ESI-MS: m/z = 619.3 [M+H]<sup>+</sup>, 641.3 [M+Na]<sup>+</sup>.

HRMS-ESI: m/z = calculated for C<sub>24</sub>H<sub>53</sub>N<sub>4</sub>O<sub>8</sub>P<sub>3</sub>+Na: 641.2969, obtained 641.2981.

**42** *(2-(aminomethyl)-1,4,7-triazacyclononane-1,4,7-triyl)tris(methylene))tris(methylphosphinic acid)*



10 mL of a 37 % HCl aqueous solution were added on 60 mg of compound **41** (0.10 mmol). The mixture was heated at 90 °C during 2 days. After evaporation, compound **42** (3 HCl) was isolated as a white powder (m = 54.4 mg, yield = 100 %).

<sup>1</sup>H NMR (300 MHz, D<sub>2</sub>O, 298 K) δ(ppm): 1.36 (d, 3H, <sup>2</sup>J = 14.2 Hz, PCH<sub>3</sub>), 1.38 (d, 3H, <sup>2</sup>J = 14.0 Hz, PCH<sub>3</sub>), 1.39 (d, 3H, <sup>2</sup>J = 13.7 Hz, PCH<sub>3</sub>), 2.79-3.54 (m, 19H).

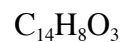
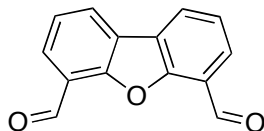
<sup>31</sup>P{<sup>1</sup>H} NMR (202 MHz, D<sub>2</sub>O, 298 K) δ(ppm): 38.4, 45.2, 49.2.

ESI-MS: m/z = 435.17 [M+H]<sup>+</sup>, 457.15 [M+Na]<sup>+</sup>.



HRMS-ESI:  $m/z$  = calculated for  $C_{13}H_{33}N_4O_6P_3+H$ : 435.1686 obtained 435.1696, calculated for  $C_{13}H_{33}N_4O_6P_3+Na$ : 457.1505 obtained 457.1511.

**43** dibenzo[b,d]furan-4,6-dicarbaldehyde



$$M = 224.21 \text{ g}\cdot\text{mol}^{-1}$$

To a solution of dibenzo[b,d]furan (20.0 g, 0.12 mol) in dry heptane (550 mL) was added TMEDA (45 mL, 0.50 mmol), followed by dropwise n-BuLi (91.0 mL, 0.22 M in hexane) at  $-78^\circ\text{C}$  under  $N_2$ . The mixture was stirred at  $-78^\circ\text{C}$  for 2 h and DMF (45 mL, 0.65 mmol) was then added. After 1 h, the mixture was poured into water (500 mL) and stirred at  $0^\circ\text{C}$  for 0.5 h. The resulting precipitate was filtered, washed with water (2\*100 mL) and then recrystallized from toluene to give **43** as yellow crystals ( $m = 14.78$  g, yield = 56 %).

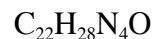
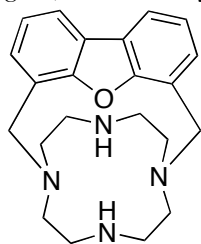
$^1\text{H}$  NMR (300 MHz, DMSO, 300 K)  $\delta$  (ppm): 7.66 (t, 2H,  $J_{\text{app}} = 7.7$  Hz), 8.06 (dd, 2H,  $^3J = 7.5$  Hz,  $^4J = 1.3$  Hz), 8.56 (dd, 2H,  $^3J = 7.5$  Hz,  $^4J = 1.3$  Hz), 10.5 (s, 2H, HC=O).

$^{13}\text{C}\{^1\text{H}\}$  NMR (125 MHz, DMSO, 300 K)  $\delta$  (ppm): 121.2 (Car), 124.1, 127.7, 128.7 (CHar), 155.0 (Car), 188.4 (C=O).

ESI-MS:  $m/z = 247.04$   $[\text{M}+\text{Na}]^+$ .

HRMS-ESI:  $m/z$  = calculated for  $C_{14}H_8O_3+Na$ : 247.0366, obtained 247.0366.

**44** 1,7-crossbridged(4,6-dimethyldibenzofuran)-1,4,7,10-tetraazacyclododecane



$$M = 364.48 \text{ g}\cdot\text{mol}^{-1}$$

A solution of **43** (2.88 g, 12.84 mmol) in 1,2-dichloroethane (40 mL) was added dropwise to a stirred solution of 1,4,7,10-tetraazacyclododecane (cyclen) (2.21 g, 12.84 mmol) and fresh sodium triacetoxyborohydride (7.61 g, 35.92 mmol) in 1,2-dichloroethane (250 mL). The solution was stirred at room temperature under  $N_2$  for 48 h. The reaction mixture was quenched by addition of a 1 M NaOH aqueous solution (300 mL), and the product extracted with chloroform (3\*200 mL). The organic layer was dried over  $MgSO_4$  and concentrated in vacuo. The crude product was washed with cyclohexane to give the compound **44** as a yellow powder ( $m = 3.51$  g, yield = 75 %).

$^1\text{H}$  NMR (500 MHz,  $\text{CDCl}_3$ , 300 K)  $\delta$  (ppm): 2.50 (bs, 2H, NH), 2.53 (m, 8H), 2.64 (m, 8H), 4.00 (s, 4H,  $\text{CH}_2$ bridge), 7.18 (m, 4H), 7.79 (m, 2H).

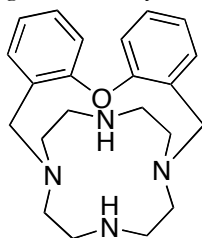
$^{13}\text{C}\{^1\text{H}\}$  NMR (125 MHz,  $\text{CDCl}_3$ , 300 K)  $\delta$  (ppm): 47.9 (\*4), 53.0 (\*4), 58.6 (\*2) ( $\text{CH}_2$ ), 120.9 (\*2), 123.1 (\*2) (CHar), 124.4 (\*2) (Car), 125.5 (\*2), 128.7 (\*2) (CHar), 154.8 (\*2) (Car).

MALDI-TOF:  $m/z = 364.9$   $[\text{M}+\text{H}]^+$ .

HRMS-ESI:  $m/z =$  calculated for  $\text{C}_{22}\text{H}_{28}\text{N}_4\text{O}+\text{H}$ : 365.2335, obtained 365.2346.

Elemental analysis for  $\text{C}_{22}\text{H}_{28}\text{N}_4\text{O}$ . Calculated: C (72.50 %), H (7.74 %), N (15.37 %). Obtained: C (72.3 %), H (7.8 %), N (15.3 %).

**45** *1,7-crossbridged(dibenzylether)-1,4,7,10-tetraazacyclododecane*



$$M = 366.50 \text{ g}\cdot\text{mol}^{-1}$$

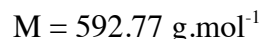
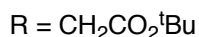
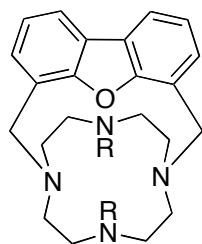
**45** was obtained from cyclen (0.78 g, 4.53 mmol) and bis(2-formylphenyl)ether (1.02 g, 4.53 mmol) in the presence of sodium triacetoxyborohydride (2.69 g, 12.68 mmol) by using the same procedure reported for **44**. The compound **45** was isolated as a white powder ( $m = 1.29$  g, yield = 78 %).

$^1\text{H}$  NMR (500 MHz,  $\text{CDCl}_3$ , 298 K)  $\delta$ (ppm): 2.05 (bs, 2H, NH), 2.45-2.82 (m, 16H), 3.33 (d, 2H,  $^2J = 12.5$  Hz,  $\text{CH}_2$ bridge), 4.13 (d, 2H,  $^2J = 12.5$  Hz,  $\text{CH}_2$ bridge), 6.65 (m, 2H), 6.96 (m, 2H), 7.15 (m, 4H).

$^{13}\text{C}\{^1\text{H}\}$  NMR (125 MHz,  $\text{CDCl}_3$ , 323 K)  $\delta$  (ppm): 48.1 (\*2), 48.4 (\*2), 53.5 (\*2), 55.9 (\*2), 59.2 (\*2) ( $\text{CH}_2$ ), 119.3 (\*2), 123.7 (\*2), 130.0 (\*2) (CHar), 130.9 (\*2) (Car), 132.5 (\*2) (CHar), 157.3 (\*2) (Car).

MALDI-TOF:  $m/z = 367.1$   $[\text{M}+\text{H}]^+$ .

Elemental analysis for  $\text{C}_{22}\text{H}_{30}\text{N}_4\text{O}$ . Calculated: C (72.08 %), H (8.26 %), N (15.29 %). Obtained: C (72.0 %), H (8.3 %), N (15.2 %).

**Compound 46**

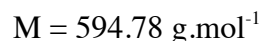
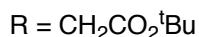
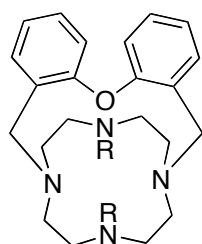
3.51 g of **44** (5.92 mmol) were dissolved in MeCN (350 mL).  $\text{K}_2\text{CO}_3$  (3.93 g, 28.52 mmol) and *tert*-butyl bromoacetate (2.78 g, 14.27 mmol) were then added, and the reaction was heated to 40 °C for 4 h. After cooling, impurities were removed by filtration, and the filtrate was evaporated under reduced pressure. Residual solvent was removed under high vacuum, and the product was triturated with diethyl ether to give the compound **46** as a yellow oil ( $m = 2.19$  g, yield = 91 %).

$^1\text{H}$  NMR (600 MHz,  $\text{CDCl}_3$ , 323 K)  $\delta$ (ppm): 1.26 (s, 18H,  $\text{CH}_3$ ), 2.68-2.71 (m, 4H), 2.88-2.94 (m, 8H), 3.01-3.05 (m, 4H), 3.14-3.18 (m, 4H), 4.67 (s, 4H), 7.33 (t, 2H,  $^3J = 7.5$  Hz), 7.51 (d, 2H,  $^3J = 7.5$  Hz), 7.92 (d, 2H,  $^3J = 7.5$  Hz), 8.52 (bs, 1H,  $\text{N}^+\text{-H}$ ).

$^{13}\text{C}\{^1\text{H}\}$  NMR (125 MHz,  $\text{CDCl}_3$ , 323 K)  $\delta$  (ppm): 27.9 (\*6), 51.8 (\*4), 53.1 (\*4), 57.8 (\*4) ( $\text{CH}_2$ ), 81.9 (\*2) (C), 119.6 (\*2), 121.5 (\*2), 123.7 (\*2) (CHar), 123.9 (\*2) (Car), 128.9 (\*2) (CHar), 158.8 (\*2) (Car), 168.8 (\*2) (C=O).

ESI-MS:  $m/z = 537.3$  [ $\text{M}+2\text{H}-^t\text{Bu}$ ] $^+$ , 593.4 [ $\text{M}+\text{H}$ ] $^+$ .

HRMS-ESI:  $m/z =$  calculated for  $\text{C}_{34}\text{H}_{48}\text{N}_4\text{O}_5+\text{H}$ : 593.3698, obtained 593.3680.

**Compound 47**

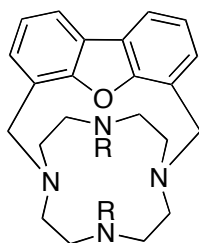
The compound **45** (1.0 g, 2.73 mmol) was dissolved in MeCN (150mL).  $\text{K}_2\text{CO}_3$  (1.51 g, 10.92 mmol) and *tert*-butyl bromoacetate (1.17 g, 6.01 mmol) were then added, and the reaction was heated to 40 °C for 4 h. After cooling, impurities were removed by filtration, and the filtrate was evaporated under reduced pressure. Residual solvent was removed under high vacuum, and the product was triturated with diethyl ether to give the compound **47** as a yellow oil ( $m = 1.20$  g, yield = 74 %).

$^1\text{H}$  NMR (600 MHz,  $\text{CDCl}_3$ , 298 K)  $\delta$ (ppm): 1.36 (s, 18H,  $\text{CH}_3$ ), 2.74 (m, 4H), 2.78-2.92 (m, 8H), 2.98-3.24 (m, 8H), 4.25 (s, 4H), 6.78 (d, 2H,  $^3J = 7.7$  Hz), 7.14 (t, 2H,  $^3J = 7.7$  Hz), 7.29 (t, 2H,  $^3J = 7.7$  Hz), 7.60 (d, 2H,  $^3J = 7.7$  Hz), 8.55 (bs,  $\text{N}^+\text{-H}$ ).

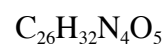
$^{13}\text{C}\{^1\text{H}\}$  NMR (75 MHz,  $\text{CDCl}_3$ , 300 K)  $\delta$  (ppm): 28.1 (\*6) ( $\text{CH}_3$ ), 47.9 (\*4), 52.7 (\*4), 54.4 (\*2), 54.9 (\*2) ( $\text{CH}_2$ ), 81.7 (\*2) (C), 116.9 (\*2), 124.1 (\*2), 125.1 (\*2) (CHar), 130.6 (\*2) (Car), 133.7 (\*2) (CHar), 154.7 (\*2) (Car), 169.5 (\*2) (C=O).

ESI-MS:  $m/z = 595.4$  [ $\text{M}+\text{H}$ ] $^+$ .

### Compound 48



R =  $\text{CH}_2\text{CO}_2\text{H}$



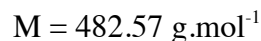
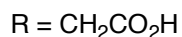
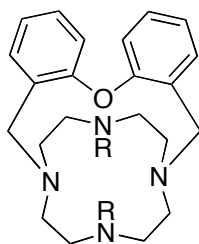
M =  $480.56 \text{ g}\cdot\text{mol}^{-1}$

2.19 g of compound **46** were dissolved in 15 mL of a 37 % HCl solution. The reaction mixture was stirred at room temperature for 10 min. Chlorhydric acid was then evaporated off, the remaining oil was dissolved in acetone, and the desired product slowly precipitated. After removal of trace solvents under high vacuum, the compound **48**•HBr•HCl•2H<sub>2</sub>O was obtained as a white solid (m = 1.49 g, yield = 67 %).

$^1\text{H}$  NMR (600 MHz,  $\text{D}_2\text{O}$ , 363 K, pD = 14)  $\delta$ (ppm): 2.52-2.56 (m, 4H), 2.63-2.71 (m, 8H), 2.98-3.02 (m, 4H), 3.12-3.17 (s, 4H), 3.74 (s, 4H), 7.31-7.32 (m, 2H), 7.34-7.36 (m, 2H), 7.90-7.92 (m, 2H).

ESI-MS:  $m/z = 481.2$  [ $\text{M}+\text{H}$ ] $^+$ , 503.2 [ $\text{M}+\text{Na}$ ] $^+$ .

Elemental analysis:  $\text{C}_{26}\text{H}_{32}\text{N}_4\text{O}_5\cdot\text{HBr}\cdot\text{HCl}\cdot 2\text{H}_2\text{O}$ . Calculated: C (49.26 %), H (6.04 %), N (8.84 %). Obtained: C (49.60 %), H (6.10 %), N (8.93 %).

**Compound 49**

1.20 g of compound **47** was dissolved in a 37 % HCl solution. The reaction mixture was stirred at room temperature for 10 min. Chlorhydric acid was then evaporated off, the remaining oil was dissolved in acetone, and the desired product slowly precipitated. After removal of trace solvents under high vacuum, the compound **49**•HBr•HCl•0.5H<sub>2</sub>O was obtained as a white solid (m = 1.12 g, yield = 80 %).

<sup>1</sup>H NMR (600 MHz, D<sub>2</sub>O, 363 K, pD = 14) δ(ppm): 3.33 (bs, 4H), 3.37-3.41 (m, 8H), 3.45-3.49 (m, 4H), 3.54-3.60 (m, 4H), 4.52 (s, 4H), 7.47 (d, 2H, <sup>3</sup>J = 7.7 Hz), 7.86 (t, 2H, <sup>3</sup>J = 7.7 Hz), 8.06 (t, 2H, <sup>3</sup>J = 7.7 Hz), 8.08 (d, 2H, <sup>3</sup>J = 7.7 Hz).

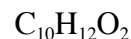
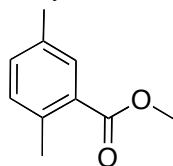
<sup>13</sup>C{<sup>1</sup>H} NMR (150 MHz, D<sub>2</sub>O, 363 K, pD = 14): 48.6 (\*4), 53.5 (\*4), 55.7 (\*2), 56.8 (\*2) (CH<sub>2</sub>), 118.0 (\*2), 124.7 (\*2), 126.4 (\*2) (CHar), 131.4 (\*2) (Car), 133.9 (\*2) (CHar), 155.6 (\*2) (Car), 179.2 (\*2) (C=O).

ESI-MS: m/z = 483.3 [M+H]<sup>+</sup>.

Elemental analysis for C<sub>26</sub>H<sub>34</sub>N<sub>4</sub>•HBr•HCl•0.5H<sub>2</sub>O. Calculated: C (51.07 %), H (5.87 %), N (9.12 %). Obtained: C (51.28 %), H (6.12 %), N (9.20 %).

### III. Experimental part Chapter III

#### 52 methyl-2,5-dimethylbenzoate <sup>261</sup>



$$M = 164.20 \text{ g}\cdot\text{mol}^{-1}$$

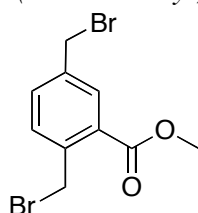
A mixture of 2,5-dimethylbenzoic acid (10.0 g, 66.6 mmol) and sulphuric acid (14 mL, 13.3 mmol) was refluxed in methanol (27 mL) for 4 h. The mixture was poured into water (250 mL) and extracted with ethyl acetate (2\*200 mL). The pooled organics were washed with saturated sodium bicarbonate (2\*50 mL) and brine (50 mL), dried over  $\text{MgSO}_4$ , and concentrated in vacuo to give **52** (m = 10.1 g, yield = 92 %) as a colorless oil.

$^1\text{H}$  NMR (300 MHz,  $\text{CDCl}_3$ , 300 K)  $\delta$  (ppm): 2.34 (s, 3H,  $\text{CH}_3$ ), 2.56 (s, 3H,  $\text{CH}_3$ ), 3.88 (s, 3H,  $\text{OCH}_3$ ), 7.12 (d, 1H,  $^3\text{J} = 7.8$  Hz, CHar), 7.24 (dd, 1H,  $^3\text{J} = 7.8$  Hz,  $^4\text{J} = 1.7$  Hz, CHar), 7.70 (d, 1H,  $^4\text{J} = 1.7$  Hz, CHar).

$^{13}\text{C}\{^1\text{H}\}$  NMR (150 MHz,  $\text{CDCl}_3$ , 300 K)  $\delta$ (ppm): 20.9, 21.4 ( $\text{CH}_3$ ), 51.9 ( $\text{OCH}_3$ ), 129.6 (Car), 131.2, 131.8, 132.9 (CHar), 135.4, 137.2 (Car), 168.4 (C=O).

ESI-MS:  $m/z = 165.31$  [ $\text{M}+\text{H}$ ] $^+$ .

#### 53 methyl-2,5-bis(bromomethyl)benzoate



$$M = 321.99 \text{ g}\cdot\text{mol}^{-1}$$

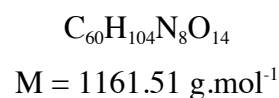
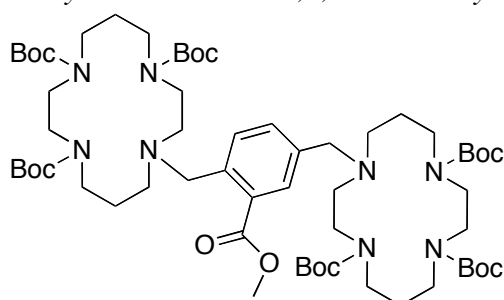
To a solution of **52** (10.1 g, 61.6 mmol) in carbon tetrachloride (300 mL) were added *N*-bromosuccinimide (23.0 g, 129.3 mmol) and benzoyl peroxide (1.0 g, 4.1 mmol). The reaction mixture was heated at reflux for 4 h. The resulting suspension was filtered, and the residue was washed with chloroform (3\*150 mL). The pooled organics were concentrated in vacuo to give a mixture of product and succinimide as determined by  $^1\text{H}$  NMR. The mixture was dissolved in dichloromethane (600 mL) and washed with water (3\*150 mL). The organic phase was dried over  $\text{MgSO}_4$  and concentrated in vacuo, and the resulting residue was purified by reverse phase flash chromatography on C18 (A:  $\text{H}_2\text{O}$ , B:  $\text{CH}_3\text{CN}$ , B 35 %  $\rightarrow$  60 %). After evaporation of acetonitrile, the aqueous solution was freeze dried to give **53** (13.9 g, yield = 70 %) as a white solid.

$^1\text{H}$  NMR (300 MHz,  $\text{CDCl}_3$ , 300 K)  $\delta$ (ppm): 3.98 (s, 3H,  $\text{OCH}_3$ ), 4.49 (s, 2H,  $\text{CH}_2$ ), 4.94 (s, 2H,  $\text{CH}_2$ ), 7.46 (d, 1H,  $^3\text{J} = 7.8$  Hz,  $\text{CHar}$ ), 7.53 (dd, 1H,  $^3\text{J} = 7.8$  Hz,  $^2\text{J} = 1.8$  Hz,  $\text{CHar}$ ), 8.00 (d, 1H,  $^4\text{J} = 1.8$  Hz,  $\text{CHar}$ ).

$^{13}\text{C}\{^1\text{H}\}$  NMR (125 MHz,  $\text{CDCl}_3$ , 300 K)  $\delta$ (ppm): 31.0, 32.0 ( $\text{CH}_2$ ), 52.6 ( $\text{CH}_3$ ), 129.7 ( $\text{Car}$ ), 132.0, 132.5, 133.2 ( $\text{CHar}$ ), 138.5, 139.6 ( $\text{Car}$ ), 166.6 ( $\text{C=O}$ ).

ESI-MS:  $m/z = 322.54$   $[\text{M}+\text{H}]^+$ .

**54** hexa-*tert*-butyl-11,11'-((2-(methoxycarbonyl)-1,4-phenylene)bis(methylene))bis(1,4,8,11-tetraazacyclotetradecane-1,4,8-tricarboxylate)



To a solution of tri-*tert*-butyl 1,4,8,11-tetraazacyclotetradecane-1,4,8-tricarboxylate (2.00 g, 3.98 mmol) in acetonitrile (20 mL) was added  $\text{K}_2\text{CO}_3$  (1.38 g, 9.99 mmol) and compound **53** (0.63 g, 1.99 mmol). The reaction mixture was heated at 40 °C overnight. After cooling, the solution was filtered on celite. The solvent was evaporated and the resulting oil was taken up in 200 mL of diethylether, washed with 2\*50 mL of water, dried over  $\text{MgSO}_4$  and concentrated in vacuo. The resulting residue was purified by flash chromatography (eluent  $\text{CH}_2\text{Cl}_2/\text{MeOH}$  65:35) to give **54** ( $m = 1.89$  g, yield = 82 %, Mp: 89 +/- 1 °C) as a white foam.

$^1\text{H}$  NMR (300 MHz,  $\text{CDCl}_3$ , 300 K)  $\delta$ (ppm): 1.32-1.43 (m, 54H,  $\text{CH}_3$ ), 1.58-1.68 (m, 4H,  $\text{CH}_2\beta$ ), 1.77-1.89 (m, 4H,  $\text{CH}_2\beta$ ), 2.16 (s, 1H), 2.29-2.36 (m, 4H), 2.53-2.62 (m, 4H), 3.14-3.35 (m, 23H), 3.49 (s, 2H), 3.79 (s, 2H), 3.82 (s, 3H,  $\text{OCH}_3$ ), 7.29 (d, 1H,  $^3\text{J} = 7.8$  Hz,  $\text{CHar}$ ), 7.41 (d, 1H,  $^3\text{J} = 7.8$  Hz,  $\text{CHar}$ ), 7.64 (s, 1H,  $\text{CHar}$ ).

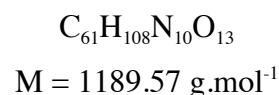
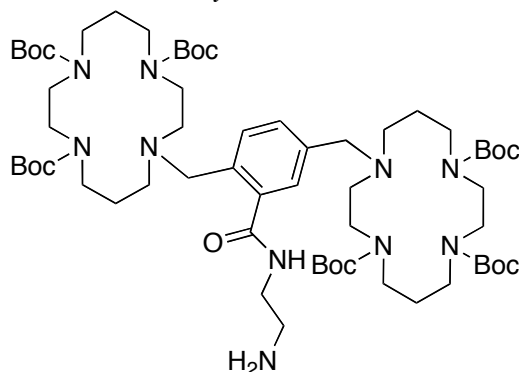
$^{13}\text{C}\{^1\text{H}\}$  NMR (125 MHz, DMSO, 343 K)  $\delta$ (ppm): 25.6 (\*2), 25.9 (\*2) ( $\text{CH}_2\beta$ ), 27.6 (\*3), 27.7 (\*3), 27.8 (\*12) ( $\text{CH}_3$ ), 45.4, 45.5, 45.7, 45.8, 45.9 (\*2), 46.0, 46.2, 46.5(\*3), 46.6, 46.7, 51.1, 51.3, 52.5, 52.7, 56.2, 57.8 ( $\text{CH}_2+\text{CH}_3$ ), 78.0 (\*2), 78.1, 78.2, 78.3, 78.4 (C), 129.6, 129.7, 130.3 ( $\text{CHar}$ ), 131.3, 137.5, 138.1 ( $\text{Car}$ ), 154.2, 154.3 (\*2), 154.4, 154.5 (\*2), 167.4 ( $\text{C=O}$ ).

ESI-MS:  $m/z = 1183.76$   $[\text{M}+\text{Na}]^+$ , 1199.73  $[\text{M}+\text{K}]^+$ .

HRMS-ESI:  $m/z =$  calculated for  $\text{C}_{60}\text{H}_{104}\text{N}_8\text{O}_{14}+\text{Na}$ : 1183.7571, obtained 1183.7564.

Elemental analysis for  $C_{60}H_{104}N_8O_{14}$ . Calculated : C (62.04 %), H (9.02 %), N (9.65 %). Obtained : C (61.62 %), H (8.98 %), N (9.55 %).

**55** hexa-*tert*-butyl-11,11'-((2-((2-aminoethyl)carbamoyl)-1,4-phenylene)bis(methylene))bis(1,4,8,11 - tetraazacyclotetradecane-1,4,8-tricarboxylate)



1.89 g of compound **54** (1.63 mmol) was dissolved in 6.5 mL of distilled ethylenediamine (30 eq.). The mixture was stirred at 40 °C for 7 days. The mixture was concentrated by evaporation and the resulting oil was taken up in acetone (200 mL). After filtration, the pooled organics were concentrated in vacuo to give a yellow foam. The resulting residue was purified by flash chromatography on silica gel (eluent  $CH_2Cl_2/MeOH$  75:15) to furnish **55** (m = 0.77 g, yield = 40 %, Mp: 98 +/- 1 °C) as a white foam.

$^1H$  NMR (500 MHz,  $CDCl_3$ , 324 K)  $\delta$ (ppm): 1.29-1.39 (m, 18H,  $CH_3$ ), 1.43-1.47 (m, 36H,  $CH_3$ ), 1.70-1.75 (m, 4H,  $CH_2\beta$ ), 1.83-1.92 (m, 4H,  $CH_2\beta$ ), 2.06-2.16 (m, 2H), 2.44 (t, 2H,  $^3J = 5.7$  Hz), 2.51 (t, 2H,  $^3J = 6.5$  Hz), 2.60-2.64 (m, 2H), 2.71 (t, 2H,  $^3J = 6.5$  Hz), 2.97 (t, 2H,  $^3J = 6.0$  Hz,  $CH_2NH_2$ ), 3.26-3.29 (m, 24H), 3.50 (q, 2H,  $^3J = 6.0$  Hz,  $CH_2NHC=O$ ), 3.54 (s, 2H,  $CH_2Ph$ ), 3.68 (s, 2H,  $CH_2Ph$ ), 7.20 (d, 1H,  $^3J = 7.3$  Hz,  $CHar$ ), 7.25 (d, 1H,  $^3J = 7.3$  Hz,  $CHar$ ), 7.49 (s, 1H,  $CHar$ ), 8.17 (bs, 1H,  $NHC=O$ ).

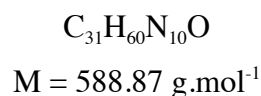
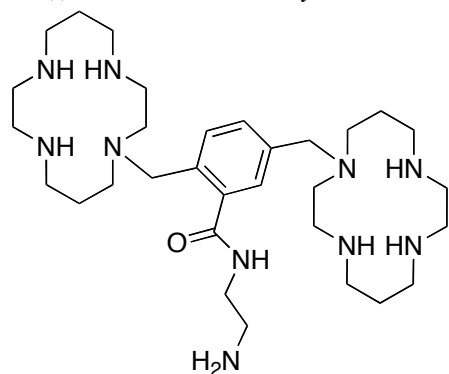
$^{13}C\{^1H\}$  NMR (125 MHz,  $CDCl_3$ , 324 K)  $\delta$ (ppm): 26.1 (\*2), 27.2 (\*2) ( $CH_2\beta$ ), 28.6 (\*3), 28.7 (\*3), 28.8 (\*9), 28.9 (\*3) ( $CH_3$ ), 42.1 (\*2), 43.1 (\*2), 46.5, 46.9, 47.3 (\*2), 47.5, 48.0, 48.1 (\*2), 50.9, 51.1, 52.1, 52.4, 52.5, 53.5, 58.0, 59.6 ( $CH_2$ ) 79.6, 79.7, 79.8, 79.9, 80.0, 80.1 (C), 129.3, 130.5, 131.2 ( $CHar$ ), 135.1, 137.4, 138.7 (Car), 155.7 (\*2), 155.9, 156.0 (\*2), 156.1, 167.4 (C=O).

ESI-MS:  $m/z = 1189.82$  [ $M+H$ ] $^+$ .

HRMS-ESI:  $m/z =$  calculated for  $C_{61}H_{108}N_{10}O_{13}+H$ : 1189.8170, obtained 1189.8212.

Elemental analysis for  $C_{61}H_{108}N_{10}O_{13}$ . Calculated : C (61.59 %), H (9.15 %), N (11.77 %). Obtained : C (61.17 %), H (9.43 %), N (11.51 %).



**56** 2,5-bis((1,4,8,11-tetraazacyclotetradecan-1-yl)methyl)-N-(2-aminoethyl)benzamide

0.47 g (0.40 mmol) of compound **55** was dissolved in 10 mL of 35 % solution of HCl. The mixture was stirred for 30 min at room temperature. The resulting solution was evaporated, taken up in 50 mL of acetone and then stirred overnight. The precipitate, which was formed, was filtered, washed with acetone (30 mL) and diethylether (30 mL) and finally dried in vacuo to yield compound **56**•9 HCl•5 H<sub>2</sub>O as a white solid (m = 0.40 g, yield = 99 %).

<sup>1</sup>H NMR (300 MHz, D<sub>2</sub>O, 300 K) δ(ppm): 2.16-2.27 (m, 8H, CH<sub>2</sub>β), 3.14-3.18 (m, 2H), 3.34-3.67 (m, 32H, CH<sub>2</sub>α), 3.78-3.82 (m, 2H), 4.29 (s, 2H, CH<sub>2</sub>Ph), 4.51 (s, 2H, CH<sub>2</sub>Ph), 7.74-7.81 (m, 2H), 7.91-7.93 (s, 1H).

<sup>13</sup>C{<sup>1</sup>H} NMR (75 MHz, D<sub>2</sub>O, 300 K) δ(ppm): 18.5, 18.8, 19.2, 19.3 (CH<sub>2</sub>β), 37.6, 37.7, 37.8, 38.1, 38.5, 38.7, 38.9, 41.0, 41.2, 41.7, 41.8, 42.1, 45.0, 45.3, 45.6, 47.8, 47.9, 48.4, 57.5, 58.1 (CH<sub>2</sub>), 130.2, 131.6, 133.4 (Car), 134.4, 134.5, 135.7 (CHar), 171.0 (C=O).

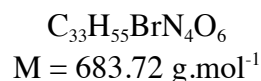
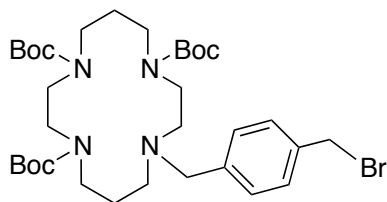
HRMS-ESI: m/z = calculated for C<sub>31</sub>H<sub>60</sub>N<sub>10</sub>O+H: 589.5024, obtained 589.5034.

Elemental analysis for C<sub>31</sub>H<sub>61</sub>N<sub>10</sub>O•9HCl•5H<sub>2</sub>O. Calculated : C (36.97 %), H (7.91 %), N (13.91 %). Obtained : C (37.13 %), H (8.06 %), N (14.33 %).

The white solid was dissolved in a 8 M solution of NaOH. After extraction of the deprotonated species with chloroform (2\*100 mL), the organic layer is dried over MgSO<sub>4</sub> and evaporated. Compound **56** was obtained as a yellow oil (m = 0.15 g, yield = 63 %).

<sup>1</sup>H NMR (300 MHz, CDCl<sub>3</sub>, 300 K) δ(ppm): 1.52-1.60 (m, 4H, CH<sub>2</sub>β), 1.67-1.80 (m, 4H, CH<sub>2</sub>β), 2.26-2.68 (m, 40H), 2.76 (t, 2H, <sup>3</sup>J = 6.1 Hz, CH<sub>2</sub>NH<sub>2</sub>), 3.32 (q, 2H, <sup>3</sup>J = 6.1 Hz, CH<sub>2</sub>NHC=O), 3.37 (s, 2H, CH<sub>2</sub>Ph), 3.51 (s, 2H, CH<sub>2</sub>Ph), 7.12 (dd, 1H, <sup>3</sup>J = 7.8 Hz, <sup>4</sup>J = 1.7 Hz), 7.37 (d, 1H, <sup>4</sup>J = 1.7 Hz), 7.41 (d, 1H, <sup>3</sup>J = 7.8 Hz), 8.64 (t, 1H, NHC=O).

<sup>13</sup>C{<sup>1</sup>H} NMR (75 MHz, CDCl<sub>3</sub>, 300 K) δ(ppm): 26.1, 26.5, 28.4, 28.6 (CH<sub>2</sub>β), 41.9, 43.1, 47.3, 47.7, 47.8, 48.2, 48.3, 48.5, 48.6, 48.7, 49.1, 49.3, 50.5, 50.9, 53.2, 53.3, 54.2, 54.6 (CH<sub>2</sub>), 55.8, 57.9 (CH<sub>2</sub>Ph), 128.0, 130.4, 130.6 (CHar), 135.7, 137.6, 137.9 (Car), 140.5 (C=O).

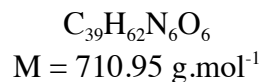
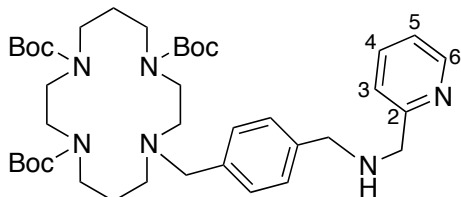
**Compound 57**

Potassium carbonate (3.6 g, 26.0 mmol) was added to a stirred solution of *p*-xylene dibromide (26.4 g, 100.0 mmol) in acetonitrile (200 mL). The solution was heated under reflux (70 °C) and a solution of triBoccyclam (10.0 g, 20.1 mmol) in acetonitrile (100 mL) was added dropwise. After the addition, the mixture was stirred at 70 °C for 4 h. The solvent was evaporated in vacuo and the resulting product was dissolved in dichloromethane (150 mL), washed with water (100 mL), brine (100 mL) and one more time with water (100 mL). The organic fractions were dried over magnesium sulfate and concentrated. The excess of *p*-xylene dibromide was extracted by recrystallization in acetonitrile. Purification by inverse phase flash chromatography on C18 (A: H<sub>2</sub>O, B: CH<sub>3</sub>CN, B 80 % → 100 %) gave **57** as a white foam (7.26 g, yield = 53 %).

<sup>1</sup>H NMR (300 MHz, CDCl<sub>3</sub>, 300 K) δ (ppm): 1.24-1.45 (m, 27H, CH<sub>3</sub>), 1.60-1.74 (m, 2H, CH<sub>2</sub>β), 1.80-1.94 (m, 2H, CH<sub>2</sub>β), 2.30-2.42 (m, 2H), 2.51-2.65 (m, 2H), 3.11-3.38 (m, 12H), 3.46 (s, 2H, CH<sub>2</sub>Ph), 4.40 (s, 2H, CH<sub>2</sub>Br), 7.17 (d, 2H, <sup>3</sup>J = 8.5 Hz, CHar), 7.25 (d, 2H, <sup>3</sup>J = 8.5 Hz, CHar).

HRMS-ESI: *m/z* = calculated for C<sub>33</sub>H<sub>55</sub>BrN<sub>4</sub>O<sub>6</sub> + H: 683.3378, obtained 683.3344.

Elemental analysis for C<sub>33</sub>H<sub>55</sub>BrN<sub>4</sub>O<sub>6</sub>•1.5H<sub>2</sub>O. Calculated : C (55.77 %), H (8.23 %), N (7.88 %). Obtained : C (55.94 %), H (8.14 %), N (8.05 %).

**Compound 58**

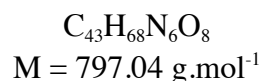
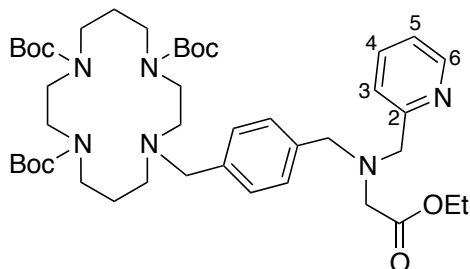
2-Aminomethylpyridine (2.36 mL, 22.95 mmol) was added to a suspension of potassium carbonate (0.95 g, 6.88 mmol) in acetonitrile (250 mL). The reaction mixture was stirred and heated under reflux. Once reflux established, a solution of **57** (3.14 g, 4.56 mmol) in acetonitrile (75 mL) was added dropwise. The resulting mixture was stirred at 80 °C for 4 h and followed by TLC. After completion of the reaction, the solvent was evaporated in vacuo. The product was dissolved in dichloromethane (50 mL), washed with water (3 x 50 mL) and dried over magnesium sulfate. The solvent was evaporated. Purification by flash chromatography on silica gel (A: CH<sub>2</sub>Cl<sub>2</sub>, B: CH<sub>3</sub>OH/CH<sub>2</sub>Cl<sub>2</sub> (10:90), B 0 % → 50 %) gave **58** as a yellow oil (2.38 g, yield = 73 %).

$^1\text{H}$  NMR (300 MHz, DMSO, 300 K)  $\delta$  (ppm): 1.23-1.45 (m, 27H,  $\text{CH}_3$ ), 1.52-1.68 (m, 2H,  $\text{CH}_2\beta$ ), 1.74-1.89 (m, 2H,  $\text{CH}_2\beta$ ), 2.23-2.37 (m, 2H), 3.10-3.19 (m, 2H), 3.21-3.37 (m, 13H), 3.47 (s, 2H,  $\text{CH}_2(1^{\text{IV}})$ ), 3.70 (s, 2H,  $\text{CH}_2(1^{\text{V}})$ ), 3.77 (s, 2H,  $\text{CH}_2(1^{\text{VI}})$ ), 7.17-7.30 (m, 5H,  $\text{CHar}$ ,  $\text{CH}(5)$ ), 7.44 (d, 1H,  $^3\text{J} = 7.7$  Hz,  $\text{CH}(3)$ ), 7.74 (td, 1H,  $^3\text{J} = 7.7$  Hz,  $^4\text{J} = 1.8$  Hz,  $\text{CH}(4)$ ), 8.45-8.51 (m, 1H,  $\text{CH}(6)$ ).

HRMS-ESI:  $m/z$  = calculated for  $\text{C}_{39}\text{H}_{62}\text{N}_6\text{O}_6 + \text{H}$ : 711.4804, obtained 711.4788.

Elemental analysis for  $\text{C}_{39}\text{H}_{62}\text{N}_6\text{O}_6 \cdot 1.5\text{H}_2\text{O}$ . Calculated : C (63.47 %), H (8.88 %), N (11.39 %).  
Obtained : C (63.54 %), H (8.85 %), N (11.32 %).

### Compound 59

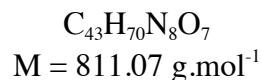
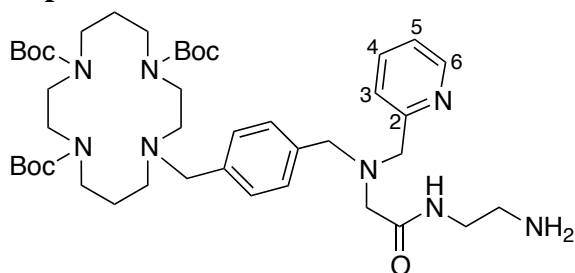


To a stirred solution of **58** (2.38 g, 3.34 mmol) in acetonitrile (35 mL) were added subsequently potassium carbonate (1.85 g, 13.36 mmol) and bromoethyl acetate (0.37 mL, 3.34 mmol). The reaction was stirred at 40 °C for one night. The suspension was filtered on a celite bed and the cake was washed with acetonitrile (100 mL). After evaporation of the solvent in vacuo, the crude was purified by flash chromatography on silica gel (A:  $\text{CH}_2\text{Cl}_2$ , B:  $\text{C}_2\text{H}_5\text{OH}$ , B 50 %) to give **59** (2.38 g, yield = 91 %) as a yellow oil.

$^1\text{H}$  NMR (300 MHz, DMSO, 300 K)  $\delta$  (ppm): 1.17 (t, 3H,  $^3\text{J} = 7.0$  Hz,  $\text{CH}_2\text{CH}_3$ ), 1.23-1.44 (m, 27H,  $\text{CH}_3$ ), 1.52-1.67 (m, 2H,  $\text{CH}_2\beta$ ), 1.72-1.88 (m, 2H,  $\text{CH}_2\beta$ ), 2.23-2.39 (m, 2H), 2.48-2.56 (m, 2H), 3.00-3.36 (m, 14H), 3.46 (s, 2H,  $\text{CH}_2\text{Ph}$ ), 3.74 (s, 2H,  $\text{CH}_2\text{Ph}$ ), 3.86 (s, 2H,  $\text{CH}_2\text{Pyr}$ ), 4.07 (q, 2H,  $^3\text{J} = 7.0$  Hz,  $\text{CH}_2\text{CH}_3$ ), 7.16-7.35 (m, 5H,  $\text{CHar}$ ,  $\text{CH}(5)$ ), 7.50 (d, 1H,  $^3\text{J} = 7.4$  Hz,  $\text{CH}(3)$ ), 7.76 (td, 1H,  $^3\text{J} = 7.8$  Hz,  $^4\text{J} = 1.9$  Hz,  $\text{CH}(4)$ ), 8.45-8.49 (m, 1H,  $\text{CH}(6)$ ).

HRMS-ESI:  $m/z$  = calculated for  $\text{C}_{43}\text{H}_{68}\text{N}_6\text{O}_8 + \text{Na}$ : 819.4991, obtained 819.4986.

Elemental analysis for  $\text{C}_{43}\text{H}_{68}\text{N}_6\text{O}_8 \cdot 2.5\text{H}_2\text{O}$ . Calculated : C (61.33 %), H (8.74 %), N (9.98 %).  
Obtained : C (61.58 %), H (9.03 %), N (9.80 %).

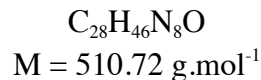
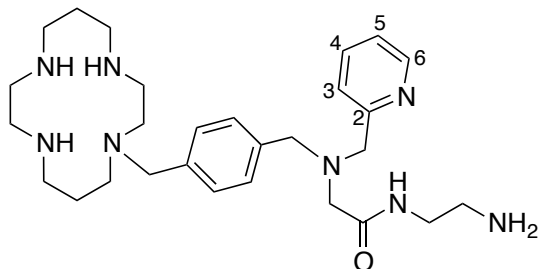
**Compound 60**

**59** (5.88 g, 7.5 mmol) was dissolved in ethylenediamine (30 mL, 450 mmol). The solution was stirred and heated at 60 °C under Ar for one week. After evaporation of the excess of ethylene diamine, the resulting oil was chromatographed on silica gel (A: CH<sub>2</sub>Cl<sub>2</sub>, B: CH<sub>3</sub>OH, B 10 %) several times in order to remove as much as possible the impurities. Finally, flash chromatography on silica gel (A: CH<sub>2</sub>Cl<sub>2</sub>, B: C<sub>2</sub>H<sub>5</sub>OH, B 10 % → 30 %) gave **60** (1.77 g, yield = 29 %) as a yellow oil.

<sup>1</sup>H NMR (300 MHz, CDCl<sub>3</sub>, 300 K) δ(ppm): 1.24-1.44 (m, 27H, CH<sub>3</sub>), 1.56-1.68 (m, 2H, CH<sub>2</sub>β), 1.77-1.91 (m, 2H, CH<sub>2</sub>β), 2.26-2.37 (m, 2H), 2.44-2.63 (m, 4H), 2.81 (t, 2H, J<sub>app</sub> = 5.8 Hz, CH<sub>2</sub>NH<sub>2</sub>), 3.15-3.33 (m, 16H), 3.43 (s, 2H, CH<sub>2</sub>Ph), 3.57 (s, 2H, CH<sub>2</sub>Ph), 3.69 (s, 2H, CH<sub>2</sub>Pyr), 7.10-7.25 (m, 6H, CH<sub>ar</sub>, CH(5), CH(3)), 7.58 (td, 1H, <sup>3</sup>J = 7.6 Hz, <sup>4</sup>J = 1.9 Hz, CH(4)), 8.39 (t, 1H, J<sub>app</sub> = 5.8 Hz, NHC=O), 8.55-8.62 (m, 1H, CH(6)).

HRMS-ESI: *m/z* = calculated for C<sub>43</sub>H<sub>70</sub>N<sub>8</sub>O<sub>7</sub> + Na: 833.5260, obtained 833.5264.

Elemental analysis for C<sub>43</sub>H<sub>70</sub>N<sub>8</sub>O<sub>7</sub>•5H<sub>2</sub>O. Calculated : C (57.31 %), H (8.95 %), N (12.46 %). Obtained : C (57.40 %), H (8.92 %), N (12.25 %).

**Compound 61**

*Route A:* **60** (689.5 mg, 0.850 mmol) was dissolved in dichloromethane (5.3 mL) and trifluoroacetic acid (8.5 mL) was added under argon atmosphere. The reaction mixture was stirred at room temperature for one night. The solvent was evaporated in vacuo. The resulting yellow oil was stirred in diethyl ether for two days until the desired product precipitates. The supernatant was eliminated and the powder was dried in vacuo. Once dry, few drops of NaOH (16 M) were added in order to obtain a viscous solution and chloroform (100 mL) was added quickly. The two layers were

separated and the organic layer was dried over magnesium sulfate. **61** (383.1 mg, yield = 88 %) was obtained as a light yellow oil.

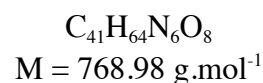
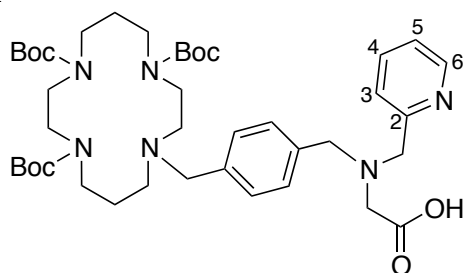
*Route B:* **63** (200.0 mg, 0.22 mmol) was dissolved in dichloromethane (1.4 mL) and trifluoroacetic acid (2.2 mL) was added under argon atmosphere. The reaction mixture was stirred at room temperature for one night. After completion of the reaction, the solvent was evaporated in vacuo. The resulting yellow oil was stirred in diethyl ether for two days until the desired product precipitates. The supernatant was eliminated and the powder was dried in vacuo. Once dry, few drops of NaOH (16 M) were added in order to obtain a viscous solution and chloroform (50 mL) was added quickly. The two layers were separated and the organic layer was dried over magnesium sulfate. **61** (104.3 mg, yield = 93 %) was obtained as a light yellow oil.

$^1\text{H}$  NMR (300 MHz,  $\text{CDCl}_3$ , 300 K)  $\delta$ (ppm): 1.62 (quint, 2H,  $J_{\text{app}} = 5.2$  Hz,  $\text{CH}_2\beta$ ), 1.81 (quint, 2H,  $J_{\text{app}} = 5.5$  Hz,  $\text{CH}_2\beta$ ), 2.90-2.34 (m, 23H), 3.20 (s, 2H), 3.30 (q, 2H,  $J_{\text{app}} = 5.9$  Hz,  $\text{CH}_2\text{NHC=O}$ ), 3.52 (s, 2H,  $\text{CH}_2\text{Ph}$ ), 3.62 (s, 2H,  $\text{CH}_2\text{Ph}$ ), 3.74 (s, 2H,  $\text{CH}_2\text{Pyr}$ ), 7.28-7.14 (m, 6H,  $\text{CHar}$ ,  $\text{CH}(3)$ ,  $\text{CH}(5)$ ), 7.61 (td, 1H,  $^3J = 7.7$  Hz,  $^4J = 1.7$  Hz,  $\text{CH}(4)$ ), 8.37 (t, 1H,  $J_{\text{app}} = 5.7$  Hz,  $\text{NHC=O}$ ), 8.56-8.62 (m, 1H,  $\text{CH}(6)$ ).

$^{13}\text{C}\{^1\text{H}\}$  NMR (150 MHz,  $\text{CDCl}_3$ , 300 K)  $\delta$ (ppm): 26.0 ( $\text{CH}_2\beta$ ), 28.1 ( $\text{CH}_2\beta$ ), 41.8 ( $\text{CH}_2\text{NH}_2$ ), 42.3 ( $\text{CH}_2\text{NHC=O}$ ), 47.3, 47.7, 48.8, 49.0, 49.3, 50.6, 53.2, 54.3, 57.5 ( $\text{CH}_2$ ), 57.6 ( $\text{CH}_2\text{Ph}$ ), 58.6 ( $\text{CH}_2\text{Ph}$ ), 60.6 ( $\text{CH}_2\text{Pyr}$ ), 122.5, 123.3 ( $\text{CHar}_{\text{pyr}}$ ), 128.8 (\*2) ( $\text{CHar}$ ), 129.4 (\*2) ( $\text{CHar}$ ), 136.5 (\*2) ( $\text{CHar}_{\text{pyr}}$ ,  $\text{Car}$ ), 138.0 ( $\text{Car}$ ), 149.7 ( $\text{CHar}_{\text{pyr}}$ ), 158.4 ( $\text{Car}_{\text{pyr}}$ ), 171.4 ( $\text{C=O}$ ).

HRMS-ESI:  $m/z$  = calculated for  $\text{C}_{28}\text{H}_{46}\text{N}_8\text{O} + \text{H}$ : 511.3867, obtained 511.3862.

## Compound 62



**59** (1.43 g, 1.8 mmol) was dissolved in ethanol (13.8 mL) and a solution of NaOH (1M) (3.6 mL, 3.6 mmol) was added. The reaction mixture was stirred during one night. After evaporation of ethanol, the resulting product was dissolved in water (200 mL) and washed with diethyl ether (100 mL). Then, the aqueous layer was acidified progressively until pH 1 and the desired product was extracted with chloroform (3\*100 mL). **62** (1.04 g, yield = 75 %) was obtained as a yellow oil.

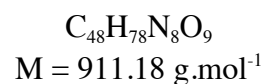
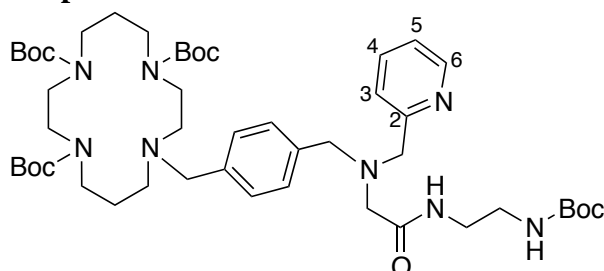
$^1\text{H}$  NMR (300 MHz,  $\text{CDCl}_3$ , 300 K)  $\delta$ (ppm): 1.26-1.48 (m, 27H,  $\text{CH}_3$ ), 1.57-1.70 (m, 2H,  $\text{CH}_2\beta$ ), 1.79-1.93 (m, 2H,  $\text{CH}_2\beta$ ), 2.28-2.41 (m, 2H), 2.48-2.66 (m, 2H), 3.13-3.41 (m, 12H), 3.47 (s, 4H),

3.82 (s, 2H, CH<sub>2</sub>Ph), 3.97 (s, 2H, CH<sub>2</sub>Pyr), 7.10-7.20 (m, 6H, CH<sub>ar</sub>, CH(5), CH(3)), 7.66 (td, 1H, <sup>3</sup>J = 7.6 Hz, <sup>4</sup>J = 1.8 Hz, CH(4)), 8.53-8.59 (m, 1H, CH(6)).

HRMS-ESI:  $m/z$  = calculated for C<sub>41</sub>H<sub>64</sub>N<sub>6</sub>O<sub>8</sub> + H: 769.4858, obtained 769.4870.

Elemental analysis for C<sub>41</sub>H<sub>64</sub>N<sub>6</sub>O<sub>8</sub>•2C<sub>2</sub>H<sub>5</sub>OH. Calculated : C (62.77 %), H (8.90 %), N (9.76 %).  
Obtained : C (62.87 %), H (8.50 %), N (9.68 %).

### Compound 63



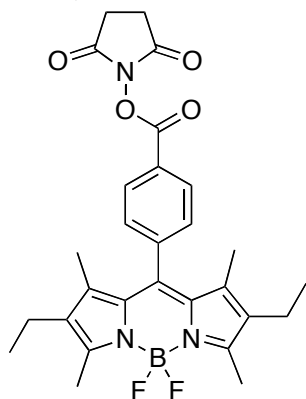
*tert*-Butyl (2-aminoethyl)carbamate (229.1 mg, 1.43 mmol), HBtu (519.6 mg, 1.37 mmol), HOBT (185.1 mg, 1.85 mmol) and *N,N*-diisopropylethylamine (339.8  $\mu\text{L}$ , 1.95 mmol) were added to a solution of **62** (1.00 g, 1.30 mmol) in dichloromethane (65 mL) under argon atmosphere. The reaction mixture was stirred for 4 hours. Dichloromethane and *N,N*-diisopropylethylamine were evaporated in vacuo. The resulting product was dissolved in dichloromethane (200 mL) and washed with a citric acid solution (2.2M) (100 mL), a saturated solution of sodium bicarbonate (100 mL) and finally water (100 mL). The organic layer was dried on magnesium sulfate and evaporated in vacuo. Flash chromatography (A: CH<sub>2</sub>Cl<sub>2</sub>, B: C<sub>2</sub>H<sub>5</sub>OH, B 10 %) gave **63** (0.73 g, yield = 62 %) as a light yellow foam.

<sup>1</sup>H NMR (300 MHz, CDCl<sub>3</sub>, 300 K)  $\delta$ (ppm): 1.25-1.46 (m, 36H, CH<sub>3</sub>), 1.55-1.68 (m, 2H, CH<sub>2</sub> $\beta$ ), 1.76-1.91 (m, 2H, CH<sub>2</sub> $\beta$ ), 2.24-2.38 (m, 2H), 2.47-2.61 (m, 2H), 3.06-3.42 (m, 18H), 3.46 (s, 2H, CH<sub>2</sub>Ph), 3.57 (s, 2H, CH<sub>2</sub>Ph), 3.69 (s, 2H, CH<sub>2</sub>Pyr), 5.77 (t, 1H,  $J_{\text{app}} = 5.7$  Hz, NHBoc), 7.00-7.20 (m, 6H, CH<sub>ar</sub>, CH(5), CH(3)), 7.63 (td, 1H, <sup>3</sup>J = 7.6 Hz, <sup>4</sup>J = 1.6 Hz, CH(4)), 8.43 (t, 1H,  $J_{\text{app}} = 5.8$  Hz, NHC=O), 8.63-8.74 (m, 1H, CH(6)).

HRMS-ESI:  $m/z$  = calculated for C<sub>48</sub>H<sub>78</sub>N<sub>8</sub>O<sub>9</sub> + H: 911.5965, obtained 911.5981.

Elemental analysis for C<sub>48</sub>H<sub>78</sub>N<sub>8</sub>O<sub>9</sub>•3.5 H<sub>2</sub>O. Calculated : C (59.18 %), H (8.79%), N (11.50 %).  
Obtained : C (59.00 %), H (8.69 %), N (11.55 %).

**64** 4,4-difluoro-8-((4-(((2,5-dioxopyrrolidin-1-yl)oxy)carbonyl)phenyl))1,3,5,7-tetramethyl-2,6-diethyl-4-bora-3a,4a-diaza-s-indacene



$$M = 521.36 \text{ g}\cdot\text{mol}^{-1}$$

54 mg of *N*-hydroxysuccinimide (0.48 mmol), 58 mg of dimethylaminopyridine (DMAP) (0.48 mmol) and 92 mg of 1-(3-dimethylaminopropyl)-3-ethylcarbodiimide hydrochloride (EDCI) (0.48 mmol) were added to a solution of 4,4-difluoro-8-(4-carboxyphenyl)-1,3,5,7-tetramethyl-2,6-diethyl-4-bora-3a,4a-diaza-s-indacene (100 mg, 0.24 mmol) in  $\text{CH}_2\text{Cl}_2$  (50 mL). The reaction was stirred at 35 °C. After complete activation of the acide function (2 h) followed by TLC, the mixture was washed with 2\*10 mL of water, the organic phase was dried over  $\text{MgSO}_4$  and the solvent was evaporated to give a red oil. The crude product was purified by chromatography on silica gel (eluent: AcOEt/hexane 50:50). Upon concentration of the pure fraction, recrystallization in a mixture of dichloromethane and hexane gave **64** as a red solid (m = 88 mg, yield = 70 %).

$^1\text{H}$  NMR (300 MHz,  $\text{CDCl}_3$ , 300 K)  $\delta$  (ppm): 0.96 (t, 6H,  $^3J = 7.5$  Hz,  $\text{CH}_2\text{CH}_3$ ), 1.25 (s, 6H,  $\text{CH}_3$ ), 2.27 (q, 4H,  $^3J = 7.5$  Hz,  $\text{CH}_2\text{CH}_3$ ), 2.51 (s, 6H,  $\text{CH}_3$ ), 2.92 (bs, 4H,  $\text{CH}_2\text{C}=\text{O}$ ), 7.47 (d, 2H,  $^3J = 8.3$  Hz,  $\text{CHar}_{\text{Bod}}$ ), 8.23 (d, 2H,  $^3J = 8.3$  Hz,  $\text{CHar}_{\text{Bod}}$ ).

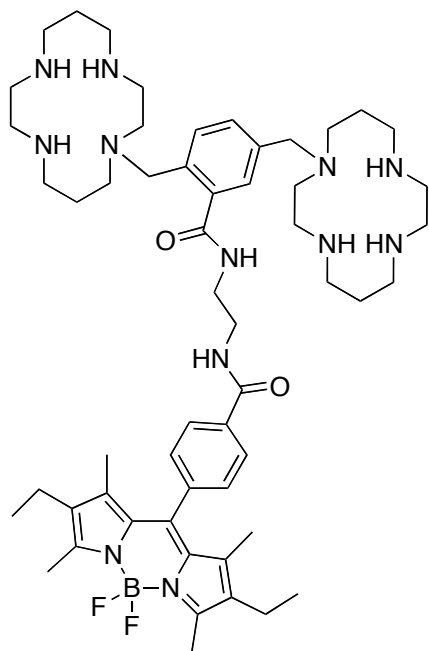
$^{13}\text{C}\{^1\text{H}\}$  NMR (75 MHz,  $\text{CDCl}_3$ , 300 K)  $\delta$  (ppm): 12.1 (\*2), 12.7 (\*2) ( $\text{CH}_3$ ), 14.6 (\*2) ( $\text{CH}_2\text{CH}_3$ ), 17.3 (\*2) ( $\text{CH}_2\text{CH}_3$ ), 25.7 (\*2) ( $\text{CH}_2\text{C}=\text{O}$ ) 125.6 ( $\text{Car}_{\text{Bod}}$ ), 129.3 (\*2) ( $\text{CHar}_{\text{Bod}}$ ), 131.2 (\*2) ( $\text{C}_{\text{pyrrole}}$ ), 133.3 (\*2) ( $\text{CHar}_{\text{Bod}}$ ), 137.7 (\*2) ( $\text{C}_{\text{pyrrole}}$ ), 138.0 (\*2) ( $\text{C}_{\text{pyrrole}}$ ), 138.7 ( $\text{C}_{\text{Bod}}$ ), 143.0 ( $\text{Car}_{\text{Bod}}$ ), 154.6 (\*2) ( $\text{C}_{\text{pyrrole}}$ ), 161.4 ( $\text{CO}_2$ ), 169.2 (\*2) ( $\text{NC}=\text{O}$ ).

$^{11}\text{B}$  NMR (192.5 MHz,  $\text{CDCl}_3$ , 300 K)  $\delta$  (ppm): 0.79 (t,  $^1J_{\text{B,F}} = 33.1$  Hz).

ESI-MS:  $m/z = 544.21$  [ $\text{M}+\text{Na}$ ] $^+$

UV-Vis ( $\text{CH}_3\text{CN}$ ),  $\lambda$  (nm) ( $\epsilon$ ,  $\text{M}^{-1}\text{cm}^{-1}$ ): 525 (73000), 492 (sh, 23200), 378 (7940)

Elemental analysis for  $\text{C}_{28}\text{H}_{30}\text{BF}_2\text{N}_3\text{O}_4$ . Calculated: C (68.50 %), H (6.67 %), N (6.39 %). Obtained: C (68.78 %), H (6.87 %), N (5.95 %).

Compound **65**

$$M = 995.15 \text{ g}\cdot\text{mol}^{-1}$$

Diisopropylethylamine (172  $\mu\text{L}$ , 1.04 mmol) was added to a solution of **56** (408 mg, 0.69 mmol) in acetonitrile (40 mL). A solution of bodipy **64** (694 mg, 0.69 mmol) in acetonitrile (10 mL) was then added and the mixture was stirred at room temperature during 6 h, until total consumption of the starting materials was observed by TLC. Solvent was evaporated, and the resulting red oil was purified by column chromatography on silica gel (eluent:  $\text{CH}_2\text{Cl}_2/\text{EtOH}/\text{NH}_4\text{OH}$  20:60:20). Precipitation from  $\text{CH}_2\text{Cl}_2$ /hexane gave the desired compound **65** as a red solid ( $m = 446 \text{ mg}$ , yield = 65 %, Mp: > 200  $^\circ\text{C}$ ).

$^1\text{H}$  NMR (300 MHz,  $\text{CDCl}_3$ , 300 K)  $\delta$  (ppm): 0.94 (t, 6H,  $^3J = 7.5 \text{ Hz}$ ,  $\text{CH}_2\text{CH}_3$ ), 1.24-1.32 (m, 9H), 1.52-1.92 (m, 8H), 2.26 (q, 4H,  $^3J = 7.5 \text{ Hz}$ ,  $\text{CH}_2\text{CH}_3$ ), 2.31-2.79 (m, 37H), 3.46-3.73 (m, 12H), 7.20 (d, 1H,  $^3J = 7.7 \text{ Hz}$ ), 7.33 (d, 2H,  $^3J = 8.2 \text{ Hz}$ ), 7.43 (s, 1H), 7.55 (d, 1H,  $^3J = 7.7 \text{ Hz}$ ), 8.12 (d, 2H,  $^3J = 8.2 \text{ Hz}$ ), 8.49-8.62 (bs, 1H), 9.67-9.80 (bs, 1H).

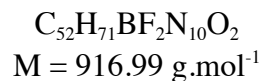
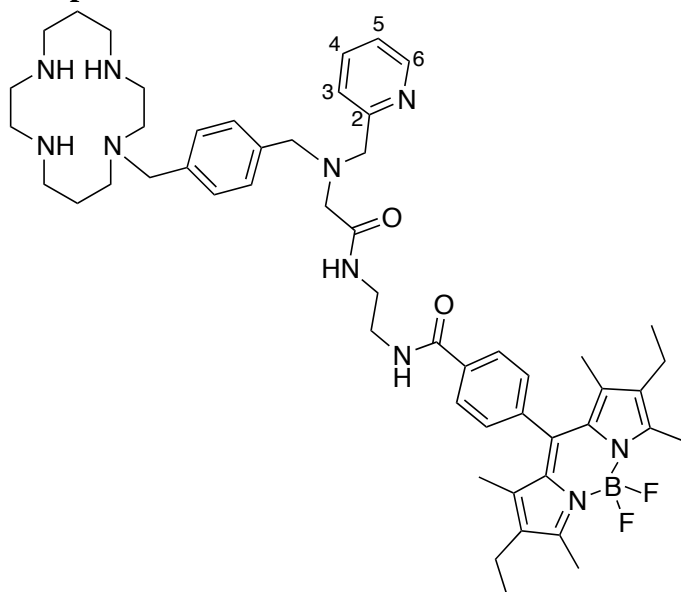
$^{13}\text{C}\{^1\text{H}\}$  NMR (75 MHz,  $\text{CDCl}_3$ , 300 K)  $\delta$  (ppm): 12.0 (\*2), 12.7 (\*2) ( $\text{CH}_3$ ), 14.8 (\*2) ( $\text{CH}_2\text{CH}_3$ ), 17.2 (\*2) ( $\text{CH}_2\text{CH}_3$ ), 26.2, 26.6, 28.6, 28.7 ( $\text{CH}_2\beta$ ), 39.7, 42.8, 47.1, 48.1, 48.4, 48.5, 48.6, 48.8, 49.4 (\*2), 49.9, 51.1, 51.3, 53.2, 53.8, 54.2, 54.6, 54.9, 55.2, 58.3 ( $\text{CH}_2$ ), 127.2 ( $\text{CHar}$ ), 128.3 (\*2), 128.8 (\*2) ( $\text{CHar}_{\text{Bod}}$ ), 130.5 ( $\text{CHar}$ ), 130.6 (\*2) ( $\text{C}_{\text{pyrrole}}$ ), 131.5 ( $\text{CHar}$ ), 133.2 (\*2) ( $\text{C}_{\text{pyrrole}}$ ), 134.5 ( $\text{Car}_{\text{Bod}}$ ), 136.1, 138.2 ( $\text{Car}$ ), 138.3 (\*2) ( $\text{C}_{\text{pyrrole}}$ ), 139.2 ( $\text{C}_{\text{Bod}}$ ), 139.3 ( $\text{Car}_{\text{Bod}}$ ), 139.8 ( $\text{Car}$ ), 154.3 (\*2) ( $\text{C}_{\text{pyrrole}}$ ), 166.6, 173.0 ( $\text{NHC=O}$ ).

$^{11}\text{B}$  NMR (96 MHz,  $\text{CDCl}_3$ , 300 K)  $\delta$  (ppm): 0.76 (t,  $^1J_{\text{B,F}} = 33.6 \text{ Hz}$ ).

ESI-MS:  $m/z = 995.7$  [ $\text{M}+\text{H}$ ] $^+$ , 1021.7 [ $\text{M}+\text{Na}$ ] $^+$ , 1033.7 [ $\text{M}+\text{K}$ ] $^+$ .

HRMS-ESI:  $m/z =$  calculated for  $\text{C}_{55}\text{H}_{85}\text{BF}_2\text{N}_{12}\text{O}_2+\text{H}$ : 995.7062, obtained 995.7012.

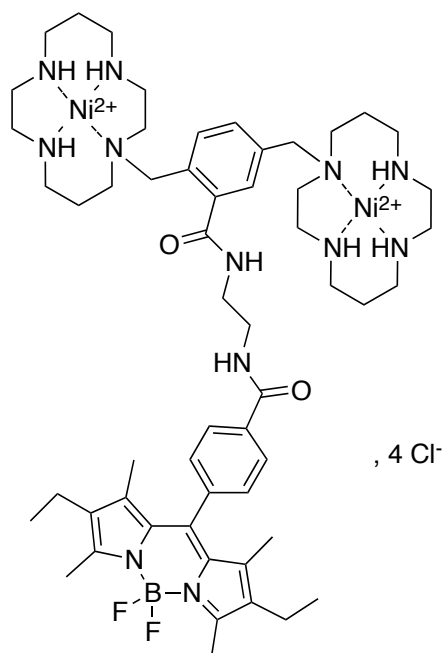


**Compound 66**

*N,N*-Diisopropylethylamine (15.7  $\mu\text{L}$ , 0.09 mmol) and **64** (49.0 mg, 0.09 mmol) were added to a solution of **61** (47.8 mg, 0.09 mmol) in acetonitrile (5 mL). The reaction mixture was stirred at room temperature for one night. The solvent was evaporated in vacuo. Chromatography on silica gel (A:  $\text{C}_2\text{H}_5\text{OH}$ , B:  $\text{NH}_3$  (25 %), B 5 %) gave **66** (55.0 mg, yield = 47 %) as a red powder.

$^1\text{H}$  NMR (300 MHz,  $\text{CDCl}_3$ , 300 K)  $\delta$ (ppm): 0.92 (t, 6H,  $^3J = 7.5$  Hz,  $\text{CH}_2\text{CH}_3$ ), 1.18 (s, 6H,  $\text{CH}_3$ ), 1.70-1.96 (m, 4H,  $\text{CH}_2\beta$ ), 2.24 (q, 4H,  $^3J = 7.5$  Hz,  $\text{CH}_2\text{CH}_3$ ), 2.39-3.00 (m, 22H), 3.07-3.32 (m, 4H), 3.42-3.59 (m, 6H), 3.64 (s, 2H,  $\text{CH}_2\text{Ph}$ ), 3.70-3.80 (m, 3H), 7.28-7.08 (m, 8H,  $\text{CHar}$ ,  $\text{CH}(5)$ ,  $\text{CH}(3)$ ,  $\text{CHar}_{\text{Bod}}$ ), 7.57 (td, 1H,  $^3J = 7.7$  Hz,  $^4J = 1.8$  Hz,  $\text{CH}(4)$ ), 7.88-7.98 (m, 2H,  $\text{CHar}_{\text{Bod}}$ ), 8.07 (t, 1H,  $J_{\text{app}} = 4.8$  Hz,  $\text{NHC=O}$ ), 8.51 (d, 1H,  $J_{\text{app}} = 4.6$  Hz,  $\text{CH}(6)$ ), 8.71 (t, 1H,  $J_{\text{app}} = 5.0$  Hz,  $\text{NHC=O}$ ).

HRMS-ESI:  $m/z$  = calculated for  $\text{C}_{52}\text{H}_{71}\text{BF}_2\text{N}_{10}\text{O}_2 + \text{H}$ : 917.5904 obtained 917.5908.

**Compound 67**

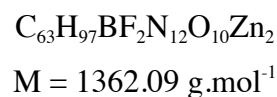
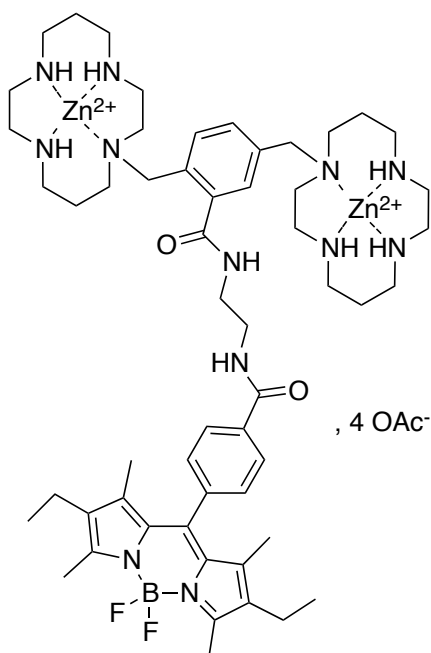
$$M = 1254.35 \text{ g}\cdot\text{mol}^{-1}$$

3.1 mg of NiCl<sub>2</sub> (0.023 mmol) was added to a solution of 10.4 mg of compound **65** (0.012 mmol) in 6 mL of methanol. The mixture was stirred at 50 °C for 2 h. After evaporation, compound **67** was obtained as a red solid (m = 14.2 mg, yield = 95 %).

ESI-MS: m/z = 555.27 [M-2H-4Cl]<sup>2+</sup>.

HRMS-ESI: m/z = calculated for C<sub>55</sub>H<sub>85</sub>BF<sub>2</sub>N<sub>12</sub>Ni<sub>2</sub>O<sub>2</sub>-2H-4Cl: 555.2740, obtained 555.2699.

### Compound 68



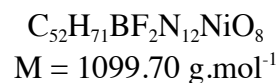
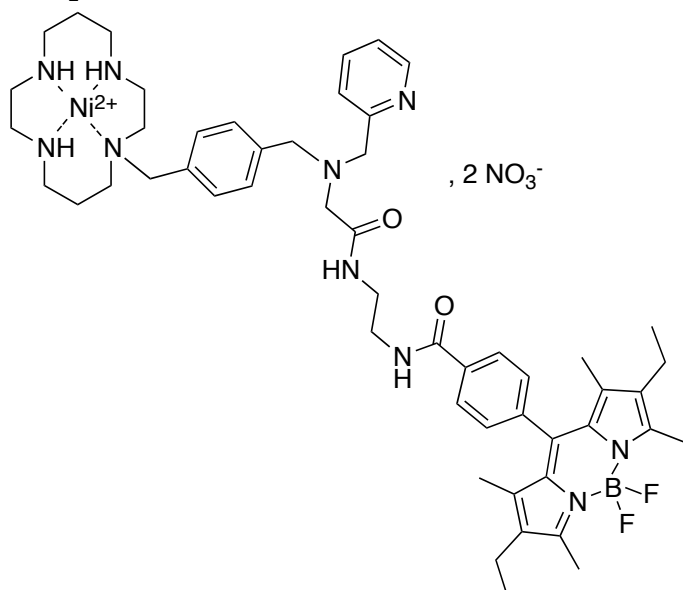
, 4 OAc<sup>-</sup>

4.7 mg of  $\text{Zn}(\text{OAc})_2(\text{H}_2\text{O})_2$  (0.021 mmol) was added to a solution of 9.5 mg of compound **65** (0.011 mmol) in 6 mL of methanol. The mixture was stirred at 50 °C for 2 h. After evaporation, compound **68** was obtained as a red solid ( $m = 27.7$  mg, yield = 97 %).

ESI-MS:  $m/z = 592.28$   $[\text{M}-\text{H}-3(\text{OAc})]^{2+}$ .

HRMS-ESI:  $m/z =$  calculated for  $\text{C}_{63}\text{H}_{97}\text{BF}_2\text{N}_{12}\text{O}_{10}\text{Zn}_2-\text{H}-3(\text{OAc})$ : 592.2783, obtained 592.2780.

### Compound 69



, 2 NO<sub>3</sub><sup>-</sup>

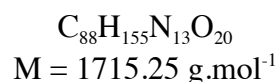
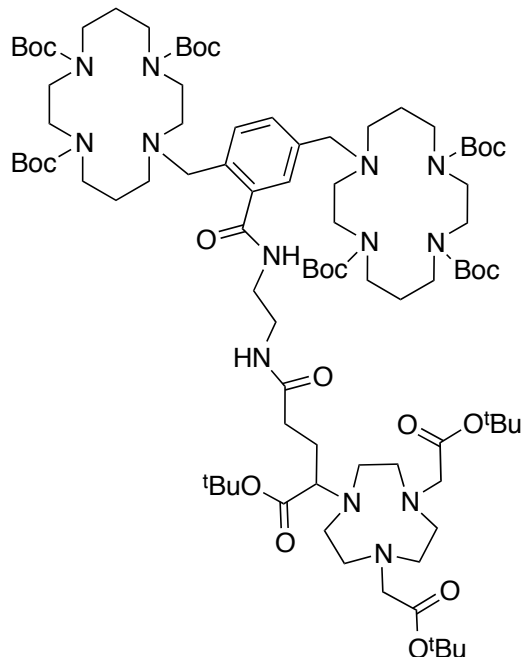
A solution of  $\text{Ni}(\text{NO}_3)_2$  in water (0.556 mL,  $c = 9.8 \times 10^{-2}$  M, 0.0545 mmol) was freeze-dried one day before the reaction.  $\text{Ni}(\text{NO}_3)_2$  was dissolved in methanol (3.5 mL) and the solution was

stirred for 3 days. A solution of **66** (50.0 mg, 0.0545 mmol) in methanol (2.0 mL) was added dropwise to the previous one. The reaction mixture was stirred for 3 days. Methanol was evaporated in vacuo giving **69** (41.2 mg, yield = 77 %) as a red powder.

MALDI :  $m/z = 973.58$  [M-H]<sup>+</sup>.

UV-Vis (CH<sub>3</sub>CN),  $\lambda$  (nm) ( $\epsilon$ , M<sup>-1</sup>cm<sup>-1</sup>): 525 (29700), 492 (sh, 12600), 378 (5420).

### Compound 70



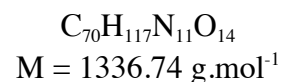
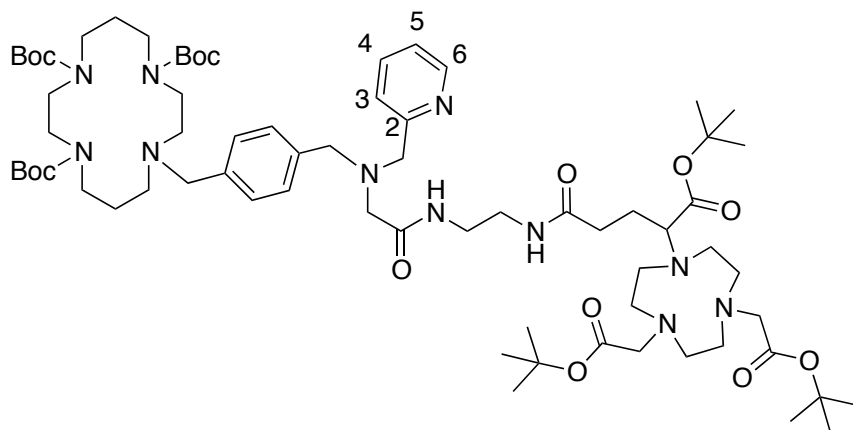
NODA-GA-tris (tBu) (125.0 mg, 0.23 mmol), HBtu (91.0 mg, 0.24 mmol), HOBt (32.5 mg, 0.24 mmol) and *N,N*-diisopropylethylamine (66.2  $\mu$ L, 0.38 mmol) were added to a solution of compound **55** in dichloromethane (12.5 mL) under argon atmosphere. The reaction mixture was stirred for one night. Dichloromethane and *N,N*-diisopropylethylamine were evaporated in vacuo. The resulting product was dissolved in dichloromethane (25 mL) and washed with a citric acid solution (2.2M, 15 mL), a saturated solution of sodium bicarbonate (15 mL) and finally water (15 mL). The organic layer was dried on magnesium sulfate and evaporated in vacuo. Inverse phase flash chromatography (A: HCOOH/H<sub>2</sub>O (0.01M), B: CH<sub>3</sub>CN, B 35 %  $\rightarrow$  60 %) gave **70** (308.7 mg, yield = 75 %) as a light yellow powder.

<sup>1</sup>H NMR (300 MHz, CDCl<sub>3</sub>, 300 K)  $\delta$ (ppm): 1.13-1.48 (m, 81H, CH<sub>3</sub>), 1.57-2.08 (m, 10H), 2.22-2.67 (m, 10H), 2.72-3.66 (m, 49H), 7.14-7.34 (m, 2H, CHar), 7.45 (bs, 1H, CHar), 8.28-8.80 (m, 2H, NHC=O).

HRMS-ESI:  $m/z =$  calculated for C<sub>88</sub>H<sub>155</sub>N<sub>13</sub>O<sub>20</sub> + H : 1715.1584 obtained 1715.1514.

Elemental analysis for  $C_{88}H_{155}N_{13}O_{20} \cdot 5.5 H_2O$ . Calculated : C (58.26 %), H (9.22 %), N (10.04 %).  
Obtained : C (58.05 %), H (8.99 %), N (10.08 %).

### Compound 71

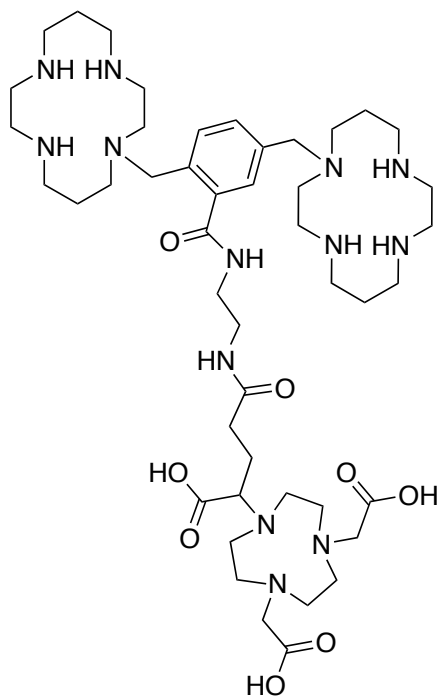


NODA-GA-tris (<sup>t</sup>Bu) (100.5 mg, 0.185 mmol), HBtu (73.68 mg, 0.194 mmol), HOBt (26.2 mg, 0.194 mmol) and N,N-diisopropylethylamine (48.3  $\mu$ L, 0.278 mmol) were added to a solution of **60** (149.89 mg, 0.185 mmol) in dichloromethane (9.2 mL) under argon atmosphere. The reaction mixture was stirred for one day. Dichloromethane and N,N-diisopropylethylamine were evaporated in vacuo. The resulting product was dissolved in dichloromethane (50 mL) and washed with a citric acid solution (2.2M) (50 mL), a saturated solution of sodium bicarbonate (50 mL) and finally water (50 mL). The organic layer was dried on magnesium sulfate and evaporated in vacuo. Inverse phase flash chromatography (A: HCOOH/H<sub>2</sub>O (0.01M), B: CH<sub>3</sub>CN, B 50 %) gave **71** (102.3 mg, yield = 42 %) as a light yellow powder.

<sup>1</sup>H NMR (300 MHz, DMSO, 300 K)  $\delta$ (ppm): 1.10-1.50 (m, 54H, CH<sub>3</sub>), 1.53-1.87 (m, 6H), 2.05-2.63 (m, 8H), 2.66-3.77 (m, 39H), 7.16-7.38 (m, 5H, CHar, CH(5)), 7.55 (d, 1H, <sup>3</sup>J (= 7.7 Hz, CH(3)), 7.76 (td, 1H, <sup>3</sup>J = 7.7 Hz, <sup>4</sup>J = 1.7 Hz, CH(4)), 7.86 (bs, 1H, NHC=O), 8.15 (bs, 1H, NHC=O), 8.51 (s, 1H, CH(6)).

HRMS-ESI:  $m/z$  = calculated for  $C_{70}H_{117}N_{11}O_{14} + H$ : 1336.8854 obtained 1336.8854.

Elemental analysis for  $C_{70}H_{117}N_{11}O_{14} \cdot 8.5 H_2O$ . Calculated : C (56.43 %), H (9.07 %), N (10.34 %).  
Obtained : C (56.29 %), H (9.40 %), N (9.95 %).

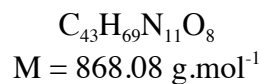
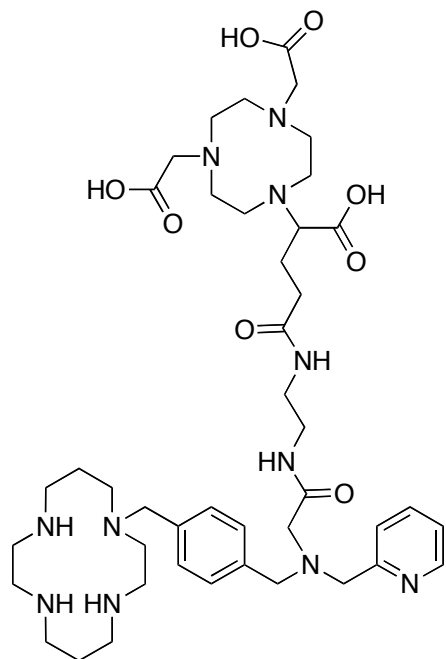
**Compound 72**

$$M = 946.23 \text{ g}\cdot\text{mol}^{-1}$$

A solution of HCl (3 M) (5.0 mL) was added to **70** (98.32 mg, 0.06 mmol) and the reaction mixture was stirred for one hour. The resulting product was left one night at room temperature. The acid was evaporated in vacuo giving **72** (32.3 mg, yield = 60 %).

HRMS-ESI:  $m/z$  = calculated for  $\text{C}_{46}\text{H}_{83}\text{N}_{13}\text{O}_8+\text{H}$ : 946.6560, obtained 946.6558.

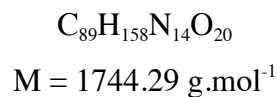
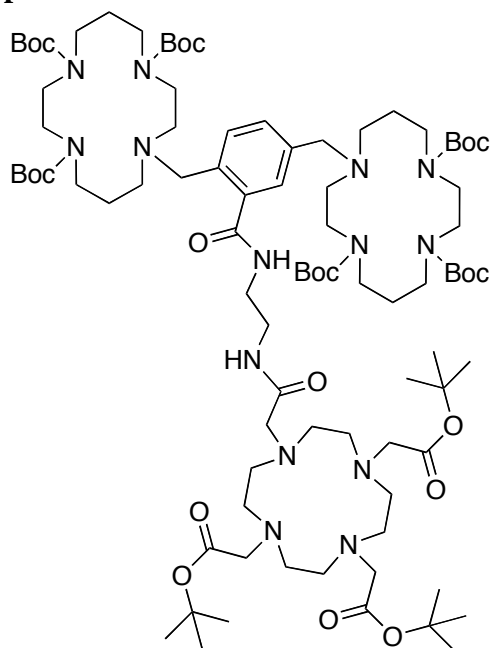
## Compound 73



A solution of 3M HCl (5.0 mL) was added to **71** (72.5 mg, 0.05 mmol) and the reaction mixture was stirred for one hour. The resulting product was left one night at room temperature. The acid was evaporated in vacuo and **73** was obtained as a white powder (18.2 mg, yield = 42 %).

ESI-MS:  $m/z = 868.54$   $[\text{M}+\text{H}]^+$ .

## Compound 74



Triethylamine (69.5  $\mu\text{L}$ , 0.5 mmol) and DOTA-tris(<sup>t</sup>Bu) ester NHS (167.5 mg, 0.25 mmol) were added subsequently to a stirred solution of compound **55** (300.0 mg, 0.25 mmol) in DMF (25

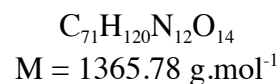
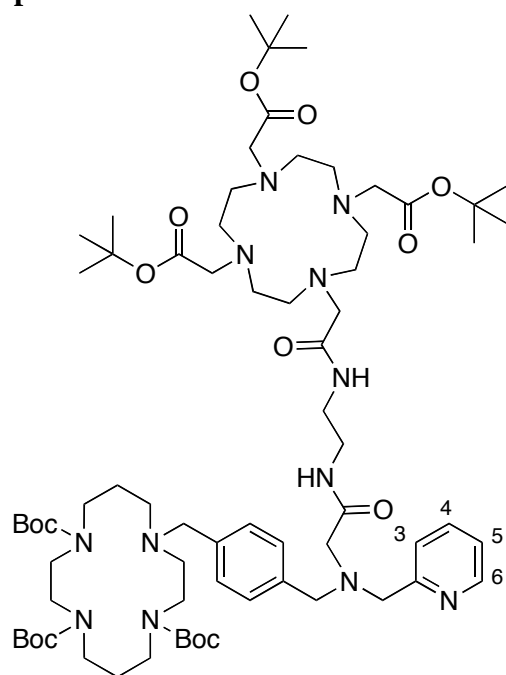
mL). The reaction mixture was stirred for one day and the solvent was evaporated in vacuo. Flash chromatography on silicate (A: CH<sub>2</sub>Cl<sub>2</sub>, B: CH<sub>3</sub>OH, B 0 % → 30 %) gave **74** (67.2 mg, 16 %) as a light yellow powder.

<sup>1</sup>H NMR (600 MHz, CDCl<sub>3</sub>, 300 K) δ (ppm): 1.07-1.48 (m, 81H, CH<sub>3</sub>), 1.53-1.70 (m, 6H), 1.70-1.92 (m, 6H), 2.29-2.69 (m, 14H), 2.94-3.55 (m, 46H), 7.16-7.36 (m, 2H, CHar), 7.38 (br.s, 1H, NHC=O), 7.47 (s, 1H, CHar), 8.49 (br.s, 1H, NHC=O).

HRMS-ESI: *m/z* = calculated for C<sub>89</sub>H<sub>158</sub>N<sub>14</sub>O<sub>20</sub>+Na: 1766.1669, obtained 1766.1686.

Elemental analysis for C<sub>89</sub>H<sub>158</sub>N<sub>14</sub>O<sub>20</sub>•HPF<sub>6</sub>•15H<sub>2</sub>O. Calculated : C (49.48 %), H (8.82 %), N (9.08 %). Obtained : C (49.56 %), H (8.73 %), N (8.95 %).

### Compound 75



Triethylamine (49.76 μL, 0.358 mmol) and DOTA-tris(<sup>t</sup>Bu) ester NHS (120.0 mg, 0.179 mmol) were added subsequently to a stirred solution of **60** (145.3 mg, 0.179 mmol) in DMF (18 mL). The reaction mixture was stirred for one day and the solvent was evaporated in vacuo. Flash chromatography (A: CH<sub>2</sub>Cl<sub>2</sub>, B: CH<sub>3</sub>OH, B 15 %) gave **75** (162.0 mg, yield = 66 %) as a light yellow powder.

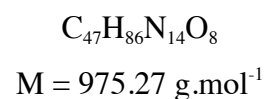
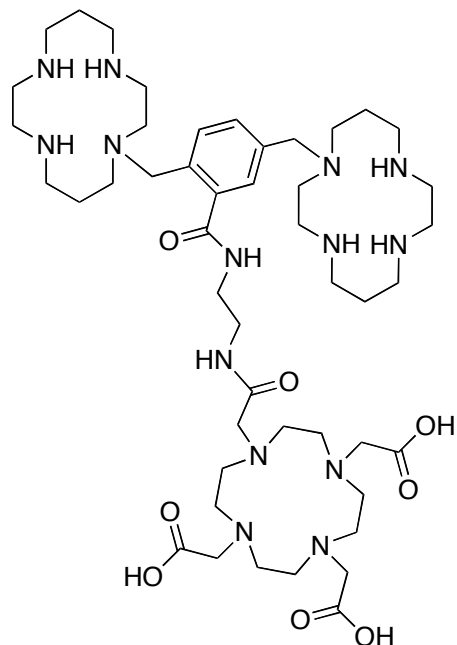
<sup>1</sup>H NMR (600 MHz, CDCl<sub>3</sub>, 300 K) δ(ppm): 1.28-1.45 (m, 54H, CH<sub>3</sub>), 1.65-1.86 (m, 4H, 2 CH<sub>2</sub>β), 2.09-2.56 (m, 8H), 2.65-3.47 (m, 36H), 3.49-3.84 (m, 8H), 7.13-7.27 (m, 5H, CHar, CH(5)), 7.32-7.45 (m, 1H, CH(3)), 7.68-7.77 (m, 1H, CH(4)), 7.96 (bs, 1H, NHC=O), 8.15 (bs, 1H, NHC=O), 8.49-8.56 (m, 1H, CH(6)).

HRMS-ESI: *m/z* = calculated for C<sub>71</sub>H<sub>120</sub>N<sub>12</sub>O<sub>14</sub> + Na: 1387.8939 obtained 1387.8923.



Elemental analysis for  $C_{71}H_{120}N_{12}O_{14} \cdot 2HPF_6 \cdot 2H_2O$ . Calculated : C (50.35 %), H (7.50 %), N (9.92 %). Obtained : C (50.43 %), H (7.63 %), N (9.96 %).

**Compound 76**

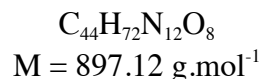
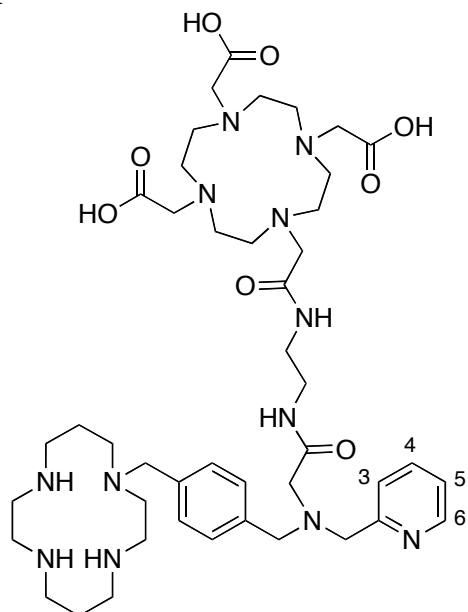


A solution of HCl (3M) (3.0 mL, 9.0 mmol) was added to **74** (50.0 mg, 0.03 mmol) and the reaction mixture was stirred for one hour. The resulting product was left one night at room temperature. The acid was evaporated in vacuo giving **76** (28.3 mg, 100 %) as a light yellow powder.

$^1\text{H}$  NMR (300 MHz,  $\text{CDCl}_3$ , 300 K)  $\delta$  (ppm): 2.16-2.35 (m, 10H), 3.06-3.94 (m, 58H), 4.38 (s, 2H), 4.56 (s, 2H), 7.71-7.87 (m, 2H, CHar), 7.98 (s, 1H, CHar).

HRMS-ESI:  $m/z$  = calculated for  $C_{47}H_{86}N_{14}O_8+H$ : 975.6826, obtained 975.6837.

## Compound 77



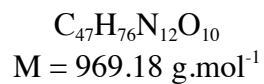
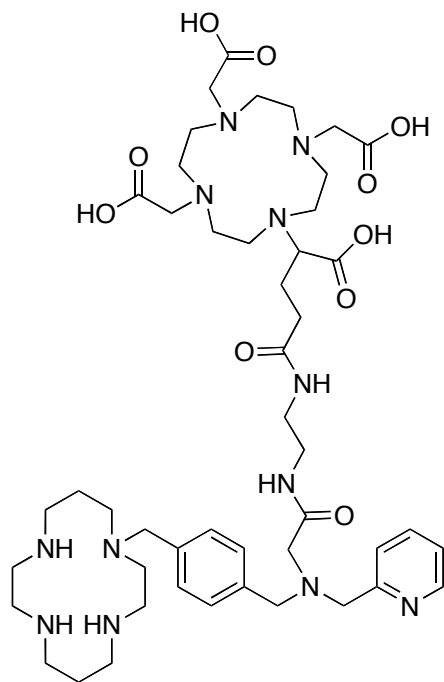
A solution of 3M HCl (5.0 mL) was added to **75** (70.3 mg, 0.05 mmol) and the reaction mixture was stirred for one hour. The resulting product was left one night at room temperature. The acid was evaporated in vacuo giving **77** (31.2 g, yield = 68%) as a brown foam.

$^1\text{H}$  NMR (600 MHz, DMSO, 365 K)  $\delta$ (ppm): 2.25-2.33 (m, 4H, 2  $\text{CH}_2\beta$ ), 3.16-3.28 (m, 16H), 3.31 (bs, 4H), 3.35-3.62 (m, 19H), 3.68 (br.s, 2H), 3.72 (bs, 4H), 3.95 (bs, 2H), 4.06 (bs, 2H), 4.15-4.25 (m, 4H), 4.44 (bs, 2H), 7.54 (d, 2H,  $^3J = 7.2$  Hz, CHar), 7.59 (d, 2H,  $^3J = 7.2$  Hz, CHar), 7.50-7.61 (m, 1H, CH(5)), 7.84 (d, 1H,  $^3J = 7.4$  Hz, CH(3)), 8.18 (t, 1H,  $J_{\text{app}} = 7.7$  Hz, CH(4)), 8.60 (bs, 1H,  $\text{NHC=O}$ ), 8.68-8.79 (m, 2H, CH(6),  $\text{NH}_{\text{C=O}}$ ), 9.70-10.30 (bs, 3H, OH).

HRMS-ESI:  $m/z$  = calculated for  $\text{C}_{44}\text{H}_{72}\text{N}_{12}\text{O}_8 + \text{H}$ : 897.5669 obtained 897.5627.

Elemental analysis for  $\text{C}_{44}\text{H}_{72}\text{N}_{12}\text{O}_8 \cdot 12\text{HCl} \cdot 7.5\text{H}_2\text{O}$ . Calculated : C (35.96 %), H (6.79 %), N (11.44 %). Obtained : C (35.57 %), H (6.37 %), N (11.46 %).

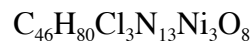
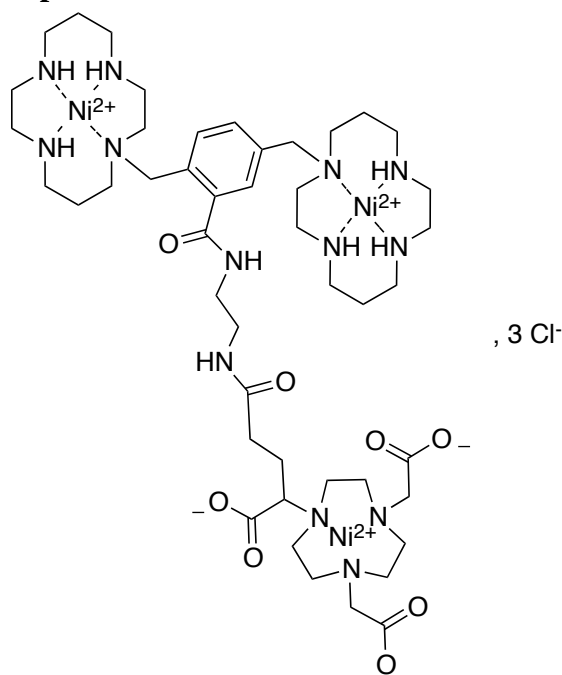
## Compound 78



Triethylamine (193.2  $\mu\text{L}$ , 1.43 mmol) and DOTA-GA anhydride (144.4 mg, 0.32 mmol) were added subsequently to a stirred solution of **61** (146.0 mg, 0.29 mmol) in DMF (15 mL). The reaction mixture was stirred for one day at 75  $^{\circ}\text{C}$ . DMSO (1 mL) was added and the reaction mixture was stirred at 75  $^{\circ}\text{C}$  for another one day. The solvents were evaporated in vacuo. Flash chromatography (A:  $\text{H}_2\text{O}$ , B:  $\text{CH}_3\text{CN}$ , B 15 %) gave **78** (20.6 mg, yield = 7 %) as a brown foam.

HRMS-ESI:  $m/z$  = calculated for  $\text{C}_{47}\text{H}_{76}\text{N}_{12}\text{O}_{10} + \text{H}$ : 969.5888 obtained 969.5847.

## Compound 79

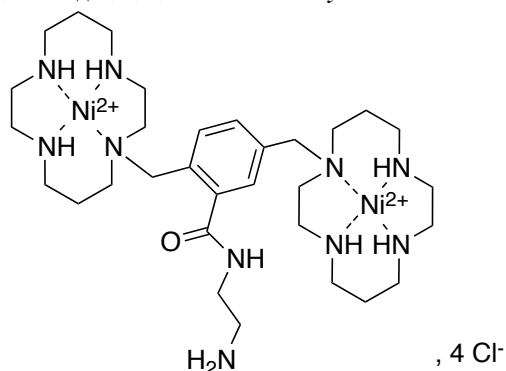


$$M = 1225.65$$

A solution of 4.3 mg of NiCl<sub>2</sub> (0.033 mmol) in 2 mL of a mixture MeOH/H<sub>2</sub>O (1:1) was added to a solution of 6.33 mg of compound **56** (0.011 mmol) in 3 mL of methanol. The mixture was stirred at 50 °C for 2 h, then filtered and evaporated *in vacuo*. Compound **79** was isolated as a green powder (m = 15.5 mg, yield = 85 %).

ESI-MS: m/z = 372.81 [M-3Cl]<sup>3+</sup>.

HRMS-ESI: m/z = calculated for C<sub>46</sub>H<sub>80</sub>N<sub>13</sub>Ni<sub>3</sub>O<sub>8</sub>-3Cl: 372.1432, obtained 372.1430.

**80** 2,5-bis((1,4,8,11-tetraazacyclotetradecan-1-yl)methyl)-N-(2-aminoethyl)benzamide, dinickel salt


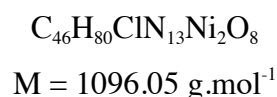
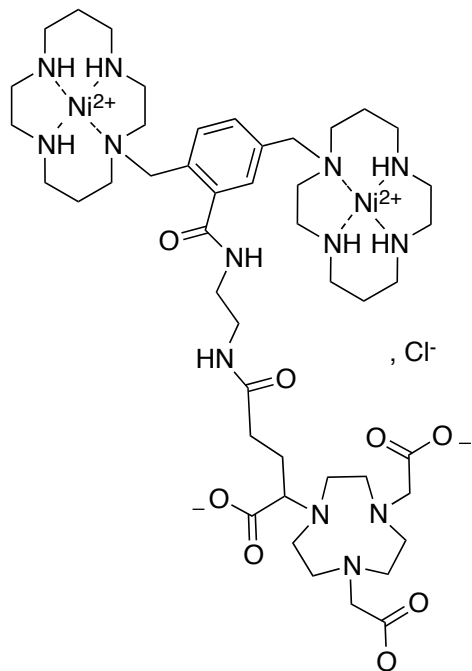
$$M = 848.07 \text{ g}\cdot\text{mol}^{-1}$$

A solution of 35.4 mg of NiCl<sub>2</sub> (0.271 mmol) in 5 mL of a mixture MeOH/H<sub>2</sub>O (1:1) was added to a solution of 80.4 mg of compound **56** (0.136 mmol) in 10 mL of methanol. The mixture was stirred at 50 °C for 2 h, then filtered and evaporated *in vacuo*. Compound **80** was isolated as an orange powder (m = 98.1 mg, yield = 85 %).

ESI-MS: m/z = 351.1712 [M-2H-4Cl]<sup>2+</sup>.

HRMS-ESI:  $m/z$  = calculated for  $C_{31}H_{60}N_{10}ONi_2 \cdot 2H \cdot 4Cl$ : 351.1746, obtained 351.1734.

**81** 2,2'-(7-(4-((2-(2,5-bis((1,4,8,11-tetraazacyclotetradecan-1-yl)methyl)benzamido)-ethyl)amino)-1-carboxy-4-oxobutyl)-1,4,7-triazacyclononane-1,4-diyl)diacetic acid, dinickel salt

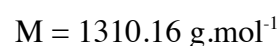
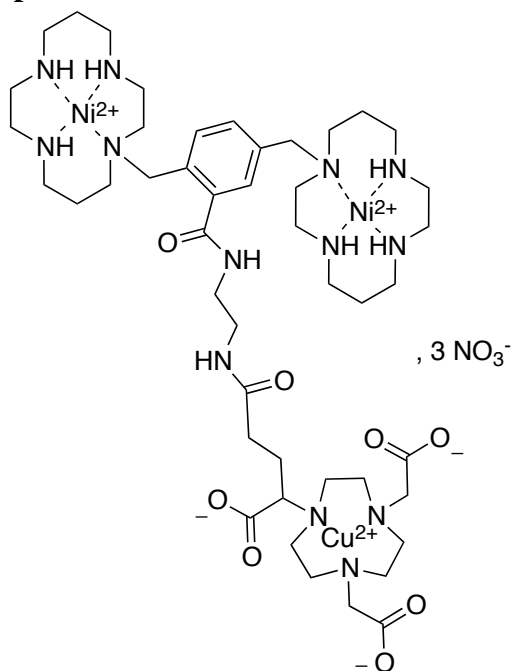


A solution of 19.7 mg of NODAGA-NHS (0.32 mmol) in 1.5 mL of dried DMF was added to a solution of 25.0 mg of compound **80** (0.032 mmol) and  $NEt_3$  (3.4 mL, 2.56 mmol) in 1.5 mL of DMF. The mixture was stirred at 50 °C for 24 h, then filtered and evaporated *in vacuo*. Compound **81** was obtained as an orange solid ( $m = 29.0 \text{ mg}$ , yield = 82 %).

MALDI:  $m/z = 1058 [M-Cl]^+$ .

ESI-MS:  $m/z = 529.7232 [M-H-Cl]^{2+}$ .

HRMS-ESI:  $m/z$  = calculated for  $C_{46}H_{80}N_{13}Ni_2O_8 \cdot H \cdot Cl$ : 529.7514, obtained 529.7523.

Compound **82**

2.7 mL of a 0.1 M solution of  $\text{Cu}(\text{NO}_3)_2$  (0.27 mmol) in 5 mL of a mixture MeOH/ $\text{H}_2\text{O}$  (1:1) was added to a solution of 15.0 mg of compound **81** (0.027 mmol) in 5 mL of methanol. The mixture was stirred at 60 °C for 5 min, then filtered and evaporated *in vacuo* to give **82** as a blue powder. (m = 32.9 mg, yield = 93 %)

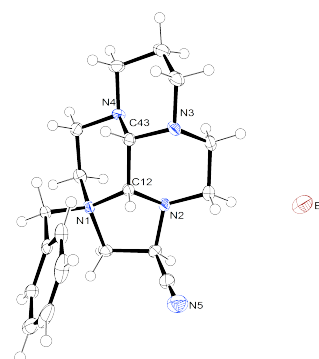
MALDI:  $m/z = 1121.36$   $[\text{M}-2\text{H}-3(\text{NO}_3)]^+$ .

HRMS-ESI:  $m/z =$  calculated for  $\text{C}_{46}\text{H}_{80}\text{CuN}_{16}\text{Ni}_2\text{O}_{17}-\text{H}-3(\text{NO}_3)$ : 560.2083, obtained 560.2102.

## IV. X-Ray Data

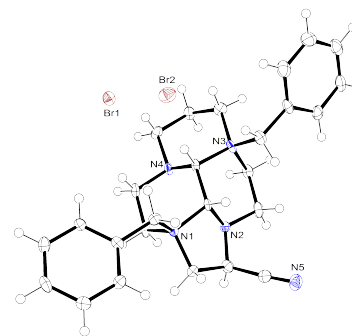
## Crystal data and structure refinement for compound 2.

Empirical formula	C <sub>20</sub> H <sub>30</sub> Br N <sub>5</sub> O	
Formula weight	436.40	
Temperature	115(2) K	
Wavelength	0.71073 Å	
Crystal description	Plate, colourless	
Crystal system	Monoclinic	
Space group	<i>P</i> 21/ <i>c</i>	
Unit cell dimensions	<i>a</i> = 14.2107(4) Å	$\alpha = 90^\circ$ .
	<i>b</i> = 9.9297(3) Å	$\beta = 122.155(2)^\circ$ .
	<i>c</i> = 17.2713(6) Å	$\gamma = 90^\circ$ .
Volume	2063.29(11) Å <sup>3</sup>	
<i>Z</i>	4	
Density (calculated)	1.405 Mg/m <sup>3</sup>	
Absorption coefficient	2.012 mm <sup>-1</sup>	
<i>F</i> (000)	912	
Crystal size	0.32 x 0.20 x 0.09 mm <sup>3</sup>	
Theta range for data collection	3.03 to 27.48°.	
Index ranges	-18 ≤ <i>h</i> ≤ 17, -8 ≤ <i>k</i> ≤ 12, -15 ≤ <i>l</i> ≤ 22	
Reflections collected	11787	
Independent reflections	4677 [ <i>R</i> (int) = 0.0437]	
Completeness to theta = 27.48°	99.0 %	
Absorption correction	Semi-empirical from equivalents	
Max. and min. transmission	0.7105 and 0.6336	
Refinement method	Full-matrix least-squares on <i>F</i> <sup>2</sup>	
Data / restraints / parameters	4677 / 0 / 245	
Goodness-of-fit on <i>F</i> <sup>2</sup>	1.044	
Final <i>R</i> indices [ <i>I</i> > 2σ( <i>I</i> )]	<i>R</i> 1 = 0.0377, <i>wR</i> 2 = 0.0880	
<i>R</i> indices (all data)	<i>R</i> 1 = 0.0569, <i>wR</i> 2 = 0.0954	
Largest diff. peak and hole	0.599 and -0.882 e.Å <sup>-3</sup>	



Crystal data and structure refinement for compound **3**.

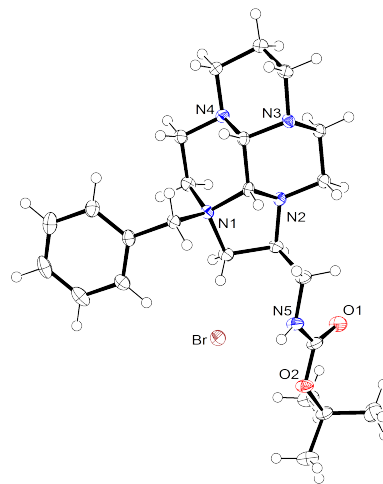
Empirical formula	C <sub>26</sub> H <sub>39</sub> Br <sub>2</sub> N <sub>5</sub> O <sub>3</sub>	
Formula weight	629.44	
Temperature	115(2) K	
Wavelength	0.71069 Å	
Crystal description	Plate, colourless	
Crystal system	Monoclinic	
Space group	<i>P</i> 21/ <i>c</i>	
Unit cell dimensions	<i>a</i> = 8.1945(3) Å	$\alpha = 90^\circ$ .
	<i>b</i> = 19.8416(7) Å	$\beta = 105.677(2)^\circ$ .
	<i>c</i> = 17.3420(6) Å	$\gamma = 90^\circ$ .
Volume	2714.78(17) Å <sup>3</sup>	
<i>Z</i>	4	
Density (calculated)	1.540 Mg/m <sup>3</sup>	
Absorption coefficient	3.023 mm <sup>-1</sup>	
<i>F</i> (000)	1296	
Crystal size	0.40 x 0.11 x 0.04 mm <sup>3</sup>	
Theta range for data collection	2.58 to 27.50°.	
Index ranges	-10 ≤ <i>h</i> ≤ 10, -23 ≤ <i>k</i> ≤ 25, -17 ≤ <i>l</i> ≤ 22	
Reflections collected	16855	
Independent reflections	6150 [ <i>R</i> (int) = 0.0752]	
Completeness to theta = 27.50°	98.6 %	
Absorption correction	Semi-empirical from equivalents	
Max. and min. transmission	0.67703 and 0.53607	
Refinement method	Full-matrix least-squares on <i>F</i> <sup>2</sup>	
Data / restraints / parameters	6150 / 9 / 343	
Goodness-of-fit on <i>F</i> <sup>2</sup>	0.961	
Final <i>R</i> indices [ <i>I</i> > 2σ( <i>I</i> )]	<i>R</i> 1 = 0.0495, <i>wR</i> 2 = 0.0951	
<i>R</i> indices (all data)	<i>R</i> 1 = 0.1111, <i>wR</i> 2 = 0.1145	
Largest diff. peak and hole	0.530 and -0.944 e.Å <sup>-3</sup>	





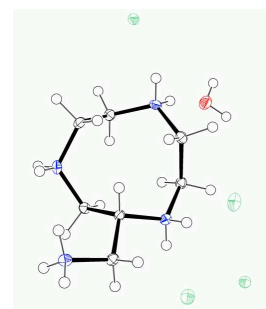
Crystal data and structure refinement for compound **8**.

Empirical formula	C <sub>28</sub> H <sub>44</sub> Br N <sub>7</sub> O <sub>2</sub>
Formula weight	590.61
Temperature	115(2) K
Wavelength	0.71073 Å
Crystal description	Prism, colourless
Crystal system	Orthorhombic
Space group	<i>P</i> c a 21
Unit cell dimensions	a = 32.4504(11) Å      α = 90°. b = 7.7984(3) Å      β = 90°. c = 11.7545(4) Å      γ = 90°.
Volume	2974.61(18) Å <sup>3</sup>
Z	4
Density (calculated)	1.319 Mg/m <sup>3</sup>
Absorption coefficient	1.419 mm <sup>-1</sup>
F(000)	1248
Crystal size	0.52 x 0.37 x 0.25 mm <sup>3</sup>
Theta range for data collection	2.90 to 27.48°.
Index ranges	-42 ≤ h ≤ 41, -9 ≤ k ≤ 10, -14 ≤ l ≤ 15
Reflections collected	15237
Independent reflections	5931 [R(int) = 0.0569]
Completeness to theta = 27.48°	98.1 %
Absorption correction	Semi-empirical from equivalents
Max. and min. transmission	0.9725 and 0.4673
Refinement method	Full-matrix least-squares on F <sup>2</sup>
Data / restraints / parameters	5931 / 1 / 348
Goodness-of-fit on F <sup>2</sup>	1.084
Final R indices [I > 2σ(I)]	R1 = 0.0412, wR2 = 0.1145
R indices (all data)	R1 = 0.0441, wR2 = 0.1185
Absolute structure parameter	0.504(10)
Largest diff. peak and hole	0.382 and -0.879 e.Å <sup>-3</sup>



Crystal data and structure refinement for **26**.

Empirical formula	C <sub>7</sub> H <sub>24</sub> Cl <sub>4</sub> N <sub>4</sub> O	
Formula weight	322.10	
Temperature	115(2) K	
Wavelength	0.71073 Å	
Crystal system	Monoclinic	
Space group	P 21/c	
Unit cell dimensions	a = 10.8478(3) Å b = 6.9249(2) Å c = 19.6388(7) Å	α = 90°. β = 102.912(2)°. γ = 90°.
Volume	1437.96(8) Å <sup>3</sup>	
Z	4	
Density (calculated)	1.488 Mg/m <sup>3</sup>	
Absorption coefficient	0.812 mm <sup>-1</sup>	
F(000)	680	
Crystal size	0.50 x 0.35 x 0.30 mm <sup>3</sup>	
Theta range for data collection	1.93 to 27.48°.	
Index ranges	-13 ≤ h ≤ 14, -8 ≤ k ≤ 8, -25 ≤ l ≤ 25	
Reflections collected	6061	
Independent reflections	3254 [R(int) = 0.0257]	
Completeness to theta = 27.48°	99.3 %	
Absorption correction	None	
Refinement method	Full-matrix least-squares on F <sup>2</sup>	
Data / restraints / parameters	3254 / 0 / 145	
Goodness-of-fit on F <sup>2</sup>	1.108	
Final R indices [I > 2σ(I)]	R1 = 0.0319, wR2 = 0.0682	
R indices (all data)	R1 = 0.0360, wR2 = 0.0704	
Largest diff. peak and hole	0.477 and -0.322 e.	





## **References**



- (1) James, M. L.; Gambhir, S. S. *Physiol. Rev.* **2012**, *92*, 897-965.
- (2) Tanaka, T.; Bai, Z.; Srinoulprasert, Y.; Yang, B. G.; Hayasaka, H.; Miyasaka, M. *Cancer Sci.* **2005**, *96*, 317-322.
- (3) Liang, X. Y. *Chem. Biol. Drug Des.* **2008**, *72*, 97-110.
- (4) Kuil, J.; Buckle, T.; van Leeuwen, F. W. B. *Chem. Soc. Rev.* **2012**, *41*, 5239-5261.
- (5) Horuk, R. *Cytokine Growth Factor Rev.* **2001**, *12*, 313-335.
- (6) Sun, X. Q.; Cheng, G. C.; Hao, M. G.; Zheng, J. H.; Zhou, X. M.; Zhang, J. A.; Taichman, R. S.; Pienta, K. J.; Wang, J. H. *Cancer Metastasis Rev.* **2010**, *29*, 709-722.
- (7) Vicari, A. P.; Caux, C. *Cytokine Growth Factor Rev.* **2002**, *13*, 143-154.
- (8) Murphy, J. W.; Cho, Y.; Sachpatzidis, A.; Fan, C. P.; Hodsdon, M. E.; Lolis, E. *J. Biol. Chem.* **2007**, *282*, 10018-10027.
- (9) Kofuku, Y.; Yoshiura, C.; Ueda, T.; Terasawa, H.; Hirai, T.; Tominaga, S.; Hirose, M.; Maeda, Y.; Takahashi, H.; Terashima, Y.; Matsushima, K.; Shimada, I. *J. Biol. Chem.* **2009**, *284*, 35240-35250.
- (10) Wu, B. L.; Chien, E. Y. T.; Mol, C. D.; Fenalti, G.; Liu, W.; Katritch, V.; Abagyan, R.; Brooun, A.; Wells, P.; Bi, F. C.; Hamel, D. J.; Kuhn, P.; Handel, T. M.; Cherezov, V.; Stevens, R. C. *Science* **2010**, *330*, 1066-1071.
- (11) Scholten, D. J.; Canals, M.; Maussang, D.; Roumen, L.; Smit, M. J.; Wijtmans, M.; de, G. C.; Vischer, H. F.; Leurs, R. *Br. J. Pharmacol.* **2012**, *165*, 1617-1643.
- (12) Choi, W. T.; Duggineni, S.; Xu, Y.; Huang, Z. W.; An, J. *J. Med. Chem.* **2012**, *55*, 977-994.
- (13) Balkwill, F. *Semin. Cancer Biol.* **2004**, *14*, 171-179.
- (14) Calandra, G.; Bridger, G.; Fricker, S. *CXCR4 in Clinical Hematology*, **2010**, Vol. 341.
- (15) Luster, A. D. *N. Engl. J. Med.* **1998**, *338*, 436-445.
- (16) De Clercq, E. *Int. J. Biochem. Cell Biol.* **2004**, *36*, 1800-1822.
- (17) Endres, M. J.; Clapham, P. R.; Marsh, M.; Ahuja, M.; Davis, T. J.; McKnight, A.; Thomas, J. F.; Stoebenau-Haggarty, B.; Choe, S.; Vance, P. J.; Wells, T. N. C.; Power, C. A.; Sutterwala, S. S.; Doms, R. W.; Landau, N. R.; Hoxie, J. A. *Cell* **1996**, *87*, 745-756.
- (18) Baribaud, F.; Edwards, T. G.; Sharron, M.; Brelot, A.; Heveker, N.; Price, K.; Mortari, F.; Alizon, M.; Tsang, M.; Doms, R. W. *J. Virol.* **2001**, *75*, 8957-8967.
- (19) Tamamura, H.; Hanaoka, H.; Tsutsumi, H.; Ohashi, N.; Tanaka, T.; Mori, T.; Mukai, T.; Doi, R.; Saji, H.; Fujii, N. *Pept. Sci.* **2006**, *43*, 254.
- (20) Loetscher, P.; Gong, J. H.; Dewald, B.; Baggiolini, M.; Clark-Lewis, I. *J. Biol. Chem.* **1998**, *273*, 22279-22283.
- (21) Luo, Z. W.; Zhou, N. M.; Luo, J. S.; Hall, J. W.; Huang, Z. W. *Biochem. Biophys. Res. Commun.* **1999**, *263*, 691-695.
- (22) Luo, J. S.; Luo, Z. W.; Zhou, N. M.; Hall, J. W.; Huang, Z. W. *Biochem. Biophys. Res. Commun.* **1999**, *264*, 42-47.
- (23) Fernandez, E. J.; Wilken, J.; Thompson, D. A.; Peiper, S. C.; Lolis, E. *Biochemistry* **2000**, *39*, 12837-12844.
- (24) Luo, Z. W.; Fan, X. J.; Zhou, N. M.; Hiraoka, M.; Luo, J. S.; Kaji, H.; Huang, Z. W. *Biochemistry* **2000**, *39*, 13545-13550.

- (25) Tamamura, H.; Kuroda, M.; Masuda, M.; Otaka, A.; Funakoshi, S.; Nakashima, H.; Yamamoto, N.; Waki, M.; Matsumoto, A.; Lancelin, J. M.; Kohda, D.; Tate, S.; Inagaki, F.; Fujii, N. *Biochim. Biophys. Acta* **1993**, *1163*, 209-216.
- (26) Masuda, M.; Nakashima, H.; Ueda, T.; Naba, H.; Ikoma, R.; Otaka, A.; Terakawa, Y.; Tamamura, H.; Ibuka, T.; Murakami, T.; Koyanagi, Y.; Waki, M.; Matsumoto, A.; Yamamoto, N.; Funakoshi, S.; Fujii, N. *Biochem. Biophys. Res. Commun.* **1992**, *189*, 845-850.
- (27) Tamamura, H.; Waki, M.; Imai, M.; Otaka, A.; Ibuka, T.; Waki, K.; Miyamoto, K.; Matsumoto, A.; Murakami, T.; Nakashima, H.; Yamamoto, N.; Fujii, N. *Bioorg. Med. Chem.* **1998**, *6*, 473-479.
- (28) Tamamura, H.; Omagari, A.; Oishi, S.; Kanamoto, T.; Yamamoto, N.; Peiper, S. C.; Nakashima, H.; Otaka, A.; Fujii, N. *Bioorg. Med. Chem. Lett.* **2000**, *10*, 2633-2637.
- (29) Tamamura, H.; Hiramatsu, K.; Kusano, S.; Terakubo, S.; Yamamoto, N.; Trent, J. O.; Wang, Z. X.; Peiper, S. C.; Nakashima, H. *Org. Biomol. Chem.* **2003**, *1*, 3656-3662.
- (30) Ueda, S.; Oishi, S.; Wang, Z. X.; Araki, T.; Tamamura, H.; Cluzeau, J.; Ohno, H.; Kusano, S.; Nakashima, H.; Trent, J. O.; Peiper, S. C.; Fujii, N. *J. Med. Chem.* **2007**, *50*, 192-198.
- (31) Tamamura, H.; Hiramatsu, K.; Ueda, S.; Wang, Z. X.; Kusano, S.; Terakubo, S.; Trent, J. O.; Peiper, S. C.; Yamamoto, N.; Nakashima, H.; Otaka, A.; Fujii, N. *J. Med. Chem.* **2005**, *48*, 380-391.
- (32) Liang, X. Y.; Sadler, P. J. *Chem. Soc. Rev.* **2004**, *33*, 246-266.
- (33) Lam, A. R.; Bhattacharya, S.; Patel, K.; Hall, S. E.; Mao, A.; Vaidehi, N. *J. Chem. Inf. Model.* **2011**, *51*, 139-147.
- (34) De Clercq, E. *Biochem. Pharmacol.* **2009**, *77*, 1655-1664.
- (35) Valks, G. C.; McRobbie, G.; Lewis, E. A.; Hubin, T. J.; Hunter, T. M.; Sadler, P. J.; Pannecouque, C.; De Clercq, E.; Archibald, S. J. *J. Med. Chem.* **2006**, *49*, 6162-6165.
- (36) Smith, R.; Huskens, D.; Daelemans, D.; Mewis, R. E.; Garcia, C. D.; Cain, A. N.; Freeman, T. N. C.; Pannecouque, C.; De, C. E.; Schols, D.; Hubin, T. J.; Archibald, S. J. *Dalton Trans.* **2012**, *41*, 11369-11377.
- (37) Hatse, S.; Princen, K.; De Clercq, E.; Rosenkilde, M. M.; Schwartz, T. W.; Hernandez-Abad, P. E.; Skerlj, R. T.; Bridger, G. J.; Schols, D. *Biochem. Pharmacol.* **2005**, *70*, 752-761.
- (38) Kawatkar, S. P.; Yan, M. C.; Gevariya, H.; Lim, M. Y.; Eisold, S.; Zhu, X. J.; Huang, Z. W.; An, J. *Exp. Biol. Med.* **2011**, *236*, 844-850.
- (39) Rosenkilde, M. M.; Gerlach, L. O.; Hatse, S.; Skerlj, R. T.; Schols, D.; Bridger, G. J.; Schwartz, T. W. *J. Biol. Chem.* **2007**, *282*, 27354-27365.
- (40) Wong, R. S. Y.; Bodart, V.; Metz, M.; Labrecque, J.; Bridger, G.; Fricker, S. P. *Mol. Pharmacol.* **2008**, *74*, 1485-1495.
- (41) Gerlach, L. O.; Jakobsen, J. S.; Jensen, K. P.; Rosenkilde, M. R.; Skerlj, R. T.; Ryde, U.; Bridger, G. J.; Schwartz, T. W. *Biochemistry* **2003**, *42*, 710-717.
- (42) Duda, D. G.; Kozin, S. V.; Kirkpatrick, N. D.; Xu, L.; Fukumura, D.; Jain, R. K. *Clin. Cancer Res.* **2011**, *17*, 2074-2080.
- (43) Azhdarinia, A.; Ghosh, P.; Ghosh, S.; Wilganowski, N.; Sevick-Muraca, E. M. *Mol. Imaging Biol.* **2012**, *14*, 261-276.

- (44) Banisadr, G.; Dicou, E.; Berbar, T.; Rostene, W.; Lombet, A.; Haour, F. *J. Neuroimmunol.* **2000**, *110*, 151-160.
- (45) Nimmagadda, S.; Pullambhatla, M.; Pomper, M. G. *J. Nucl. Med.* **2009**, *50*, 1124-1130.
- (46) Aberg, O.; Pisaneschi, F.; Smith, G.; Nguyen, Q. D.; Stevens, E.; Aboagye, E. O. *J. Fluorine Chem.* **2012**, *135*, 200-206.
- (47) Jacobson, O.; Weiss, I. D.; Kiesewetter, D. O.; Farber, J. M.; Chen, X. Y. *J. Nucl. Med.* **2010**, *51*, 1796-1804.
- (48) Wadas, T. J.; Wong, E. H.; Weisman, G. R.; Anderson, C. J. *Chem. Rev.* **2010**, *110*, 2858-2902.
- (49) Lattuada, L.; Barge, A.; Cravotto, G.; Giovenzana, G. B.; Tei, L. *Chem. Soc. Rev.* **2011**, *40*, 3019-3049.
- (50) Ferreira, C. L.; Lamsa, E.; Woods, M.; Duan, Y.; Fernando, P.; Bensimon, C.; Kordos, M.; Guenther, K.; Jurek, P.; Kiefer, G. E. *Bioconjugate Chem.* **2010**, *21*, 531-536.
- (51) Bass, L. A.; Wang, M.; Welch, M. J.; Anderson, C. J. *Bioconjugate Chem.* **2000**, *11*, 527-532.
- (52) Silversides, J. D.; Smith, R.; Archibald, S. J. *Dalton Trans.* **2011**, *40*, 6289-6297.
- (53) Brechbiel, M. W. *Q. J. Nucl. Med. Mol. Imaging* **2008**, *52*, 166-173.
- (54) Anderson, C. J.; Welch, M. J. *Chem. Rev.* **1999**, *99*, 2219-2234.
- (55) Zeglis, B. M.; Lewis, J. S. *Dalton Trans.* **2011**, *40*, 6168-6195.
- (56) Bartholoma, M. D.; Louie, A. S.; Valliant, J. F.; Zubieta, J. *Chem. Rev.* **2010**, *110*, 2903-2920.
- (57) Correia, J. D. G.; Paulo, A.; Raposinho, P. D.; Santos, I. *Dalton Trans.* **2011**, *40*, 6144-6167.
- (58) Liu, S. *Adv. Drug Delivery Rev.* **2008**, *60*, 1347-1370.
- (59) Mewis, R. E.; Archibald, S. J. *Coord. Chem. Rev.* **2010**, *254*, 1686-1712.
- (60) Benmelouka, M.; Borel, A.; Moriggi, L.; Helm, L.; Merbach, A. E. *J. Phys. Chem. B* **2007**, *111*, 832-840.
- (61) Ferdani, R.; Stigers, D. J.; Fiamengo, A. L.; Wei, L. H.; Li, B. T. Y.; Golen, J. A.; Rheingold, A. L.; Weisman, G. R.; Wong, E. H.; Anderson, C. J. *Dalton Trans.* **2012**, *41*, 1938-1950.
- (62) Guo, Y.; Ferdani, R.; Anderson, C. J. *Bioconjugate Chem.* **2012**, *23*, 1470-1477.
- (63) Notni, J.; Hermann, P.; Havlickova, J.; Kotek, J.; Kubicek, V.; Plutnar, J.; Loktionova, N.; Riss, P. J.; Rosch, F.; Lukes, I. *Chem. Eur. J.* **2010**, *16*, 7174-7185.
- (64) Notni, J.; Wester, H.-J.; Hermann, P., **2012**, WO2012095347A1.
- (65) Simecek, J.; Schulz, M.; Notni, J.; Plutnar, J.; Kubicek, V.; Havlickova, J.; Hermann, P. *Inorg. Chem.* **2012**, *51*, 577-590.
- (66) Simecek, J.; Zemek, O.; Hermann, P.; Wester, H.-J.; Notni, J. *ChemMedChem* **2012**, *7*, 1375-1378.
- (67) Notni, J.; Simecek, J.; Hermann, P.; Wester, H.-J. *Chem. Eur. J.* **2011**, *17*, 14718-14722.
- (68) Kubicek, V.; Havlickova, J.; Kotek, J.; Tircso, G.; Hermann, P.; Toth, E.; Lukes, I. *Inorg. Chem.* **2010**, *49*, 10960-10969.



- (69) Andre, J. P.; Maecke, H. R.; Zehnder, M.; Macko, L.; Akyel, K. G. *Chem. Commun.* **1998**, 1301-1302.
- (70) Riss, P. J.; Kroll, C.; Nagel, V.; Roesch, F. *Bioorg. Med. Chem. Lett.* **2008**, *18*, 5364-5367.
- (71) Eisenwiener, K. P.; Powell, P.; Macke, H. R. *Bioorg. Med. Chem. Lett.* **2000**, *10*, 2133-2135.
- (72) Ruser, G.; Ritter, W.; Maecke, H. R. *Bioconjugate Chem.* **1990**, *1*, 345-349.
- (73) Lewis, E. A.; Boyle, R. W.; Archibald, S. J. *Chem. Commun.* **2004**, 2212-2213.
- (74) Wadas, T. J.; Eiblmaier, M.; Zheleznyak, A.; Sherman, C. D.; Ferdani, R.; Liang, K.; Achilefu, S.; Anderson, C. J. *J. Nucl. Med.* **2008**, *49*, 1819-1827.
- (75) Smith, S. V. *J. Inorg. Biochem.* **2004**, *98*, 1874-1901.
- (76) Shokeen, M.; Anderson, C. J. *Acc. Chem. Res.* **2009**, *42*, 832-841.
- (77) Jones-Wilson, T. M.; Deal, K. A.; Anderson, C. J.; McCarthy, D. W.; Kovacs, Z.; Motekaitis, R. J.; Sherry, A. D.; Martell, A. E.; Welch, M. J. *Nucl. Med. Biol.* **1998**, *25*, 523-530.
- (78) Fani, M.; Del Pozzo, L.; Abiraj, K.; Mansi, R.; Tamma, M. L.; Cescato, R.; Waser, B.; Weber, W. A.; Reubi, J. C.; Maecke, H. R. *J. Nucl. Med.* **2011**, *52*, 1110-1118.
- (79) Silversides, J. D.; Allan, C. C.; Archibald, S. J. *Dalton Trans.* **2007**, 971-978.
- (80) Woodin, K. S.; Heroux, K. J.; Boswell, C. A.; Wong, E. H.; Weisman, G. R.; Niu, W. J.; Tomellini, S. A.; Anderson, C. J.; Zakharov, L. N.; Rheingold, A. L. *Eur. J. Inorg. Chem.* **2005**, 4829-4833.
- (81) Pandya, D. N.; Dale, A. V.; Kim, J. Y.; Lee, H.; Ha, Y. S.; An, G. I.; Yoo, J. *Bioconjugate Chem.* **2012**, *23*, 330-335.
- (82) Odendaal, A. Y.; Fiamengo, A. L.; Ferdani, R.; Wadas, T. J.; Hill, D. C.; Peng, Y. J.; Heroux, K. J.; Golen, J. A.; Rheingold, A. L.; Anderson, C. J.; Weisman, G. R.; Wong, E. H. *Inorg. Chem.* **2011**, *50*, 3078-3086.
- (83) Cai, H. C.; Li, Z. B.; Huang, C. W.; Park, R.; Shahinian, A. H.; Conti, P. S. *Nucl. Med. Biol.* **2010**, *37*, 57-65.
- (84) Cooper, M. S.; Ma, M. T.; Sunassee, K.; Shaw, K. P.; Williams, J. D.; Paul, R. L.; Donnelly, P. S.; Blower, P. J. *Bioconjugate Chem.* **2012**, *23*, 1029-1039.
- (85) Fichna, J.; Janecka, A. *Bioconjugate Chem.* **2003**, *14*, 3-17.
- (86) Hermanson, G. T. *Bioconjugate Techniques*; Academic press, **1996**.
- (87) Montalbetti, C. A. G. N.; Falque, V. *Tetrahedron* **2005**, *61*, 10827-10852.
- (88) Dijkgraaf, I.; Rijnders, A. Y.; Soede, A.; Dechesne, A. C.; Van Esse, G. W.; Brouwer, A. J.; Corstens, F. H. M.; Boerman, O. C.; Rijkers, D. T. S.; Liskamp, R. M. J. *Org. Biomol. Chem.* **2007**, *5*, 935-944.
- (89) Mindt, T. L.; Mueller, C.; Melis, M.; De Jong, M.; Schibli, R. *Bioconjugate Chem.* **2008**, *19*, 1689-1695.
- (90) Struthers, H.; Spingler, B.; Mindt, T. L.; Schibli, R. *Chem. Eur. J.* **2008**, *14*, 6173-6183.
- (91) Martin, M. E.; Parameswarappa, S. G.; O'Dorisio, M. S.; Pigge, F. C.; Schultz, M. K. *Bioorg. Med. Chem. Lett.* **2010**, *20*, 4805-4807.
- (92) Misra, P.; Humblet, V.; Pannier, N.; Maison, W.; Frangioni, J. V. *J. Nucl. Med.* **2007**, *48*, 1379-1389.

- (93) Misra, P.; Lebeche, D.; Ly, H.; Schwarzkopf, M.; Diaz, G.; Hajjar, R. J.; Schechter, A. D.; Frangioni, J. V. *J. Nucl. Med.* **2008**, *49*, 963-969.
- (94) Hanaoka, H.; Mukai, T.; Tamamura, H.; Mori, T.; Ishino, S.; Ogawa, K.; Iida, Y.; Doi, R.; Fujii, N.; Saji, H. *Nucl. Med. Biol.* **2006**, *33*, 489-494.
- (95) Buckle, T.; Van den Berg, N. S.; Kuil, J.; Bunschoten, A.; Oldenburg, J.; Borowsky, A. D.; Wesseling, J.; Masada, R.; Oishi, S.; Fujii, N.; Van Leeuwen, F. W. B. *Am. J. Nucl. Med. Mol. Imaging* **2012**, *2*, 99-109.
- (96) Hennrich, U.; Seyler, L.; Schafer, M.; Bauder-Wust, U.; Eisenhut, M.; Semmler, W.; Bauerle, T. *Bioorg. Med. Chem.* **2012**, *20*, 1502-1510.
- (97) Jacobson, O.; Weiss, I. D.; Szajek, L. P.; Niu, G.; Ma, Y.; Kiesewetter, D. O.; Farber, J. M.; Chen, X. Y. *Theranostics* **2011**, *1*, 251-262.
- (98) Jacobson, O.; Weiss, I. D.; Szajek, L. P.; Niu, G.; Ma, Y.; Kiesewetter, D. O.; Peled, A.; Eden, H. S.; Farber, J. M.; Chen, X. Y. *J. Control. Release* **2012**, *157*, 216-223.
- (99) Demmer, O.; Gourni, E.; Schumacher, U.; Kessler, H.; Wester, H. J. *ChemMedChem* **2011**, *6*, 1789-1791.
- (100) Gourni, E.; Demmer, O.; Schottelius, M.; D'Alessandria, C.; Schulz, S.; Dijkgraaf, I.; Schumacher, U.; Schwaiger, M.; Kessler, H.; Wester, H. J. *J. Nucl. Med.* **2011**, *52*, 1803-1810.
- (101) Jacobson, O.; Weiss, I. D.; Szajek, L.; Farber, J. M.; Kiesewetter, D. O. *Bioorg. Med. Chem.* **2009**, *17*, 1486-1493.
- (102) Nimmagadda, S.; Pullambhatla, M.; Stone, K.; Green, G.; Bhujwalla, Z. M.; Pomper, M. G. *Cancer Res.* **2010**, *70*, 3935-3944.
- (103) Weiss, I. D.; Jacobson, O.; Kiesewetter, D. O.; Jacobus, J. P.; Szajek, L. P.; Chen, X. Y.; Farber, J. M. *Mol. Imaging Biol.* **2012**, *14*, 106-114.
- (104) Zhang, J. M.; Tian, J. H.; Li, T. R.; Guo, H. Y.; Shen, L. *Chin. Chem. Lett.* **2010**, *21*, 461-463.
- (105) De Silva, R. A.; Peyre, K.; Pullambhatla, M.; Fox, J. J.; Pomper, M. G.; Nimmagadda, S. *J. Nucl. Med.* **2011**, *52*, 986-993.
- (106) Luo, S. L.; Zhang, E. L.; Su, Y. P.; Cheng, T. M.; Shi, C. M. *Biomaterials* **2011**, *32*, 7127-7138.
- (107) Lavis, L. D.; Raines, R. T. *ACS Chem. Biol.* **2008**, *3*, 142-155.
- (108) Kobayashi, H.; Ogawa, M.; Alford, R.; Choyke, P. L.; Urano, Y. *Chem. Rev.* **2010**, *110*, 2620-2640.
- (109) Dar, A.; Goichberg, P.; Shinder, V.; Kalinkovich, A.; Kollet, O.; Netzer, N.; Margalit, R.; Zsak, M.; Nagler, A.; Hardan, I.; Resnick, I.; Rot, A.; Lapidot, T. *Nat. Immunol.* **2005**, *6*, 1038-1046.
- (110) Meincke, M.; Tiwari, S.; Hattermann, K.; Kalthoff, H.; Mentlein, R. *Clin. Exp. Metastasis* **2011**, *28*, 713-720.
- (111) Nishizawa, K.; Nishiyama, H.; Oishi, S.; Tanahara, N.; Kotani, H.; Mikami, Y.; Toda, Y.; Evans, B. J.; Peiper, S. C.; Saito, R.; Watanabe, J.; Fujii, N.; Ogawa, O. *Int. J. Cancer* **2010**, *127*, 1180-1187.
- (112) Nomura, W.; Tanabe, Y.; Tsutsumi, H.; Tanaka, T.; Ohba, K.; Yamamoto, N.; Tamamura, H. *Bioconjugate Chem.* **2008**, *19*, 1917-1920.

- (113) Oishi, S.; Masuda, R.; Evans, B.; Ueda, S.; Goto, Y.; Ohno, H.; Hirasawa, A.; Tsujimoto, G.; Wang, Z. X.; Peiper, S. C.; Naito, T.; Kodama, E.; Matsuoka, M.; Fujii, N. *ChemBioChem* **2008**, *9*, 1154-1158.
- (114) Khan, A.; Silversides, J. D.; Madden, L.; Greenman, J.; Archibald, S. J. *Chem. Commun.* **2007**, 416-418.
- (115) Knight, J. C.; Hallett, A. J.; Brancale, A.; Paisey, S. J.; Clarkson, R. W. E.; Edwards, P. G. *ChemBioChem* **2011**, *12*, 2692-2698.
- (116) Louie, A. Y. *Chem. Rev.* **2010**, *110*, 3146-3195.
- (117) Culver, J.; Akers, W.; Achilefu, S. *J. Nucl. Med.* **2008**, *49*, 169-172.
- (118) Waghorn, P. A.; Jones, M. W.; McIntyre, A.; Innocenti, A.; Vullo, D.; Harris, A. L.; Supuran, C. T.; Dilworth, J. R. *Eur. J. Inorg. Chem.* **2012**, *2012*, 2898-2907.
- (119) Kuil, J.; Velders, A. H.; van Leeuwen, F. W. B. *Bioconjugate Chem.* **2010**, *21*, 1709-1719.
- (120) Kuil, J.; Buckle, T.; Yuan, H. S.; van den Berg, N. S.; Oishi, S.; Fujii, N.; Josephson, L.; van Leeuwen, F. W. B. *Bioconjugate Chem.* **2011**, *22*, 859-864.
- (121) Kuil, J.; Buckle, T.; Oldenburg, J.; Yuan, H.; Borowsky, A. D.; Josephson, L.; van, L. F. W. B. *Mol. Pharmaceutics* **2011**, *8*, 2444-2453.
- (122) Boschetti, F.; Denat, F.; Espinosa, E.; Tabard, A.; Dory, Y.; Guillard, R. *J. Org. Chem.* **2005**, *70*, 7042-7053.
- (123) Boschetti, F.; Denat, F.; Espinosa, E.; Guillard, R. *Chem. Commun.* **2002**, 312-313.
- (124) Rousselin, Y.; Sok, N.; Boschetti, F.; Guillard, R.; Denat, F. *Eur. J. Org. Chem.* **2010**, 1688-1693.
- (125) Chuburu, F.; Tripier, R.; Le Baccon, M.; Handel, H. *Eur. J. Org. Chem.* **2003**, 1050-1055.
- (126) Claudon, G.; Le Bris, N.; Bernard, H.; Handel, H. *Eur. J. Org. Chem.* **2004**, 5027-5030.
- (127) Delepine, A.-S.; Tripier, R.; Bernard, H.; Le, B. N.; Handel, H. *Tetrahedron Lett.* **2009**, *50*, 2521-2524.
- (128) Le Baccon, M.; Chuburu, F.; Toupet, L.; Handel, H.; Soibinet, M.; Dechamps-Olivier, I.; Barbieri, J. P.; Aplincourt, M. *New J. Chem.* **2001**, *25*, 1168-1174.
- (129) Boschetti, F.; Denat, F.; Espinosa, E.; Lagrange, J.-M.; Guillard, R. *Chem. Commun.* **2004**, 588-589.
- (130) Weisman, G. R.; Ho, S. C. H.; Johnson, V. *Tetrahedron Lett.* **1980**, *21*, 335-338.
- (131) Royal, G.; Dahaoui-Gindrey, V.; Dahaoui, S.; Tabard, A.; Guillard, R.; Pullumbi, P.; Lecomte, C. *Eur. J. Org. Chem.* **1998**, 1971-1975.
- (132) Bucher, C.; Royal, G.; Barbe, J. M.; Guillard, R. *Tetrahedron Lett.* **1999**, *40*, 2315-2318.
- (133) Baker, W. C.; Choi, M. J.; Hill, D. C.; Thompson, J. L.; Petillo, P. A. *J. Org. Chem.* **1999**, *64*, 2683-2689.
- (134) Rohovec, J.; Gyepes, R.; Cisarova, I.; Rudovsky, J.; Lukes, I. *Tetrahedron Lett.* **2000**, *41*, 1249-1253.
- (135) Kotek, J.; Hermann, P.; Vojtisek, P.; Rohovec, J.; Lukes, I. *Collect. Czech. Chem. Commun.* **2000**, *65*, 243-266.
- (136) Lewis, E. A.; Allan, C. C.; Boyle, R. W.; Archibald, S. J. *Tetrahedron Lett.* **2004**, *45*, 3059-3062.

- (137) Wong, E. H.; Weisman, G. R.; Hill, D. C.; Reed, D. P.; Rogers, M. E.; Condon, J. S.; Fagan, M. A.; Calabrese, J. C.; Lam, K. C.; Guzei, I. A.; Rheingold, A. L. *J. Am. Chem. Soc.* **2000**, *122*, 10561-10572.
- (138) Hervé, G.; Bernard, H.; Le Bris, N.; Yaouanc, J. J.; Handel, H. *Tetrahedron Lett.* **1998**, *39*, 6861-6864.
- (139) Develay, S. P.; Tripier, R.; Chuburu, F.; Le Baccon, M.; Handel, H. *Eur. J. Org. Chem.* **2003**, 3047-3050.
- (140) Weisman, G. R.; Rogers, M. E.; Wong, E. H.; Jasinski, J. P.; Paight, E. S. *J. Am. Chem. Soc.* **1990**, *112*, 8604-8605.
- (141) Weisman, G. R.; Wong, E. H.; Hill, D. C.; Rogers, M. E.; Reed, D. P.; Calabrese, J. C. *Chem. Commun.* **1996**, 947-948.
- (142) Kolinski, R. A.; Riddell, F. G. *Tetrahedron Lett.* **1981**, *22*, 2217-2220.
- (143) Bernier, N.; Allali, M.; Tripier, R.; Conan, F.; Patinec, V.; Develay, S.; Le Baccon, M.; Handel, H. *New J. Chem.* **2006**, *30*, 435-441.
- (144) Bernier, N.; Tripier, R.; Patinec, V.; Le Baccon, M.; Handel, H. *C. R. Chim.* **2007**, *10*, 832-838.
- (145) Yamamoto, H.; Maruoka, K. *J. Am. Chem. Soc.* **1981**, *103*, 4186-4194.
- (146) Richman, J. E.; Atkins, T. J. *J. Am. Chem. Soc.* **1974**, *96*, 2268-2270.
- (147) Tabushi, I.; Taniguchi, Y.; Kato, H. *Tetrahedron Lett.* **1977**, 1049-1052.
- (148) Bernhard, C., *Thesis*, Université de Bourgogne, **2011**.
- (149) Farrugia, L. J. *J. Appl. Crystallogr.* **1997**, *30*, 565.
- (150) Haines, R. I. *Rev. Inorg. Chem.* **2001**, *21*, 165-205.
- (151) Wainwright, K. P. *Coord. Chem. Rev.* **1997**, *166*, 35-90.
- (152) Hage, R.; Iburg, J. E.; Kerschner, J.; Koek, J. H.; Lempers, E. L. M.; Martens, R. J.; Racherla, U. S.; Russell, S. W.; Swarthoff, T. *Nature* **1994**, *369*, 637-639.
- (153) Hage, R.; Nuhlen, D.; Weyhermuller, T.; Wieghardt, K., **2001**, WO2001064826A2.
- (154) Adams, N.; Arts, H. J.; Bolton, P. D.; Cowell, D.; Dubberley, S. R.; Friederichs, N.; Grant, C. M.; Kranenburg, M.; Sealey, A. J.; Wang, B.; Wilson, P. J.; Zuideveld, M.; Blake, A. J.; Schroeder, M.; Mountford, P. *Organometallics* **2006**, *25*, 3888-3903.
- (155) Sakai, T., **1998**, EP816387A1.
- (156) Chin Quee-Smith, V.; DelPizzo, L.; Jureller, S. H.; Kerschner, J. L.; Hage, R. *Inorg. Chem.* **1996**, *35*, 6461-6465.
- (157) De Vos, D.; Bein, T. *J. Am. Chem. Soc.* **1997**, *119*, 9460-9465.
- (158) Gilbert, B. C.; Lindsay, S. J. R.; Mairata, i. P. A.; Oakes, J.; Pons, i. P. R. *J. Mol. Catal. A: Chem.* **2004**, *219*, 265-272.
- (159) Handervan, C.; Ge, R.; Feringa, B. L. *Chem. Commun.* **1997**, 419-420.
- (160) Johnson, D. L.; Martin, L. L. *J. Am. Chem. Soc.* **2005**, *127*, 2018-2019.
- (161) Tolman, W. B. *Acc. Chem. Res.* **1997**, *30*, 227-237.
- (162) Parker, R. J.; Spiccia, L.; Berry, K. J.; Fallon, G. D.; Moubaraki, B.; Murray, K. S. *Chem. Commun.* **2001**, 333-334.
- (163) Sokol, J. J.; Hee, A. G.; Long, J. R. *J. Am. Chem. Soc.* **2002**, *124*, 7656-7657.

- (164) Liang, F.; Wan, S. H.; Li, Z.; Xiong, X. Q.; Yang, L.; Zhou, X.; Wu, C. T. *Curr. Med. Chem.* **2006**, *13*, 711-727.
- (165) Hoye, R. C.; Richman, J. E.; Dantas, G. A.; Lightbourne, M. F.; Shinneman, L. S. *J. Org. Chem.* **2001**, *66*, 2722-2725.
- (166) Martin, A. E.; Ford, T. M.; Bulkowski, J. E. *J. Org. Chem.* **1982**, *47*, 412-415.
- (167) Chong, H. S.; Brechbiel, M. W. *Synth. Commun.* **2003**, *33*, 1147-1154.
- (168) Sessler, J. L.; Sibert, J. W.; Lynch, V. *Inorg. Chem.* **1990**, *29*, 4143-4146.
- (169) Kovacs, Z.; Sherry, A. D. *Tetrahedron Lett.* **1995**, *36*, 9269-9272.
- (170) Van Westrenen, J.; Sherry, A. D. *Bioconjugate Chem.* **1992**, *3*, 524-532.
- (171) Madison, S. A.; Batal, D. J., **1994**, WO9400439A1.
- (172) Weisman, G. R.; Vachon, D. J.; Johnson, V. B.; Gronbeck, D. A. *J. Chem. Soc., Chem. Commun.* **1987**, 886-887.
- (173) Roger, M.; Patinec, V.; Bourgeois, M.; Tripier, R.; Triki, S.; Handel, H. *Tetrahedron* **2012**, *68*, 5637-5643.
- (174) Craig, A. S.; Helps, I. M.; Jankowski, K. J.; Parker, D.; Beeley, N. R. A.; Boyce, B. A.; Eaton, M. A. W.; Millican, A. T.; Millar, K.; Phipps, A.; Rhind, S. K.; Harrison, A.; Walker, C. *J. Chem. Soc., Chem. Commun.* **1989**, 794-796.
- (175) Scheuermann, J. E. W.; Sibbons, K. F.; Benoit, D. M.; Motevalli, M.; Watkinson, M. *Org. Biomol. Chem.* **2004**, *2*, 2664-2670.
- (176) Argouarch, G.; Gibson, C. L.; Stones, G.; Sherrington, D. C. *Tetrahedron Lett.* **2002**, *43*, 3795-3798.
- (177) Argouarch, G.; Stones, G.; Gibson, C. L.; Kennedy, A. R.; Sherrington, D. C. *Org. Biomol. Chem.* **2003**, *1*, 4408-4417.
- (178) Stones, G.; Argouarch, G.; Kennedy, A. R.; Sherrington, D. C.; Gibson, C. L. *Org. Biomol. Chem.* **2003**, *1*, 2357-2363.
- (179) Koek, J. H.; Kohlen, E. W. J. M. *Tetrahedron Lett.* **2006**, *47*, 3673-3675.
- (180) Rousselin, Y., *Thesis*, Université de Bourgogne, **2007**.
- (181) Rowe, B. J.; Wallace, R. A.; White, D. H.; Kaspar, D. L., **2007**, WO2007142804A2.
- (182) Rodriguez, E.; Nilges, M.; Weissleder, R.; Chen, J. W. *J. Am. Chem. Soc.* **2010**, *132*, 168-177.
- (183) Siddiqui, T. S.; Jani, A.; Williams, F.; Muller, R. N.; Vander Elst, L.; Laurent, S.; Yao, F.; Wadghiri, Y. Z.; Walters, M. A. *J. Colloid Interface Sci.* **2009**, *337*, 88-96.
- (184) Bernhard, C.; Moreau, M.; Lhenry, D.; Goze, C.; Boschetti, F.; Rousselin, Y.; Brunotte, F.; Denat, F. *Chem. Eur. J.* **2012**, *18*, 7834-7841.
- (185) Lux, F.; Mignot, A.; Mowat, P.; Louis, C.; Dufort, S.; Bernhard, C.; Denat, F.; Boschetti, F.; Brunet, C.; Antoine, R.; Dugourd, P.; Laurent, S.; Vander Elst, L.; Muller, R.; Sancey, L.; Jossierand, V.; Coll, J. L.; Stupar, V.; Barbier, E.; Remy, C.; Broisat, A.; Ghezzi, C.; Le Duc, G.; Roux, S.; Perriat, P.; Tillement, O. *Angew. Chem. Int. Ed.* **2011**, *50*, 12299-12303.
- (186) Moreau, M.; Raguin, O.; Vrigneaud, J.-M.; Collin, B.; Bernhard, C.; Tizon, X.; Boschetti, F.; Duchamp, O.; Brunotte, F.; Denat, F. *Bioconjugate Chem.* **2012**, *23*, 1181-1188.
- (187) Tornøe, C. W.; Christensen, C.; Meldal, M. *J. Org. Chem.* **2002**, *67*, 3057-3064.

- (188) Bernardin, A.; Cazet, A.; Guyon, L.; Delannoy, P.; Vinet, F.; Bonnaffe, D.; Texier, I. *Bioconjugate Chem.* **2010**, *21*, 583-588.
- (189) Prasuhn, D. E., Jr.; Yeh, R. M.; Obenaus, A.; Manchester, M.; Finn, M. G. *Chem. Commun.* **2007**, 1269-1271.
- (190) Muller, C.; Mindt, T. L.; De Jong, M.; Schibli, R. *Eur. J. Nucl. Med. Mol. Imaging* **2009**, *36*, 938-946.
- (191) Mezzanotte, L.; Que, I.; Kaijzel, E.; Branchini, B.; Roda, A.; Lowik, C. *PLoS One* **2011**, *6*, e19277.
- (192) Rostovtsev, V. V.; Green, L. G.; Fokin, V. V.; Sharpless, K. B. *Angew. Chem. Int. Ed.* **2002**, *41*, 2596-2599.
- (193) Mindt, T. L.; Schweinsberg, C.; Brans, L.; Hagenbach, A.; Abram, U.; Tourwe, D.; Garcia-Garayo, E.; Schibli, R. *ChemMedChem* **2009**, *4*, 529-539.
- (194) Yu, M.; Price, J. R.; Jensen, P.; Lovitt, C. J.; Shelper, T.; Duffy, S.; Windus, L. C.; Avery, V. M.; Rutledge, P. J.; Todd, M. H. *Inorg. Chem.* **2011**, *50*, 12823-12835.
- (195) Yim, C.-B.; Boerman, O. C.; De Visser, M.; De Jong, M.; Dechesne, A. C.; Rijkers, D. T. S.; Liskamp, R. M. J. *Bioconjugate Chem.* **2009**, *20*, 1323-1331.
- (196) Knoer, S.; Modlinger, A.; Poethko, T.; Schottelius, M.; Wester, H.-J.; Kessler, H. *Chem. Eur. J.* **2007**, *13*, 6082-6090.
- (197) Lebedev, A. Y.; Holland, J. P.; Lewis, J. S. *Chem. Commun.* **2010**, *46*, 1706-1708.
- (198) Pal, M.; Parasuraman, K.; Yeleswarapu, K. R. *Org. Lett.* **2003**, *5*, 349-352.
- (199) Sok, N., *Thesis*, Université de Bourgogne, **2010**.
- (200) Aime, S.; Batsanov, A. S.; Botta, M.; Dickins, R. S.; Faulkner, S.; Foster, C. E.; Harrison, A.; Howard, J. A. K.; Moloney, J. M.; Norman, T. J.; Parker, D.; Royle, L.; Williams, J. A. G. *J. Chem. Soc., Dalton Trans.* **1997**, 3623-3636.
- (201) Huskens, J.; Sherry, A. D. *Inorg. Chem.* **1996**, *35*, 5137-5143.
- (202) Kotkova, Z.; Pereira, G. A.; Djanashvili, K.; Kotek, J.; Rudovsky, J.; Hermann, P.; Elst, L. V.; Muller, R. N.; Geraldes, C. F. G. C.; Lukes, I.; Peters, J. A. *Eur. J. Inorg. Chem.* **2009**, 119-136.
- (203) Huskens, J.; Sherry, A. D. *J. Am. Chem. Soc.* **1996**, *118*, 4396-4404.
- (204) Senanayake, K.; Thompson, A. L.; Howard, J. A. K.; Botta, M.; Parker, D. *Dalton Trans.* **2006**, 5423-5428.
- (205) Pulukkody, K. P.; Norman, T. J.; Parker, D.; Royle, L.; Broan, C. J. *J. Chem. Soc., Perkin Trans. 2* **1993**, 605-620.
- (206) Parker, D.; Senanayake, K.; Williams, J. A. G. *Chem. Commun.* **1997**, 1777-1778.
- (207) Picazo, O.; Alkorta, I.; Elguero, J.; Mo, O.; Yanez, M. *J. Phys. Org. Chem.* **2005**, *18*, 491-497.
- (208) Kang, S.-O.; Llinares, J. M.; Day, V. W.; Bowman-James, K. *Chem. Soc. Rev.* **2010**, *39*, 3980-4003.
- (209) Ambrosi, G.; Dapporto, P.; Formica, M.; Fusi, V.; Giorgi, L.; Guerri, A.; Micheloni, M.; Paoli, P.; Pontellini, R.; Rossi, P. *Inorg. Chem.* **2006**, *45*, 304-314.
- (210) Dietrich, B.; Lehn, J. M.; Sauvage, J. P. *Tetrahedron Lett.* **1969**, 2885-2888.
- (211) Pederson, C. J.; Lehn, J. M.; Cram, D. J. *Resonance* **2001**, *6*, 71-79.

- (212) An, H. Y.; Bradshaw, J. S.; Izatt, R. M. *Chem. Rev.* **1992**, *92*, 543-572.
- (213) Boswell, C. A.; Regino, C. A. S.; Baidoo, K. E.; Wong, K. J.; Bumb, A.; Xu, H.; Milenic, D. E.; Kelley, J. A.; Lai, C. C.; Brechbiel, M. W. *Bioconjugate Chem.* **2008**, *19*, 1476-1484.
- (214) Broge, L.; Pretzmann, U.; Jensen, N.; Sotofte, I.; Olsen, C. E.; Springborg, J. *Inorg. Chem.* **2001**, *40*, 2323-2334.
- (215) Di Bartolo, N. M.; Sargeson, A. M.; Donlevy, T. M.; Smith, S. V. *J. Chem. Soc., Dalton Trans.* **2001**, 2303-2309.
- (216) Jana, A.; Jang, S. Y.; Shin, J.-Y.; De, A. K.; Goswami, D.; Kim, D.; Bharadwaj, P. K. *Chem. Eur. J.* **2008**, *14*, 10628-10638.
- (217) Springborg, J. *Dalton Trans.* **2003**, 1653-1665.
- (218) Springborg, J.; Kofod, P.; Olsen, C. E.; Toftlund, H.; Sotofte, I. *Acta Chem. Scand.* **1995**, *49*, 547-554.
- (219) Springborg, J.; Pretzmann, U.; Nielsen, B.; Olsen, C. E.; Sotofte, I. *Acta Chem. Scand.* **1998**, *52*, 212-217.
- (220) Springborg, J.; Pretzmann, U.; Olsen, C. E. *Acta Chem. Scand.* **1996**, *50*, 294-298.
- (221) Springborg, J.; Sotofte, I. *Acta Chem. Scand.* **1997**, *51*, 357-366.
- (222) Fabbrizzi, L.; Pallavicini, P.; Parodi, L.; Taglietti, A. *Inorg. Chim. Acta* **1995**, *238*, 5-8.
- (223) Dearling, J. L. J.; Voss, S. D.; Dunning, P.; Snay, E.; Fahey, F.; Smith, S. V.; Huston, J. S.; Meares, C. F.; Treves, S. T.; Packard, A. B. *Nucl. Med. Biol.* **2011**, *38*, 29-38.
- (224) Di Bartolo, N.; Sargeson, A. M.; Smith, S. V. *Org. Biomol. Chem.* **2006**, *4*, 3350-3357.
- (225) Sargeson, A. M. *Pure Appl. Chem.* **1984**, *56*, 1603-1619.
- (226) Sargeson, A. M. *Coord. Chem. Rev.* **1996**, *151*, 89-114.
- (227) Bazzicalupi, C.; Bellusci, A.; Bencini, A.; Berni, E.; Bianchi, A.; Ciattini, S.; Giorgi, C.; Valtancoli, B. *J. Chem. Soc., Dalton Trans.* **2002**, 2151-2157.
- (228) Bencini, A.; Biagini, S.; Giorgi, C.; Handel, H.; Le Baccon, M.; Mariani, P.; Paoletti, P.; Paoli, P.; Rossi, P.; Tripier, R.; Valtancoli, B. *Eur. J. Org. Chem.* **2009**, 5610-5621.
- (229) Boswell, C. A.; Sun, X. K.; Niu, W. J.; Weisman, G. R.; Wong, E. H.; Rheingold, A. L.; Anderson, C. J. *J. Med. Chem.* **2004**, *47*, 1465-1474.
- (230) Broge, L.; Sotofte, I.; Jensen, K.; Jensen, N.; Pretzmann, U.; Springborg, J. *Dalton Trans.* **2007**, 3826-3839.
- (231) Bazzicalupi, C.; Bencini, A.; Bianchi, A.; Borsari, L.; Danesi, A.; Giorgi, C.; Lodeiro, C.; Mariani, P.; Pina, F.; Santarelli, S.; Tamayo, A.; Valtancoli, B. *Dalton Trans.* **2006**, 4000-4010.
- (232) Bazzicalupi, C.; Bencini, A.; Ciattini, S.; Giorgi, C.; Masotti, A.; Paoletti, P.; Valtancoli, B.; Navon, N.; Meyerstein, D. *J. Chem. Soc., Dalton Trans.* **2000**, 2383-2391.
- (233) Li, F.; Delgado, R.; Coelho, A.; Drew, M. G. B.; Felix, V. *Tetrahedron* **2006**, *62*, 8550-8558.
- (234) Chaux, F., *Thesis*, Université de Bourgogne, **2005**.
- (235) Chaux, F.; Denat, F.; Espinosa, E.; Guillard, R. *Chem. Commun.* **2006**, 5054-5056.
- (236) Bazzicalupi, C.; Bencini, A.; Bianchi, A.; Fusi, V.; Mazzanti, L.; Paoletti, P.; Valtancoli, B.; Golub, G.; Cohen, H.; Meyerstein, D. *J. Chem. Soc., Dalton Trans.* **1995**, 2377-2384.

- (237) Bazzicalupi, C.; Bencini, A.; Bianchi, A.; Fusi, V.; Paoletti, P.; Valtancoli, B. *J. Chem. Soc., Perkin Trans. 2* **1994**, 815-820.
- (238) Bencini, A.; Fusi, V.; Giorgi, C.; Micheloni, M.; Nardi, N.; Valtancoli, B. *J. Chem. Soc., Perkin Trans. 2* **1996**, 2297-2302.
- (239) Bardazzi, E.; Ciampolini, M.; Fusi, V.; Micheloni, M.; Nardi, N.; Pontellini, R.; Romani, P. *J. Org. Chem.* **1999**, *64*, 1335-1337.
- (240) Brandès, S.; Cocolios, P.; Guillard, R. *C. R. Ac. Sci.* **1996**, *322*, 827-833.
- (241) Brandès, S.; Denat, F.; Lacour, S.; Rabiet, F.; Barbette, F.; Pullumbi, P.; Guillard, R. *Eur. J. Org. Chem.* **1998**, 2349-2360.
- (242) AbdelMagid, A. F.; Carson, K. G.; Harris, B. D.; Maryanoff, C. A.; Shah, R. D. *J. Org. Chem.* **1996**, *61*, 3849-3862.
- (243) Habata, Y.; Osaka, F.; Yamada, S. *J. Heterocycl. Chem.* **2006**, *43*, 157-161.
- (244) Maffeo, D.; Williams, J. A. G. *Inorg. Chim. Acta* **2003**, *355*, 127-136.
- (245) Xue, G. P.; Bradshaw, J. S.; Dalley, N. K.; Savage, P. B.; Izatt, R. M.; Prodi, L.; Montalti, M.; Zaccheroni, N. *Tetrahedron* **2002**, *58*, 4809-4815.
- (246) Kuehm-Caubere, C.; AdachBecker, S.; Fort, Y.; Caubere, P. *Tetrahedron* **1996**, *52*, 9087-9092.
- (247) Skar, M. L.; Svendsen, J. S. *Tetrahedron* **1997**, *53*, 17425-17440.
- (248) Bazzicalupi, C.; Bencini, A.; Ciattini, S.; Denat, F.; Desogere, P.; Goze, C.; Matera, I.; Valtancoli, B. *Dalton Trans.* **2010**, *39*, 11643-11653.
- (249) Li, F.; Li, L.; Delgado, R.; Drew, M. G. B.; Felix, V. *Dalton Trans.* **2007**, 1316-1324.
- (250) Oltmanns, D.; Zitzmann-Kolbe, S.; Mueller, A.; Bauder-Wuest, U.; Schaefer, M.; Eder, M.; Haberkorn, U.; Eisenhut, M. *Bioconjugate Chem.* **2011**, *22*, 2611-2624.
- (251) Zitzmann-Kolbe, S.; Bauder-Wuest, U.; Eisenhut, M.; Oltmanns, D., **2010**, WO2010006755A2.
- (252) Zitzmann-Kolbe, S.; Oltmanns, D.; Eisenhut, M.; Bauder-Wuest, U., **2010**, EP2149567A1.
- (253) Schutters, K.; Reutelingsperger, C. *Apoptosis* **2010**, *15*, 1072-1082.
- (254) Brandès, S.; Gros, C.; Denat, F.; Pullumbi, P.; Guillard, R. *Bull. Soc. Chim. Fr.* **1996**, *133*, 65-73.
- (255) Bridger, G. J.; Boehringer, E. M.; Wang, Z.; Schols, D.; Skerlj, R. T.; Bogucki, D. E., **2003**, US6506770B1.
- (256) Bridger, G. J.; Padmanabhan, S.; Skerlj, R. T.; Thornton, D. M., **1993**, WO9312096A1.
- (257) Bridger, G. J.; Skerlj, R. T.; Hernandez-Abad, P. E.; Bogucki, D. E.; Wang, Z. R.; Zhou, Y. X.; Nan, S.; Boehringer, E. M.; Wilson, T.; Crawford, J.; Metz, M.; Hatse, S.; Princen, K.; De Clercq, E.; Schols, D. *J. Med. Chem.* **2010**, *53*, 1250-1260.
- (258) Dessolin, J.; Galea, P.; Vlieghe, P.; Chermann, J. C.; Kraus, J. L. *J. Med. Chem.* **1999**, *42*, 229-241.
- (259) Moret, V.; Dereudre-Bosquet, N.; Clayette, P.; Laras, Y.; Pietrancosta, N.; Rolland, A.; Weck, C.; Marc, S.; Kraus, J. L. *Bioorg. Med. Chem. Lett.* **2006**, *16*, 5988-5992.
- (260) Tanaka, T.; Narumi, T.; Ozaki, T.; Sohma, A.; Ohashi, N.; Hashimoto, C.; Itotani, K.; Nomura, W.; Murakami, T.; Yamamoto, N.; Tamamura, H. *ChemMedChem* **2011**, *6*, 834-839.



- (261) Baell, J. B.; Gable, R. W.; Harvey, A. J.; Toovey, N.; Herzog, T.; Hansel, W.; Wulff, H. J. *Med. Chem.* **2004**, *47*, 2326-2336.
- (262) Acherar, S.; Jamart-Gregoire, B. *Tetrahedron Lett.* **2009**, *50*, 6377-6379.
- (263) Hudnall, T. W.; Lin, T. P.; Gabbai, F. P. *J. Fluorine Chem.* **2010**, *131*, 1182-1186.
- (264) Kand, D.; Mishra, P. K.; Saha, T.; Lahiri, M.; Talukdar, P. *Analyst* **2012**, *137*, 3921-3924.
- (265) Lemcke, S.; Honnscheidt, C.; Waschatko, G.; Bopp, A.; Lutjohann, D.; Bertram, N.; Gehrig-Burger, K. *Mol. Cell. Endocrinol.* **2010**, *314*, 31-40.
- (266) Liu, K. M.; Tsai, M. S.; Jan, M. S.; Chau, C. M.; Wang, W. J. *Tetrahedron* **2011**, *67*, 7919-7922.
- (267) Lee, J.-J.; Lee, S.-C.; Zhai, D.; Ahn, Y.-H.; Yeo, H. Y.; Tan, Y. L.; Chang, Y.-T. *Chem. Commun.* **2011**, *47*, 4508-4510.
- (268) Kang, G.; Son, H.; Lim, J. M.; Kweon, H.-S.; Lee, I. S.; Kang, D.; Jung, J. H. *Chem. Eur. J.* **2012**, *18*, 5843-5847.
- (269) Loudet, A.; Burgess, K. *Chem. Rev.* **2007**, *107*, 4891-4932.
- (270) Haughland, R. P. *The Handbook. A Guide to Fluorescent Probes and Labeling Technologies.*; 10th ed.; Molecular Probes, **2005**.
- (271) Ulrich, G.; Ziessel, R.; Harriman, A. *Angew. Chem. Int. Ed.* **2008**, *47*, 1184-1201.
- (272) Atilgan, S.; Ozdemir, T.; Akkaya, E. U. *Org. Lett.* **2008**, *10*, 4065-4067.
- (273) Tasiar, M.; O'Shea, D. F. *Bioconjugate Chem.* **2010**, *21*, 1130-1133.
- (274) Niu, S. L.; Massif, C.; Ulrich, G.; Ziessel, R.; Renard, P. Y.; Romieu, A. *Org. Biomol. Chem.* **2011**, *9*, 66-69.
- (275) Niu, S. L.; Ulrich, G.; Ziessel, R.; Kiss, A.; Renard, P.-Y.; Romieu, A. *Org. Lett.* **2009**, *11*, 2049-2052.
- (276) Bernhard, C.; Goze, C.; Rousselin, Y.; Denat, F. *Chem. Commun.* **2010**, *46*, 8267-8269.
- (277) Brellier, M.; Duportail, G.; Baati, R. *Tetrahedron Lett.* **2010**, *51*, 1269-1272.
- (278) Amendola, V.; Fabbrizzi, L.; Licchelli, M.; Mangano, C.; Pallavicini, P.; Parodi, L.; Poggi, A. *Coord. Chem. Rev.* **1999**, *192*, 649-669.
- (279) Barefield, E. K.; Wagner, F.; Herlinger, A. W.; Dahl, A. R. *Inorg. Synth.* **1976**, *16*, 220-225.
- (280) De Santis, G.; Fabbrizzi, L.; Licchelli, M.; Pallavicini, P. *J. Chem. Soc., Dalton Trans.* **1991**, 2925-2928.
- (281) Barefield, E. K. *Inorg. Chem.* **1972**, *11*, 2273-2274.
- (282) Barefield, E. K.; Wagner, F.; Hodges, K. D. *Inorg. Chem.* **1976**, *15*, 1370-1377.
- (283) Fabbrizzi, L.; Gatti, F.; Pallavicini, P.; Zambarbieri, E. *Chem.--Eur. J.* **1999**, *5*, 682-690.
- (284) Otwinowski, Z. M., W.; Carter, C. W. Jr. *Methods Enzymol.* **1997**, *276*, 307-326.
- (285) Blessing, R. H. *Acta Crystallogr., Sect. A: Found. Crystallogr.* **1995**, *A51*, 33-38.
- (286) Altomare, A.; Cascarano, G.; Giacovazzo, C.; Guagliardi, A. *J. Appl. Crystallogr.* **1993**, *26*, 343-350.
- (287) Sheldrick, G. M. *SHELX-97, Program for the Refinement of Crystal Structures*, **1997**.
- (288) Sheldrick, G. M. *Acta Cryst., Sect. A* **2008**, *64*, 112-122.

## **Publications and communications**



**Publications and patents:**

“Synthesis of triazacyclononane (TACN) and new *N*- and *C*-functionalized TACN.” P. Désogère, C. Bernhard, Y. Rousselin, F. Boschetti, F. Denat, **2012**, FR1261091.

“Remarkable inertness of Copper(II) chelates of a cyclen-based rigid cryptand with two trans-*N*-acetate arms.” C. V. Esteves, P. Lamosa, R. Delgado, J. Costa, P. Désogère, Y. Rousselin, C. Goze, Franck Denat, *Chemistry*. **In preparation**.

“Selectively Functionalized Constrained Polyazamacrocycles: Building Blocks for Multifunctional Chelating Agents.” P. Désogère, C. Bernhard, C. Goze, Marie José Penouilh, Y. Rousselin, F. Denat, *Eur. J. Org. Chem.* **Accepted**.

“Proton and metal binding by cyclen-based highly rigid cryptands.” C. Bazzicalupi, A. Bencini, S. Ciattini, F. Denat, P. Désogère, C. Goze, I. Matera, B. Valtancoli, *Dalton Trans.*, **2010**, 39, 1-11.

**Oral communications:**

“*New imaging agents based on AMD 3100 and 3465 for targeting chemokine receptor CXCR4.*” P. Désogère, S. Poty, M. Fani, H. Maecke, F. Boschetti, C. Goze, F. Denat, **2012**, XIII<sup>th</sup> doctoral school days, Dijon, France, Besançon.

→ Best oral communication awarded by the Young Researchers Club of the French Chemical Society (SFC).

“*Imaging CXCR4 expression with new AMD 3100 analogues.*” P. Désogère, M. Fani, H. Maecke, F. Boschetti, C. Goze, F. Denat, **2012**, Young researchers days of the Therapeutic Chemistry Society, Paris.

“*New imaging agents for targeting chemokine receptor CXCR4.*” P. Désogère, M. Fani, H. Maecke, F. Boschetti, C. Goze, F. Denat, **2012**, Coordination Chemistry Days, Strasbourg.

→ Best oral communication awarded by the French Chemical Society (SFC).

“*Synthesis of new copper chelators based on reinforced cyclams.*” P. Désogère, C. Goze, F. Denat, **2010**, Advances in the synthesis of molecularly ordered structures (ASMOS), 6<sup>th</sup> workshop Germany France, Dijon.

“*Synthesis and study of new constrained cyclams.*” P. Désogère, C. Goze, F. Denat, **2010**, 1<sup>st</sup> workshop France - Czech Republic, Dijon.

**Posters:**

“*Synthesis of new copper chelators based on reinforced tetraazamacrocycles.*” P. Désogère, C. Bernhard, N. Sok, Y. Rousselin, F. Denat, **2011**, 4<sup>th</sup> Workshop GPOL, Toulouse.

“*New imaging agents for targeting chemokine receptor CXCR4.*” P. Désogère, S. Poty, M. Fani, H. Maecke, F. Boschetti, C. Goze, F. Denat, **2012**, Gecom Concoord, Metabief.

“*Thermodynamic and kinetic consequences of a cross-bridged dicarboxylic cyclam unit with an ethylene chain on proton and Cu(II) binding.*” T. Vu, M. Meyer, P. Désogère, F. Denat, **2012**, Coordination Chemistry Days, Strasbourg.

“*Synthesis of new copper chelators based on reinforced tetraazamacrocycles.*” P. Désogère, C. Bernhard, N. Sok, Y. Rousselin, F. Denat, **2011**, ISRS, Amsterdam.

“*Synthesis of new C-functionalized reinforced cyclams.*” P. Désogère, N. Sok, Y. Rousselin, F. Denat, **2010**, 3<sup>rd</sup> Workshop GPOL (Groupe d'études en chimie des polyamines cycliques), Orléans.

“*New building blocks for the synthesis of molecular contrast agents.*” C. Bernhard, P. Désogère, F. Boschetti, C. Goze, Y. Rousselin, F. Denat, **2009**, 4<sup>th</sup> International Symposium on Macrocyclic and Supramolecular Chemistry, Maastricht.

## ABSTRACT

The objective of this thesis work was to develop CXCR4-targeted tools to localize and treat cancer at an early stage. In this line, we investigated the synthesis of new target-specific radiopharmaceuticals. The work focused on two main axes, *i.e.* the chelating agent and the carrier, by using the know-how and the expertise of our group in polyazacycloalkanes synthesis and functionalization.

In the first part, we were interested in developing new macrocyclic scaffolds of high potential for copper and gallium chelation. We first focused on the development of a new powerful route towards selectively functionalized constrained homocyclens. The second part was based on *C*-functionalized 1,4,7-triazacyclononane (TACN) and its derivatives. From a synthetic route previously developed in our group, we were able to facilitate and optimize the synthesis of selectively *N*- and *C*-functionalized TACN. By varying the grafting functions and the pendant coordinating arms, we prepared several really promising bifunctional chelating agents for copper and gallium chelation. We also investigated the synthesis of new cryptands based on cyclen and we studied their properties towards copper complexation.

In the second part of this thesis work, we were interested in generating a new family of imaging agents based on well-known CXCR4 antagonists, *i.e.* AMD3100 and AMD3465. The access towards these agents first required the preparation of original building blocks by modification of the AMD3100 and AMD3465 cores. The conjugation of such platforms onto the appropriate probe enabled the synthesis of various systems for optical and nuclear imaging. Thus, we were able to introduce a bodipy dye and several chelators adapted for gallium, copper and indium chelation.

### Keywords:

CXCR4	Macrocycles	1,4,7-triazacyclononane
AMD3100/AMD3465	Cryptand	<i>C</i> -functionalization
Copper/Gallium chelation	Homocyclen	Bifunctional chelating agents

## RESUME

L'objectif de ce travail de thèse était de développer des outils pour détecter et traiter le cancer à un stade précoce. Nous avons donc entrepris la synthèse de nouveaux radiopharmaceutiques ciblant spécifiquement le récepteur CXCR4, en utilisant le savoir-faire et l'expertise de notre groupe dans la synthèse et la fonctionnalisation des polyazacycloalcanes. Nous avons travaillé simultanément sur deux aspects : l'agent chélatant et la molécule vectrice.

Dans un premier temps, les travaux ont concerné la conception, la synthèse et la caractérisation de nouveaux macrocycles à fort potentiel pour la chélation du cuivre et du gallium. Nous avons tout d'abord développé une nouvelle voie de synthèse permettant d'accéder à des dérivés homocyclènes C-fonctionnalisés. Nous nous sommes ensuite intéressés aux dérivés du 1,4,7-triazacyclononane (TACN). En optimisant une voie de synthèse déjà développée au laboratoire, nous avons facilité l'accès à des dérivés TACN *N*- et *C*-fonctionnalisés. Nous avons ainsi préparé une série de nouveaux agents chélatants bifonctionnels adaptés pour la complexation du cuivre ou du gallium, en variant la nature de la fonction de greffage et des bras coordinants. Nous avons également réalisé la synthèse de nouveaux cryptands en série cyclène et nous avons étudié leur propriété de complexation vis à vis du cuivre.

Dans un second temps, nous avons développé une nouvelle famille d'agents imageants du CXCR4 en modifiant la structure des AMD3100 et AMD3465. Ce travail a tout d'abord nécessité la mise au point de nouvelles méthodes de fonctionnalisation de ces structures. Nous avons ainsi pu préparer de nouveaux synthons porteur d'une fonction de greffage dans les deux séries. Nous avons ensuite introduit différentes sondes imageantes, telles que des chélates adaptés pour la complexation du cuivre, gallium et indium ainsi que des sondes fluorescentes de type bodipy.

### Mots clés :

CXCR4	Macrocycles	1,4,7-triazacyclononane
AMD3100/AMD3465	Cryptand	C-fonctionnalisation
Complexation Cuivre/Gallium	Homocyclène	Agents bifonctionnels chélatants